

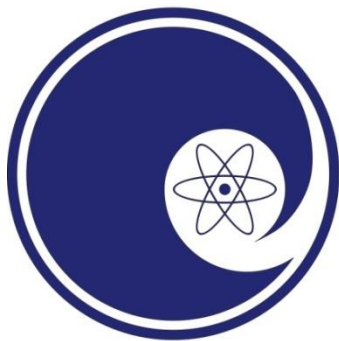
Cavity Fabrication Final Report

Cavity ID: TB9NR016

**FNAL 1.3GHz 9-cell
10 cavity order**

January 20, 2012

FNAL PO # 593451



NIOWAVE
www.niowaveinc.com

Executive Summary

This report contains all the pertinent design and fabrication procedures for the fabrication of this 1.3 GHz 9-cell cavity. All cavity components were manufactured by Niowave with the use of Sciaky EBW chambers at both Sciaky, Inc. and C.F. Roark Welding & Engineering Co. Both the DESY Cavity Spec and FNAL Cavity Specs (Appendix A) were utilized in the fabrication of this 9-cell cavity. The RF and mechanical measurements, as well as all material certifications are also included in this report.

OUTLINE

1. Design	4
a. RF Design	4
i. PRSTAB for ILC TESLA 1.3 GHz 9-cell Cavity	4
ii. ILC 1.3 GHz 9-cell Cavity Theoretical Parameters	5
b. Mechanical Design	6
2. Fabrication	25
a. Cavity Photo	25
b. RF Measurements	25
c. Mechanical Assembly	31
i. Cavity Components	31
ii. Key Parameters	32
iii. Fabrication Observations	32
3. Appendices	33
a. References	33
b. DESY & FNAL Cavity Fabrication Specifications	34
c. PRSTAB for ILC TESLA 1.3 GHz 9-cell Cavity	62
d. Material Certifications	87
e. Component Fabrication Logs	110
f. Equator Weld Repair Plan	182

1. Design

a. RF Design

i. ILC 1.3 GHz 9-cell Cavity

As described in the relevant literature [1], the TESLA-style cavities chosen for the International Linear Collider are 9-cell structures operating in a standing-wave mode. Relevant parameters for the design and performance of these cavities are presented in Table 1. The Physical Review Special Topics – Accelerators and Beams article describing the design of the ILC 1.3 GHz 9-cell is attached in appendix a, section c. The structures are built from bulk niobium and intended to be cooled to 2 K with superfluid helium, as required to reach the cavity Q levels shown in the table.

The choice of the cavity frequency considers the dominance of residual resistance and cavity size at lower frequencies (below 300 MHz or so, where the effective resistance increases as $1/f$) and the higher BCS resistance, which increases the effective surface resistance according to f^2 at high frequencies. Because high-power RF sources (klystrons) are available at 1.3 GHz, this frequency was eventually chosen.

The geometry of the cells was carefully designed with a number of parameters in mind, including multipacting trajectories, cell-to-cell coupling, wakefields, and peak electric and magnetic fields on the niobium surface relative to the accelerating field. Because of the importance of the geometry, a number of steps are taken by Niowave in the manufacturing process to check and preserve

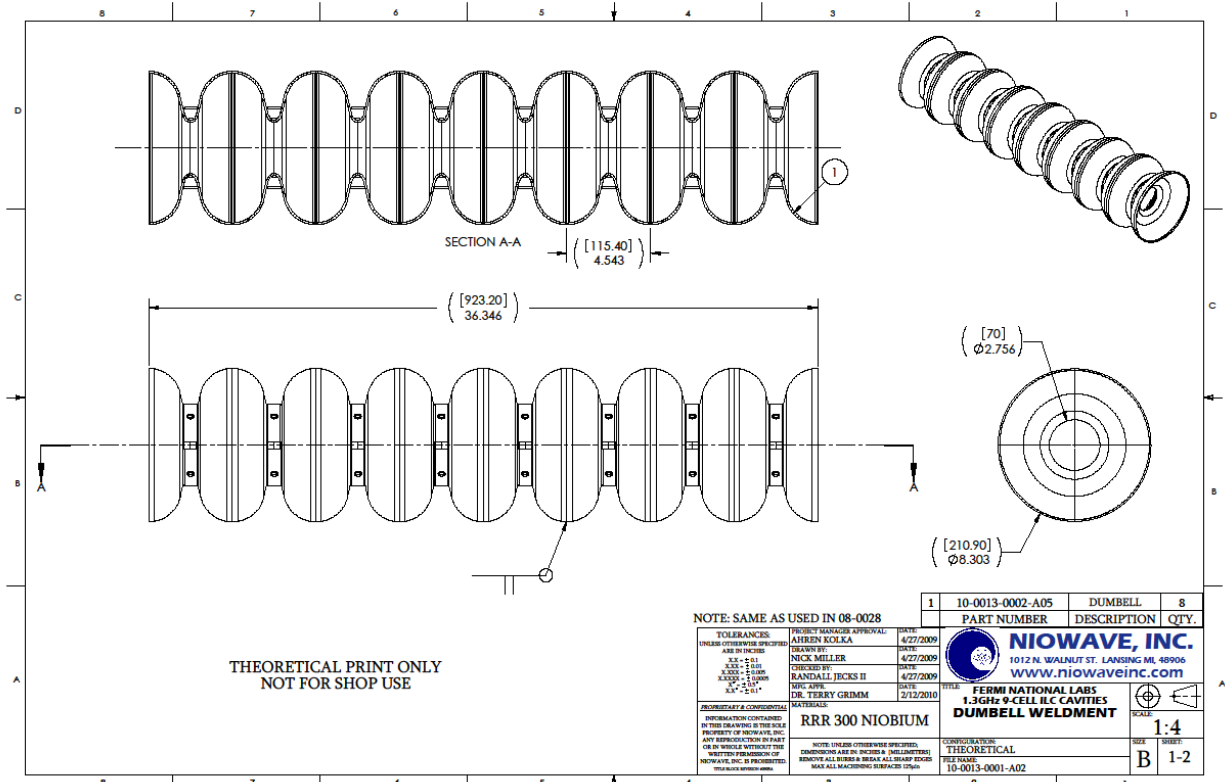
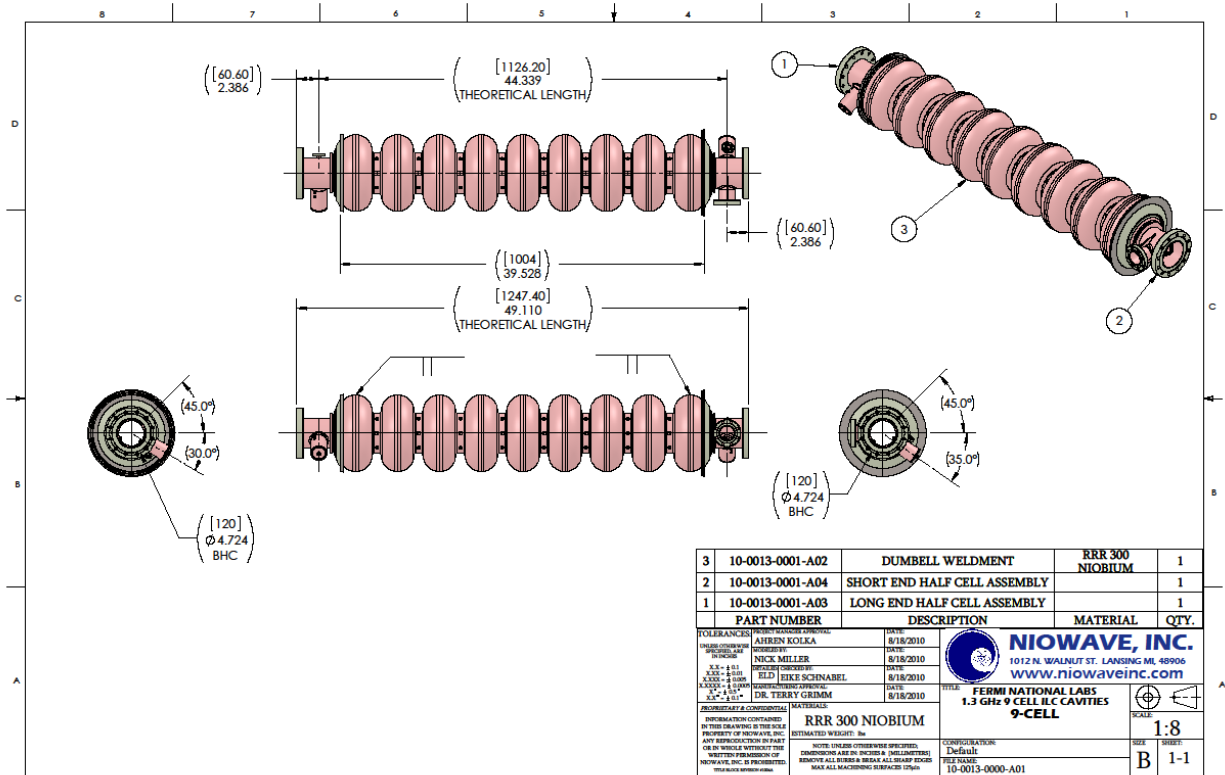
the contours of the dumbbells through the manufacturing process – these procedures are described in a later section.

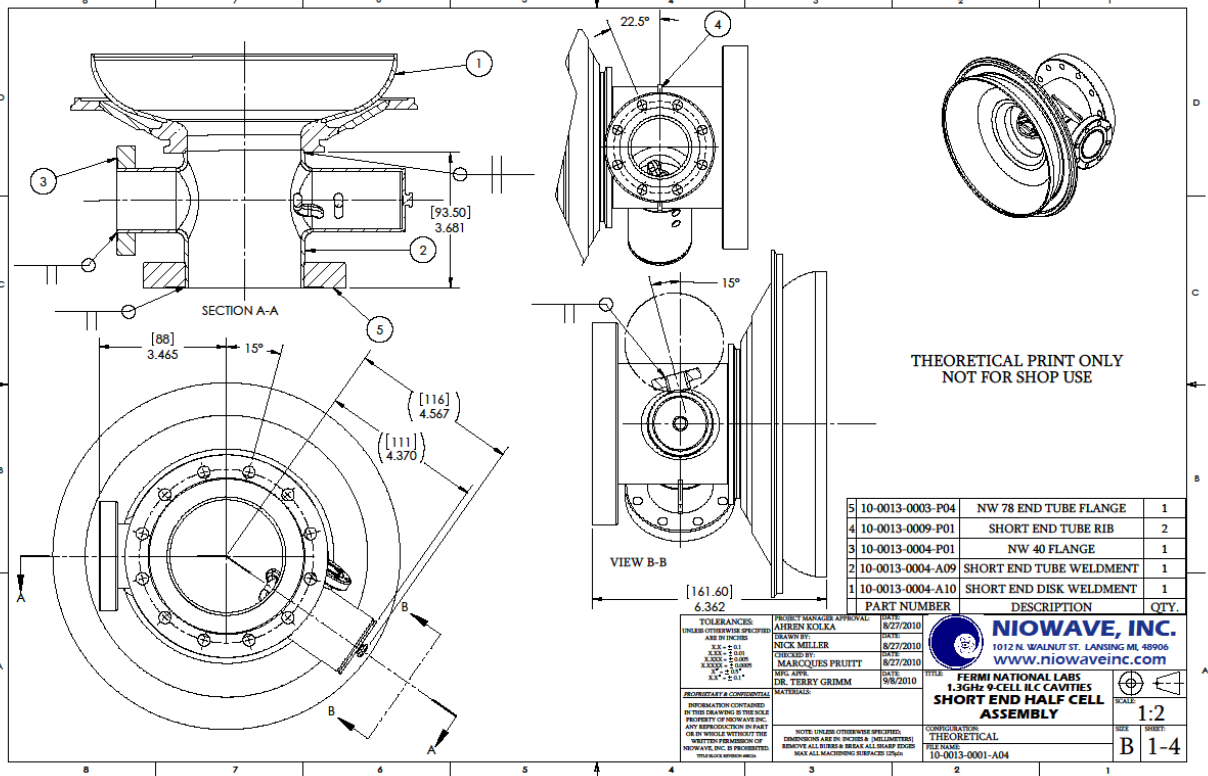
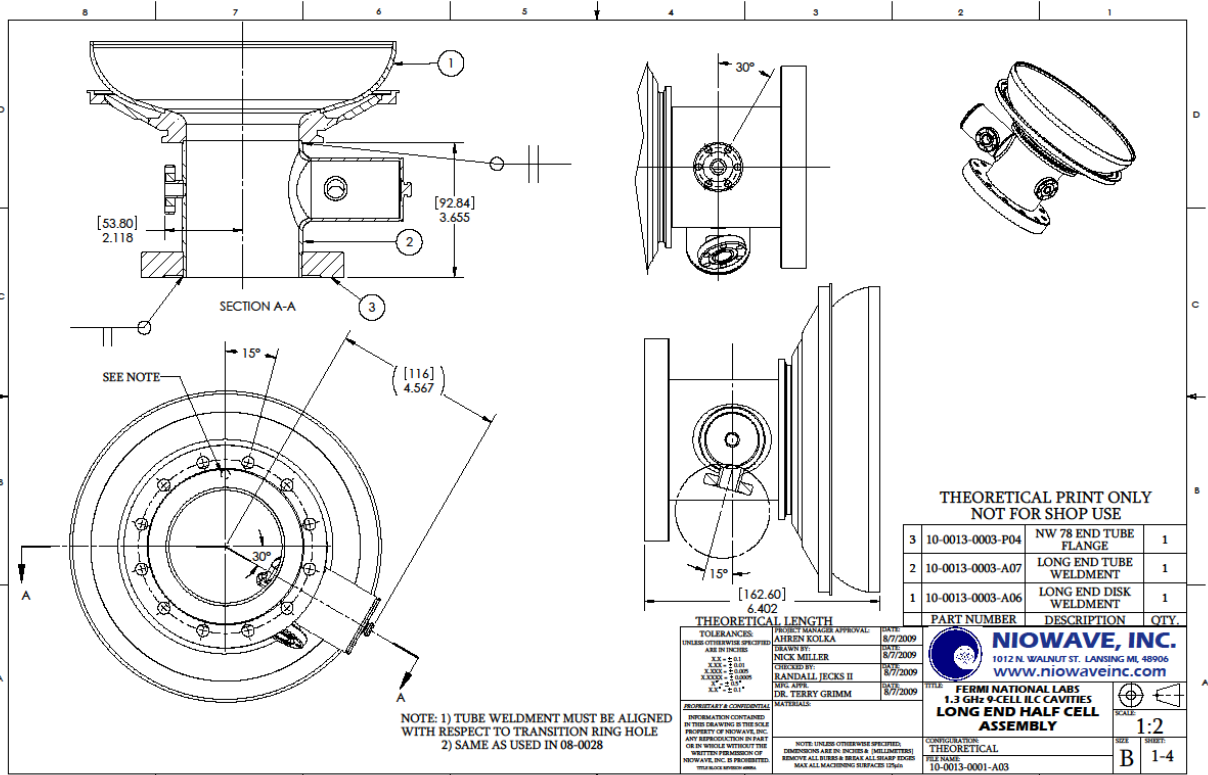
ii. ILC 1.3 GHz 9-cell Cavity Theoretical Parameters

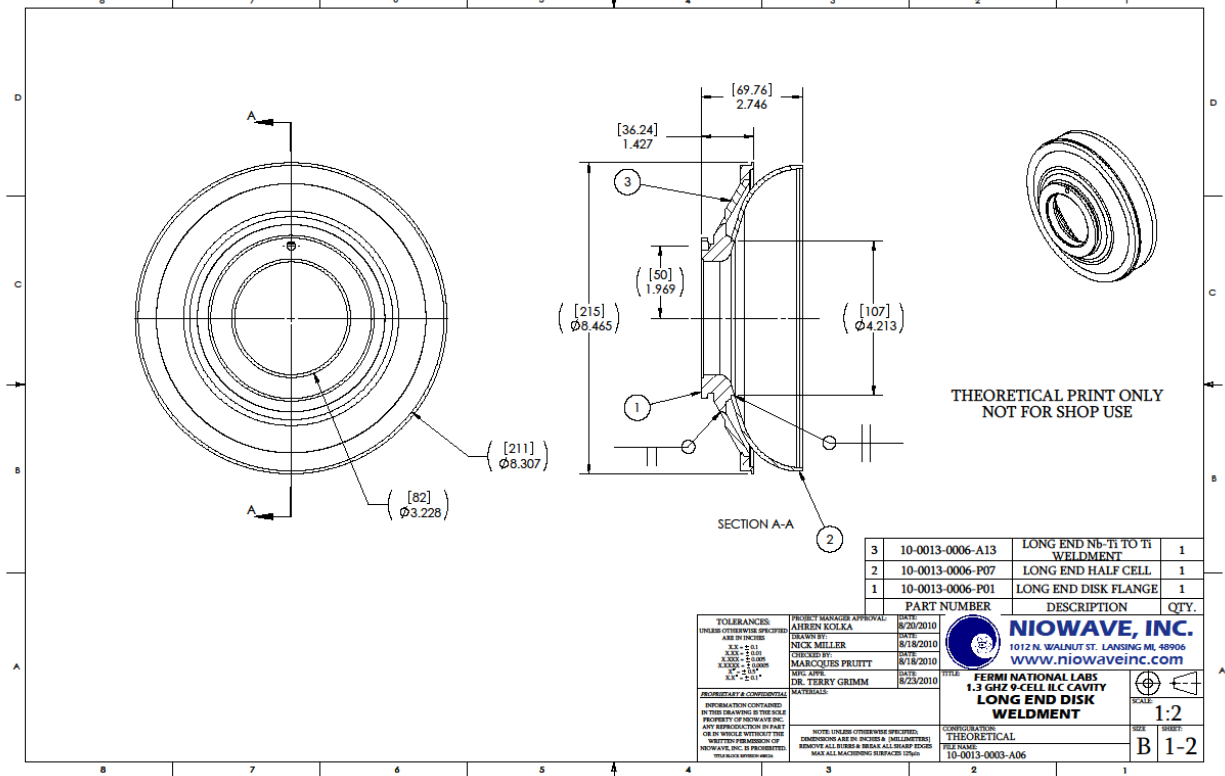
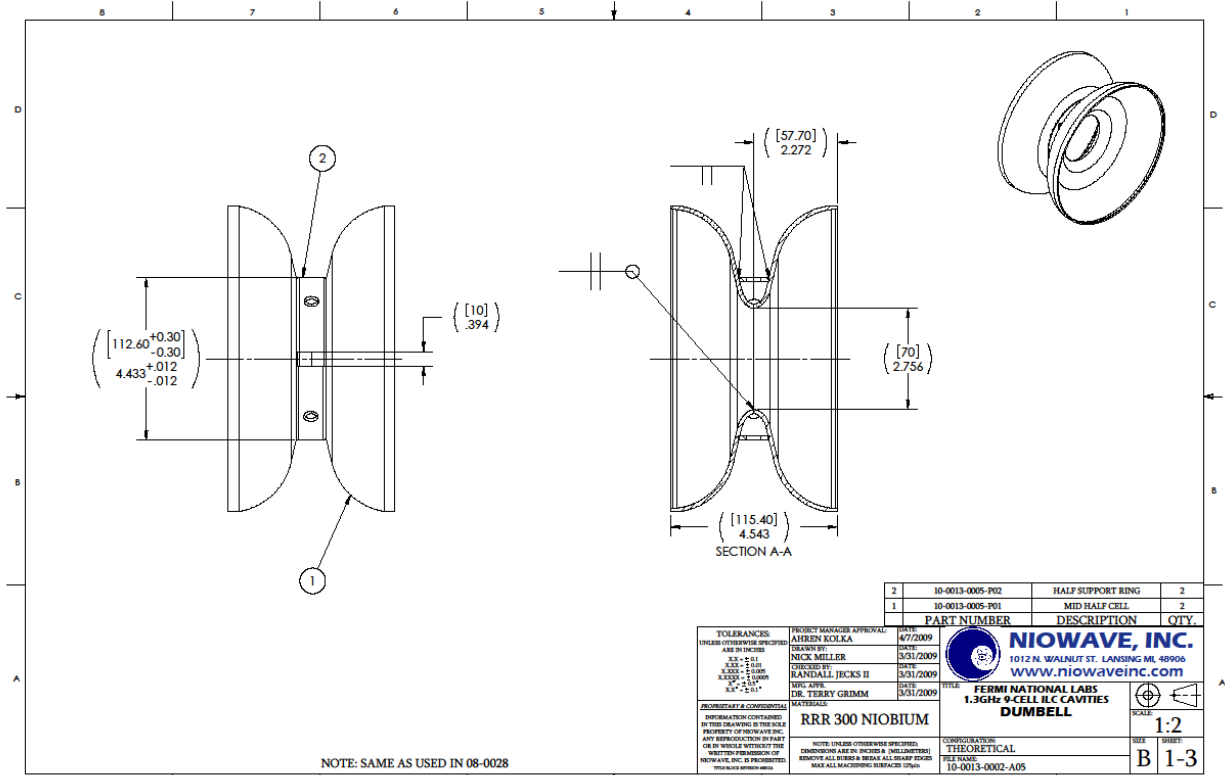
frequency	1300 MHz
TESLA design quality factor, Q_0	5.3×10^9
ILC operational linac quality factor, Q_0	1×10^{10}
R/Q (circuit definition)	518 Ω
geometry factor	270 Ω
theoretical BCS resistance (for 1300 MHz)	17 n Ω
assumed residual resistance for $Q_0=10^{10}$	10 n Ω
ILC design accelerating gradient, vertical test	35 MV/m
peak surface electric field at 35 MV/m gradient	70 MV/m
peak surface magnetic field at 35 MV/m gradient	149 mT
tuning range	6300 kHz
differential tuning with length df/dl	315 kHz/mm
cell-to-cell coupling	1.87%
iris diameter	70 mm
accelerating mode	standing wave, TM010, π -mode
highest impedance parasitic modes	TM011 $\pi/9 - f = 2454$ MHz, R/Q = 80 Ω $2\pi/9 - f = 2443$ MHz, R/Q = 67 Ω
cavity longitudinal loss factor for $\sigma_z=0.7$ mm	10.2 V/pC
cavity transverse loss factor for $\sigma_z=0.7$ mm	15.1 —

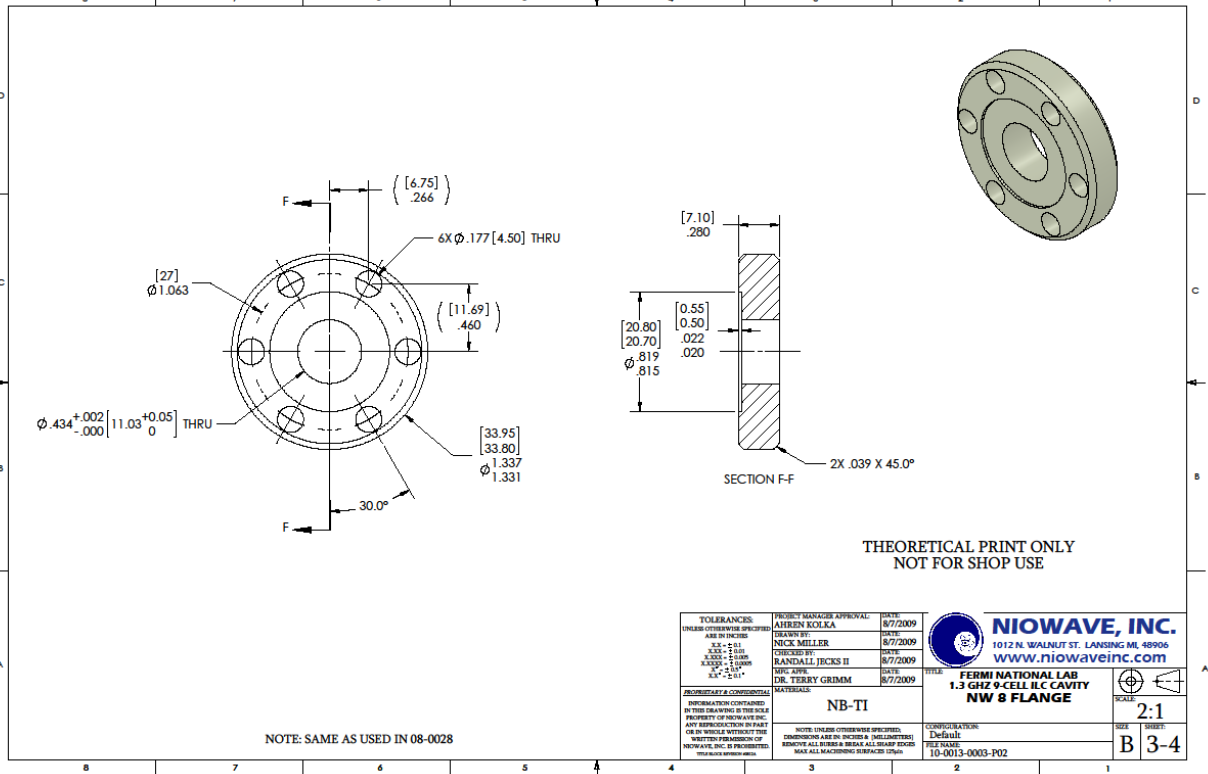
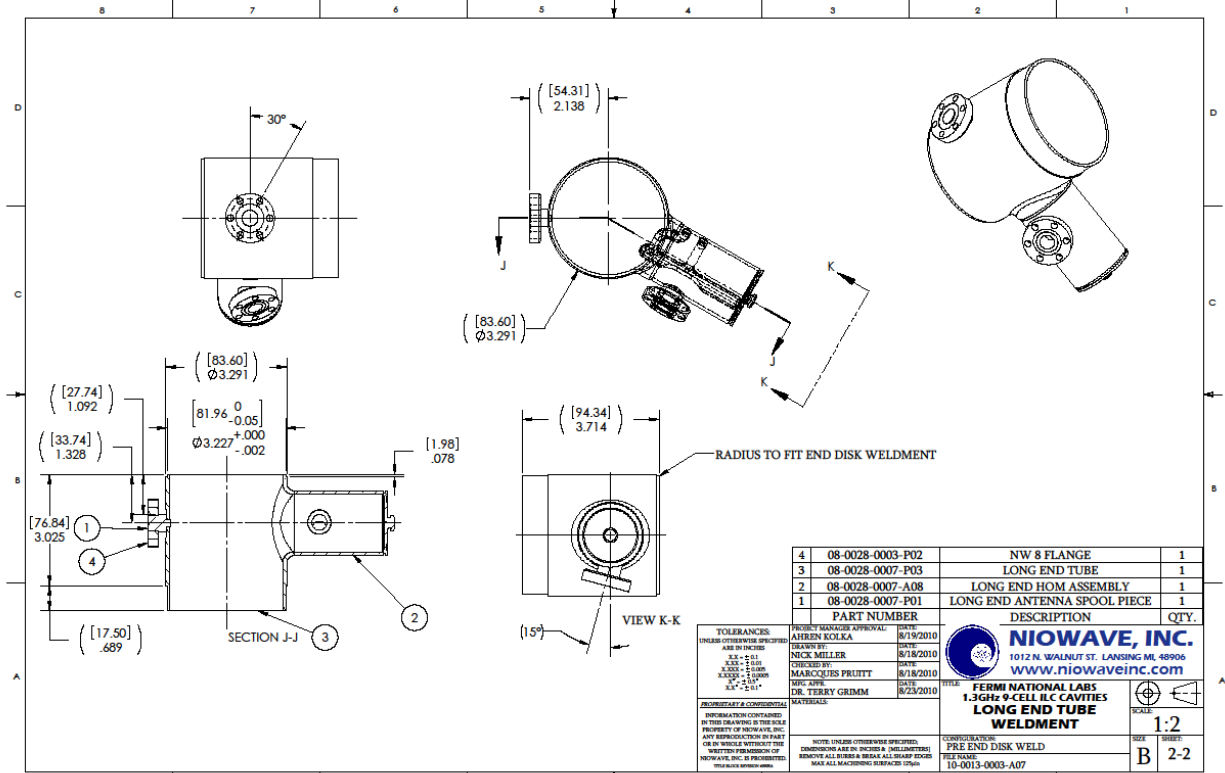
Table 1 ILC 1.3 GHz 9-cell cavity parameters [1,2]

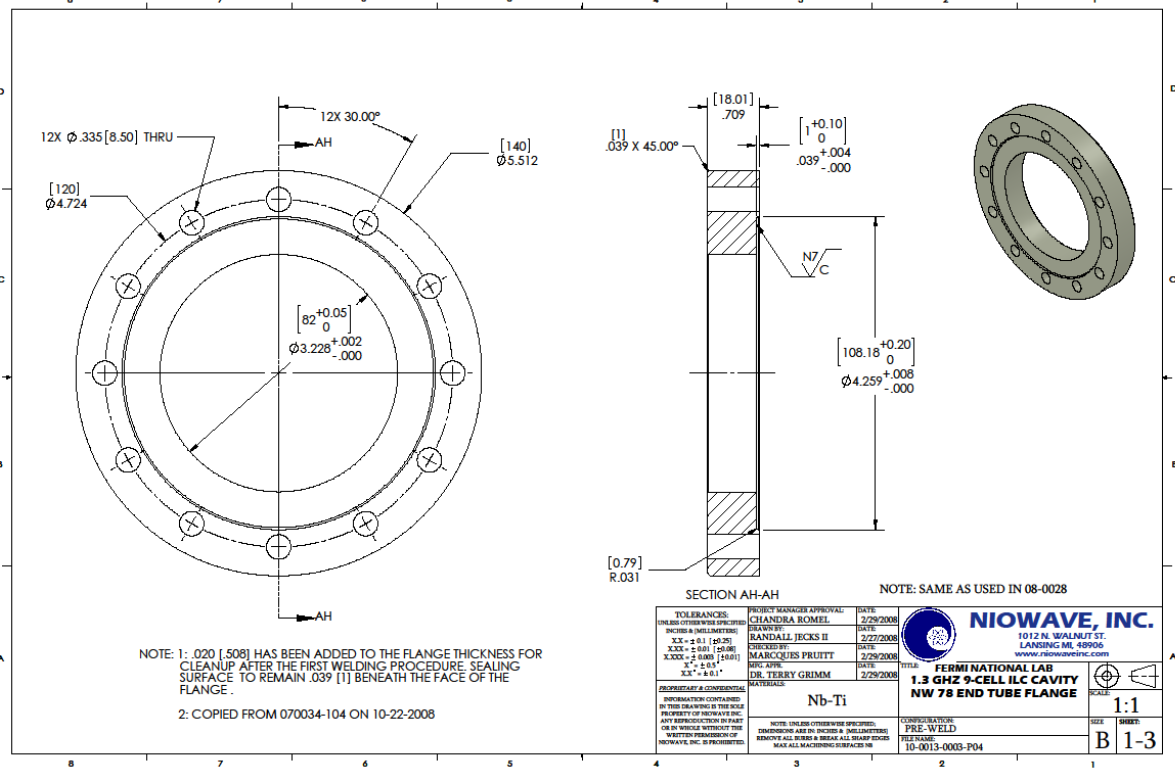
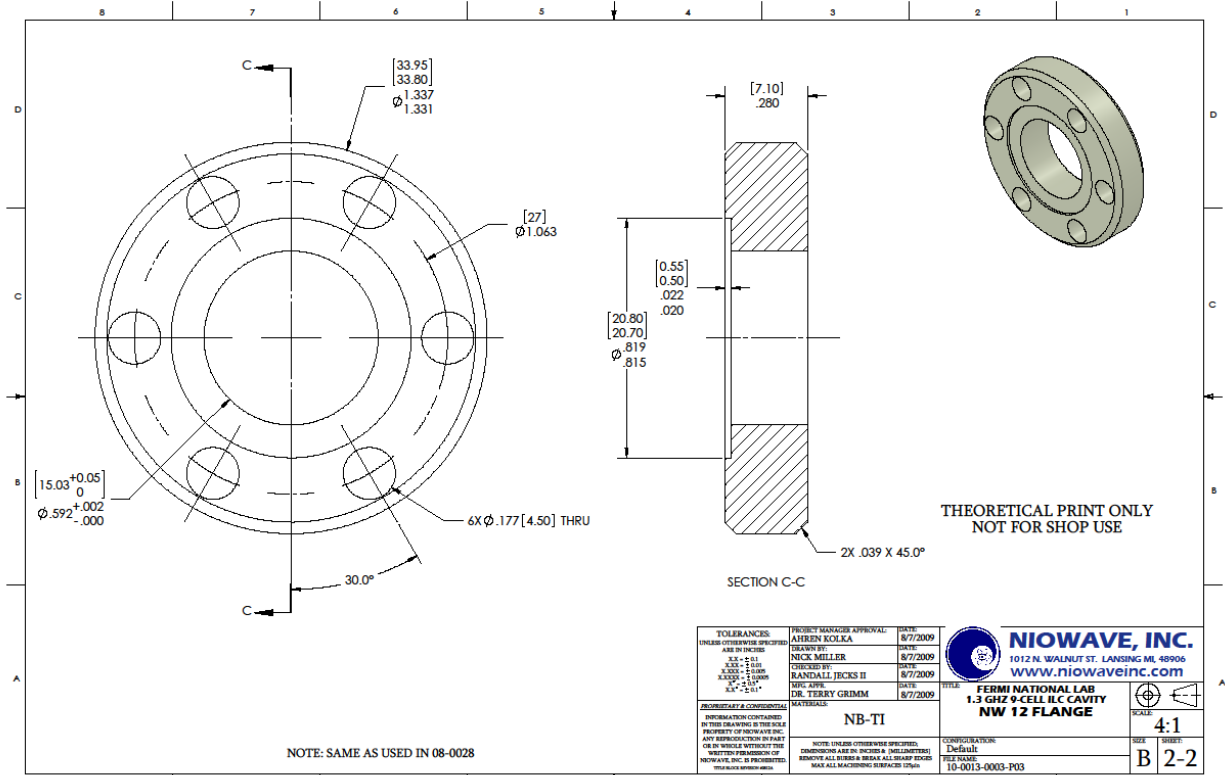
b. Mechanical Design

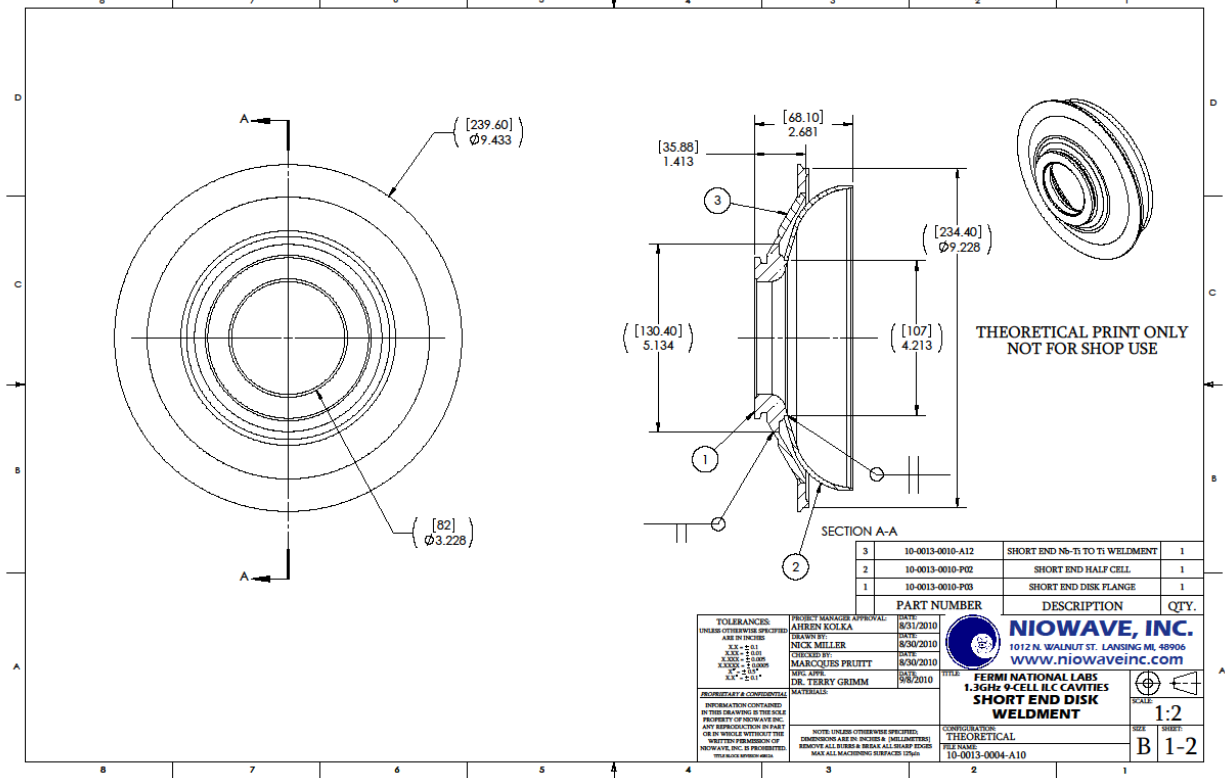
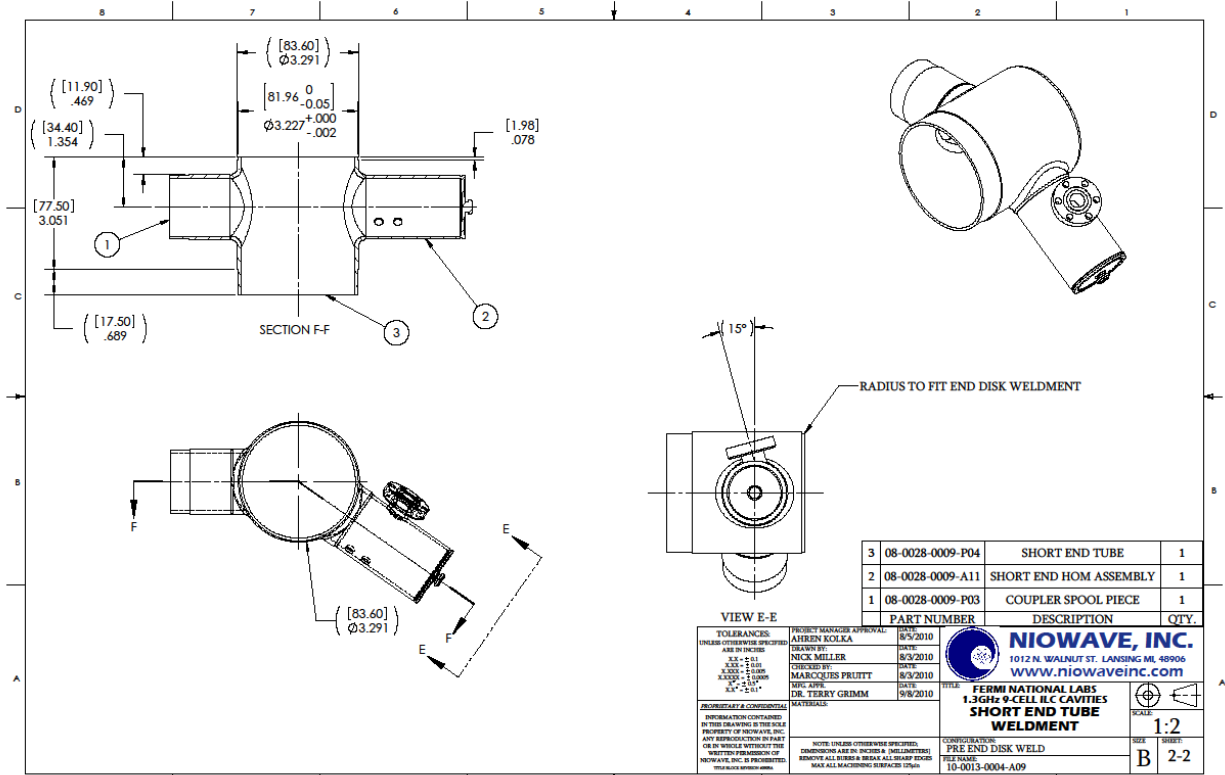


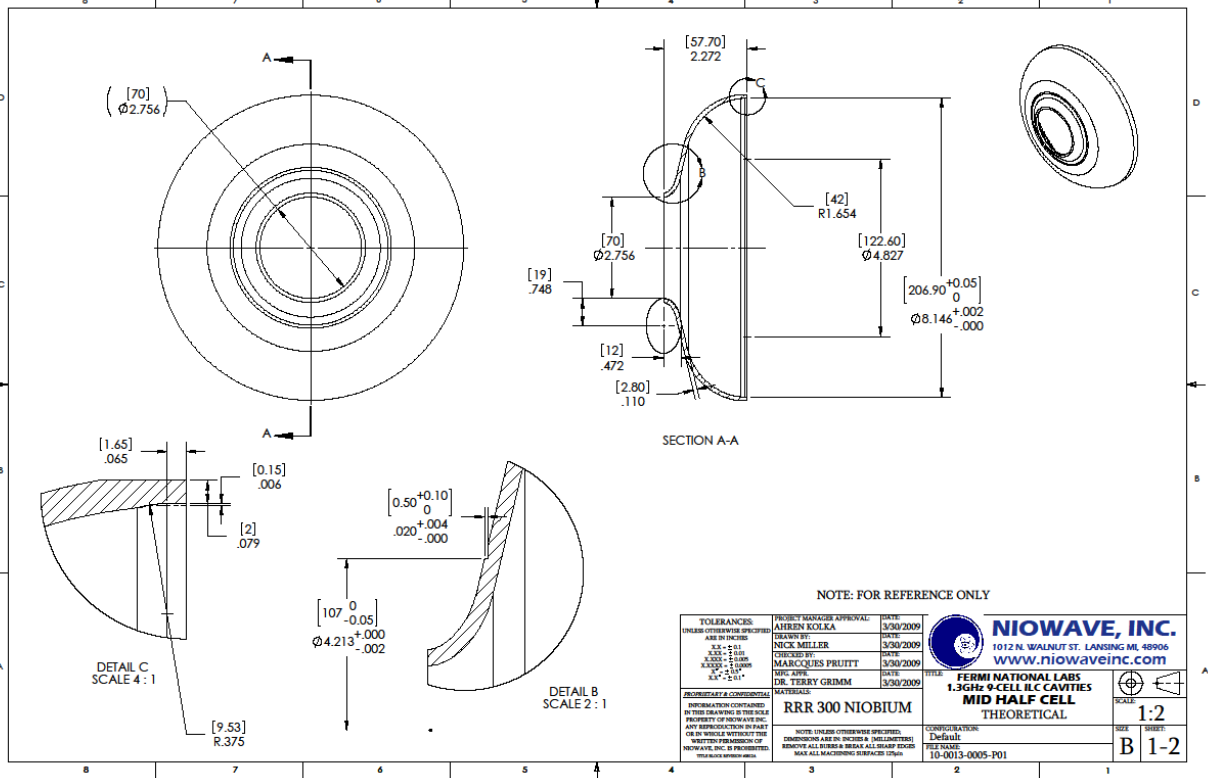
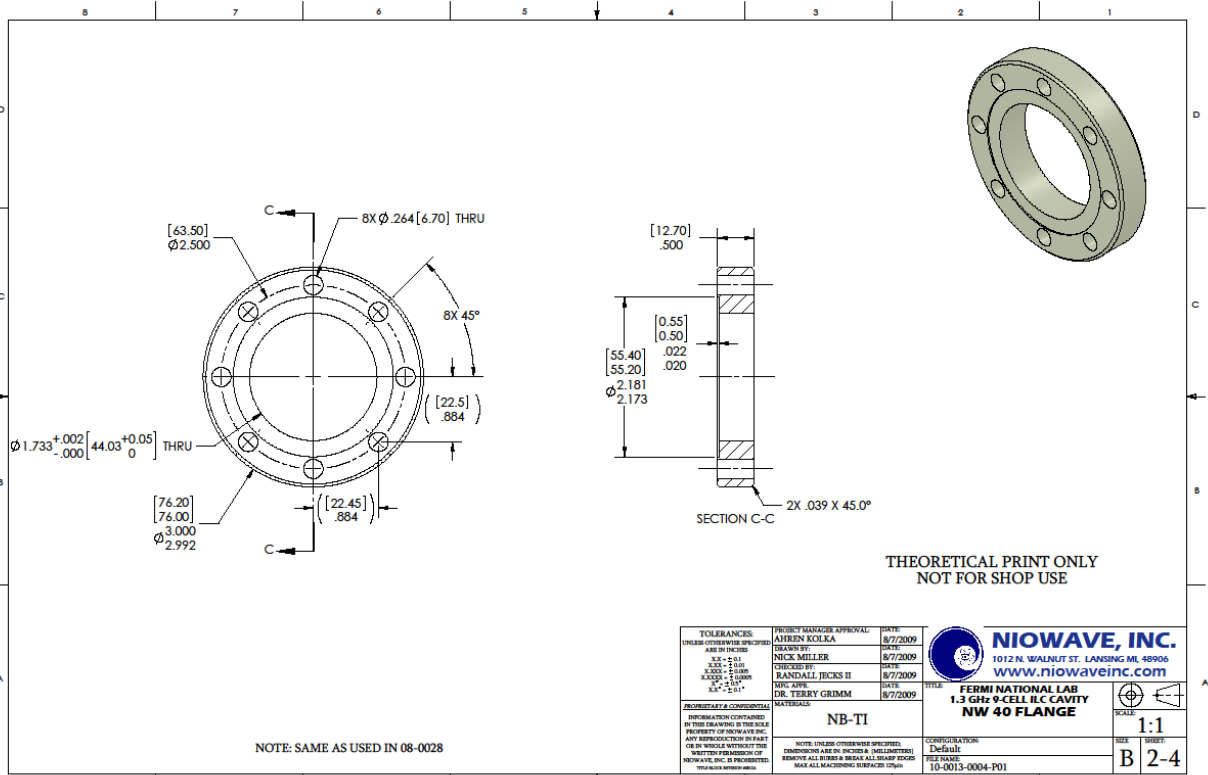


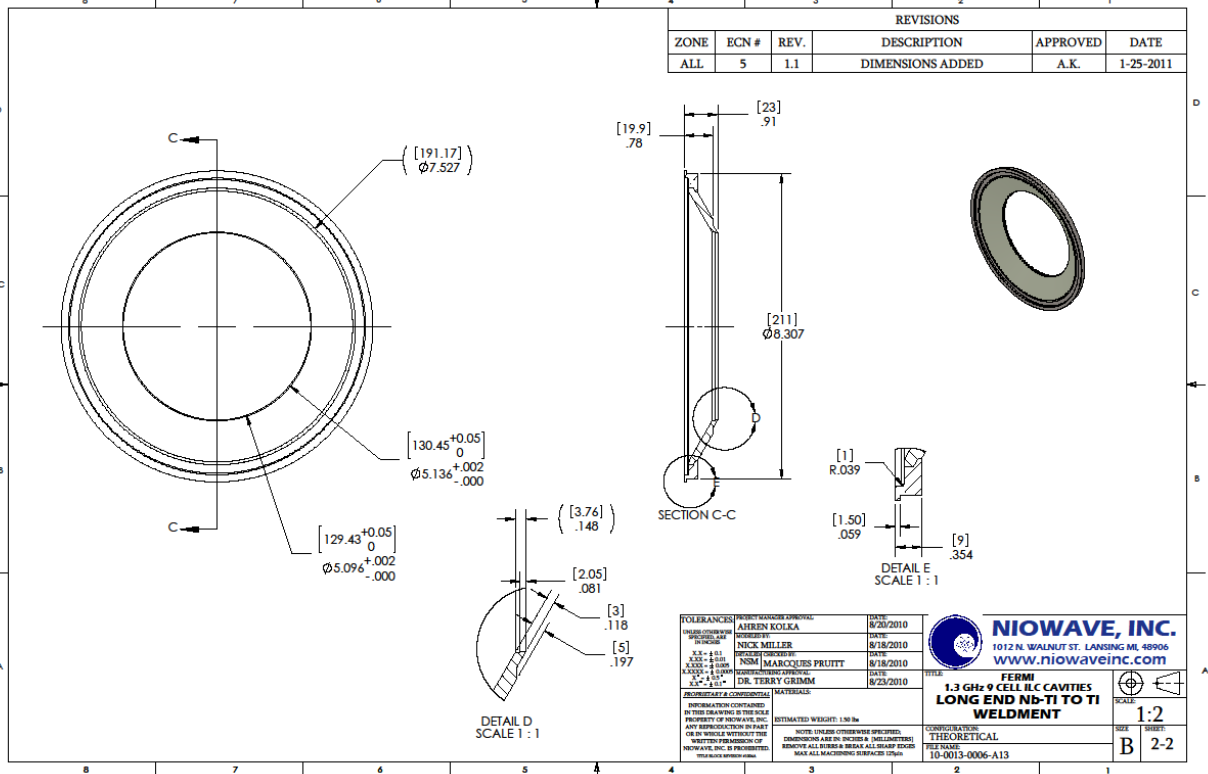
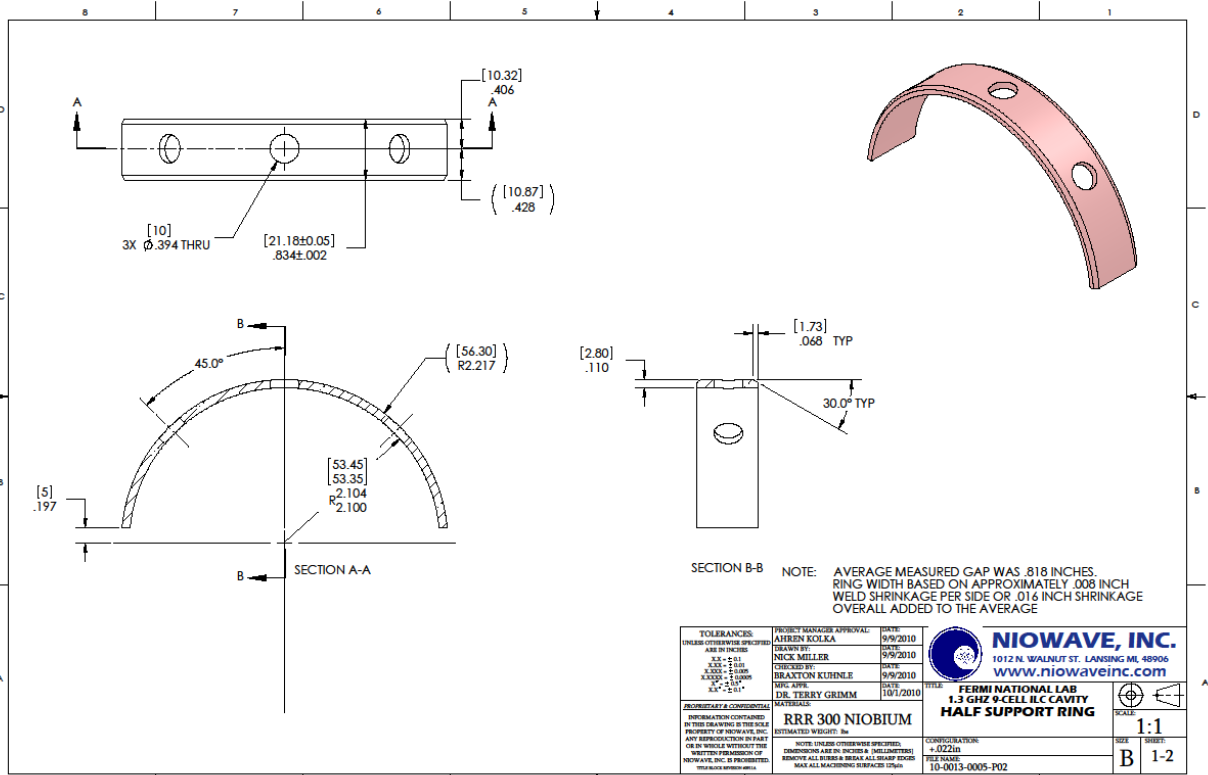


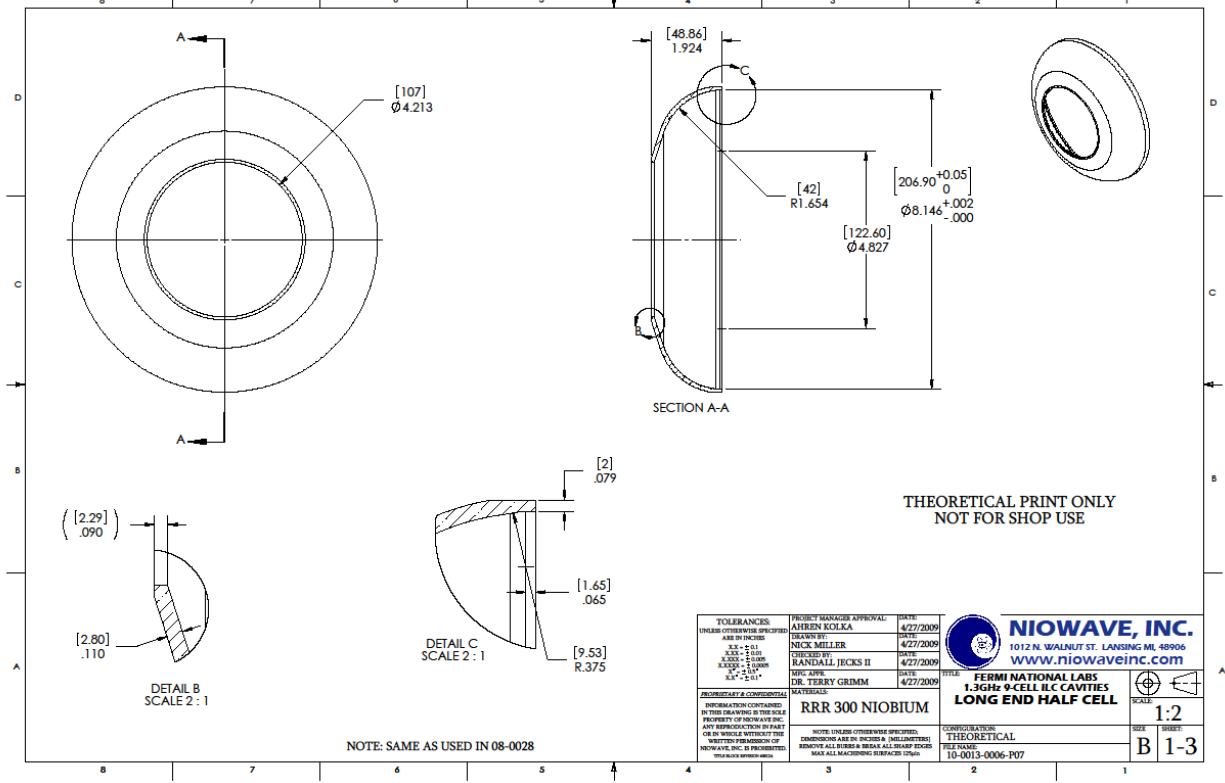
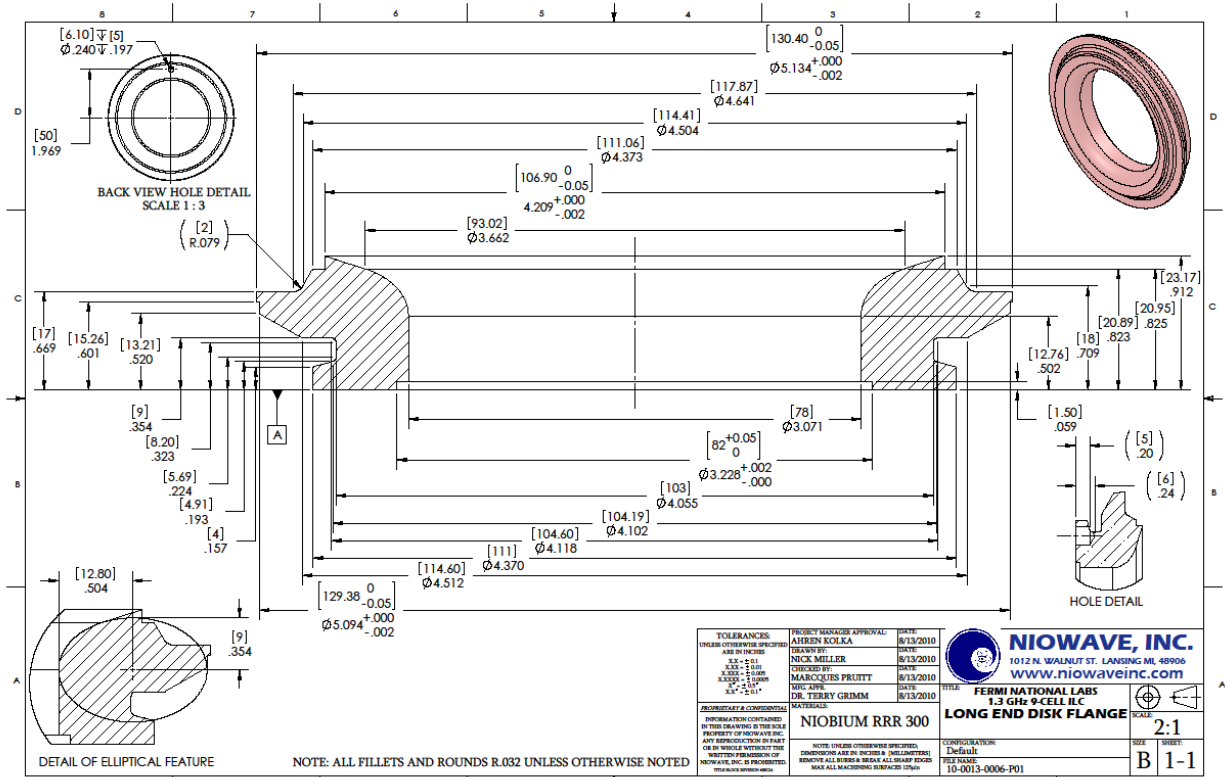


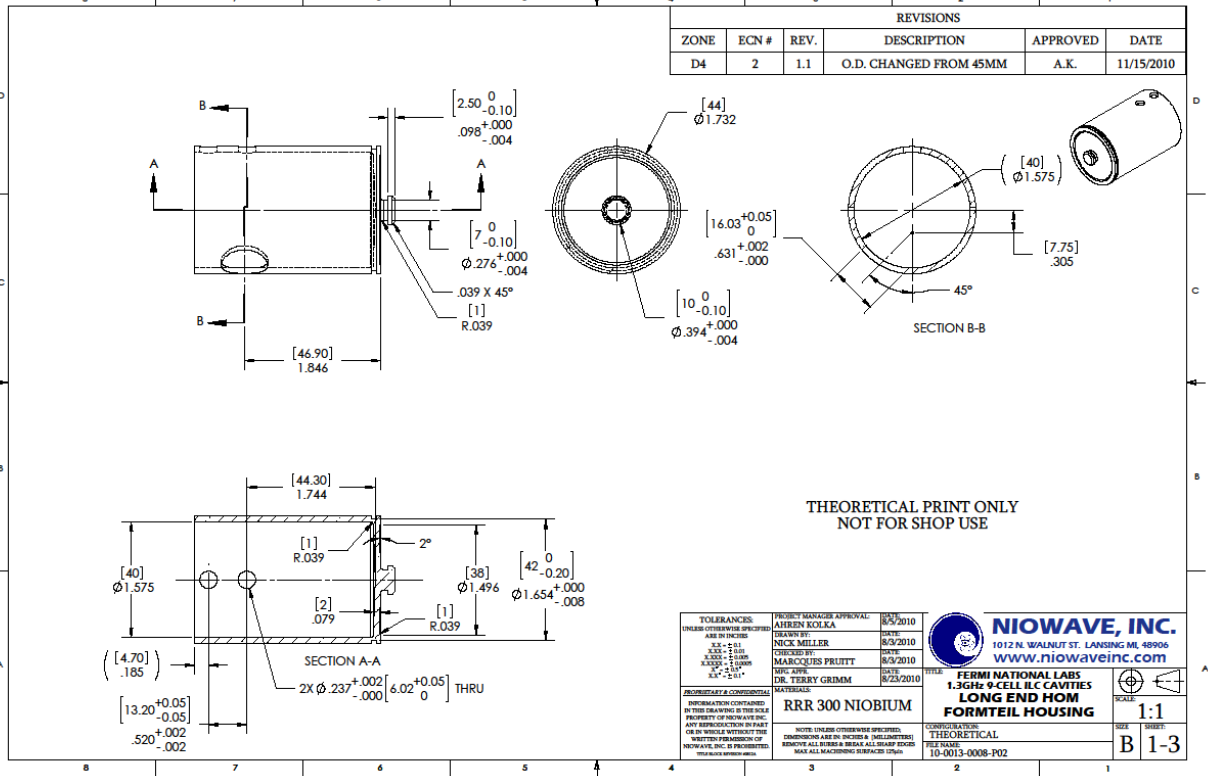
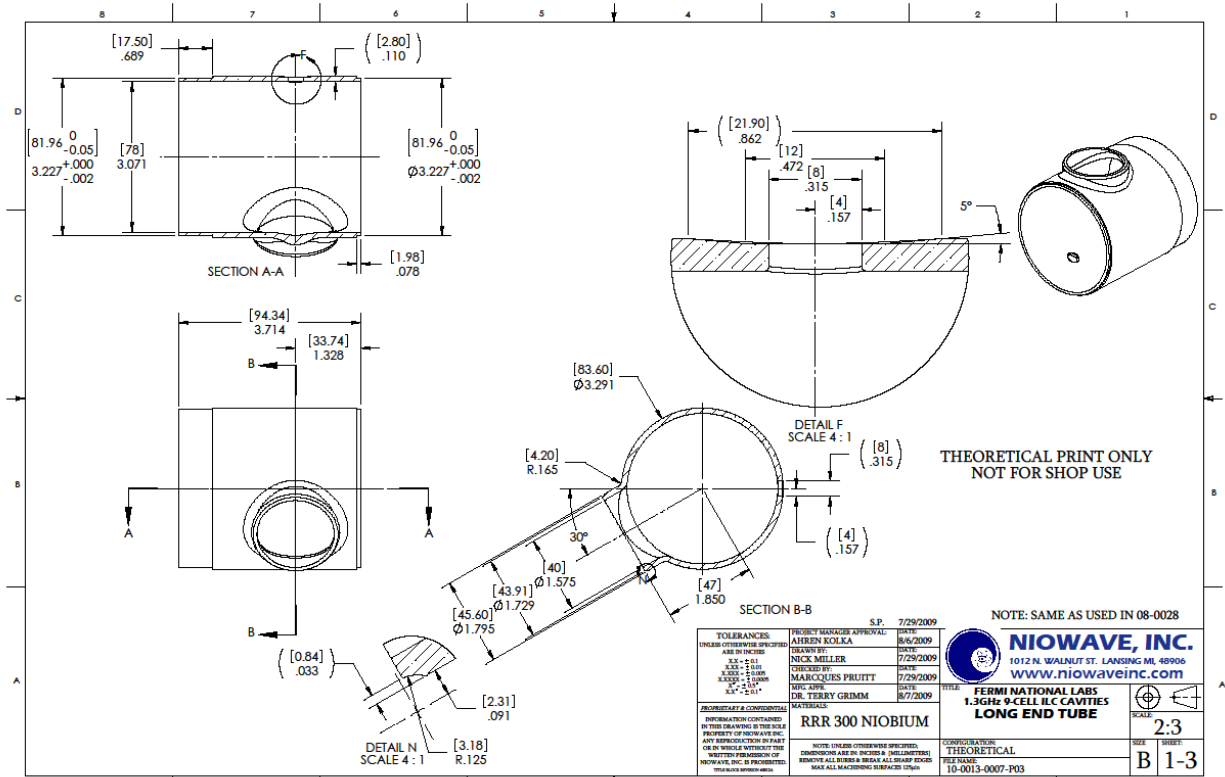


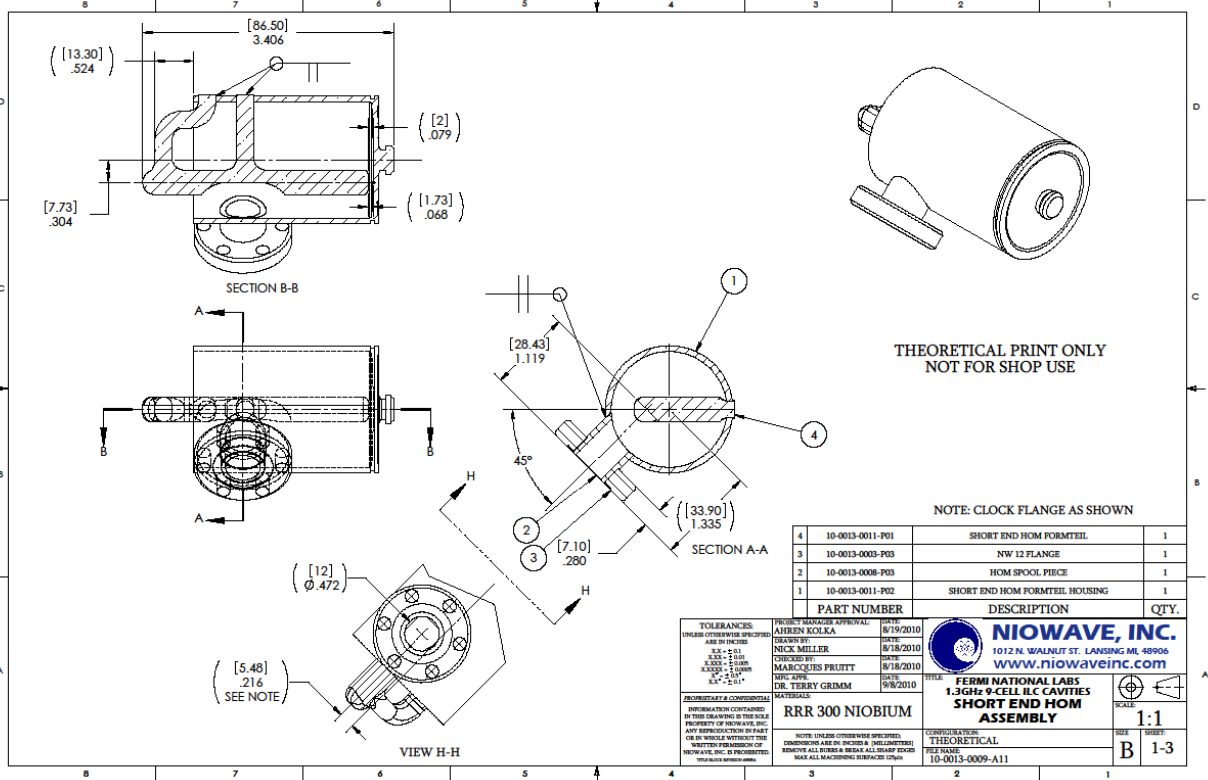
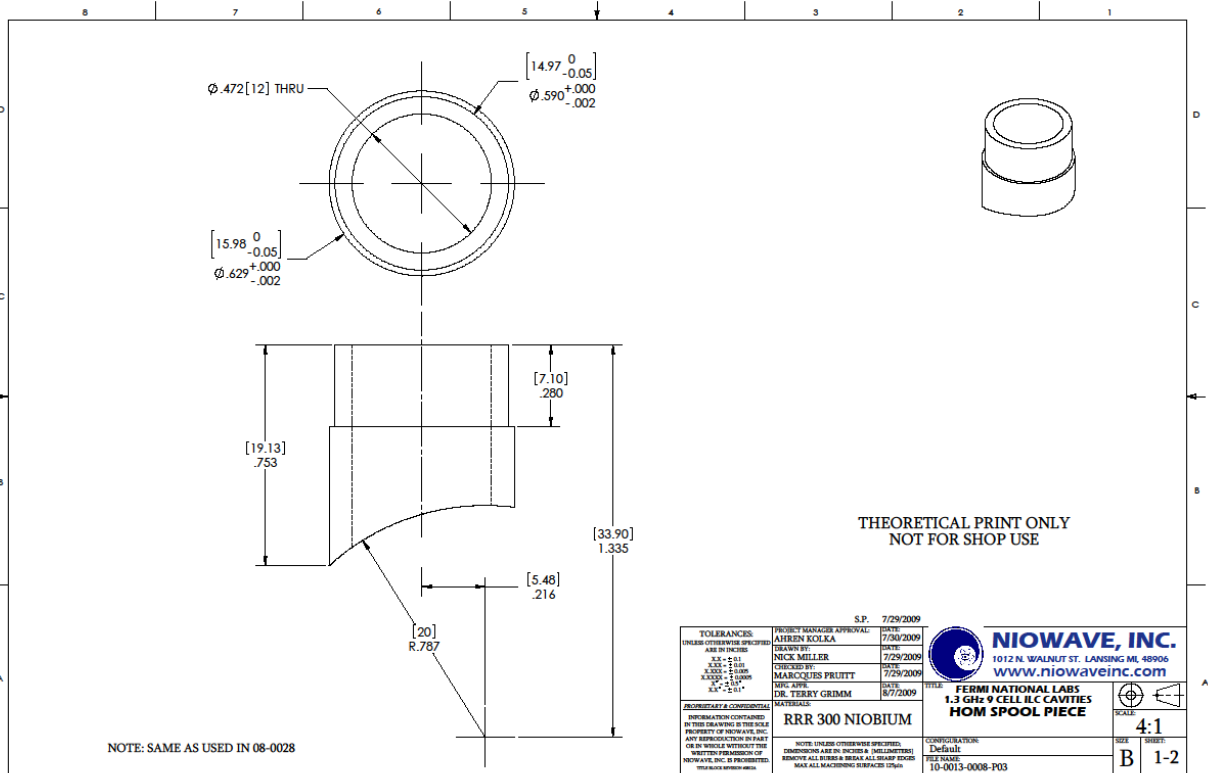


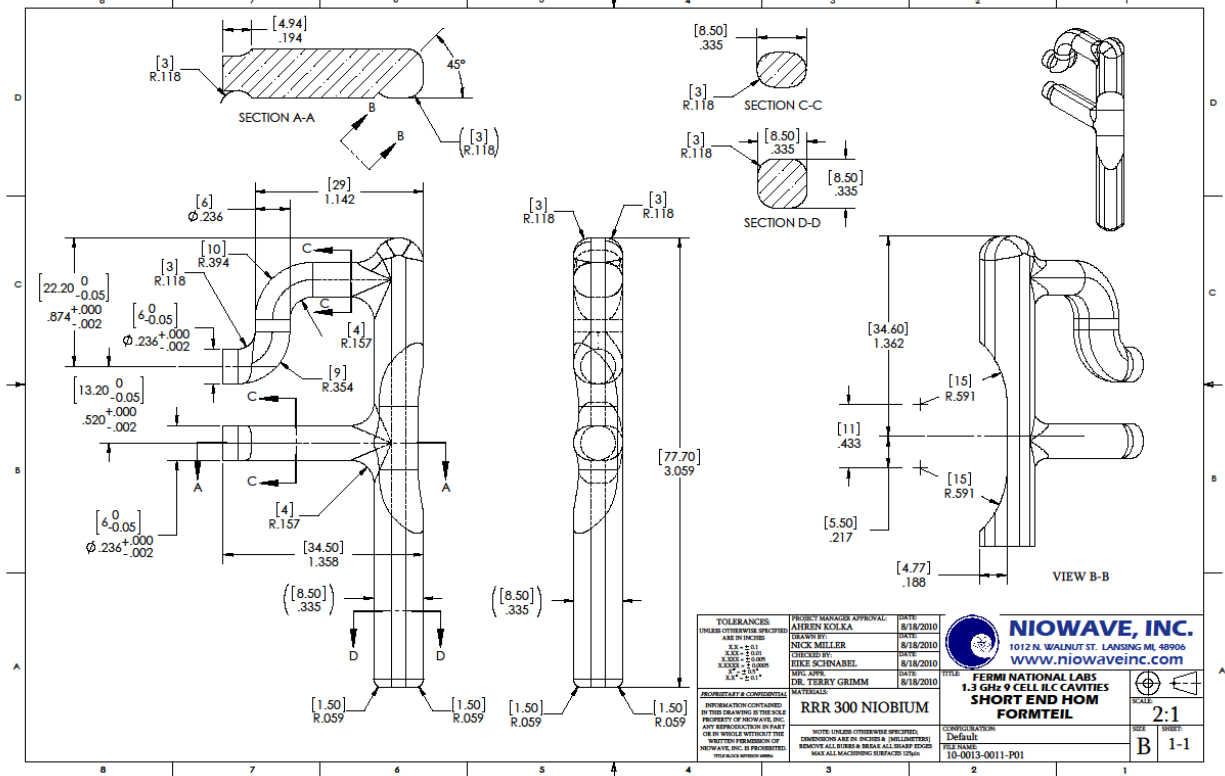
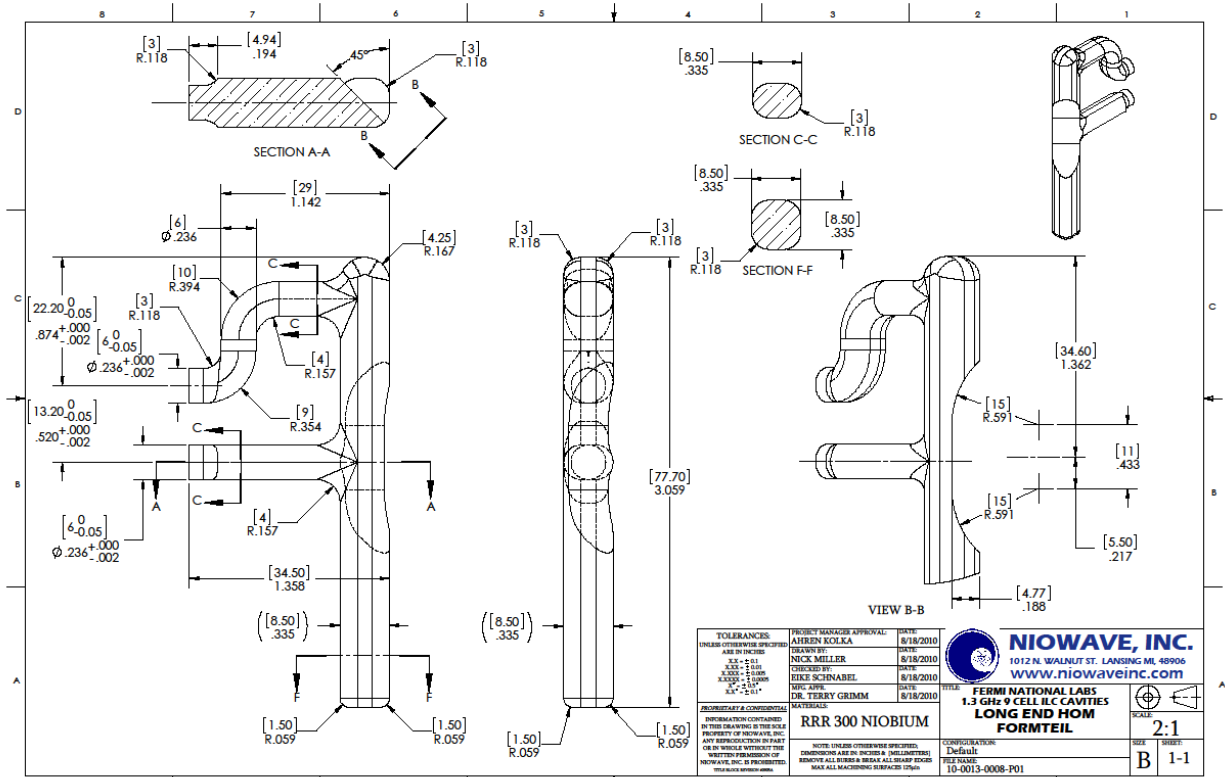


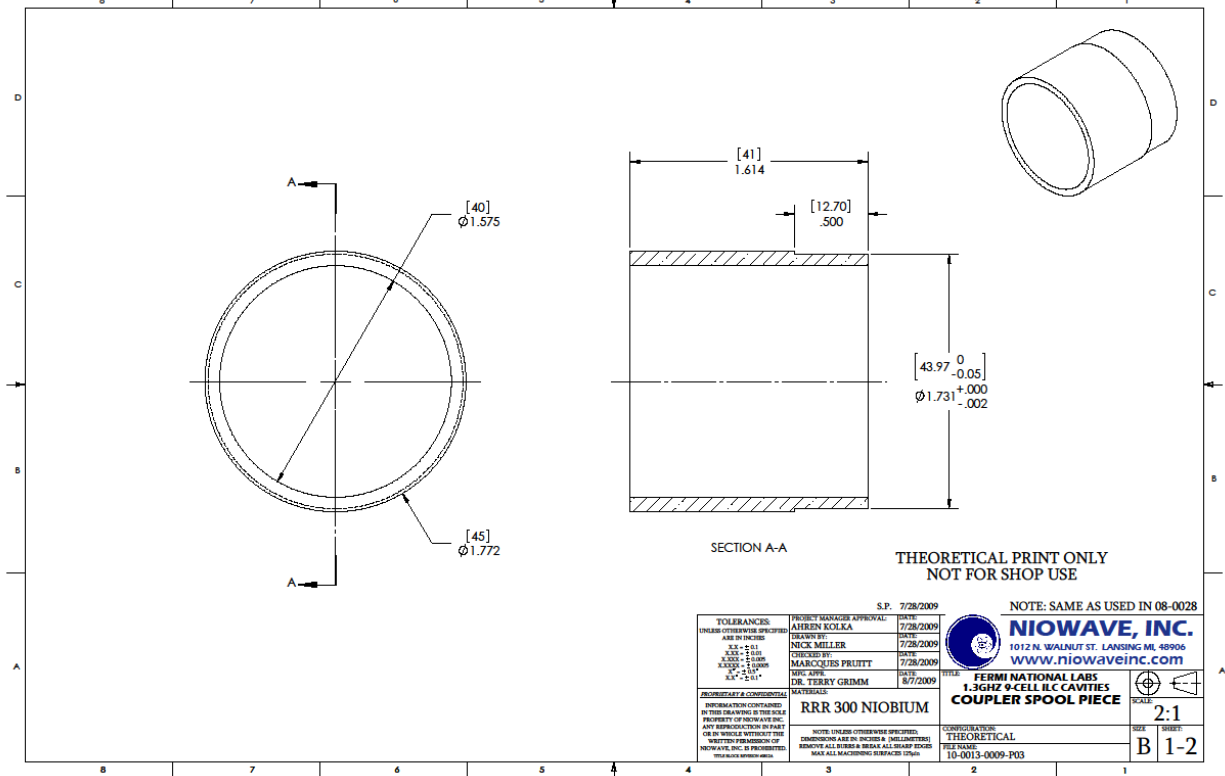
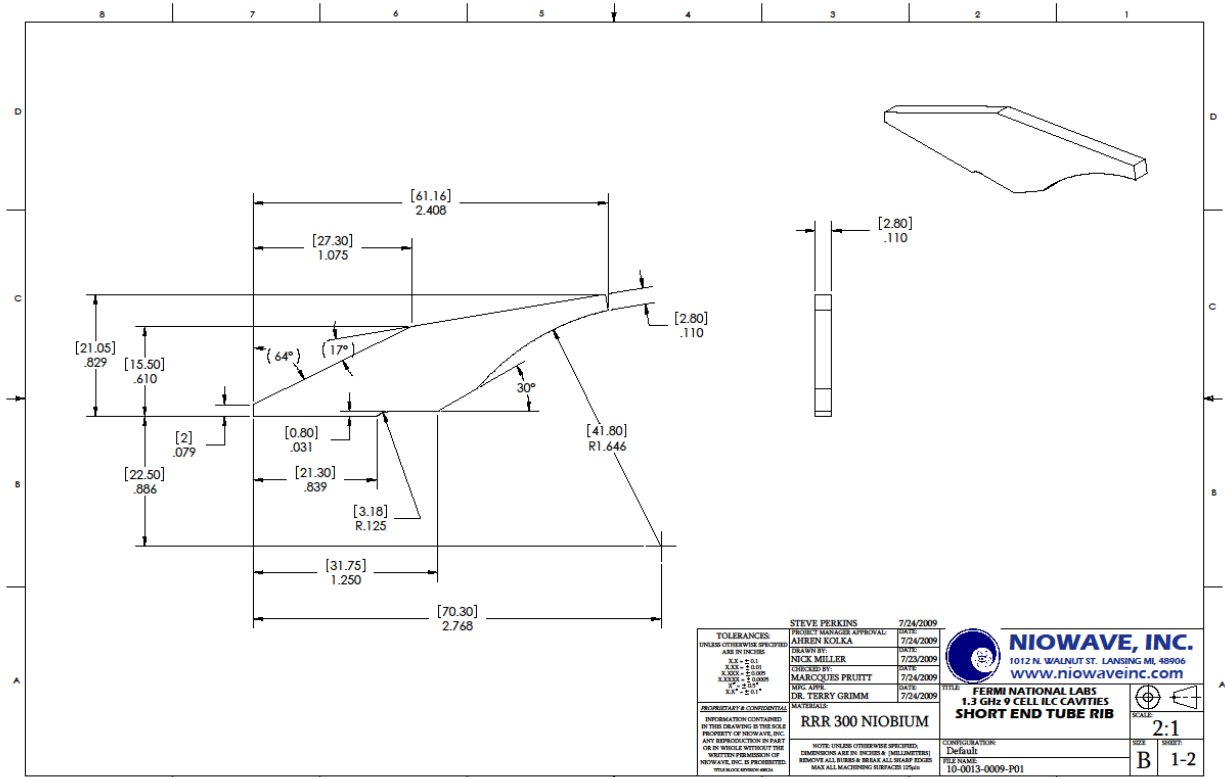


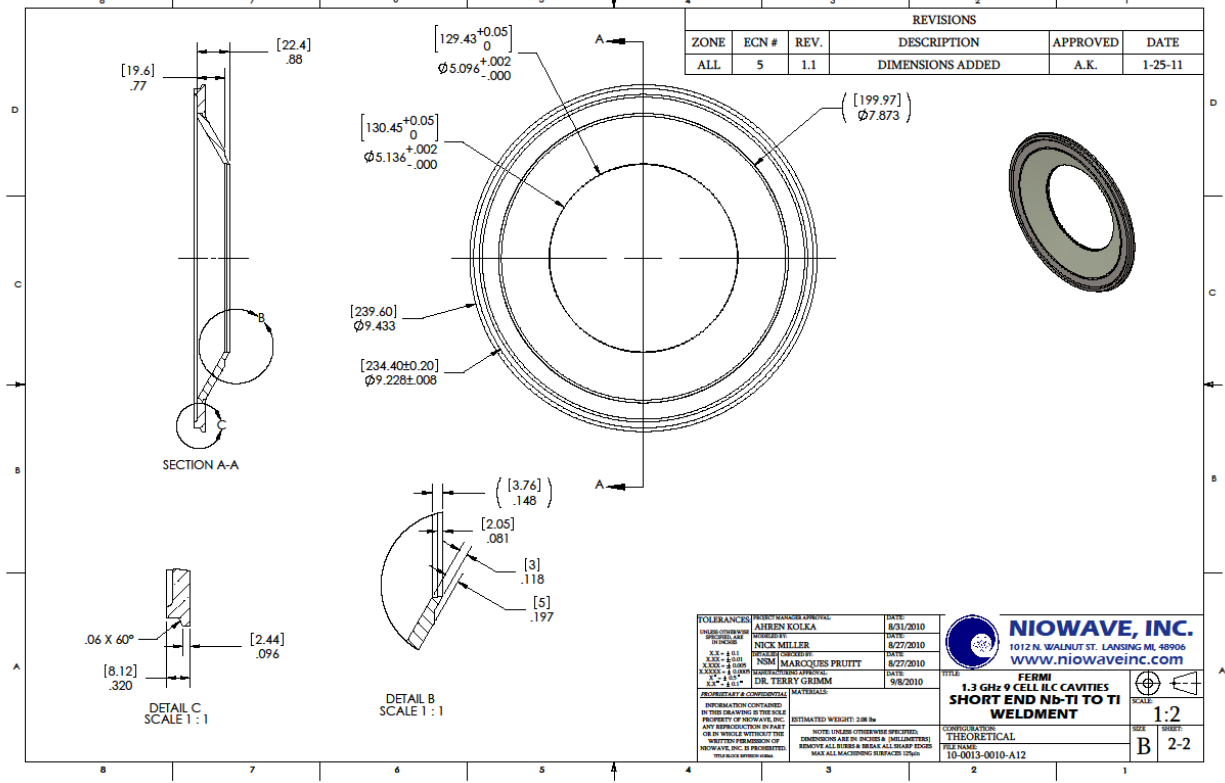
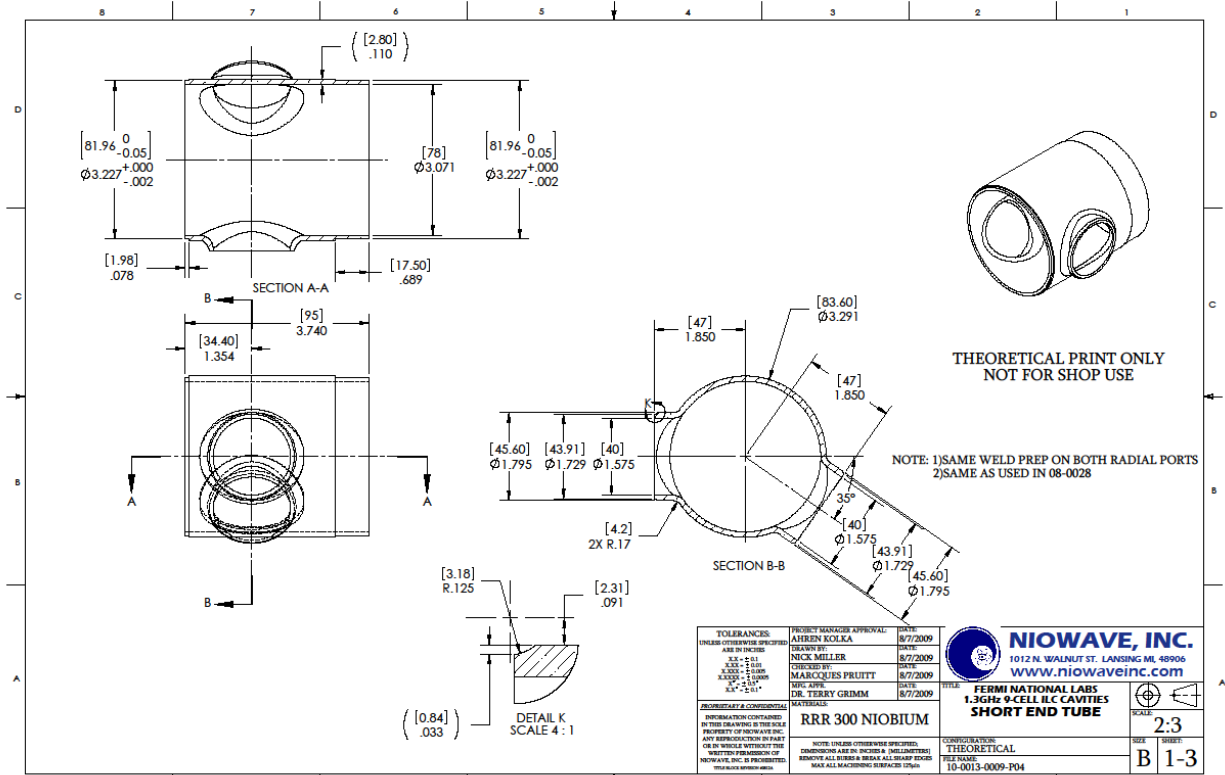


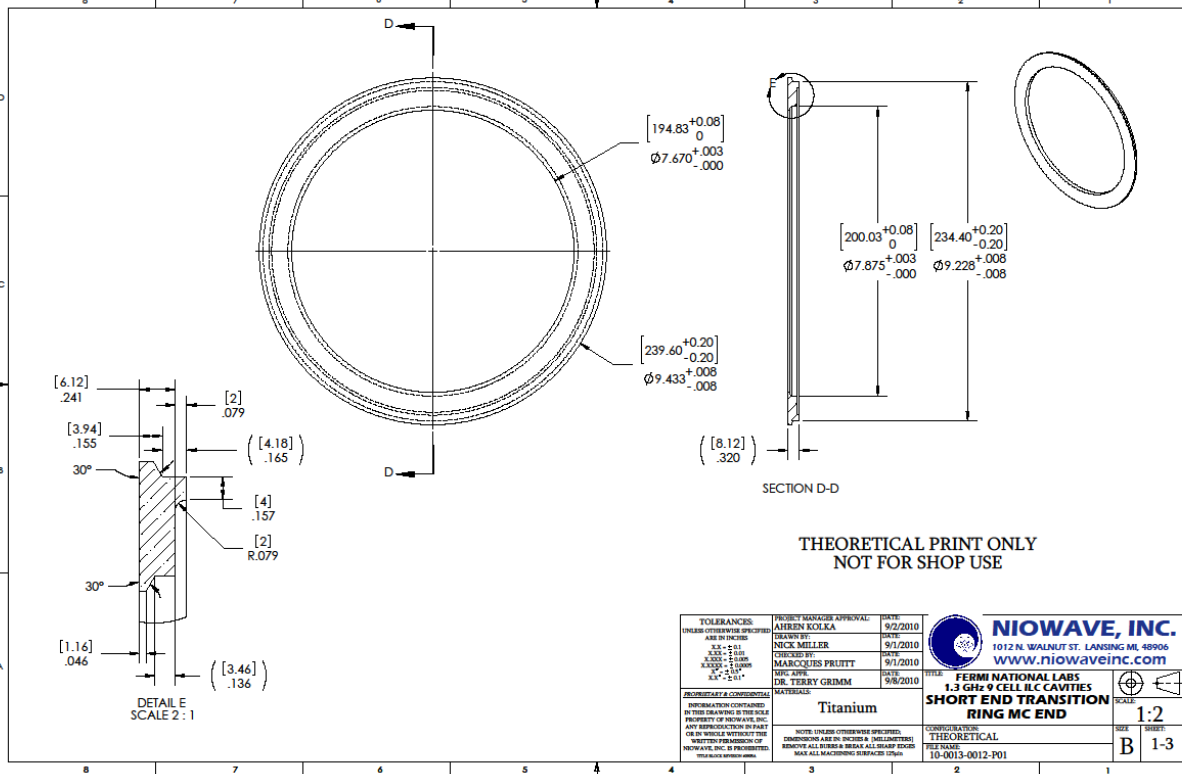
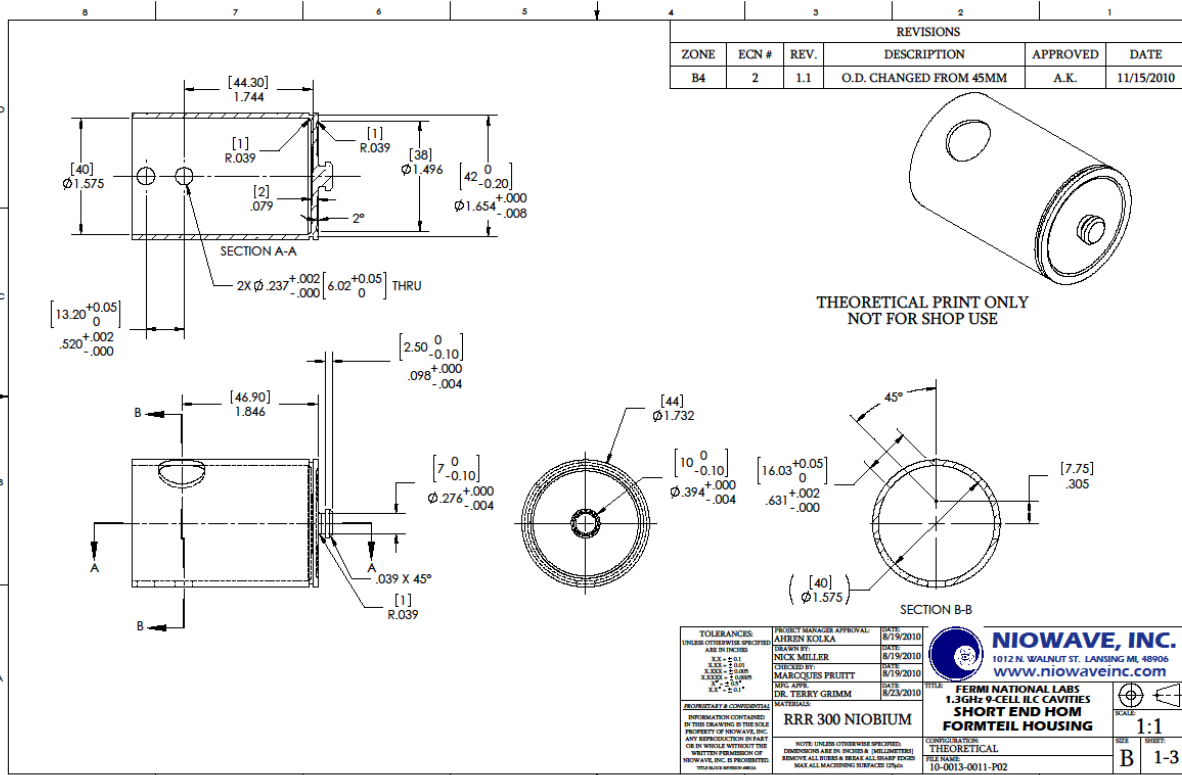


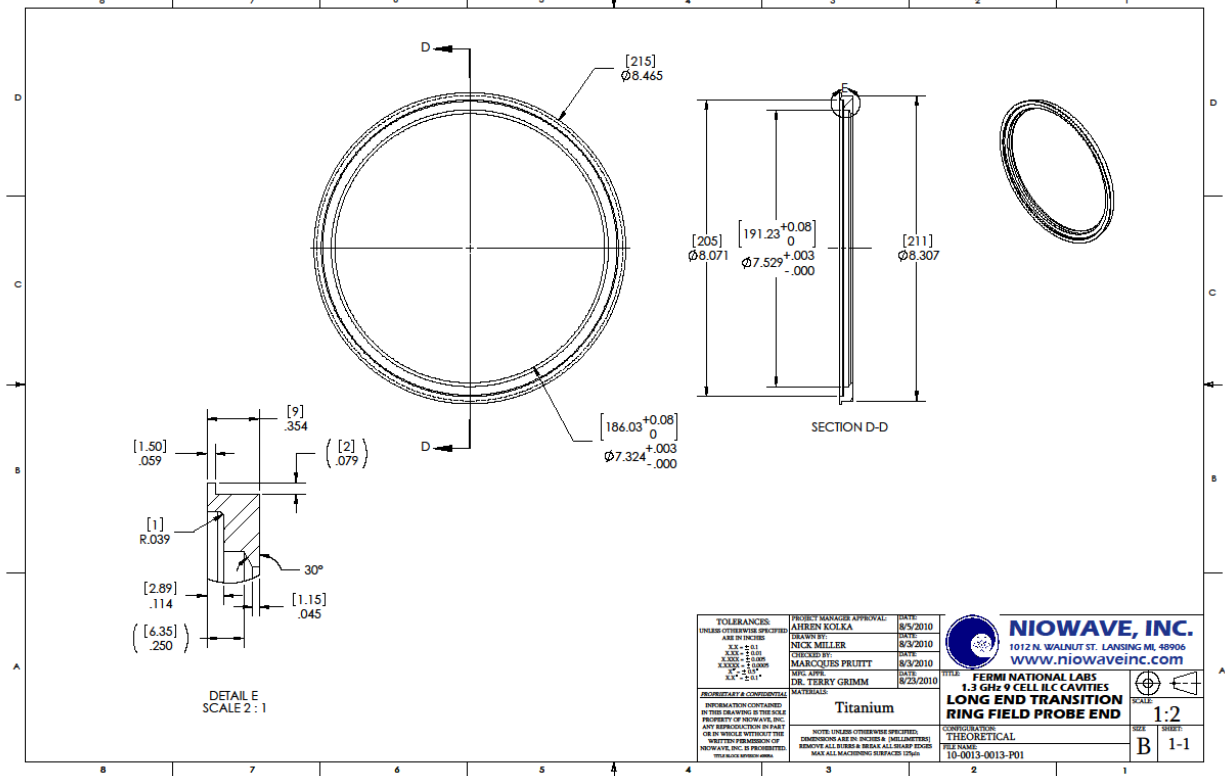
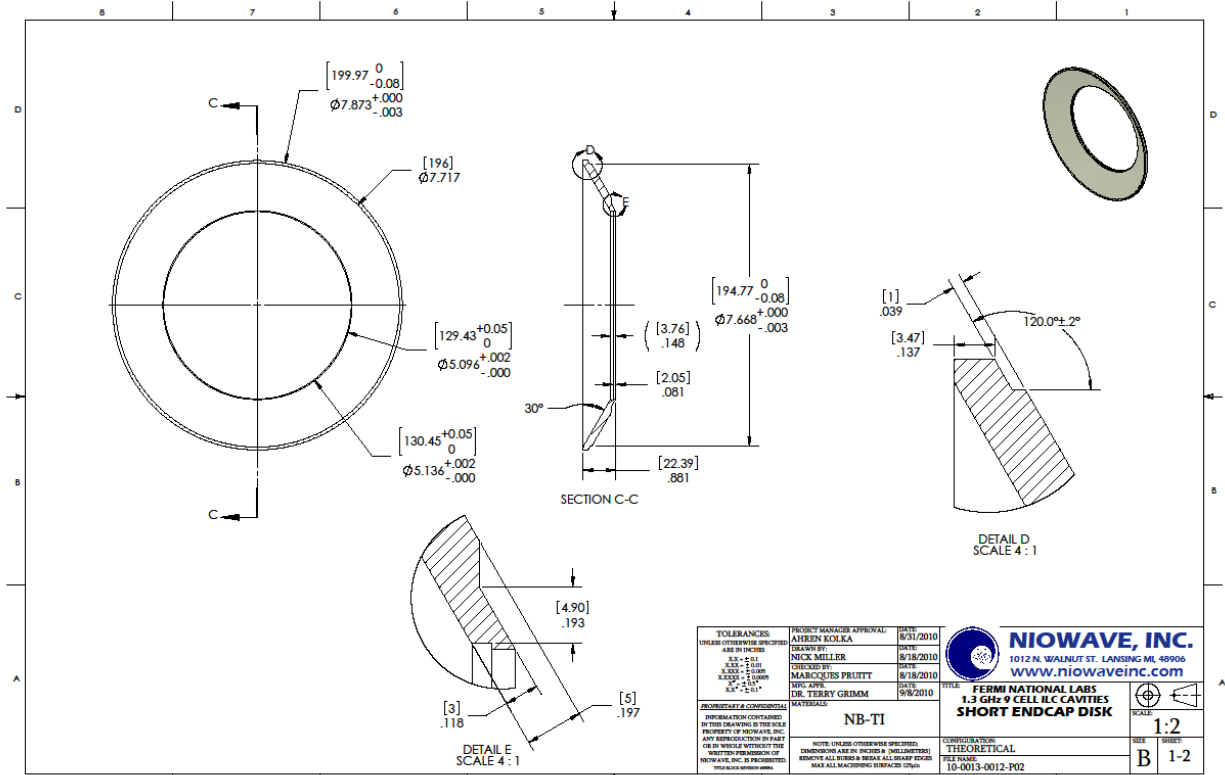


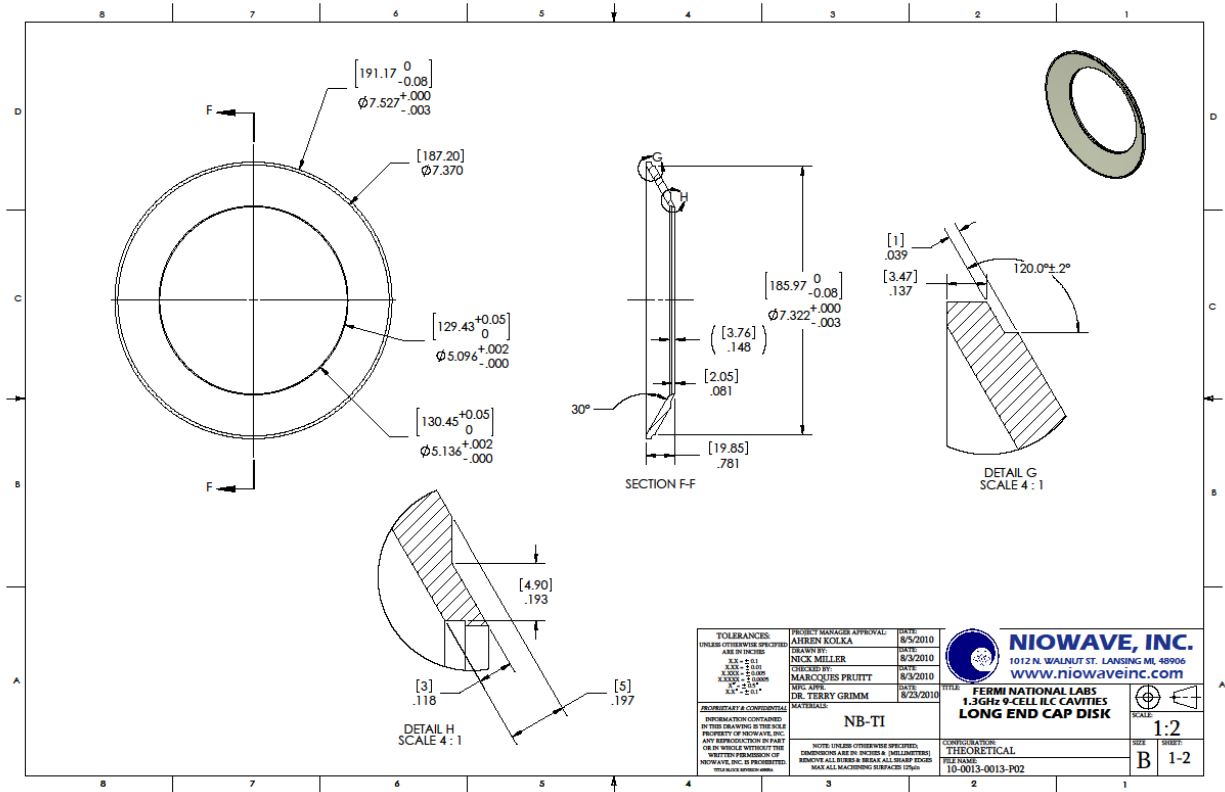












2. Fabrication

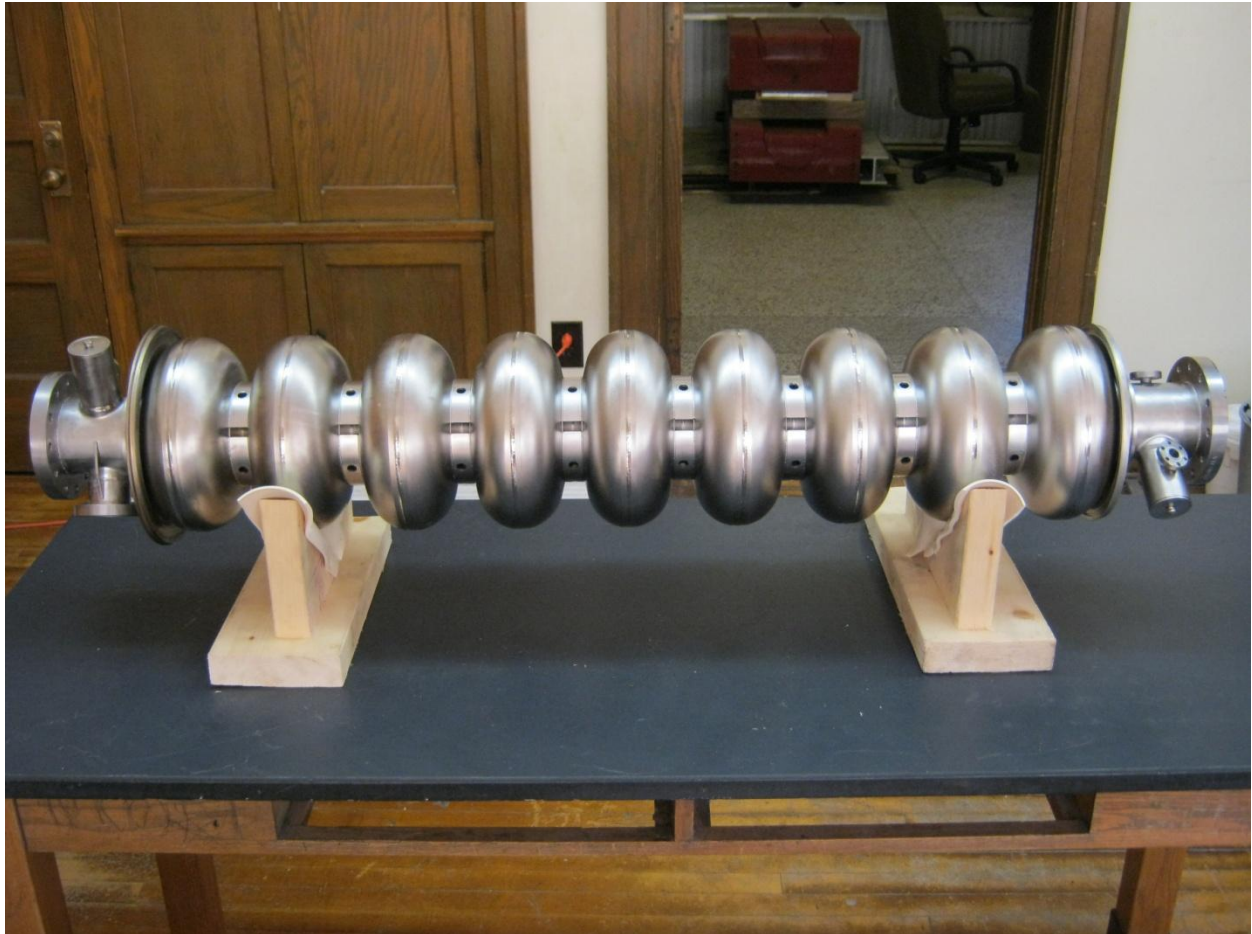


Figure 2.1 Completed 1.3 GHz ILC 9-cell

b. RF Measurements

Tuning stock is left on each dumbbell so that the frequency of each cell can be precisely matched. This is necessary because the flatness of the field from cell to cell depends on the resonant frequency of each cell. The Niowave tuning setup includes a set of six tuning plates which simulate trimming of the dumbbells by adjusting the location of the electric short at the dumbbell ends (equators). An example of a dumbbell in one of the check fixtures is shown in Figure 2.2.

To check how well this tuning has been performed, a bead pull of each manufactured cavity is performed after welding. In this procedure a small metal bead moves on a string through each of the cavity's 9 cells. The strength of the frequency perturbation of the pi-mode as the bead moves through each cell corresponds to the magnitude of the field in that cell. A photograph of the bead pull setup is shown in Figure 1. The most effective cavity is one where the fields are equal in each cell so that maximum fields can be achieved uniformly through the structure.

For the most recent set of manufactured cavities (TB9NR007 – TB9NR016), the cavity frequencies were measured after welding, field flatness was measured by the bead pull technique for each cavity, and both HOM cup notch filter frequencies (in the short and long end assemblies) were checked. The results for the group and details for cavity TB9NR016 are presented here.



Figure 2.2 Dumbbell frequency measurement setup.

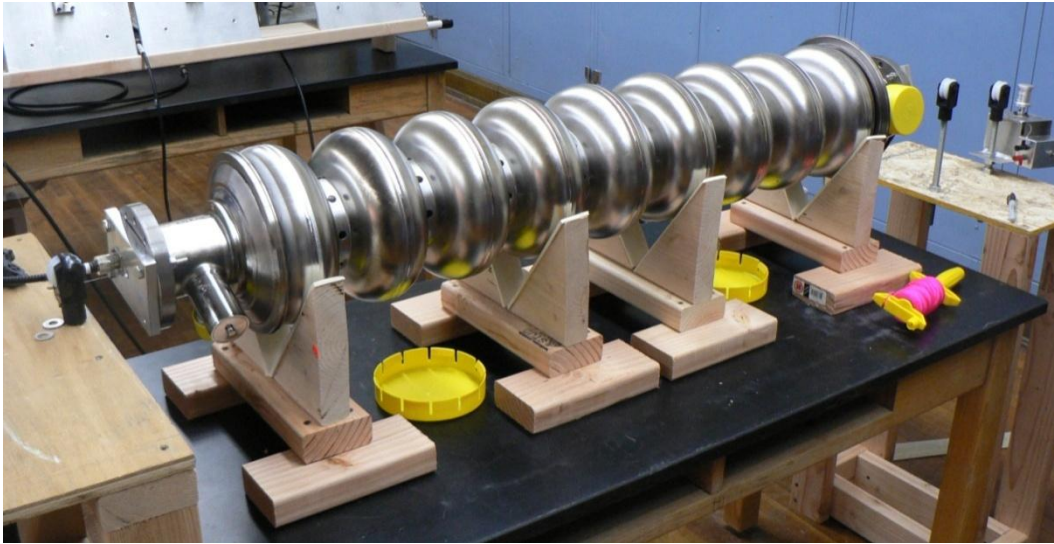


Figure 1.3 Bead pull testing setup for welded 9-cell cavities

The target frequency for the just-welded 9-cell cavities at room temperature and pressure is 1298.6 MHz. Chemical polishing reduces the frequency 1.0-1.5 MHz, pumping down to vacuum increases the frequency about 0.4 MHz, and shrinkage on cooldown increases the frequency by 1.9 MHz. The net result of these operations leaves the cavity at 1299.7 MHz, and the tuner is used to reach the operating frequency of 1300 MHz. This set of eight cavities has an average frequency of 1299.4 MHz, somewhat higher than the warm target – the distribution of frequencies is shown in Figure . The standard deviation of the eight frequencies is 0.1 MHz – the good reproducibility will allow the tuning processes to be adjusted to bring the mean closer to the target.

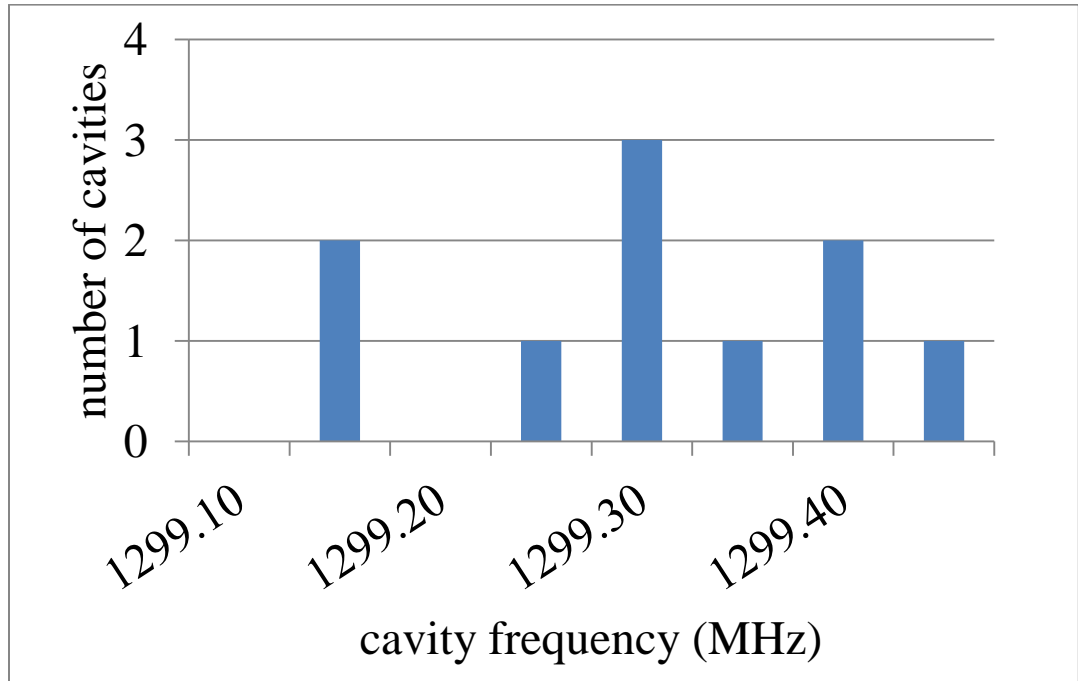


Figure 2.4 Distribution of frequencies of ten just-welded cavities.

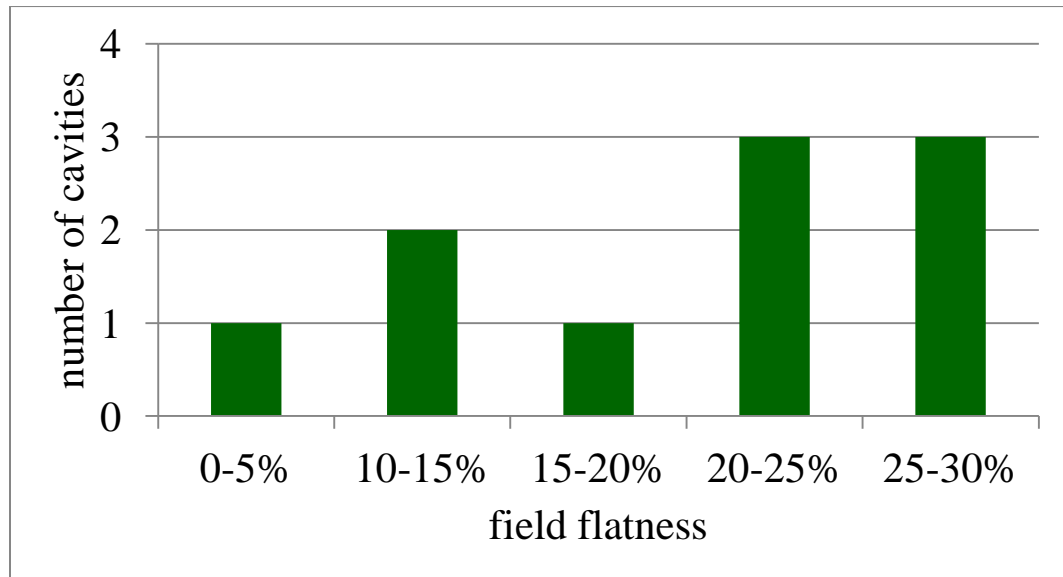


Figure 2.5 Distribution of field flatness for the ten just-welded cavities as measured by bead pulls.

As discussed, the field distribution in the 9 cells of the cavity is measured by the bead pull technique. The field flatness is then calculated according to

$$\left(\sqrt{\frac{\Delta\phi_{\max}}{\Delta\phi_{\min}}} - 1 \right) \times 100\%$$

The distribution of results for the field flatness is shown in Figure 2.5. All eight of the recently manufactured cavities have a field flatness of 30% or less. The bead pull data for cavity TBN9NR016 is shown in Figure 2.6.

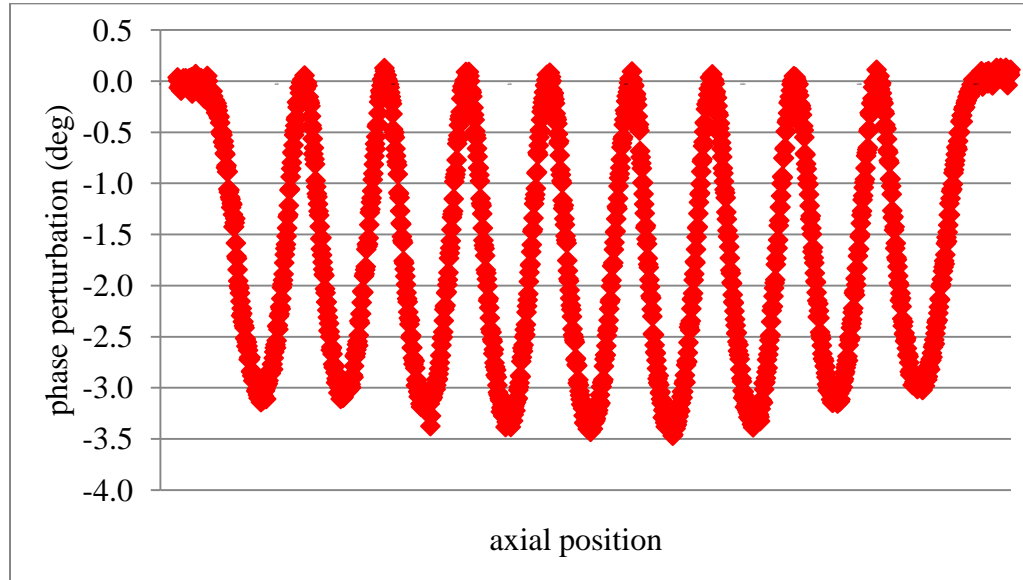


Figure 2.6 Bead pull data for 9-cell cavity TB9NR016 showing the perturbation of phase as the bead moves through the cavity.

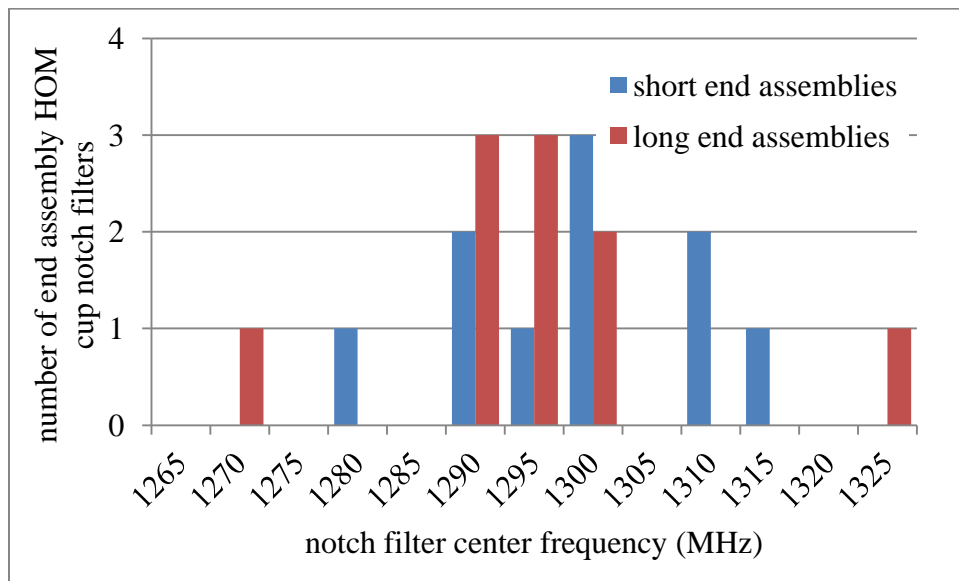


Figure 2.7 Distribution of HOM cup notch filter center frequencies.

The center frequencies of the HOM cup notch filters has also been checked for each of the cavities. To properly reject the fundamental mode, this frequency should be 1300 MHz – the width of the notch allows a window of ± 30 MHz to be considered

acceptable. All 20 of the HOM cup notch filters on these 10 cavities meet the specification as shown in Figure 2.7. An example of the data for a notch filter is given in figure 2.8.

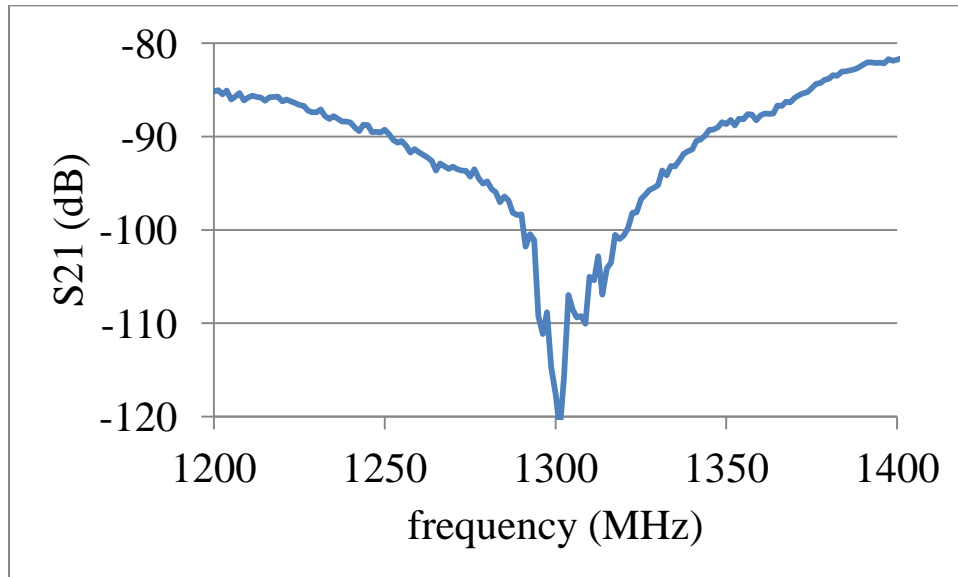


Figure 2.8 Transmitted power plot from the network analyzer characterizing the HOM cup notch filter on short end assembly 1S, part of cavity TB9NR007.

c. Mechanical Assembly

i. Cavity Components

Part/Assm.	Tracking #	Material Vendor	Lot #	Internal #
Long End Half Cell	P7-4-5	Plansee	90512418	P7
Long End Disk Flange (Trans. Ring)	L10	Heraeus	3199/S103183	H8
Long Endcap Disk (NbTi)	12L	Ningxia	2010-4-9-368-101014	N8
Long End Ti Transition Ring (MCE)	10	Titanium Industries	232542	
Long End Beam Tube	4L	Ningxia	W2009-02-16-090323	N3
Antenna Spool	3	Heraeus	3199/S103036	H7
Antenna Port Flange (NW 8)	4	Ningxia	Nb-55TiD-2-10001	N6
Long End Beam Tube Flange (NW 78)	16	Ningxia	Nb-55TiD-2-10001	N6
Long End HOM Housing	L4	Heraeus	3192	H4
Long End HOM Spool	10	Heraeus	3199/S103036	H7
Long End Formteil	10	Ningxia	2010-4-9-368-101207	N15
Long End HOM Flange (NW 12)	13	Ningxia	Nb-55TiD-2-10001	N6
Mid-cell ID	N4-16-5	Ningxia	2010-4-9-368-100909	N4
Mid-cell ID	N4-17-1	Ningxia	2010-4-9-368-100909	N4
Mid-cell ID	N4-19-3	Ningxia	2010-4-9-368-100909	N4
Mid-cell ID	N4-24-2M	Ningxia	2010-4-9-368-101018	N4
Mid-cell ID	N4-3-9	Ningxia	2010-4-9-368-1008171	N4
Mid-cell ID	N4-3-2	Ningxia	2010-4-9-368-1008171	N4
Mid-cell ID	N4-6-1	Ningxia	2010-4-9-368-1008171	N4
Mid-cell ID	N4-1-1	Ningxia	2010-4-9-368-1008171	N4
Mid-cell ID	N4-5-7	Ningxia	2010-4-9-368-1008171	N4
Mid-cell ID	N4-1-4	Ningxia	2010-4-9-368-1008171	N4
Mid-cell ID	N4-8-7	Ningxia	2010-4-9-368-1008171	N4
Mid-cell ID	N4-9-4	Ningxia	2010-4-9-368-1008171	N4
Mid-cell ID	N4-23-9	Ningxia	2010-4-9-368-101111	N4
Mid-cell ID	N4-4-9	Ningxia	2010-4-9-368-1008171	N4
Mid-cell ID	N4-16-3	Ningxia	2010-4-9-368-100909	N4
Mid-cell ID	N4-24-6	Ningxia	2010-4-9-368-101018	N4
Short End Half Cell	P7-6-4	Plansee	90512418	P7
Short End Disk Flange (Trans. Ring)	S1	Heraeus	3199/S103183	H8
Short Endcap Disk (NbTi)	5S	Ningxia	2010-4-9-368-101014	N8
Short End Ti Transition Ring (MCE)	1	Titanium Industries	232542	
Short End Beam Tube	3S	Ningxia	W2009-02-16-090323	N3
Coupler Spool	3	Heraeus	3199/S103036	H7
Coupler Port Flange (NW 40)	2	Ningxia	Nb-55TiD-2-10001	N6
Short End Beam Tube Flange (NW 78)	25	Ningxia	Nb-55TiD-2-10001	N6
Short End HOM Housing	S12	Heraeus	3192	H4
Short End HOM Spool	17	Heraeus	3199/S103036	H7
Short End Formteil	17	Ningxia	2010-4-9-368-101207	N15
Short End HOM Flange (NW 12)	16	Ningxia	Nb-55TiD-2-10001	N6

* Material certifications are attached in appendix C

ii. Key Parameters

The interior cavity profile must be within +/- 0.2 mm of the nominal design. This profile has been verified with a check fixture for all dumbbells and end groups. This check has been logged in the process sheets contained in appendix d.

All electron beam welds were inspected after each welding operation to verify both the proper weld penetration and appearance. Leonardo Ristori (FNAL) recorded video of one of the equator welds as an example of the interior weld quality for the end groups. The remaining equator welds were inspected by an operator utilizing a manual bore scope.

Cavity length is also an important parameter to track, and it goes hand in hand with cavity frequency. As each cavity is tuned by FNAL personnel, the overall cavity length will change. The current as-welded (not yet tuned) cavity length has been recorded in the cavity inspection documentation in appendix d.

iii. Fabrication Observations

The vast majority of the cavity dimensions meet design specifications, but – as with any production project – there are a few minor observations to report on this cavity. In order to enhance the welding efficiency of the dumbbells, they were welded over multiple shifts with different weld operators and welding technicians. Unfortunately, this resulted in some small variations ($< 0.080''$ on the diameter) in the stiffening ring placement for nearly all of the dumbbells. We will be revising the tooling for stiffening ring installation to remedy this

observation on future cavity fabrication efforts. This cavity was one of two from the batch that had a blow-through on one of the full penetration equator welds. The blow-through has been repaired, and the area of the repair is marked on the outside of the long end group beam flange for future reference. The repair work is documented in more detail in appendix f below. There is also a small variation in the ID of the short end beam tube that was spotted at the interface between the beam tube and the Nb end disk flange. The last observation to report is that the overall cavity length is approximately 3mm too long.

3. Appendices

a. References

- [1] B. Aune, R. Bandelmann, D. Bloess, B. Bonin, A. Bosotti, M. Champion, C. Crawford, G. Deppe, B. Dwersteg, D. A. Edwards, H. T. Edwards, M. Ferrario, M. Fouaidy, P.-D. Gall, A. Gamp, A. Gössel, J. Graber, D. Hubert, M. Hüning, M. Juillard, T. Junquera, H. Kaiser, G. Kreps, M. Kuchnir, R. Lange, M. Leenen, M. Liepe, L. Lilje, A. Matheisen, W.-D. Möller, A. Mosnier, H. Padamsee, C. Pagani, M. Pekeler, H.-B. Peters, O. Peters, D. Proch, K. Rehlich, D. Reschke, H. Safa, T. Schilcher, P. Schmüser, J. Sekutowicz, S. Simrock, W. Singer, M. Tigner, D. Trines, K. Twarowski, G. Weichert, J. Weisend, J. Wojtkiewicz, S. Wolff, and K. Zapfe, *Phys. Rev. ST Accel. Beams* **3**, 092001 (2000).
- [2] E. Elsen, M. Harrison, L. Hesla, M. Ross, P. Royole-Degieux, R. Takahashi, N. Walker, B. Warmbein, A. Yamamoto, K. Yokoya, and M. Zhang, *The International Linear Collider: A Technical Progress Report* (2011).

b. DESY & FNAL Cavity Fabrication Specifications

DESY SPECIFICATION OF WELDED 1.3 GHz SUPERCONDUCTING RESONATORS FOR TTF/VUV-FEL

D. PROCH, MHF-SL 09-2005

DESY EDMS DOCUMENT NO

303237 B,1,1

1

TABLE OF CONTENTS

1 INTRODUCTION 5

2 FABRICATION DRAWINGS..... 5

3 SUPPLY OF MATERIAL 6

3.1 Nb QUANTITY 6

3.2 INCOMING INSPECTION..... 6

3.3 SHEET MATERIAL FOR HALF CELLS 6

4 PRODUCTION OF PARTS 6

4.1 NbTi FLANGES (DRAWING NO. 3 03 7248/0.001, 3 93 2214/0.021, 4 93 2214/0.022, 3 03 7248/D.004) 6

4.2 END TUBES (DRAWING NO. 3 93 2214/B.006, 3 93 2214/c.005)..... 6

4.3 HOM COUPLER PARTS (DRAWING No 1 03 7248/D.000, 3 03 7248/D.001, 2 03 7248/D.002, 4 03 7248/D.003, 3 03 7248/D.004, 1 03 7248/E.000, 3 03 7248/E.001, 2 03 7248/E.002) 7

4.4 STIFFENING RING (DRAWING NO 4 93 2214/A.002) 7

4.5 PICK UP AT LONG END TUBE AND HOM COUPLERS 7

4.6 CONICAL DISK (DRAWING NO 4 93 2214/B.004, 4 93 2214/c.003)..... 7

4.7 CONNECTING FLANGE (DRAWING NO 3 93 2214/0.002)..... 7

5 PRODUCTION OF SUBGROUPS 7

5.1 HOM COUPLER 7

5.2 END GROUPS 8

5.3 FREQUENCY MEASUREMENT OF END GROUPS..... 9

6 PRODUCTION OF CELLS 9

6.1 DEEP DRAWING OF HALF CELL 9

6.2 PREPARATION OF HALF CELLS FOR DUMB-BELL WELDING..... 9

6.3 FREQUENCY MEASUREMENT OF HALF CELLS 10

6.4 WELDING OF DUMB-BELL 10

6.5 FREQUENCY MEASUREMENT OF DUMB-BELLS 10

6.6 ANODISATION AND GRINDING OF DUMB-BELLS 11

7 WELDING OF CAVITY 11

7.1 WELDING OF DUMB-BELL TO DUMB-BELL 11

7.2 WELDING OF END GROUP TO DUMB-BELL 11

7.3 SEQUENCE OF HALF CELL AND DUMB-BELL TREATMENT, CLEANING AND WELDING 11

8 FINAL TEST OF CAVITY 13

8.1 LEAK CHECK 13

8.2 MECHANICAL MEASUREMENT..... 13

9 PACKING AND SHIPPING..... 13

10 TIME SCHEDULE..... 13

11 PROGRESS REPORT 13

12 QUALITY ASSURANCE DOCUMENTATION..... 14

13 APPENDIX..... 15

13.1 LIST OF PARTS..... 15

13.2 DEGREASING, ULTRASONIC CLEANING, DRYING..... 15

13.3 CHEMICAL CLEANING, RINSING, DRYING..... 16

13.4 HANDLING AND STORAGE CONDITIONS..... 16

13.5 WELDING PREPARATION..... 16

13.6 GENERAL ELECTRON BEAM WELDING CONDITIONS..... 17

13.7 ANODISING..... 17

 13.7.1 Introduction..... 17

 13.7.2 Process..... 18

 13.7.3 Procedure..... 18

13.8 GRINDING..... 19

13.9 Nb SPECIFICATION..... 20

13.10 SURFACE CONTAMINATION..... 20

13.11 CAVITY CONTOUR, FREQUENCY AND LENGTH..... 20

13.12 LIST OF DRAWINGS..... 21

13.13 QUALITY CONTROL REQUIREMENT..... 21

1 INTRODUCTION

This specification describes fabrication details of the superconducting resonators for the acceleration of electrons in the TTF/VUV-FEL. TTF/VUV-FEL is an extension of the experimental linear accelerator TTF (TESLA Test Facility) and will mainly serve as a FEL radiation source.

The resonator is joined from deep drawn half cells and special end sections entirely by electron beam welding. Correct cell form is important to reach the desired resonant frequencies (accelerating mode and some important higher frequency resonances) at specified cell- and resonator lengths.

The HOM-coupler are described in this specification and in bill of material 9 03 7248/D.000 and 9 03 7248/E.000 and drawings contained therein.

The accuracy of form of single cells and the complete 9-cell structure as required by drawing 0 03 7248/0.000 call for accurate deep drawing of half cells, and suitable weld preparation and control of welding parameters.

This specification is an update of the former DESY specification of 24 welded 1.3 GHz Superconducting Resonators for TESLA Test Facility TTF. There are changes which are based on the experience with the last cavity production: tight frequency control of half cells and dumb-bell, more tight welding conditions, compensating slight contour deviations of the half cells by trimming the equator region at the stage of dumb-bells, more chemical cleaning of half cells and HOM parts, more strict quality control on mechanical tolerances and an extended description of cleaning and handling necessities.

2 FABRICATION DRAWINGS

The DESY drawings are listed with actualization index in Appendix "13.12". Upon any change in a drawing, it will receive a new actualization index and a new drawing list will be issued which invalidates earlier issues.

On the basis of the DESY drawings the contractor produces his own fabrication drawings for the resonator. The dimensions in these drawings must allow for the material removal by etching and weld shrinkage such that after etching and welding the tolerances specified by the DESY drawings are achieved. He also prepares prescriptions for chemical treatment and controls of drawings of tools and fixtures for production. For the content of the documents he prepares the contractor is responsible exclusively.

DESY is furnished with a full set of the above mentioned fabrication documents at least 2 weeks prior to their use for production. DESY will check if the specified characteristics of the resonator may be achieved with these documents. Possible comments from DESY pertaining to these documents are without any liability. DESY finally receives a set of the documents actually used for production. In view of the still ongoing development work, DESY may wish to modify details of the current design of the resonator. Such modifications will be carried out by the contractor.

3 SUPPLY OF MATERIAL

3.1 Nb QUANTITY

The niobium stock is furnished by DESY. Appendix "13.1" lists all parts needed to fabricate one 9-cell resonator. DESY delivers this amount per cavity plus a reserve of ca. 10 %. If the contractor requires still more stock, he may buy more from DESY. All stock for the half cells is eddy current scanned by DESY to detect and sort out material with inclusions of foreign materials or other defects. Any left over niobium stock and scrap pieces of more than 20 grams will be returned to DESY with the last resonator shipment.

3.2 INCOMING INSPECTION

Upon receipt, the contractor will inspect the niobium stock for conformity with specification. In case of nonconformity DESY will inspect the material at the contractor's plant and replace the material.

3.3 SHEET MATERIAL FOR HALF CELLS

All sheet material for the half cells has been eddy current scanned at DESY. The later "outer" surface is marked by DESY by methods to be agreed on by the contractor. This mark should be visible after deep drawing, welding and chemical cleaning. The opposite sheet surface is the "inner" surface which carries the superconducting surface current. This surface shall not be contaminated by any handling procedure (see Appendix "13.4, 13.10")

4 PRODUCTION OF PARTS

4.1 NbTi FLANGES (DRAWING NO. 3 03 7248/0.001, 3 93 2214/0.021, 4 93 2214/0.022, 3 03 7248/D.004)

All flanges (2 x beam pipe, 1 x pick up, 1 x input coupler, 2 x output of HOM coupler) are made from NbTi. A rod of diameter 147mm NbTi material is furnished by DESY. The smaller diameter flanges are made from inner the cut out of the large flanges. The sealing surface must have a very good surface quality (Ra 0.8) and must be free of any scratches, especially radial ones. Therefore the surface finish must be done with a method which removes the material tangential to the circle of the sealing area. The finished sealing surface shall be protected by plastic half cells (soft polyvinyl chloride is acceptable). The removal rate for NbTi by the standard chemical etching mixture (see App. "13.3") is a factor of two larger as compared to niobium.

The connection of the NbTi flanges to the Nb tube was done in the last production by EB welding from the front side (sealing surface) of the NbTi flange. The surface finish of this weld was not always smooth, as required. Furthermore there was a gap between the NbTi flange and the Nb tube at the backside of the flange. Therefore it may be considered by the contractor to carry out butt welding between the NbTi flange and the Nb tube at the backside of the NbTi flange. The contractor is requested to reconsider the welding procedure of all subgroups containing NbTi flanges and consult with DESY on the welding procedure.

4.2 BEAM TUBES (DRAWING NO. 393 2214/B.006, 393 2214/C.005)

Seamless tubes of length 105 mm (short end tube) and of length 140 mm (long end tube) are

furnished by DESY.

4.3 HOM COUPLER PARTS (DRAWING NO 1 03 7248/D.000, 3 03 7248/D.001, 3 03 7248/D.002, 4 03 7248/D.003, 3 03 7248/D.004, 1 03 7248/E.000, 3 03 7248/E.001, 2 03 7248/E.002)

The HOM coupler will carry sizeable RF surface currents (inner surface of "coupler housing", "F part"). Therefore these parts must be treated with the same care as the inner surface of the half cells and dumb-bell. The inner surface of the coupler housing as delivered by DESY has a smooth, scratch free surface. This surface shall not be contaminated by other material or scratches. The surface of the "F part" must fulfill the surface conditions as described for the inner surface of the half cells and dumb-bells.

4.4 STIFFENING RING (DRAWING NO 4 93 2214/A.002)

Stiffening rings are welded to the outer side of the half cells when completing the dumb-bells. It is necessary to assure a 100 % penetration weld in order to avoid cracks at the backside of the stiffening rings. This would weaken the mechanical strength and risk contamination by chemistry, since the acid cannot be removed out of the cracks. The geometry of the welding cut at the stiffening ring and at the mating part of the outer surface of the half cells must be chosen to assure the quality of the desired welding.

4.5 PICK UP AT LONG END TUBE AND HOM COUPLERS

The small pick up tube is EB welded to the large diameter beam pipe. It is important to produce a 100 % penetration weld. In case of gaps or cracks at the inner surface, acid will penetrate during etching and contaminate that region. In some of the recently produced cavities inner grinding was applied to eliminate those cracks. This method cannot be accepted, because it is very difficult to inspect this area for any remaining small crack. Therefore a welding geometry has to be chosen by the contractor which assures a full penetration welding seam.

4.6 CONICAL DISK (DRAWING NO 4 93 2214/B.004, 4 93 2214/C.003)

The conical disk is the connecting part between Nb cavity and Ti tank. For a tight fit of the connecting parts to the Ti tank, it is important to establish an only small planarity error at the outer shoulder ($\varnothing 186\text{mm}$ and $\varnothing 194.8\text{mm}$, please note that the conical disk at the short and long end tube are of different outer diameter). This is established by cutting the shoulder (3 mm) after finishing all welding to the conical disk. For the welding to the Ti tank it is required that a cylindrical part ($\varnothing 186\text{ mm}$ and $\varnothing 194.8\text{ mm}$) of at least 0.5 mm remains in order to avoid a blow through of the welding beam.

4.7 CONNECTING FLANGE (DRAWING NO 3 93 2214/0.002)

The connecting flange will locate precisely the tuner assembly and serve as reference for alignment of the cavities. Therefore a tight tolerance, as given in the drawings, is necessary. As consequence the final machining must be done after finishing all welding to avoid deformation of the connecting flange.

5 PRODUCTION OF SUBGROUPS

5.1 HOM COUPLER

The "F-part" is cut from a 8.5 mm thick RRR 300 Nb sheet. In order to save Nb material, the

"F-part" should be arranged in an interlaced geometry. Cutting the Nb material should not deteriorate the bulk properties. Water cutting or spark erosion can be used for this purpose. A removal of the damaged surface layer of 0.5 mm is necessary after the last mechanical treatment. The "F-part" must have a smooth, defect free and scratch free surface.

Before welding the "F parts" to the coupler housing, both parts must be cleaned by removing 20 μm by the standard chemistry for Nb (see App. "13.3"). Cleaning with ultrapure water, drying and storage shall be done according to conditions described in App. "13.3, 13.4". If welding cannot be carried out within 8 hours after the chemical cleaning, another flash of 3 μm chemical etching is necessary immediately before welding.

5.2 END GROUPS

The sub-assemblies called: "short end group" (drawing no 1 03 7248/A.000) and "long end group" (drawing no 1 93 2214/B.000) are shown for the cavity version with welded HOM coupler. The two end half cells as well as the two end tubes of the resonator are different.

No more than 8 hours before welding the surfaces of the end tubes and end tube sections ("end tube") are degreased, ultrasonic cleaned, etched by 3 μm , rinsed with ultrapure water, dried and stored described in section "13.3, 13.4".

The resonance frequency of the end half cells (before welding to the connecting flange) has to be measured according to "6.3". At this stage the end half cells are longer by 1 mm at the equator (in addition to the expected welding shrinkage at equator and iris). Another frequency measurement shall be done after welding the connecting flange plus part of the beam tube to the end cell. As in the case of dumb-bell frequency measurement, possible contour changes by the welding procedure will be uncovered hereby. The frequency measurement will determine the amount of trimming at the equator. The end tube is joined via the end tube section to the iris of the end half cell by welding from the inside.

The connecting flange among other things serves the same function as the stiffening ring of the dumb-bell and carries the conical disk. The short end tube is made from the same stock as the long end tube. For all welding of the end group, "General electron beam welding requirements" ("13.6") needs to be observed.

The finished sealing surfaces of the above mentioned flanges shall be protected by plastic caps (soft polyvinyl chloride is acceptable) at all times, except for flange dimensions measurements and inspection of finish of sealing surfaces.

After finishing all welds, the connecting flange and conical disc are machined, with the end group held from the inner surface of the half cell, analogously as described in "6.2".

As pointed out in "Error! Reference source not found.", the cylindrical part of the shoulder at the conical disc (O 186 mm, O 194.8 mm) should have a minimum width of 0.5 mm. The exact contour of the connecting flange should be checked with an original assembly ring of the tuner. DESY will supply this assembly ring.

Finally, the end group is chemically cleaned ("13.3") with 20 μm of removal (the NbTi flanges must be protected from the acid), then inspected for defects, and treated in all respects like the dumb-bell (Anodising and grinding "6.6").

5.3 FREQUENCY MEASUREMENT OF END GROUPS

The frequency of the end half cells is measured according to "6.3" and "7.3", steps 4 to 8. After welding the end half cell to the end group the frequency of this unit is measured. Afterwards the equator is trimmed to length accordingly.

6 PRODUCTION OF CELLS

6.1 DEEP DRAWING OF HALF CELL

From the square plates provided, discs with or without a central hole are produced (depending on choice of contractor) and then deep drawn into half cells. It must be assured, that the marked sheet surface will be the outer half cell surface after deep drawing. The "inner" surface of the Nb sheet must be handled with greatest care to avoid any contamination and damage by the deep drawing process. One of the scrap corners of each plate is marked identically to the half cell made from the plate, and stored in a sealed plastic bag for possible future material tests.

For establishing the form of the deep-drawing tooling the spring-back and thickness tolerance of the niobium sheet material has to be taken into consideration. It is also important that at the end of the deep-drawing operation the inner surface of the half cell is everywhere in intimate contact with the mandrel. Possible seizing marks or other damage on the inner resonator surface must be strictly avoided. The surfaces of the tooling and the niobium disc must be carefully cleaned prior to each deep drawing operation, such that no dirt, metal particles or other matter can become embedded in the niobium surface. As stated before, any lubricants or deep-drawing foil used must be completely removable by the ensuing cleaning operations.

Further, the form of deep-drawing tooling must also take into consideration the change of mechanical dimensions caused by etching the dumb-bell. For first deep-drawing tests copper has been successfully used. As material for the mandrel, aluminum alloy, hard anodized, is recommended.

6.2 PREPARATION OF HALF CELLS FOR DUMB-BELL WELDING

The weld preparation of the half cells has three main purposes:

- It must allow assembly of half cells into a resonator with the accuracy required by drawing 0 03 7248/0.000 while considering weld shrinkage and material removal by etching. It may also be so shaped as to center the half cells with respect to each other.
- It must produce correct and uniform wall thickness at iris (smaller diameter) and equator (larger diameter) to avoid locally burning through during welding and to achieve a smooth weld surface on the inner surface of the resonator if welding proceeds from the outside.
- It must allow longitudinal and radial locating of the prefabricated stiffening rings in proper relation to the inner surface of the half cell.

It is advisable to machine **in one clamping** in a lathe all the weld preparations of the half cell including that for the stiffening ring. For this the half cell is located on a fixture from its inner surface which must not be damaged thereby. By this method unroundness at the equator can be eliminated *during* the machining operations, and the various weld preparations can be prepared at the proper location with respect to the contour of the inner surface of half cell.

At this stage the iris is cut to a length which takes into account the welding shrinkage. At the equator, the half cell is longer by 1 mm plus welding shrinkage. The equator will be cut to the right length after frequency measurement of the dumb-bell (see section "6.5") again taking into consideration the weld shrinkage. The details of the weld preparations contemplated by the contractor need to be approved by DESY.

The finished half cells must be inspected with respect to inside contour and the proper relation of the various weld preparations to it. Use of templates, among other tools, is acceptable for this purpose.

At a rate of 5 % of the half cells, the inner contour has to be measured by 3D technique. The samples are selected randomly. All end half cells have to be measured by the 3D technique.

6.3 FREQUENCY MEASUREMENT OF HALF CELLS

After degreasing the half cells, the resonant frequency is measured for all parts. Equipment and manpower is supported by DESY. This frequency measurement will deliver information about

- the accuracy of the contour of the half cells by the average value of the resonant frequencies,
- the reproducibility of shaping the half cells by the spread of resonant frequency,
- the status of the half cells before dumb-bell welding.

Non acceptable deviations of the resonant frequency of half cells or a too large spread in frequency must be reduced by modifying tools or forming parameters.

6.4 WELDING OF DUMB-BELL

The half cells are ultrasonically cleaned, etched 20 μm (one side) rinsed, dried and stored as specified in "13.2, 13.3, 13.4". No longer than 8 h before E.B. welding are the niobium parts etched 3 μm (one side), rinsed, dried and stored as specified in "13.4".

Two normal half cells (drawing 1 93 2214/A.001) are welded together at their irises into a "dumb-bell". The selection of two half cells for one dumb-bell is guided by the evaluation of the resonance frequency measurement "6.3" to yield an average frequency as close as possible to the design value. The requirements of welding conditions ("13.6") have to be observed. It is recommended that this weld receives its smooth surface on the inside by welding from inside. To the dumb-bell is welded the stiffening ring (drawing 4 93 2214/A.002). Execution and sequence of welds while considering weld shrinkage have to be chosen as to produce dumb-bells with which the cell form tolerance in drawings 0 03 7248/0.000 is achieved. If needed, form correction by plastic deformation of dumb-bell is acceptable after coordination with DESY.

The execution of a full penetration weld at the stiffening ring might result in a slight distortion of the cavity shape. Just underneath the weld of the stiffening ring there might be a slight elevation. This local distortion must be investigated by test welds and will be judged by DESY for approval.

It seems advisable to use a welding fixture that ensures parallelism of the equator planes of the 2 half cells to be joined, while leaving axial freedom to accommodate weld shrinkage. The fixture must not touch the inner half cell surface.

The dumb-bell is finally inspected for correct dimensions and weld characteristics.

6.5 FREQUENCY MEASUREMENT OF DUMB-BELLS

After completion of the dumb-bells (iris and stiffening ring welding) the resonance frequency is measured again. The evaluation of this measurement will determine the amount of trimming at the equator to achieve simultaneously the correct length and the correct frequency of the finished

resonator. It also serves as a measure of contour change and reproducibility of iris and stiffening ring welding.

Both ends of the dumb-bell will be cut to the length determined by the evaluation of the frequency measurement done at DESY. For the trimming the dumb-bell is located on a fixture from the inner surface which must not be damaged thereby. By this method both equatorial planes will be cut parallel.

6.6 ANODISATION AND GRINDING OF DUMB-BELLS

Next, the dumb-bell is degreased, ultrasonically cleaned, etched by 20 μm , rinsed and dried as required in "13.2, 13.3, 13.4". An anodization is now made ("13.7"). The RF-surface is inspected jointly with DESY and, where deemed to be defective ground with abrasive material according to appendix "13.8". If no grinding needs to be carried out, the dumb bell is stored in accordance with appendix "13.4". The anodization will be removed by the 3 μm pre-welding etching.

Grinding should be avoided as much as possible. If, however, grinding has to be applied, the dumb bell is etched another 20 μm , rinsed, dried, anodized again, and stored as prescribed in appendix "13.2, 13.3, 13.4". If again surface defects are detected, another sequence of grinding, etching and anodisation is necessary.

7 WELDING OF CAVITY

7.1 WELDING OF DUMB-BELL TO DUMB-BELL

8 dumb-bells, a long end group and a short end group are joined in accordance with "13.6" with equator-welds from the outside. The contractor may also elect to execute the equator welds from the inside. Please note that a repair of an equatorial weld defect cannot be accepted (see "13.6").

Out-of-roundness of half cells at the equator, if present, results in a deviation from planarity of the weld preparation at the equator. The planarity, necessary for avoiding gaps at weld seam, can be achieved by using a tool that keeps the half cells round during tack welding. Also in these welds, niobium vapor must be prevented by suitable shields from being deposited on yet unwelded weld preparations. Since a complete shielding is very difficult it is requested to chemically clean (3 μm) the neighboring two equator areas before the next welding.

7.2 WELDING OF END GROUP TO DUMB-BELL

Welding of the end group to the dumb-bell is done in the same way as welding dumb-bell to dumb-bell. Please note, that a repair of a weld defect of the equatorial weld cannot be accepted (see "13.6").

7.3 SEQUENCE OF HALF CELL AND DUMB-BELL TREATMENT, CLEANING AND WELDING

In the following overview the sequence of half cells, dumb-bell and cavity body fabrication is summarized.

1. Optical, mechanical inspection of Nb sheets
2. Cutting Nb sheets to disc
3. Deepdrawing of half cells ("inner side" of half cells!)
4. Cutting half cells to length $L = L_{nom} + \delta L_{equ} + \delta L_{iris} + 1 \text{ mm}$ (L_{nom} = nominal length, δL_{equ} = welding shrinkage at equator, δL_{iris} = welding shrinkage at iris + stiffening ring)
5. Prepare welding steps at iris and stiffening ring
6. Degreasing, ultrasonic cleaning, rinsing
7. Frequency measurement, selection of half cells for dumb-bells
8. 20 μm chemical cleaning of half cells (inner and outer surface), rinsing, storage
9. 3 μm chemical cleaning at iris area, rinsing
10. Welding of iris within 8 hours after step 9
11. Welding of stiffening ring
12. Frequency measurement of dumb-bells
13. Cutting equators of dumb-bells to right length according to frequency measurement ("12"), machining welding area (drawing No 393 2214/A.000)
14. Degreasing
15. Frequency measurement of dumb-bells, selection of dumb-bells for welding sequence of cavity
16. Degreasing of dumb-bell
17. 20 μm chemical cleaning of dumb-bells
18. Anodising of dumb-bells
19. Inspection of "inner" dumb-bell surface for defects, if OK, continue at step 23
20. Grinding of defects
21. 20 μm chemical cleaning of dumb-bells for cleaning of surface from grinding dirt
22. go back to step 18
23. Storage of dumb-bell
24. 3 μm chemical cleaning at equator region of the dumb-bell to be welded

25. Welding of two dumb-bells at equator within 8 hours after step 24

26. Repeat step 24 with longer cavity section

8 FINAL TEST OF CAVITY

8.1 LEAK CHECK

Before lowering the internal pressure, the resonator must be constrained against becoming shorter and thus being permanently deformed, by fixing its connecting flanges to external braces. Silicon grease must be strictly avoided.

The finished resonator is subjected to a leak test. The prescribed leak-tightness of

$$\leq 1 \times 10^{-10} \text{ mbar l/s}$$

must be determined with the sensitivity of the helium leak tester such that full range of its instrument corresponds to

$$\leq 1 \times 10^{-9} \text{ mbar l/s}$$

A plot of the indication of the leak tester as function of time shall be made over ca. 5 min before and ca. 5 min after application of ca. 1 bar helium, with time of application of He marked in the plot. This plot shall be included in the quality control documentation.

Repair of leaks requires in all cases prior approval of DESY as to the method, and possible risks.

8.2 MECHANICAL MEASUREMENT

Dimensions, inner surface, welds and other features of the resonator are inspected as per paragraph "12".

All results of measurements and inspections are recorded in a protocol and sent to DESY prior to shipment of resonator.

9 PACKING AND SHIPPING

The degreased resonator, with all plastic flange caps in place, is sealed into a clean polyethylene foil and mounted in a transport box. The resonator is to be fastened only on the 2nd and 8th cell and must be secured against axial displacement. Transport is by truck or airplane (rail excluded).

10 TIME SCHEDULE

A reliable time schedule has to be provided by the contractor when signing the contract. It must contain reasonable details to follow closely the production as well as state milestones, e.g. frequency measurement of half cells and dumb-bells, start of welding the cavity body and delivery of individual resonators.

11 PROGRESS REPORT

The contractor shall submit a monthly progress report to the DESY technical representative. The progress report shall provide full details concerning the contractor's progress during the previous month. The progress report shall be submitted until the 15th day of the following month in which progress is reported.

12 QUALITY ASSURANCE DOCUMENTATION

Appendix "13.12" lists tables of quality assurance measurements. The individual parts (see section "4"), subgroups (see section "5") and cavity body components (see section "6" and "7") have to be measured. The method of measurement is proposed by the contractor and must be agreed on by DESY. Any nonconformity of parts, subgroups or cavity body items with the specification has to be reported to DESY prior to continuation of the production. DESY will decide whether to use or reject the part.

13 APPENDIX

13.1 LIST OF PARTS

Material (Quality)	Delivered amount	Material	Purpose
RRR 300	18	Nb sheets 265 x 265 x 2.8	Half cell
NbTi	2	Nb rings 220 x 100 x 5 ± 0.2 mm	Conical disk
RRR 40	Length 217 mm	Nb sheets 3 ± 0.15 x 360 x fabrication length (> 2134 mm)	Stiffening ring
RRR 300	Length 50 mm	Nb sheet 1000 x 300 x 8.5 ± 0.2 mm	Inner part, coupler
RRR 40	Length 50 mm	Nb rod Ø 20 x 700	Forged bar, antenna neck
RRR 300	1	Seamless Nb tubes IØ 78 ± 0.2 x 3 ± 0.3 x 105 mm	Short end tube
RRR 300	1	Seamless Nb tubes IØ 78 ± 0.2 x 3 ± 0.3 x 140 mm	Long end tube
RRR 300	1	Seamless Nb tubes IØ 40 ± 0.15 x 2.5 ± 0.15 x 155 mm	Maincoupler port
RRR 300	2	Forged Nb rings 135 x 75 x 27 mm	Connecting flange
RRR 300	2	Pre-formed part according to DESY MPL drawing 3 93 4417/0.001	Coupler housing
NbTi	Ø 147 mm, length 20 mm	Rundstab Nb 55% Ti	Flange DN78
Nb Ti	"	Rundstab Nb 55% Ti	Flange DN40
NbTi	"	Rundstab Nb 55% Ti	Flange DN12
NbTi	"	Rundstab Nb 55% Ti	Flange DN8

13.2 DEGREASING, ULTRASONIC CLEANING, DRYING

Degreasing and ultrasonic cleaning with "Ticopus" or equivalent, followed by rinsing in de-ionized, filtered (0.2 µm particle size) water, precedes all etching operations. Rinsing is done until a resistivity of 10 MΩcm is reached. Hot water (temperature about 60 °C) is preferred for more intense cleaning action. For selection of baths for degreasing and ultrasonic cleaning the contractor will contact DESY. Drying is carried out in laminar airflow in a clean room of class 1000 or better. The parts must be supported in places well away from the weld preparations and the RF surfaces to avoid

drying stains there.

13.3 CHEMICAL CLEANING, RINSING, DRYING

Generally, all etching operations are carried out with the niobium part immersed in the acid mixture, i.e. over the entire surface. The acid mixture consists of HF (48 % conc.), HNO₃ (65 %) and H₃PO₄ (85 conc.) in the volume ratio 1 : 1 : 2, respectively. All acids are p.a. grade. The removal rate is roughly 1 μm/min for fresh acid at 15 °C, but depends on agitation as well as niobium content and temperature of acid mixture. Before etching resonator parts, a test etching must be made. After etching, the parts are quickly (within max. 15 sec) immersed in a rinsing bath. At no time during etching and transfer to the rinsing bath may the acid temperature be permitted to exceed 20°C.

The acid mixture is replaced when its niobium content reaches 10 g/l, corresponding to an etch rate of about 0.5 μm/min.

For all etching operations there shall be recorded in a protocol: Part type and serial number, bath temperature, duration and thickness removed (determined by weighing of at least one sample out of each batch).

Removal of thickness always is understood to refer to one surface only.

The etched parts are rinsed with de-ionized, to 0.2~μm particle size filtered water until resistivity of 10 MΩcm is reached.

Drying is carried out in laminar airflow in a clean room of class 1000 or better. The parts must be supported in places well away from the weld preparations and the RF surfaces to avoid drying stains there.

13.4 HANDLING AND STORAGE CONDITIONS

Contact of the niobium surfaces with substances that the cleaning and etching processes described in "13.2, 13.3" will not completely remove must be prevented. Such forbidden materials include silicone products, chemically very stable plastics such as Teflon, fingerprints and others. They can disturb etching processes and limit RF performance. General precautions against contamination of the Nb parts include use of suitable lint free gloves, keeping work areas and tools used in clean condition, and protection against dust during storage and assembly of cavity components.

Anodization of niobium surfaces serves for the detection of possible surface defects and handling pollution (e.g. fingerprints). The details of the anodization process are described in appendix "13.7" Cleaned parts are protected during storage and transport from dust, contact with "forbidden" materials and mechanical damage. For this purpose clean, closed polyethylene boxes have proven useful.

The parts should not be supported on weld areas. The half cells should be supported on the outer surface. The dumb bells must be stored with horizontal axis.

13.5 WELDING PREPARATION

Before welding, all parts must be cleaned by 3 μm chemical etching at the welding area. Welds at the equator and iris of cells and at the HOM coupler parts will be exposed to high magnetic or electric fields. Therefore absolutely clean conditions must be assured during welding. These parts must undergo a chemical cleaning of 20 μm after the last mechanical treatment. Another 3 μm

chemical cleaning is necessary if the time between last chemical cleaning and welding exceeds 8 hours. Touching the weld preparation area after the last cleaning must be strictly avoided. Especially storing the half cells or dumb-bells with the equator/iris weld preparation area touching the storage table is not allowed. Also wiping the welding step with some alcohol soaked "dust free" cloth must be avoided. A last cleaning of the welding step from dust by blowing with clean and dry nitrogen gas is recommended. Ionized gas may be helpful to remove dust.

13.6 GENERAL ELECTRON BEAM WELDING CONDITIONS

To prevent oxidation and other contamination of weld preparations, welding shall generally commence within the same work shift in which the parts were cleaned, etched, rinsed and dried.

The pressure in the welding chamber has to be less than 5×10^{-5} mbar during welding. The welding chamber shall be vented with clean nitrogen only after the temperature of the niobium part has dropped to 100 °C at the hottest spot.

All welds must have full penetration, be smooth and of uniformly wide root on the inside surface of resonator and must neither protrude nor stay back by more than 0.1 mm with respect to the neighboring surface. Some larger protrusion might occur locally underneath the stiffening ring welding (see section "6.4"). Welding from the inside (RF-side) is recommended, wherever possible. Wiggling the electron beam according to a suitable pattern has been found to be very useful in producing uniformly wide and flat roots and to reduce risk of burning holes. By suitable shields niobium vapor from welding must be prevented from contaminating weld preparations elsewhere.

The contractor shall, after optimization of welding parameters, demonstrate by test welds to DESY that the RRR in the welds and weld overlaps is not degraded by more than 10 % over that of the unwelded niobium. No cracks, pores, inclusions of foreign materials or other defects are allowed in welds. DESY will check that these requirements are met on test- and production welds by eddy current- and other methods. During the weld tests the welding-chamber gas is analyzed with a mass spectrometer (DESY can assist with equipment and personnel). The final welding parameters for production are subject to approval by DESY.

The experience with the earlier cavity production has provided clear evidence, that there exists no appropriate procedure to repair a hole in the equatorial weld. Although the visual appearance of a repaired weld looks good, the RF performance of such a cell is degraded: quenches at the repaired area limit the accelerating gradient far below the design value of 25 MV/m. Therefore a repaired equatorial weld cannot be accepted. In such a case the contractor has to inform DESY and propose a procedure to cut the damaged cell and replace it by a cell which is free of welding defects. The repair procedure has to be agreed on by DESY but will be carried out at the contractor's risk and cost.

Any repair of a weld other than at the equator, contemplated by the contractor, requires in each instance prior approval of the methods by DESY.

13.7 ANODISING

13.7.1 INTRODUCTION

Anodization means the electro-chemical oxidation of metal surfaces like aluminum, titanium or niobium. It results in a colored surface depending on the experimental conditions. For the

production of niobium cavities the better contrast of the colorated surface allows the detection of defects and inclusions of foreign material.

13.7.2 PROCESS

The electro-chemical process of anodization builds up an oxide layer of Nb_2O_5 thicker than the natural layer formed in air. Due to the inference of reflected light, the color of the surface is correlated directly to the thickness of the oxide layer.

The thickness of the layer grows with 2 nm per volt. Each voltage leads to a typical color. For example, for niobium a voltage of 20 V results in a dark blue color with good contrast to other materials. Materials not affected by the electro-chemical reaction like stainless steel, brass etc. retain their original color. Aluminium shows up in different color, but the color of titanium is close to that of niobium.

The coloration of the niobium depending on the voltage is shown in Table 1.

The Nb_2O_5 layer is an electrical insulator, while the niobium has a low electrical resistivity. If the voltage is applied, the niobium piece – used as the anode – the electrical conducting solution and the cathode constitute almost a short circuit for the power supply. The current flowing in the bath has to be limited. During the forming of the pent-oxide layer, the current density reduces exponentially. The oxide layer is formed uniformly, when the current has reduced to $1/e$ of the starting value.

For a controlled process the power supply needs to be voltage stabilized and the maximum current flow in the beginning of the process has to be limited. Too high current densities ($j > 5 \text{ mA/cm}^2$) can lead to the formation of sub-oxides (NbO , NbO_2) with completely different characteristics.

To prevent contamination of the niobium piece to be checked, the bath containers should be made of polyethylene or any other acid/alkaline resistant plastic. The power leads and contacts have to be made from Nb of reactor grade or better. Any tooling necessary in the solution should be fabricated of either polyethylene (acid/alkaline resistant plastic) or Nb of reactor grade or better.

Safety regulations for handling and storage of the acid/alkaline as well as electrical precautions have to be checked with the local authorities.

13.7.3 PROCEDURE

Solution: Two mixtures are in use for the process:

- a) A mixture of deionized (DI) water ($> 10 \text{ M}\Omega\text{cm}$) and nitric acid (HNO_3 in 'pro analysi/'selectipur'-quality) in a composition of 5: 1 to 9: 1.
- b) A mixture of DI water ($> 10 \text{ M}\Omega\text{cm}$) and ammonia-hydroxide $NH_4(OH)$ (in 'pro analysi/'selectipur'-quality) in a composition of 5: 1.

The solution is mixed well and the temperature has to be $20 - 25 \text{ }^\circ\text{C}$ before starting the anodization.

The Nb pieces, cleaned by $20 \mu\text{m}$ chemical etching ("13.3") are placed in the bath and connected to the power supply. The contacts are on the backside of the surface to be checked. Within the solution Nb current leads have to be used.

The voltage of the power supply is increased from 0 to 20 V. The current flowing in the bath has to be controlled and limited to around 1 mA/cm^2 . A current density of 5 mA/cm^2 must not be

exceeded. At the nominal voltage of 20 V the current reduces exponentially. The current can be switched off, if it is around 0.1 mA/cm².

The Nb pieces are removed from the solution without touching the surface and dipped in DI water (> 10 MΩcm). Extensive rinsing under flowing DI water (> 10 MΩcm) has to be done. The rinsing and drying procedures have to be done carefully in a clean environment (cleanroom class 10000 or better). No mechanical contact to the Nb surface to be checked is allowed and no drying stains or residues of the chemical should remain on the surface.

Handling the Nb pieces during the whole process after precleaning until the completed inspection has to be done wearing latex or rubber gloves. Grease and sweat lead to chemical reactions affecting the NbO₅-layer, which gets in discolorations of the surface.

Voltage	Color
0 V	Metallic
10 V	Slightly darkened
11 – 14 V	gold – brown (varying)
16 V	Purple –red
17 –20 V	Purple changing to dark blue
20 V	Dark blue
20 – 40 V	Dark blue changing to light blue
> 40 V	Red and green colors
> 100 V	Danger of grey oxides

Table 1 Coloration of niobium by an electron-chemical anodizing process

13.8 GRINDING

Grinding of defects at the "inner" cavity surface has proven to avoid performance limitations of superconducting resonators. Grinding should be restricted to the defect area and produce a smooth surface. The pressure and velocity of the grinding wheel should be chosen so that

- no heating of the ground Nb area occurs,
- no deep scratches are produced at the ground area,
- a smooth transition is gained at the border from the ground to the untreated surface area.

Two different types of grinding tools have been successfully applied: rubberized abrasives of various shapes (cylinders, cones, thin wheels, ..) and flapped wheel (fan shaped rotating grinding paper). Two types of abrasives are commonly in use: silicon carbide and aluminum oxide (Korund). Both materials are only slowly dissolved by the Nb-chemistry ("13.3"). Therefore the size of the abrasive particles should be not larger than 50 μm. In this case any imbedded abrasive particle will be removed from the bulk Nb when etching a layer of 150 μm during final preparation of the resonator.

Recommended abrasive wheel: CRATEX, No. 545097, rubberized abrasive 120 No 83C

Recommended flapped wheel: "Pferd", abrasive size 320 or higher.

13.9 NB SPECIFICATION

The Nb sheets for half cells are specified in "Technical Specification for Niobium Applied for the Fabrication of 1.3 GHz Superconducting Cavities (RRR 300 (200)), Version D".

13.10 SURFACE CONTAMINATION

The "inner" surface of the half cell, dumb-bell and HOM coupler must be free of surface contaminations:

- Scratches deeper than 15 μ m
- Mechanical damage larger 15 μ m
- Imprints of foreign material
- Fingerprints
- Silicon grease

13.11 CAVITY CONTOUR, FREQUENCY AND LENGTH

In the accelerator the cavity has to operate at exactly the frequency of 1300 MHz. The resonant frequency of the cavity is determined by the shape of the cells. Major parameters are the equator diameter and the length of the individual cells. The drawing of the cavity shape (drawing no 0 03 7248/0.000) describes the contour of the resonator as delivered. Frequency change by succeeding etching and thermal shrinkage during cool down are taken into account in the fabrication drawing.

The change of the resonance frequency by changing mechanical dimensions is given by

- a) increasing the height of a half cell by extending the equator by 0.1 mm: -0.53 MHz
- b) increasing the height of one half cell by extending the iris by 0.1 mm: -0.155 MHz
- c) changing the contour of one half cell by uniform removal of a surface layer of 0.1 mm (as in the case of chemical etching): -1 MHz
- d) increasing the total length of a 9 cell resonator in the tuning machine by equally tuning each of the 9 cells: +320 kHz/1 mm

Welding shrinkage will influence the cavity resonance according to a) and b): contour deviations are partially described by c).

The delivered cavity is tuned at DESY to establish the right resonance frequency and equal electrical excitation of the individual 9 cells. This is accomplished by slightly changing the length of the individual cells. Any deviation of the ideal cavity contour will be compensated hereby but with the consequence of changing the total cavity length. To keep the cavity length in the specified tolerance of ± 3 mm it is therefore necessary to assure strict individual tolerances. Ideally one would request a contour deviation of no more than ± 0.1 mm, which is hard to achieve. Experience with the previous production of half cells showed that there is a negative contour change (smaller volume) at the iris region whereas the equator region has a positive one. These areas are sampled by dominant electric and magnetic field, respectively, and the resultant frequency changes are of opposite sign so that the result of contour changes is cancelled to some extent. On the other hand, the other mechanical tolerances as given above might add up. Therefore the acceptable tolerances are

- ± 0.1 mm for welding shrinkage,
- ± 0.2 mm for contour change of the half cells.

During the last cavity production a 100 % frequency check of half cells and dumb-bells was performed and deviations of the ideal contour were detected and corrected. Measurement and calculation of the height correction is done by DESY. The correction is done by cutting the height of a cell and a dumb-bell to an intermediate length in such a way, that a too long completed cavity was shortened the right amount when tuned to the correct frequency in the 9 cell tuning machine.

Most of the cavities of the latest production stayed within the length tolerance of ± 3 mm at the design frequency of 1.3 GHz. The described tuning philosophy is based on adjusting contour errors by tuning the fundamental mode (1.3 GHz) properties. It turned out, however, that in some cavities important higher order mode frequencies were distorted too much. In most cases this was due to imperfect end half cells, thus destroying the asymmetry of the right and left end cells. For this reason all end half cells have to be measured with the 3D technique and frequency-checked before and after welding.

13.12 LIST OF DRAWINGS

The list of drawings is attached separately.

13.13 QUALITY CONTROL REQUIREMENT

The quality control requirement is attached separately.

FABRICATION OF 1.3 GHZ NINE-CELL SUPERCONDUCTING RF CAVITIES

Prepared by: M. H. Foley
Date: May 1, 2006
First Revision: April 4, 2007
Second Revision: August 7, 2008
Third Revision: November 12, 2009

1. INTRODUCTION

This document describes the required specifications and conditions for the fabrication of nine-cell SCRF cavities. The cavities described herein are designed to operate in the TM010 accelerating mode at a frequency of 1.3 GHz.

SCRF cavities are formed by electron beam welding multiple, deep drawn (or hydroformed), niobium half-cells and end assemblies. The shape of the inner surface of these half-cells is designed so that the welded cells will electrically resonate at a precise frequency. Mechanical tolerances are strict. Adherence to established procedures is essential to avoid contamination during fabrication.

Throughout this document FNAL will refer to Fermi National Accelerator Laboratory, DESY will refer to the German National Electron Acceleration Facility, and potential vendors will be referred to as "the contractor".

2. SCOPE OF WORK

The contractor will: (1) Develop their own fabrication drawings from the attached FNAL cavity drawings, (2) Design and fabricate all required tooling and welding fixtures, (3) Develop the required e-beam welding parameters, and (4) Fabricate 20 SCRF cavities in accordance with the attached DESY fabrication specification [1] as amended in Section 3 below. The contractor will provide all supervision, engineering, necessary materials, labor, QC inspections, and other services required to fabricate the cavities. All necessary facilities (e.g., buildings, machine shop, clean room, ultra pure water system, ultrasonic cleaning, chemical etching, devices for mechanical inspection, and leak detection equipment) will be the responsibility of the contractor, unless otherwise specified. All drawings, tooling and welding fixtures will become the property of FNAL upon completion of the contract.

Records of all fabrication measurements and inspections for each cavity, as specified in the attached QC document [2], will be submitted to FNAL with the completed cavities.

11/12/2009

p. 1 of 7

The FNAL cavity drawings are an Americanized version of the DESY cavity drawings. The drawings, the fabrication specification [1] and the QC document [2] are the property of DESY, and DESY maintains all rights according to DIN 34/ISO 16016.

FNAL reserves the right to observe all processes, and to invite the advice and collaboration of established experts in the field.

2.1 Fabrication Plan

The contractor will submit a fabrication plan to FNAL for acceptance by the date specified in the contract. The plan will identify and describe all aspects of the work to be executed from the point of initial inspection of the niobium material through delivery of the cavities. The fabrication plan will include the following:

- (1) Fabrication drawings for the various parts adapted from the FNAL cavity drawings.
- (2) Procedure for identification marking of niobium half-cell blanks.
- (3) Proposed method for machining weld preparations on cavity components.
- (4) Procedures for cleaning and chemical etching of components before welding.
- (5) Procedures and proposed vessels for storage and transportation of components to the welding site.
- (6) Procedures for verifying sufficient weld penetration: i.e., micrographs of all sample welds performed using the finalized, production EB weld parameters.

FNAL must accept the fabrication plan prior to the start of work.

2.2 Schedule

The contractor will submit a detailed schedule including milestones with the initial proposal. Cavities are to be fabricated in three batches as follows:

Batch 1	6 cavities due 12 months from date of order
Batch 2	6 cavities due 21 months from date of order
Batch 3	8 cavities due 30 months from date of order

Subassemblies, including dumbbells and end groups, can be produced in batches or as a single production run. FNAL must approve the proposed schedule prior to the start of work.

2.3 Quality Assurance Plan

The contractor will submit a Quality Assurance Plan to FNAL for acceptance by the date specified in the contract. FNAL must accept the Quality Assurance Plan prior to the start of work.

3. DESY FABRICATION SPECIFICATION

The attached DESY fabrication specification [1] must be adhered to in all respects, with exceptions listed below by section number. Note that in the fabrication specification, any reference to DESY should be replaced by FNAL, excepting reference to the supply of material or components.

2. FABRICATION DRAWINGS

A complete list of the DESY drawing numbers mapped to their corresponding FNAL drawing numbers is attached (follow the column marked "Short End Tubes" where there is a discrepancy). A BOM listing the material necessary to build a cavity is contained in the Appendix of this document.

3. SUPPLY OF MATERIAL

All material (Niobium and Nb55Ti) will be procured by the contractor and can be ordered at one time. FNAL approved suppliers are: Teledyne Wah Chang, Tokyo Denkai and Plansee/Heraeus. Niobium must conform to the FNAL material specification [3] attached to this document. Upon receipt the contractor will inspect the material for conformity with dimensional tolerances. Niobium sheets for forming half-cells will be eddy current scanned by FNAL to detect possible inclusions of foreign material or other defects. FNAL may choose to conduct further analysis (e.g., mechanical properties, RRR measurements, etc.) of selected material samples. FNAL reserves the right to reject substandard material.

4.2 BEAM TUBES

End tubes will be formed by the method of choice of the contractor: seamless tube drawn from sheet, or rolled and seam welded tube. If seam welded, the inner weld bead must be fully eliminated by machining. The "long" end tube will be shortened to 105 mm; i.e., the cavity end tubes will be symmetric in length.

5.3 FREQUENCY MEASUREMENT OF END GROUPS

After welding the end half-cell to the end group the frequency of this unit is measured. Evaluation of the frequency measurements and determination of the amount of material to trim from the end half-cell equators will be agreed upon jointly by the contractor and FNAL.

6.1 DEEP DRAWING OF HALF CELLS

Half-cells may be formed by a method of the contractor's choice (e.g., deep drawing or hydroforming). The proposed method must be approved by FNAL.

A preliminary batch of six "proof-of-principle" half-cells (two normal, two short end and two long end) will be formed by the contractor and shipped to FNAL for coordinate measuring machine (CMM) profiling and frequency measurements. This step will verify the final die contours.

6.2 PREPARATION OF HALF CELLS FOR DUMBBELL WELDING

The contours of the inner surface of each half-cell will be inspected by the contractor using templates or other means proposed by the contractor and approved by FNAL. FNAL will perform 3D contour measurements (CMM) on a subset of the formed half-cells, as specified in Section 6.2.

6.4 WELDING OF DUMBBELLS

Execution of the welds at stiffening rings may cause distortion of the inner cavity surface in the region of the weld. This distortion should be less than 0.4 mm in depth as measured over a region ~ 5 mm x 5 mm. Local distortion must be investigated by performing test welds and frequency measurements. Results must be approved by FNAL.

Prior to production welding, the contractor will provide e-beam weld samples to FNAL to be evaluated for RRR values in the weld region. Components must be jointly inspected with FNAL.

6.5 FREQUENCY MEASUREMENT OF DUMBBELLS

Evaluation of the frequency measurements and determination of the amount of material to trim from the dumbbell equators will be agreed upon jointly by the contractor and FNAL.

6.6 ANODIZING

Anodizing is not necessary. Strict handling procedures must be followed.

7. WELDING OF CAVITY

Preparation of the equator joints for EB welding will be by the method of choice of the contractor. The proposed method must be approved by FNAL.

Equator welds on Batch 2 cavities must not be made until Batch 1 cavities have been processed and tested. Equator welds on Batch 3 cavities must not be made until Batch 2 cavities have been processed and tested.

13.1 LIST OF PARTS

The Appendix of this document lists the material required to fabricate one nine-cell 1.3 GHz SCRF cavity with symmetric end tubes.

13.5 & 13.6 WELDING PREPARATION/GENERAL ELECTRON BEAM WELDING CONDITIONS

All niobium components must undergo a 20 μ m BCP etch after the final machining operation and before welding. If more than eight hours (< 5 days) is expected to expire between the 20 μ m etch and welding, the parts must be stored in a vacuum vessel evacuated to less than 0.05 atm and backfilled with nitrogen, argon or other inert gas. The parts must be stored in the vessel such that the edges to be welded do not touch any surface. Once exposed to air, welding must occur within two hours. **It is mandatory that surfaces to be welded do not come in contact with any foreign body or surface before welding.**

If parts which have undergone the primary 20 μ m BCP etch have exceeded the eight hour requirement, or have been stored under vacuum for five or more days, they must undergo a secondary 3 μ m BCP etch before welding. After the 3 μ m BCP etch, the same storage requirements as above apply.

Vacuum pumps on the EB welding machine must be oil-free or utilize silicone-free lubricants.

The contractor may use a method of his choice to execute full penetration fusion welds; e.g., butt welds or step joint welds.

13.13 QUALITY CONTROL

A copy of the Quality Control (QC) document [2] or equivalent traveler will follow each cavity through the fabrication process. The contractor will record required dimensional measurements and tolerances listed in the QC document. Any deviations will be rectified by the contractor or discussed with FNAL.

4. REFERENCES

- [1] "DESY Specification of Welded 1.3 GHz Superconducting Resonators for TTF/VUV-FEL", D. Proch, MHF-SL 09-2005.
- [2] English translation of the DESY Quality Control (QC) Document.
- [3] "Technical Specifications for High RRR Grade Niobium Sheet and Rod for use in Superconducting Cavities", Lance Cooley, 5500-ES-371037 Revision A, July 9, 2007.

11/12/2009

p. 6 of 7

5. APPENDIX

Parts List for 1.3 GHz 9-cell SCRF Cavity

Quality	Material (dimensions/tolerances)	Application	Quantity
RRR300	Nb sheet 265 x 265 x 2.8 +/- 0.1 mm	Half cells	18
Nb55Ti	NbTi plate Ø205 x 25 + 1.0/- 0.0 mm	End cap disks	2
RRR300	Nb sheet 3 +/- 0.15 x 415 x 230 mm	Stiffening rings	1
RRR300	Nb sheet 300 x 100 x 10 +/- 0.2 mm	F-parts	1
RRR300	Seamless Nb tube ID 78 +/- 0.2 x 3.0 +/- 0.3 x 115 mm	End tubes Spool pieces	2
RRR300	Seamless Nb tube ID 40 +/- 0.15 x 2.5 +/- 0.15 x 50 mm	Main coupler tube	1
RRR300	Forged Nb ring 135 x 75 x 27 mm	End disk flanges	2
Nb55Ti	Rod Ø147 mm +/- 0.3 mm x 80 mm (forged, annealed & surface turned)	Beam tube, main coupler, HOM coupler and pick up port flanges	1
RRR300	Nb rod Ø 50 mm x 250 mm Long	HOM coupler housings	2
RRR300	Nb rod Ø 20.0 x 150 mm Long	HOM spool pieces Antenna spool piece	1

11/12.2009

p. 7 of 7

c. PRSTAB for ILC TESLA 1.3 GHz 9-cell Cavity

PHYSICAL REVIEW SPECIAL TOPICS - ACCELERATORS AND BEAMS, VOLUME 3, 092001 (2000)

Superconducting TESLA cavities

B. Aune,¹ R. Bandelmann,⁴ D. Bloess,² B. Bonin,^{1,*} A. Bosotti,⁷ M. Champion,⁵ C. Crawford,⁵ G. Deppe,⁴ B. Dwersteg,⁴ D. A. Edwards,^{4,5} H. T. Edwards,^{4,5} M. Ferrario,⁶ M. Fouaidy,⁹ P.-D. Gall,⁴ A. Gamp,⁴ A. Gössel,⁴ J. Graber,^{4,7} D. Hubert,⁴ M. Hüning,⁴ M. Juillard,¹ T. Junquera,⁹ H. Kaiser,⁴ G. Kreps,⁴ M. Kuchnir,⁵ R. Lange,⁴ M. Leenen,⁴ M. Liepe,⁴ L. Lilje,⁴ A. Matheisen,⁴ W.-D. Möller,⁴ A. Mosnier,⁷ H. Padamsee,³ C. Pagani,⁷ M. Pekeler,^{4,7} H.-B. Peters,⁴ O. Peters,⁴ D. Proch,⁴ K. Rehlich,⁴ D. Reschke,⁴ H. Safa,¹ T. Schilcher,^{4,5} P. Schmüser,⁸ J. Sekutowicz,⁴ S. Simrock,⁴ W. Singer,⁴ M. Tigner,³ D. Trines,⁴ K. Twarowski,^{4,10} G. Weichert,⁴ J. Weisend,^{4,11} J. Wojtkiewicz,⁴ S. Wolff,⁴ and K. Zapfe⁴

¹CEA Saclay, Gif-sur-Yvette, France

²CERN, Geneva, Switzerland

³Cornell University, Ithaca, New York

⁴Deutsches Elektronen-Synchrotron, Hamburg, Germany

⁵FNAL, Batavia, Illinois

⁶INFN Frascati, Frascati, Italy

⁷INFN Milano, Milano, Italy

⁸II. Institut für Experimentalphysik, Universität Hamburg, Hamburg, Germany

⁹IPN, Orsay, Orsay, France

¹⁰Institute of Physics, Polish Academy of Sciences, Warsaw, Poland

(Received 19 April 2000; published 22 September 2000)

The conceptional design of the proposed linear electron-positron collider TESLA is based on 9-cell 1.3 GHz superconducting niobium cavities with an accelerating gradient of $E_{acc} \geq 25$ MV/m at a quality factor $Q_0 \geq 5 \times 10^9$. The design goal for the cavities of the TESLA Test Facility (TTF) linac was set to the more moderate value of $E_{acc} \geq 15$ MV/m. In a first series of 27 industrially produced TTF cavities the average gradient at $Q_0 = 5 \times 10^9$ was measured to be 20.1 ± 6.2 MV/m, excluding a few cavities suffering from serious fabrication or material defects. In the second production of 24 TTF cavities, additional quality control measures were introduced, in particular, an eddy-current scan to eliminate niobium sheets with foreign material inclusions and stringent prescriptions for carrying out the electron-beam welds. The average gradient of these cavities at $Q_0 = 5 \times 10^9$ amounts to 25.0 ± 3.2 MV/m with the exception of one cavity suffering from a weld defect. Hence only a moderate improvement in production and preparation techniques will be needed to meet the ambitious TESLA goal with an adequate safety margin. In this paper we present a detailed description of the design, fabrication, and preparation of the TESLA Test Facility cavities and their associated components and report on cavity performance in test cryostats and with electron beam in the TTF linac. The ongoing research and development towards higher gradients is briefly addressed.

PACS numbers: 84.40.-x, 41.20.-q, 41.75.Ht, 74.60.-w

I. INTRODUCTION

In the past 30 years, electron-positron collisions have played a central role in the discovery and detailed investigation of new elementary particles and their interactions. The highly successful standard model of the unified electromagnetic and weak interactions and quantum chromodynamics, the quantum field theory of quark-gluon interactions, are to a large extent based on the precise data

collected at electron-positron colliders. Important questions still remain to be answered, in particular, the origin of the masses of field quanta and particles—within the standard model explained in terms of the so-called Higgs mechanism—and the existence or nonexistence of supersymmetric particles which appear to be a necessary ingredient of any quantum field theory attempting to unify all four forces known in nature: the gravitational, weak, electromagnetic, and strong forces. There is general agreement in the high energy physics community that, in addition to the Large Hadron Collider under construction at CERN, a lepton collider will be needed to address these fundamental issues.

Electron-positron interactions in the center-of-mass (cm) energy range from 200 GeV to more than a TeV can no longer be realized in a circular machine such as LEP since the E^4 dependence of the synchrotron radiation loss would lead to prohibitive operating costs. Instead,

*Current address: CEA/IPSN, Fontenay, France.

¹Current address: Center for Advanced Biotechnology, Boston University, Boston, Massachusetts.

²Current address: ACCEL Instruments GmbH, Bergisch-Gladbach, Germany.

³Current address: Paul Scherrer Institut, Villigen, Switzerland.

¹¹Current address: SLAC, Stanford, California.

the linear collider concept must be employed. This new principle was successfully demonstrated with the Stanford Linear Collider (SLC) providing a cm energy of more than 90 GeV. Worldwide there are different design options towards the next generation of linear colliders in the 100 GeV to TeV regime. Two main routes are followed: colliders equipped with normal-conducting (nc) cavities (NLC, JLC, VLEPP, and CLIC) or with superconducting (sc) cavities (TESLA). The normal-conducting designs are based on high frequency structures (6 to 30 GHz), while the superconducting TESLA collider employs the comparatively low frequency of 1.3 GHz. The high conversion efficiency from primary electric power to beam power (about 20%) in combination with the small beam emittance growth in low-frequency accelerating structures makes the superconducting option an ideal choice for a high-luminosity collider.

The first international TESLA workshop was held in 1990 [1]. At that time superconducting rf cavities in particle accelerators were usually operated in the 5 MV/m regime. Such low gradients, together with the high cost of cryogenic equipment, would have made a superconducting linear electron-positron collider totally noncompetitive with the normal-conducting colliders proposed in the U.S. and Japan. The TESLA Collaboration, formally established in 1994 with the aim of developing a 500 GeV center-of-mass energy superconducting linear collider, set out with the ambitious goal of increasing the cost effectiveness of the superconducting option by more than 1 order of magnitude: first, by raising the accelerating gradient by a factor of 5 from 5 to 25 MV/m, and, second, by reducing the cost per unit length of the linac by using economical cavity production methods and a greatly simplified cryostat design. Important progress has been achieved in both directions; in particular, the gradient of 25 MV/m is essentially in hand, as will be shown below. To allow for a gradual improvement in the course of the cavity research and development (R&D) program, a more moderate goal of 15 MV/m was set for the TESLA Test Facility (TTF) linac [2].

The TESLA cavities are quite similar in their layout to the 5-cell 1.5 GHz cavities of the electron accelerator CEBAF in Newport News, Virginia, which were made by an industrial company [3]. These cavities exceeded the specified gradient of 5 MV/m considerably and, hence, offered the potential for further improvement. While the CEBAF cavity fabrication methods were adopted for TTF without major modifications, important new steps were introduced in the cavity preparation: (i) chemical removal of a thicker surface layer, (ii) a 1400 °C annealing with titanium getter to improve the Nb heat conductivity and to homogenize the material, (iii) rinsing with ultrapure water at high pressure (100 bar) to remove surface contaminants, and (iv) destruction of field emitters by a technique called high power processing.

The application of these techniques, combined with extremely careful handling of the cavities in a clean room

environment, has led to a significant increase in accelerating field.

The TTF has been set up at DESY to provide the necessary infrastructure for the chemical and thermal treatment, clean room assembly, and testing of industrially produced multicell cavities. In addition, a 500 MeV electron linac is being built as a test bed for the performance of the sc accelerating structures with an electron beam of high bunch charge. At present, more than 30 institutes from Armenia, People's Republic of China, Finland, France, Germany, Italy, Poland, Russia, and the U.S. participate in the TESLA Collaboration and contribute to TTF.

The low frequency of 1.3 GHz permits the acceleration of long trains of particle bunches with very low emittance making a superconducting linac an ideal driver of a free electron laser (FEL) in the vacuum ultraviolet and x-ray regimes. For this reason, the TTF linac has recently been equipped with undulator magnets, and its energy will be upgraded to 1 GeV in the coming years to provide an FEL user facility in the nanometer wavelength range. An x-ray FEL facility with wavelengths below 1 Å is an integral part of the TESLA collider project [4].

The present paper is organized as follows: Sec. II is devoted to the basics of rf superconductivity and the properties and limitations of superconducting cavities for particle acceleration. The design of the TESLA cavities and the auxiliary equipment are presented in Sec. III. The fabrication and preparation steps of the cavities are described in Sec. IV. The test results obtained on all TTF cavities are presented in Sec. V, together with a discussion of errors and limitations encountered during cavity production at industry and the quality control measures taken. The rf control and cavity performance with electron beam in the TTF linac are described in Sec. VI. A summary and outlook are given in Sec. VII, where the ongoing research towards higher gradients is also briefly addressed.

II. BASICS OF RF SUPERCONDUCTIVITY AND PROPERTIES OF SUPERCONDUCTING CAVITIES FOR PARTICLE ACCELERATION

A. Basic principles of rf superconductivity and choice of superconductor

The existing large scale applications of superconductors in accelerators are twofold: in magnets and in accelerating cavities. While there are some common requirements, such as the demand for as high a critical temperature as possible,¹ there are also characteristic differences. In magnets operated with a dc or a low-frequency ac current, the

¹The high- T_c ceramic superconductors have not yet found widespread application in magnets mainly due to technical difficulties in cable production and coil winding. Cavities with high- T_c sputter coatings on copper have shown much inferior performance in comparison to niobium cavities.

so-called “hard” superconductors are needed featuring high upper critical magnetic fields (15–20 T) and strong flux pinning in order to obtain high critical current density; such properties can only be achieved using alloys such as niobium-titanium or niobium-tin. In microwave applications the limitation of the superconductor is not given by the upper critical field but rather by the so-called “superheating field” which is well below 1 T for all known superconductors. Moreover, strong flux pinning appears undesirable in microwave cavities as it is coupled with hysteretic losses. Hence a “soft” superconductor must be used and pure niobium is still the best candidate although its critical temperature is only 9.2 K and the superheating field about 240 mT. Niobium-tin (Nb₃Sn) looks more favorable at first sight since it has a higher critical temperature of 18 K and a superheating field of 400 mT; however, the gradients achieved in Nb₃Sn coated single-cell copper cavities were below 15 MV/m, probably due to grain boundary effects in the Nb₃Sn layer [5]. For these reasons the TESLA Collaboration decided to use niobium as the superconducting material, as in all other large scale installations of sc cavities. Here two alternatives exist: the cavities are fabricated from solid niobium sheets or a thin niobium layer is sputtered onto the inner surface of a copper cavity. Both approaches have been successfully applied, the former at Cornell (CESR), KEK (TRISTAN), DESY (PETRA, HERA), Darmstadt (SDALINAC), Jefferson Lab (CEBAF), and other laboratories, the latter, in particular, at CERN in the electron-positron storage ring LEP. From the test results on existing cavities, the solid-niobium approach promised higher accelerating gradients, hence it was adopted as the baseline for the TTF cavity R&D program.

1. Surface resistance

In contrast to the dc case, superconductors are not free from energy dissipation in microwave fields. The reason is that the rf magnetic field penetrates a thin surface layer and induces oscillations of the electrons which are not bound in Cooper pairs. The number of these “free electrons” drops exponentially with temperature. According to the Bardeen-Cooper-Schrieffer (BCS) theory of superconductivity the surface resistance in the range $T < T_c/2$ is given by the expression

$$R_{\text{BCS}} \propto \frac{\omega^2}{T} \exp(-1.76T_c/T), \quad (2.1)$$

where $f = \omega/2\pi$ is the microwave frequency. In the two-fluid model of superconductors one can derive a refined expression for the surface resistance [6,7]

$$R_{\text{BCS}} = \frac{1}{2} \omega^2 \mu_0^2 \Lambda^3 \sigma_n. \quad (2.2)$$

Here σ_n is the normal-state conductivity of the material, and Λ is an effective penetration depth, given by

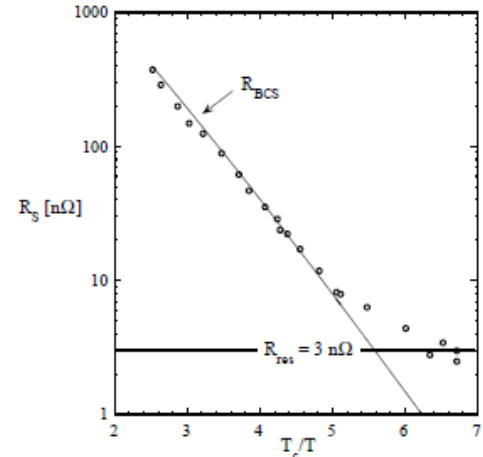


FIG. 1. The surface resistance of a 9-cell TESLA cavity plotted as a function of T_c/T . The residual resistance of 3 nΩ corresponds to a quality factor of $Q_0 = 10^{11}$.

$$\Lambda = \lambda_L \sqrt{1 + \xi_0/\ell},$$

where λ_L is the London penetration depth, ξ_0 is the coherence length, and ℓ is the mean free path of the unpaired electrons. The fact that σ_n is proportional to the mean free path ℓ leads to the surprising conclusion that the surface resistance does not assume its minimum value when the superconductor is as pure as possible ($\ell \gg \xi_0$) but rather in the range $\ell \approx \xi_0$. For niobium, the BCS surface resistance at 1.3 GHz amounts to about 800 nΩ at 4.2 K and drops to 15 nΩ at 2 K; see Fig. 1. The exponential temperature dependence is the reason that operation at 1.8–2 K is essential for achieving high accelerating gradients in combination with very high quality factors. Superfluid helium is an excellent coolant owing to its high heat conductivity.

In addition to the BCS term there is a residual resistance R_{res} caused by impurities, frozen-in magnetic flux, or lattice distortions. This term is temperature independent and amounts to a few nΩ for very pure niobium but may readily increase if the surface is contaminated.

2. Heat conduction in niobium

The heat produced at the inner cavity surface has to be guided through the cavity wall to the superfluid helium bath. Two quantities characterize the heat flow: the thermal conductivity of the bulk niobium and the temperature drop at the niobium-helium interface caused by the Kapitza resistance. For niobium with a residual resistivity

ratio² RRR of $\mathcal{R}_{\text{RRR}} = 500$, the two contributions to the temperature rise at the inner cavity surface are about equal. The thermal conductivity of niobium at cryogenic temperatures scales approximately with the RRR, a rule of thumb being

$$\lambda(4.2 \text{ K}) \approx 0.25 \mathcal{R}_{\text{RRR}} [\text{W/mK}].$$

However, λ is strongly temperature dependent and drops by about 1 order of magnitude when lowering the temperature to 2 K, as shown in Fig. 2.

Impurities influence the RRR and the thermal conductivity of niobium. Bulk niobium is contaminated by interstitial (mostly hydrogen, carbon, nitrogen, oxygen) and metallic impurities (mostly tantalum). The resulting RRR can be calculated by summing the individual contributions [10]

$$\mathcal{R}_{\text{RRR}} = \left(\sum_i f_i / r_i \right)^{-1}, \quad (2.3)$$

where the f_i denotes the fractional contents of impurity i (measured in wt. ppm) and the r_i denotes the corresponding resistivity coefficients which are listed in Table I.

A good thermal conductivity is the main motivation for using high purity niobium with RRR ≈ 300 as the material for cavity production. The RRR may be further improved by postpurification of the entire cavity (see Sec. V).

The Kapitza conductance depends on temperature and surface conditions. For pure niobium in contact

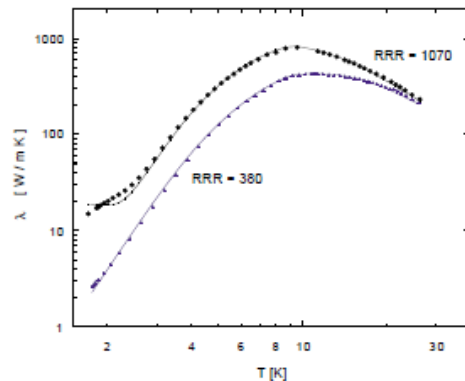


FIG. 2. The measured heat conductivity in niobium as a function of temperature [8]. Continuous curves: parametrization by Bonin, using the RRR and the average grain size as input parameters [9]. These data do not show an enhancement at 2 K (the so-called “phonon peak”) which was observed in some earlier experiments [5].

²RRR is defined as the ratio of the resistivities at room temperature and at liquid helium temperature. The low temperature resistivity is measured either just above T_c or at 4.2 K, applying a magnetic field to assure the normal state.

TABLE I. Resistivity coefficients of common impurities in Nb [10].

Impurity atom i	N	O	C	H	Ta
r_i in 10^4 wt. ppm	0.44	0.58	0.47	0.36	111

with superfluid helium at 2 K it amounts to about $6000 \text{ W}/(\text{m}^2\text{K})$ [11].

3. Influence of magnetic fields

Superheating field. Superconductivity breaks down when the rf magnetic field exceeds the critical field of the superconductor. In the high frequency case the so-called superheating field is relevant which, for niobium, is about 20% higher than the thermodynamical critical field of 200 mT [12,13].

Trapped magnetic flux. Niobium is, in principle, a soft type II superconductor without flux pinning. In practice, however, weak magnetic dc fields are not expelled upon cooldown but remain trapped in the niobium. Each flux line contains a normal-conducting core whose area is roughly $\pi \xi_0^2$. The coherence length ξ_0 amounts to 40 nm in Nb. Trapped magnetic dc flux therefore results in a surface resistance [6]

$$R_{\text{mag}} = (B_{\text{ext}}/2B_{c2})R_n, \quad (2.4)$$

where B_{ext} is the externally applied field, B_{c2} is the upper critical field, and R_n is the surface resistance in the normal state.³ At 1.3 GHz the surface resistance caused by trapped flux amounts to $3.5 \text{ n}\Omega/\mu\text{T}$ for niobium. Cavities which are not shielded from the Earth’s magnetic field are therefore limited to Q_0 values below 10^9 .

B. Advantages and limitations of superconducting cavities

The fundamental advantage of superconducting cavities is the extremely low surface resistance of about $10 \text{ n}\Omega$ at 2 K. The typical quality factors of normal conducting cavities are 10^4 – 10^5 while for sc cavities they may exceed 10^{10} , thereby reducing the rf losses by 5 to 6 orders of magnitude. In spite of the low efficiency of refrigeration there are considerable savings in primary electric power. Only a tiny fraction of the incident rf power is dissipated in the cavity walls, most of it is either transferred to the beam or reflected into a load.

The physical limitation of a sc resonator is given by the requirement that the rf magnetic field at the inner surface has to stay below the superheating field of the superconductor (200–240 mT for niobium). For the TESLA cavities this implies a maximum accelerating field of 50–60 MV/m. In principle, the quality factor should

³Benvenuti *et al.* [14] attribute the magnetic surface resistance in niobium sputter layers to flux flow.

stay roughly constant when approaching this fundamental superconductor limit, but in practice the “excitation curve” $Q_0 = Q_0(E_{acc})$ ends at considerably lower values, often accompanied with a strong decrease of Q_0 towards the highest gradient reached in the cavity. The main reasons for the performance degradation are excessive heating at impurities on the inner surface, field emission of electrons, and multipacting.⁴

Thermal instability and field emission

One basic limitation of the maximum field in a superconducting cavity is thermal instability. Temperature mapping at the outer cavity wall usually reveals that the heating by rf losses is not uniform over the whole surface but that certain spots exhibit larger temperature rises, often beyond the critical temperature of the superconductor. Hence the cavity becomes partially normal conducting, associated with strongly enhanced power dissipation. Because of the exponential increase of surface resistance with temperature, this may result in a runaway effect and eventually a quench of the entire cavity. Analytical models as well as numerical simulations are available to describe such an avalanche effect. Input parameters are the thermal conductivity of the superconductor, the size and resistance of the normal conducting spot, and the Kapitza resistance. The tolerable defect size depends on the RRR of the material and the desired field level. As a typical number, the diameter of a normal-conducting spot must exceed $50 \mu\text{m}$ to be able to initiate a thermal instability at 25 MV/m for $\text{RRR} > 200$.

There have been many attempts to identify defects which were localized by temperature mapping. Examples of defects are drying spots, fibers from tissues, foreign material inclusions, weld splatter, and cracks in the welds. There are two obvious and successful methods for reducing the danger of thermal instability: (i) avoid defects by preparing and cleaning the cavity surface with extreme care

⁴“Multipacting” is a commonly used abbreviation for “multiple impacting” and designates the resonant multiplication of field emitted electrons which gain energy in the rf electromagnetic field and impact on the cavity surface where they induce secondary electron emission.

and (ii) increase the thermal conductivity of the superconductor. Considerable progress has been achieved in both aspects over the past ten years.

Field emission of electrons from sharp tips is the most severe limitation in high-gradient superconducting cavities. In field-emission loaded cavities, the quality factor drops exponentially above a certain threshold and x rays are observed. The field emission current density is given by the Fowler-Nordheim equation [15]

$$j_{\text{FE}} = c_1 E_{\text{loc}}^{2.5} \exp\left(-\frac{c_2}{\beta E_{\text{loc}}}\right), \quad (2.5)$$

where E_{loc} is the local electric field, β is a so-called field enhancement factor, and c_1 and c_2 are constants. There is experimental evidence that small particles on the cavity surface (e.g., dust) act as field emitters. Therefore, perfect cleaning, for example by high-pressure water rinsing, is the most effective remedy against field emission. By applying this technique it has been possible to raise the threshold for field emission in multicell cavities from about 10 MV/m to more than 20 MV/m in the past few years.

The topics of thermal instability and field emission are discussed at much greater detail in the book by Padamsee, Knobloch, and Hays [16].

III. DESIGN OF THE TESLA CAVITIES

A. Overview

The TTF cavity is a 9-cell standing wave structure of about 1 m length whose lowest TM mode resonates at 1300 MHz . A photograph is shown in Fig. 3. The cavity is made from solid niobium and is cooled by superfluid helium at 2 K .

Each 9-cell cavity is equipped with its own titanium helium tank, a tuning system driven by a stepping motor, a coaxial rf power coupler capable of transmitting more than 200 kW , a pickup probe, and two higher-order mode (HOM) couplers. To reduce the cost for cryogenic installations, eight cavities and a superconducting quadrupole are mounted in a common vacuum vessel and constitute the so-called cryomodule of the TTF linac, shown in Fig. 4. Within the module the cavity beam pipes are joined by stainless steel bellows and flanges with metallic gaskets. The cavities are attached to a rigid 300 mm diameter helium supply tube which provides positional accuracy of the cavity axes of better than 0.5 mm . Invar rods ensure



FIG. 3. Superconducting 1.3 GHz 9-cell cavity for the TESLA Test Facility.

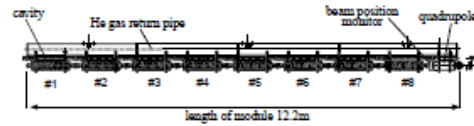


FIG. 4. Cryogenic module of the TESLA Test Facility linac comprising eight 9-cell cavities and a superconducting quadrupole.

that the distance between adjacent cavities remains constant during cooldown. Radiation shields at 5 and 60 K together with 30 layers of superinsulation limit the static heat load on the 2 K level to less than 3 W for the 12 m long module.

B. Layout of the TESLA cavities

1. Choice of frequency

The losses in a microwave cavity are proportional to the product of conductor area and surface resistance. For a given length of a multicell resonator, the area scales with $1/f$ while the surface resistance of a superconducting cavity scales with f^2 for $R_{BCS} \gg R_{res}$ and is independent of f for $R_{BCS} \ll R_{res}$. At an operating temperature $T = 2$ K, the BCS term dominates above 3 GHz and, hence, the losses grow linearly with frequency, whereas, for frequencies below 300 MHz, the residual resistance dominates and the losses grow with $1/f$. To minimize the dissipation in the cavity wall one should therefore select f in the range 300 MHz to 3 GHz.

Cavities in the 350 to 500 MHz regime are in use in electron-positron storage rings. Their large size is advantageous to suppress wake field effects and higher-order mode losses. However, for a linac of several 10 km length the niobium and cryostat costs for these bulky cavities would be prohibitive, hence a higher frequency has to be chosen. Considering material costs $f = 3$ GHz might appear the optimum, but there are compelling arguments for choosing about half this frequency:

(i) The wake field losses scale with the second to third power of the frequency ($W_{||} \propto f^2$, $W_{\perp} \propto f^3$). Beam emittance growth and beam-induced cryogenic losses are therefore much higher at 3 GHz.

(ii) The f^2 dependence of the BCS resistance sets an upper limit⁵ of about 30 MV/m at 3 GHz, hence, choosing this frequency would definitely preclude a possible upgrade of TESLA to 35–40 MV/m [17].

The choice for 1.3 GHz was motivated by the availability of high power klystrons.

⁵See Fig. 11.22 in [16].

2. Cavity geometry

A multicell resonator is advantageous for maximizing the active acceleration length in a linac of a given size. With the increasing number of cells per cavity, however, difficulties arise from trapped modes, uneven field distribution in the cells, and too high power requirements on the input coupler. Extrapolating from the experience with 4-cell and 5-cell cavities, a 9-cell structure appeared manageable. A side view of the TTF cavity with the beam tube sections and the coupler ports is given in Fig. 5.

The design of the cell shape was guided by the following considerations: (i) a spherical contour near the equator with low sensitivity for multipacting, (ii) minimization of electric and magnetic fields at the cavity wall to reduce the danger of field emission and thermal breakdown, and (iii) a large iris radius to reduce wake field effects.

The shape of the cell was optimized using the code URMEL [18]. The resonator is operated in the π mode with 180° phase difference between adjacent cells. The longitudinal dimensions are determined by the condition that the electric field has to be inverted in the time a relativistic particle needs to travel from one cell to the next. The separation between two irises is therefore $c/(2f)$. The iris radius R_{iris} influences the cell-to-cell coupling⁶ k_{cell} , the excitation of higher-order modes, and other important cavity parameters, such as the ratio of the peak electric (magnetic) field at the cavity wall to the accelerating field and the ratio (R/Q) of shunt impedance to the quality factor. For the TESLA Test Facility cavities, $R_{iris} = 35$ mm was chosen, leading to $k_{cell} = 1.87\%$ and $E_{peak}/E_{acc} = 2$. The most important parameters are listed in Table II.

The contour of a half-cell is shown in Fig. 6. It is composed of a circular arc around the equator region and an elliptical section near the iris. The dimensions are listed in Table III. The half-cells at the end of the 9-cell resonator need a slightly different shape to ensure equal field amplitudes in all 9 cells. In addition, there is a slight asymmetry

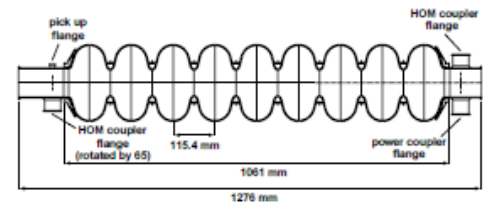


FIG. 5. Side view of the 9-cell TTF cavity with the ports for the main power coupler and two HOM couplers.

⁶The coupling coefficient is related to the frequencies of the coupled modes in the 9-cell resonator by the formula $f_n = f_0/\sqrt{1 + 2k_{cell}\cos(n\pi/9)}$ where f_0 is the resonant frequency of a single cell and $1 \leq n \leq 9$.

TABLE II. TTF cavity design parameters.^a

Type of accelerating structure	Standing wave
Accelerating mode	TM ₀₁₀ , π mode
Fundamental frequency	1300 MHz
Design gradient E_{acc}	25 MV/m
Quality factor Q_0	$>5 \times 10^9$
Active length L	1.038 m
Number of cells	9
Cell-to-cell coupling	1.87%
Iris diameter	70 mm
Geometry factor	270 Ω
R/Q	518 Ω
E_{peak}/E_{acc}	2.0
B_{peak}/E_{acc}	4.26 mT MV ⁻¹ m ⁻¹
Tuning range	± 300 kHz
$\Delta f/\Delta L$	315 kHz/mm
Lorentz force detuning at 25 MV/m	≈ 600 Hz
Q_{ext} of input coupler	3×10^6
Cavity bandwidth at $Q_{ext} = 3 \times 10^6$	430 Hz
rf pulse duration	1330 μ s
Repetition rate	5 Hz
Fill time	530 μ s
Beam acceleration time	800 μ s
rf power peak/average	208 kW/1.4 kW
Number of HOM couplers	2
Cavity longitudinal loss factor $k_{ }$ for $\sigma_z = 0.7$ mm	10.2 V/pC
Cavity transversal loss factor k_{\perp} for $\sigma_z = 0.7$ mm	15.1 VpC ⁻¹ m ⁻¹
Parasitic modes with the highest impedance: type	TM ₀₁₁
$\pi/9$ (R/Q)/frequency	80 Ω /2454 MHz
$2\pi/9$ (R/Q)/frequency	67 Ω /2443 MHz
Bellows longitudinal loss factor $k_{ }$ for $\sigma_z = 0.7$ mm	1.54 V/pC
Bellows transversal loss factor k_{\perp} for $\sigma_z = 0.7$ mm	1.97 VpC ⁻¹ m ⁻¹

^aFollowing common usage in ac circuits and the convention adopted in Ref. [19], p. 523, we define the shunt impedance by the relation $R = V^2/2P$, where P is the dissipated power and V is the peak voltage in the equivalent parallel LCR circuit. Note that another definition is common, which has also been used in the TESLA Conceptual Design Report, $R = V^2/P$, leading to a factor of 2 larger shunt impedance.

between the left and right end cell which prevents trapping of higher-order modes (see Sec. III E).

3. Lorentz-force detuning and cavity stiffening

The electromagnetic field exerts a Lorentz force on the currents induced in a thin surface layer. The resulting pressure acting on the cavity wall

$$p = \frac{1}{4}(\mu_0 H^2 - \epsilon_0 E^2) \quad (3.1)$$

leads to a deformation of the cells in the μ m range and a change ΔV of their volume. The consequence is a frequency shift according to Slater's rule

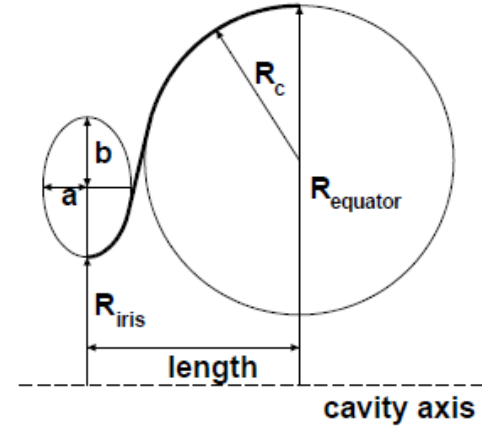


FIG. 6. Contour of a half-cell.

$$\frac{\Delta f}{f_0} = \frac{1}{4W} \int_{\Delta V} (\epsilon_0 E^2 - \mu_0 H^2) dV. \quad (3.2)$$

Here,

$$W = \frac{1}{4} \int_V (\epsilon_0 E^2 + \mu_0 H^2) dV \quad (3.3)$$

is the stored energy and f_0 is the resonant frequency of the unperturbed cavity. The computed frequency shift at 25 MV/m amounts to 900 Hz for an unstiffened cavity of 2.5 mm wall thickness. The bandwidth of the cavity equipped with the main power coupler ($Q_{ext} = 3 \times 10^6$) is about 430 Hz, hence, a reinforcement of the cavity is needed. Niobium stiffening rings are welded in between adjacent cells as shown in Fig. 7. They reduce the frequency shift to about 500 Hz for a 1.3 ms long rf pulse⁷; see Fig. 26.

The deformation of the stiffened cell is negligible near the iris where the electric field is large, but remains nearly the same as in the unstiffened cell near the equator where the magnetic field dominates. The deformation in this region can be reduced only by increasing the wall thickness.

TABLE III. Half-cell shape parameters (all dimensions in mm).

Cavity shape parameter	Midcup	Endcup 1	Endcup 2
Equator radius R_{equat}	103.3	103.3	103.3
Iris radius R_{iris}	35	39	39
Radius R_{arc} of circular arc	42.0	40.3	42
Horizontal half axis a	12	10	9
Vertical half axis b	19	13.5	12.8
Length l	57.7	56.0	57.0

⁷Part of this shift is due to an elastic deformation of the tuning mechanism.

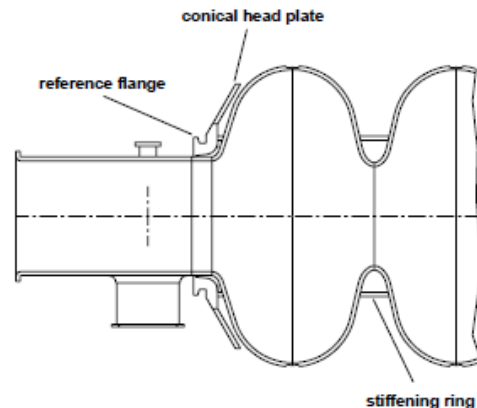


FIG. 7. The end section of a cavity with stiffening ring, conical head plate for welding into the helium tank, and reference flange for alignment.

4. Magnetic shielding

As shown in Sec. II A 3, the ambient magnetic field must be shielded to a level of about a μT to reduce the magnetic surface resistance to a few $\text{n}\Omega$. This is accomplished with a two-stage passive shielding, provided by the conventional steel vacuum vessel of the cryomodule and a high-permeability cylinder around each cavity. To remove the remanence from the steel vessel, the usual demagnetization technique is applied. The resulting attenuation of the ambient field is found to be better than expected from a cylinder without any remanence. The explanation is that the procedure does not really demagnetize the steel but rather *remagnetizes* it in such a way that the axial component of the ambient field is counteracted. This interpretation (see also Ref. [20]) becomes obvious if the cylinder is turned by 180° : in that case the axial field measured inside the steel cylinder is almost twice as large as the ambient longitudinal field component; see Fig. 8(a).

The shielding cylinders of the cavities are made from Cryoperm⁸ which retains a high permeability of more than 10 000 when cooled to liquid helium temperature. Figure 8(b) shows the measured horizontal, vertical, and axial components inside a cryoperm shield at room temperature, which was exposed to the Earth's field. The combined action of remagnetized vacuum vessel and cryoperm shield is more than adequate to reduce the ambient field to the level of some μT . An exception is the end cells of the first and the last cavity near the end of the cryomodule where the vessel is not effective in attenuating longitudinal fields. Here an active field compensation by means of Helmholtz

⁸Cryoperm is made by Vacuumschmelze Hanau, Germany.

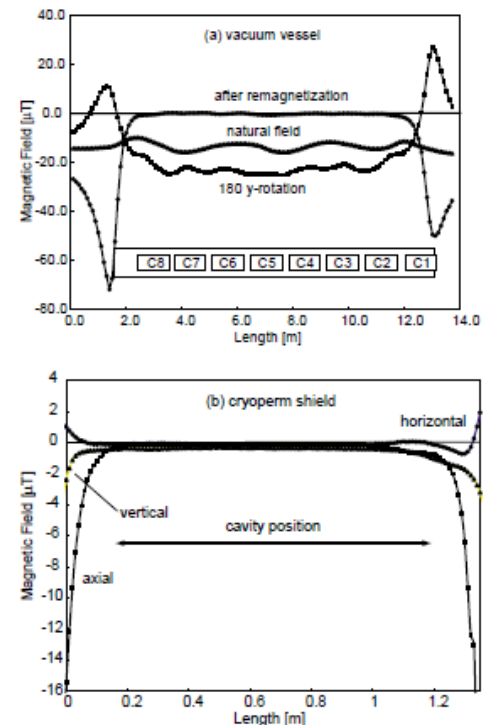


FIG. 8. Shielding of the Earth's magnetic field. (a) Shielding of an axial component by the steel vacuum vessel of the cryomodule. Also shown is the arrangement of the cavity string in the vessel. (b) Shielding of the axial, horizontal, and vertical field components by the cryoperm cylinder surrounding the cavity (measured without vacuum vessel).

coils could reduce the fringe field at the last cavity to a harmless level.

C. Helium vessel and tuning system

The helium tank contains the superfluid helium needed for cooling and serves at the same time as a mechanical support of the cavity and as a part of the tuning mechanism. The tank is made from titanium whose differential thermal contraction relative to niobium is 20 times smaller than for stainless steel. Cooldown produces a stress of only 3 MPa in a cavity that was stress free at room temperature. Titanium has the additional advantage that it can be directly electron-beam (EB) welded to niobium while stainless steel-niobium joints would require an intermediate metal layer.

The assembly of the cavity and helium tank proceeds in the following sequence: a titanium bellows is electron-beam welded to the conical Nb head plate at one side of the cavity, a titanium ring is EB welded to the conical Nb

head plate at the other side (see Fig. 7). The cavity is then inserted into the tank and the bellows as well as the titanium ring are tungsten inert gas (TIG) welded to the Ti vessel.

The tuning system consists of a stepping motor with a gear box and a double lever arm. The moving parts operate at 2 K in vacuum. The tuning range is about ± 1 mm, corresponding to a frequency range of ± 300 kHz. The resolution is 1 Hz. The tuning system is adjusted in such a way that after cooldown the cavity is always under compressive force to avoid a backlash if the force changes from pushing to pulling.

D. Main power coupler

1. Design requirements

A critical component of a superconducting cavity is the power input coupler. Several coaxial couplers have been developed for TIF [21], consisting of a "cold part," which is mounted on the cavity in the clean room and closed by a ceramic window, and a "warm part," which is assembled after installation of the cavity in the cryomodule. The warm section contains the transition from waveguide to coaxial line. This part is evacuated and sealed against the air-filled waveguide by a second ceramic window. The elaborate two-window solution was chosen to get optimum protection of the cavity against contamination during mounting in the cryomodule and against window fracture during linac operation.

The couplers must allow for some longitudinal motion⁹ inside the 12 m long cryomodule when the cavities are cooled down from room temperature to 2 K. For this reason, bellows in the inner and outer conductors of the coaxial line are needed. Since the coupler connects the room-temperature waveguide with the 2 K cavity, a compromise must be found between a low thermal conductivity and a high electrical conductivity. This is achieved by several thermal intercepts and by using stainless steel pipes or bellows with a thin copper plating (10–20 μm) at the radio frequency surface. The design heat loads of 6 W at 70 K, 0.5 W at 4 K, and 0.06 W at 2 K have been undercut in practice.

2. Electrical properties

An instantaneous power of 210 kW has to be transmitted to provide a gradient of 25 MV/m for an 800 μs long beam pulse of 8 mA. The filling time of the cavity amounts to 530 μs and the decay time, after the beam pulse is over, to an additional 500 μs . At the beginning of the filling,

⁹The motion of the coupler ports is up to 15 mm in the first cryomodules but has been reduced to about 1 mm in the most recent cryostat design by fixing the distance between neighboring cavities with invar rods.

most of the rf wave is reflected leading to voltage enhancements by a factor of 2. The external quality factor of the coupler is $Q_{\text{ext}} = 3 \times 10^6$ at 25 MV/m. By moving the inner conductor of the coaxial line, Q_{ext} can be varied in the range 1×10^6 – 9×10^6 to allow not only for different beam loading conditions but also to facilitate an *in situ* high power processing of the cavities. This feature has proved extremely useful on several occasions to eliminate field emitters that entered the cavities at the last assembly stage.

3. Input coupler A

The coupler version A is shown in Fig. 9. It has a conical ceramic window at 70 K and a commercial planar waveguide window at room temperature.

A conical shape was chosen for the cold ceramic window to obtain broad band impedance matching. The Hewlett-Packard high frequency structure simulator program HFSS was used to model the window and to optimize the shape of the tapered inner conductor. The reflected power is below 1%. The ceramic window is made from Al_2O_3 with a purity of 99.5%. Oxygen-free high-conductance copper rings are brazed to the ceramic using Au/Cu (35%/65%) braze alloy. The inner conductors on each side of the ceramic are electron-beam welded, the outer conductors are TIG welded. The ceramic is coated on both sides with a 10 nm titanium nitride layer to reduce multipacting.

The waveguide-to-coaxial transition is realized using a cylindrical knob such as the impedance-transforming device and a planar waveguide window. Matching posts are required on the air side of the window for impedance matching at 1.3 GHz.

4. Input couplers B, C

Coupler version B also uses a planar waveguide window and a doorknob transition from the waveguide to the coaxial line, but a cylindrical ceramic window at 70 K without direct view of the beam. Because of a shortage in commercial waveguide windows, a third type, C, was developed using a cylindrical window also at the waveguide-

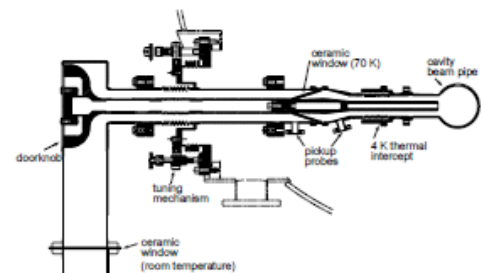


FIG. 9. A simplified view of the power input coupler version A.

coaxial transition. It features a 60 mm diameter coaxial line with reduced sensitivity to multipacting and the possibility of applying a dc potential to the center conductor. In the case of the LEP couplers [22], a dc bias has proved very beneficial in suppressing multipacting. Similar observations were made at DESY. All couplers needed some conditioning but have then performed according to specification.

E. Higher-order modes

The intense electron bunches excite eigenmodes of higher frequency in the resonator which must be damped to avoid multibunch instabilities and beam breakup. This is accomplished by extracting the stored energy via HOM couplers mounted on the beam pipe sections of the 9-cell resonator. A problem arises from “trapped modes” which are concentrated in the center cells and have a low field amplitude in the end cells. An example is the TE_{121} mode. By an asymmetric shaping of the end half-cells, one can enhance the field amplitude of the TE_{121} mode in one end cell while preserving the “field flatness” of the fundamental mode and also the good coupling of the HOM couplers to the untrapped modes TE_{111} , TM_{110} , and TM_{011} . The effects of asymmetric end cell tuning are sketched in Fig. 10.

The two polarization states of dipole modes would, in principle, require two orthogonal HOM couplers at each side of the cavity. In a string of cavities, however, this complexity can be avoided since the task of the “orthogonal” HOM coupler can be taken over by the HOM coupler of the neighboring cavity. The viability of this idea was verified in measurements.

HOM coupler design

The HOM couplers are mounted at both ends of the cavity with a nearly perpendicular orientation¹⁰ to ensure

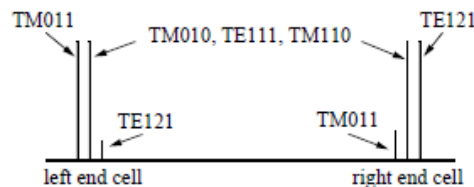


FIG. 10. The effect of asymmetric end cell shaping on various modes. The main accelerating mode TM_{010} and the higher modes TE_{111} and TM_{110} are not affected while TM_{011} is enhanced in the left end cell and TE_{121} is enhanced in the right end cell. Using HOM couplers at both ends, all higher-order modes can be extracted.

¹⁰The angle between the two HOM couplers is not 90° but 115° to also provide damping of quadrupole modes.

damping of dipole modes of either polarization. A 1.3 GHz notch filter is incorporated to prevent energy extraction from the accelerating mode. Two types of HOM couplers have been developed and tested, one mounted on a flange, the other welded to the cavity.

The demountable HOM coupler is shown in Fig. 11(a). An antenna loop couples mainly to the magnetic field for TE modes and to the electric field for TM modes. The pickup antenna is capacitively coupled to an external load. The 1.3 GHz notch filter is formed by the inductance of the loop and the capacity at the 1.9 mm wide gap between loop and wall. A niobium bellows permits tuning of the filter without opening the cavity vacuum. The antenna is thermally connected to the 2 K helium bath. In a continuous wave (cw) test at an accelerating field of 21 MV/m the antenna reached a maximum temperature of 4 K, which is totally uncritical.

The welded version of the HOM coupler is shown in Fig. 11(b). It resembles the couplers used in the 500 MHz HERA cavities which have been operating for several years without quenches. The good cooling of the superconducting inner conductor by two stubs makes the design insensitive to γ radiation and electron bombardment.

Both HOM couplers permit tuning of the fundamental mode rejection filter when mounted on the cavity. It is possible to achieve a Q_{ext} of more than 10^{11} thereby limiting power extraction to less than 50 mW at 25 MV/m.

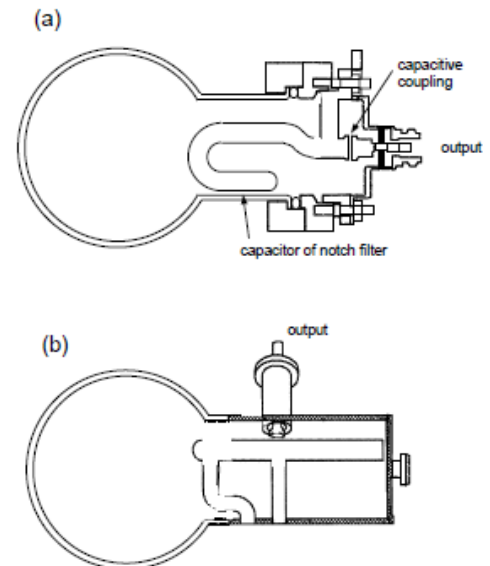


FIG. 11. The higher-order-mode couplers: (a) demountable HOM coupler and (b) welded HOM coupler.

IV. CAVITY FABRICATION AND PREPARATION

A. Cavity fabrication

1. Niobium properties

The 9-cell resonators are made from 2.8 mm thick sheet niobium by deep drawing of half-cells, followed by trimming and electron beam welding. Niobium of high purity is needed. Tantalum with a typical concentration of 500 ppm is the most important metallic impurity. Among the interstitially dissolved impurities, oxygen is dominant due to the high affinity of Nb for O₂ above 200°C. Interstitial atoms act as scattering centers for the unpaired electrons and reduce the RRR and the thermal conductivity; see Sec. II A. The niobium ingot is highly purified by several remelting steps in a high vacuum electron beam furnace. This procedure reduces the interstitial oxygen, nitrogen, and carbon contamination to a few ppm. The niobium specification for the TTF cavities is listed in Table IV.

After forging and sheet rolling, the 2.8 mm thick Nb sheets are degreased, a 5 μm surface layer is removed by etching, and then the sheets are annealed for 1–2 h at 700°C–800°C in a vacuum oven at a pressure of 10⁻⁵–10⁻⁶ mbar to achieve full recrystallization and a uniform grain size of about 50 μm.

2. Deep drawing and electron-beam welding

Half-cells are produced by deep drawing. The dies are usually made from a high yield strength aluminum alloy. To achieve the small curvature required at the iris, an additional step of forming, e.g., coining, may be needed. The half-cells are machined at the iris and the equator. At the iris the half-cell is cut to the specified length (allowing for weld shrinkage) while at the equator an extra length of 1 mm is left to retain the possibility of a precise length trimming of the dumbbell after frequency measurement (see below). The accuracy of the shape is controlled by sandwiching the half-cell between two metal plates and measuring the resonance frequency. The half-cells are thoroughly cleaned by ultrasonic degreasing, 20 μm chemical etching, and ultrapure water rinsing. Two half-cells are then joined at the iris with an EB weld to form a “dumbbell.” The EB welding is usually done from the

inside to ensure a smooth weld seam at the location of the highest electric field in the resonator. Since niobium is a strong getter material for oxygen, it is important to carry out the EB welds in a sufficiently good vacuum. Tests have shown that RRR = 300 niobium is not degraded by welding at a pressure of less than 5 × 10⁻⁵ mbar.

The next step is the welding of the stiffening ring. Here the weld shrinkage may lead to a slight distortion of the cell shape which needs to be corrected. Afterwards, frequency measurements are made on the dumbbells to determine the correct amount of trimming at the equators. After proper cleaning by a 30 μm etching, the dumbbells are visually inspected. Defects and foreign material imprints from previous fabrication steps are removed by grinding. After the inspection and proper cleaning (a few μm etching followed by ultraclean water rinsing and clean room drying), eight dumbbells and two beam-pipe sections with attached end half-cells are stacked in a precise fixture to carry out the equator welds which are done from the outside. The weld parameters are chosen to achieve full penetration. A reliable method for obtaining a smooth weld seam of a few mm width at the inner surface is to raster a slightly defocused beam in an elliptic pattern and to apply 50% of beam power during the first weld pass and 100% of beam power in the second pass.

B. Cavity treatment

Experience has shown that a damage layer of the order of 100 μm has to be removed from the inner cavity surface to obtain good rf performance in the superconducting state. The standard method applied at DESY and many other laboratories is called buffered chemical polishing (BCP), using an acid mixture of HF (48%), HNO₃ (65%), and H₃PO₄ (85%) in the ratio 1:1:2 (at CEBAF the ratio was 1:1:1). The preparation steps adopted at DESY for the industrially produced TTF cavities are as follows: A layer of 80 μm is removed by BCP from the inner surface and 30 μm from the outer surface.¹¹ The cavities are rinsed with ultraclean water and dried in a class 100 clean room. The next step is a 2 h annealing at 800°C in an ultrahigh vacuum (UHV) oven which serves to remove dissolved hydrogen from the niobium and relieves mechanical stress in the material. In the initial phase of the TTF program many cavities were tested after this step, applying a 20 μm BCP and ultraclean water rinsing before mounting in the cryostat and cooldown.

Presently, the cavities are rinsed with clean water after the 800°C treatment and then immediately transferred to another UHV oven in which they are heated to

TABLE IV. Technical specification for niobium used in TTF cavities

Impurity content in ppm (wt.)			Mechanical properties	
Ta	≤500	H ≤2	RRR	≥300
W	≤70	N ≤10	Grain size	≈50 μm
Ti	≤50	O ≤10	Yield strength	>50 MPa
Fe	≤30	C ≤10	Tensile strength	>100 MPa
Mo	≤50		Elongation at break	30%
Ni	≤30		Vickers hardness HV 10	≤50

¹¹These numbers are determined by weighing the cavity before and after etching and represent, therefore, the average over the whole surface. Frequency measurements indicate that more material is etched away at the iris than at the equator.

1350 °C–1400 °C. At this temperature, all dissolved gases diffuse out of the material and the RRR increases by about a factor of 2 to values around 500. To capture the oxygen coming out of the niobium and to prevent oxidation by the residual gas in the oven (pressure $<10^{-7}$ mbar), a thin titanium layer is evaporated on the inner and outer cavity surface, Ti being a stronger getter than Nb. The high-temperature treatment with Ti getter is often called postpurification. The titanium layer is removed afterwards by a 800 μm BCP of the inner surface. A BCP of about 30 μm is applied at the outer surface since the Kapitza resistance of titanium-coated niobium immersed in superfluid helium is about a factor of 2 larger than that of pure niobium [11]. After final heat treatment and BCP the cavities are mechanically tuned to adjust the resonance frequency to the design value and to obtain equal field amplitudes in all 9 cells. This is followed by a slight BCP, three steps of high-pressure water rinsing (100 bar), and drying in a class 10 clean room. As a last step, the rf test is performed in a superfluid helium bath cryostat.

A severe drawback of the postpurification is the considerable grain growth accompanied by a softening of the niobium. Postpurified-treated cavities are quite vulnerable to plastic deformation and have to be handled with great care.

V. RESULTS ON CAVITY PERFORMANCE AND QUALITY CONTROL MEASURES

A. Overview

Figure 12 shows the excitation curve of the best 9-cell resonator measured so far; plotted is the quality factor¹² Q_0 as a function of the accelerating electric field E_{acc} . An

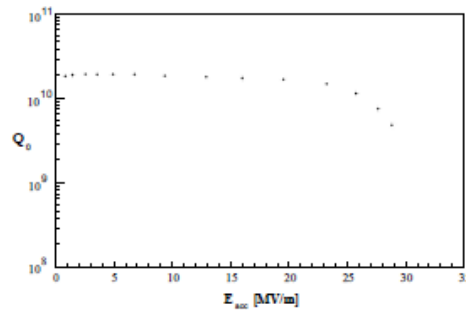


FIG. 12. Excitation curve of the best TESLA 9-cell cavity measured to date. The cavity was cooled by superfluid helium of 2 K.

¹²The quality factor is defined as $Q_0 = f/\Delta f$, where f is the resonance frequency and Δf is the full width at half height of the resonance curve of the “unloaded” cavity.

almost constant and high value of 2×10^{10} is observed up to 25 MV/m.

The importance of various cavity treatment steps for arriving at such a good performance is illustrated in the next figure. A strong degradation is usually observed if a foreign particle is sticking on the cavity surface, leading either to field emission of electrons or to local overheating in the rf field. At Cornell University an *in situ* method for destroying field emitters was invented [23], called “high power processing,” which in many cases can improve the high-field capability; see Fig. 13(a). Removal of field-emitting particles by high-pressure water rinsing, a technique developed at CERN [24], may dramatically improve the excitation curve [Fig. 13(b)]. The beneficial effect of a 1400 °C heat treatment, first tried out at Cornell [25] and Saclay [26], is seen in Fig. 13(c). Finally, an incomplete removal of the titanium surface layer in the BCP following the 1400 °C heat treatment may strongly limit the attainable gradient. Here additional BCP is advantageous [Fig. 13(d)].

B. Results from the first series of TTF cavities

After the successful test of two prototype 9-cell resonators, a total of 27 cavities equipped with main power and HOM coupler flanges were ordered at four European companies. These cavities were foreseen for installation in the TTF linac with an expected gradient of at least 15 MV/m at $Q_0 > 3 \times 10^9$. However, in the specification given to the companies no guaranteed gradient was required. According to the test results obtained at TTF these resonators can be classified into four categories: (1) 16 cavities without any known material and fabrication defects, or with minor defects which could be repaired; (2) three cavities with serious material defects; (3) six cavities with imperfect equator welds; (4) two cavities with serious fabrication defects (not fully penetrated electron beam welds or with holes burned during welding; these were rejected). One cavity has not yet been tested.

The test results for the cavities of class 1 in a vertical bath cryostat with superfluid helium cooling at 2 K are summarized in Fig. 14. It is seen that the TTF design goal of 15 MV/m is clearly exceeded. Nine of the resonators fulfill even the more stringent specification of TESLA ($E_{\text{acc}} \geq 25$ MV/m at $Q_0 \geq 5 \times 10^9$).

The excitation curves of the class 2 cavities (Fig. 15) are characterized by sudden drops in quality factor with increasing field and rather low maximum gradients.

Temperature mapping revealed spots of excessive heating at isolated spots which were far away from the EB welds. An example is shown in Fig. 16(a). The defective cell was cut from the resonator and subjected to further investigation [27]. An eddy-current scan, performed at the Bundesanstalt für Materialforschung (BAM) in Berlin, showed a pronounced signal at the defect location. With x-ray radiography, also carried out at BAM, a dark spot with

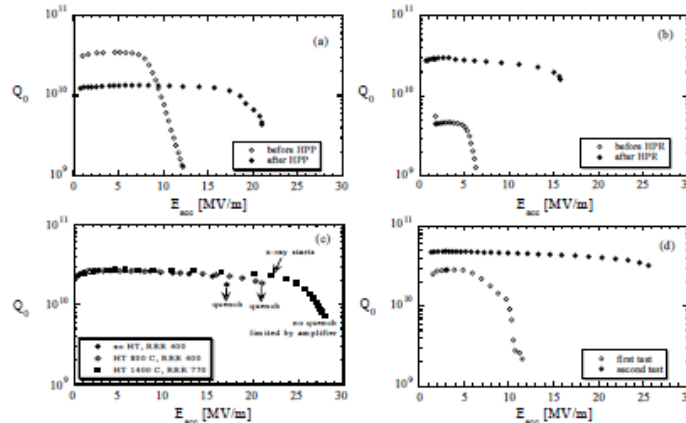


FIG. 13. Improvement in cavity performance due to various treatments: (a) high power processing (HPP), (b) high pressure water rinsing (HPR), (c) successive application of 800 °C and 1400 °C heat treatment (HT), and (d) removal of surface defects or titanium in grain boundaries by additional BCP.

a size of 0.2–0.3 mm was seen [Fig. 16(b)] indicating an inclusion of foreign material with a higher nuclear charge than niobium. Neutron absorption measurements at the Forschungszentrum GKSS in Geesthacht gave no signal, indicating that the neutron absorption coefficient of the unknown contamination was similar to that of Nb. The identification of the foreign inclusion was finally accomplished using x-ray fluorescence at the Hamburger Synchrotronstrahlungslabor (HASYLAB) at DESY. Fluorescence was observed at photon energies corresponding to the characteristic x-ray lines of tantalum $L_1 = 11.682$ keV, $L_2 = 11.136$ keV, and $L_3 = 9.881$ keV.

The synchrotron radiation fluorescence analysis method features sufficient sensitivity to perform a scan of the tantalum contents in the niobium by looking at the lines $TaK_{\alpha 1} = 57.532$ keV, $TaK_{\alpha 2} = 56.277$ keV, and $TaK_{\beta} = 65.223$ keV. The average Ta content in the bulk

Nb was about 200 ppm but rose to 2000 ppm in the spot region. The RRR dropped correspondingly from 330 to about 60.

The six cavities in class 3 were produced by one company and exhibited premature quenches at gradients of 10–14 MV/m and a slope in the $Q(E)$ curve (Fig. 17). Two of the resonators were investigated in greater detail [28]. Temperature mapping revealed strong heating at several spots on the equator weld [Fig. 18(b)]. The temperature rise as a function of the surface magnetic field is plotted in Fig. 18(c) for one sensor position above the weld and three positions on the weld. In the first case a growth proportional to B^2 is observed as expected for a constant surface resistance. On the weld, however, a much stronger rise is seen ranging from B^5 to B^8 . This is clear evidence for a contamination of the weld seam.

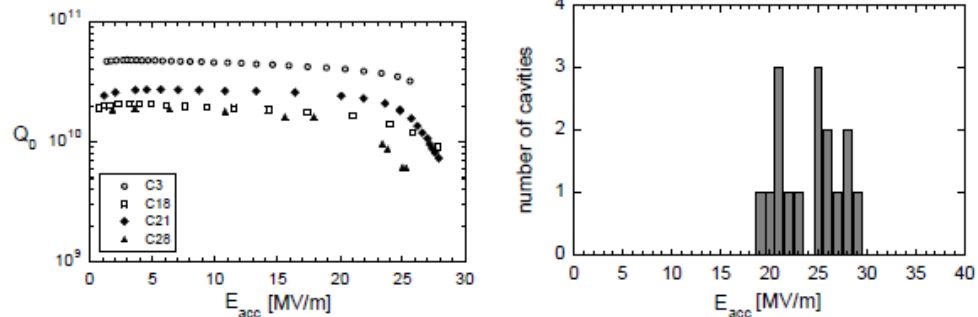


FIG. 14. (a) Excitation curves of the best 9-cell resonator of each of the four manufacturers. (b) Distribution of maximum gradients for the resonators of class 1, requiring a quality factor $Q_0 \geq 5 \times 10^9$.

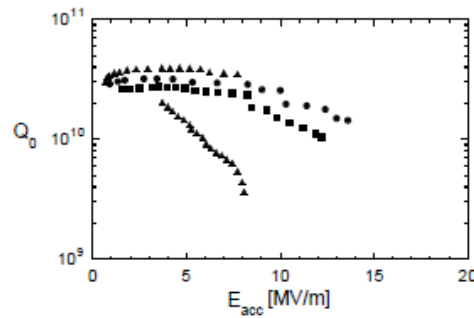


FIG. 15. Excitation curves of three cavities with serious material defects (class 2). Cavity C5 (▲) exhibited a jump in quality factor.

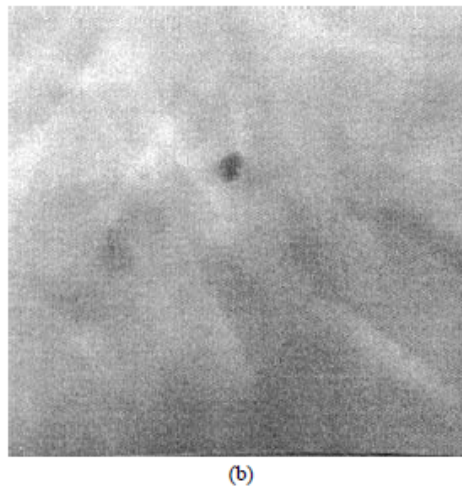
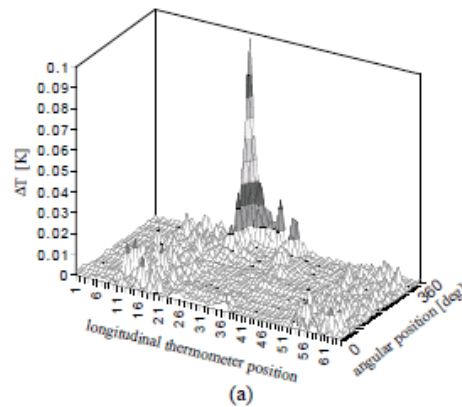


FIG. 16. (a) Temperature map of cell 5 of cavity C6 showing excessive heating at a localized spot. (b) Positive print of an x-ray radiograph showing the “hot spot” as a dark point.

092001-14

Once the reason for the reduced performance of the cavities in class 3 had been identified, a new 9-cell resonator was manufactured by the same company applying careful preparation steps of the weld region: a $2\ \mu\text{m}$ chemical etching not more than 8 h in advance of the EB welding, rinsing with ultrapure water and drying in a clean room. A rastered electron beam was used for welding with 50% penetration in the first weld layer and 100% in the second. The new cavity indeed showed excellent performance and achieved $24.5\ \text{MV/m}$; see Fig. 17. The same applies for later cavities made by this company.

The average gradient of the cavities without serious material or fabrication defects amounts to $20.1 \pm 6.2\ \text{MV/m}$ at $Q_0 = 5 \times 10^9$, where the error represents the rms of the distribution.

C. Diagnostic methods and quality control

The deficiencies encountered in the first series production of TESLA cavities have initiated the development of diagnostic methods and quality control procedures.

1. Electron microscopy

Scanning electron microscopy with energy-dispersive x-ray analysis (EDX) is used to identify foreign elements on the surface. Only a depth of about $1\ \mu\text{m}$ can be penetrated, so one has to remove layer by layer to determine the diffusion depth of titanium or other elements. Alternatively, one can cut the material and scan the cut region. The titanium layer applied in the high temperature treatment has been found to extend to a depth of about $10\ \mu\text{m}$ in the bulk niobium. The sensitivity of the EDX method is rather limited; a Ti fraction below 0.5% is undetectable. Auger electron spectroscopy offers higher sensitivity, and, using this method, titanium migration at grain boundaries has been found to a depth of $50\text{--}100\ \mu\text{m}$. Hence this large

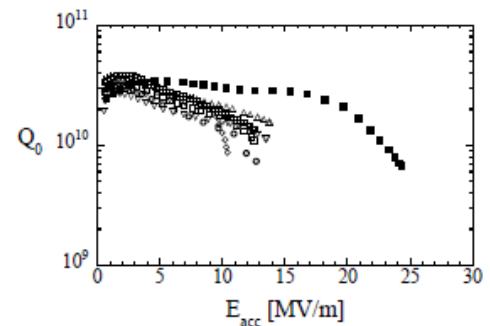


FIG. 17. Excitation curves of six cavities with imperfect equator welds (class 3). Also shown is a resonator (■) made later by the same company, following stringent cleaning procedures at the equator welds.

092001-14

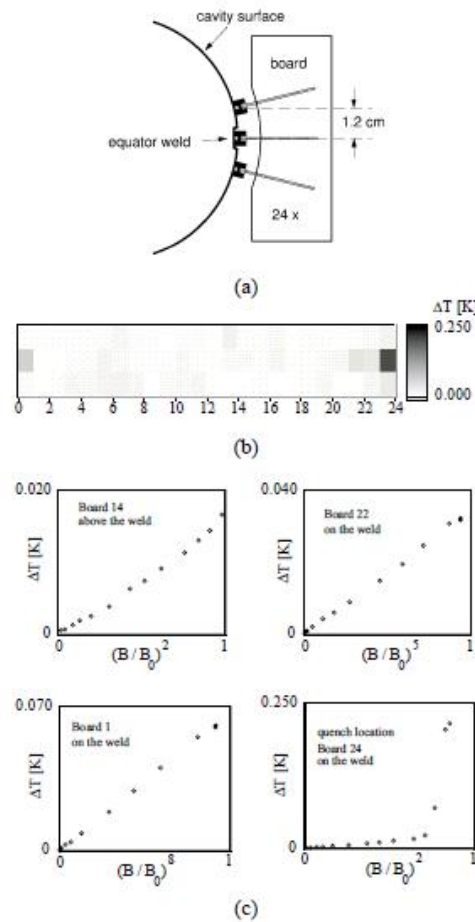


FIG. 18. (a) Location of temperature sensors to determine heating at the equator weld. (b) Temperature map of the equator region from cell 5 of cavity C9 just below the quench. (c) Temperature rise at various locations as a function of $(B/B_0)^n$ with n between 2 and 8 and $B_0 = 50$ mT.

thickness must be removed from the rf surface by BCP after postpurification with a Ti getter. The detrimental effect of insufficient titanium removal has already been shown in Fig. 13(d). The microscopic methods are restricted to small samples and cannot be used to study entire cavities.

2. X-ray fluorescence

The narrow band x-ray beams at HASYLAB permit element identification via fluorescence analysis. In principle the existing apparatus allows the scanning of a whole niobium sheet such as is used for producing a half-cell; however, the procedure would be far too time consuming.

A practical device for the quality control of all niobium sheets going into cavity production is a high-resolution eddy-current system developed by the BAM in Berlin. The apparatus is shown in Fig. 19. The frequency used is

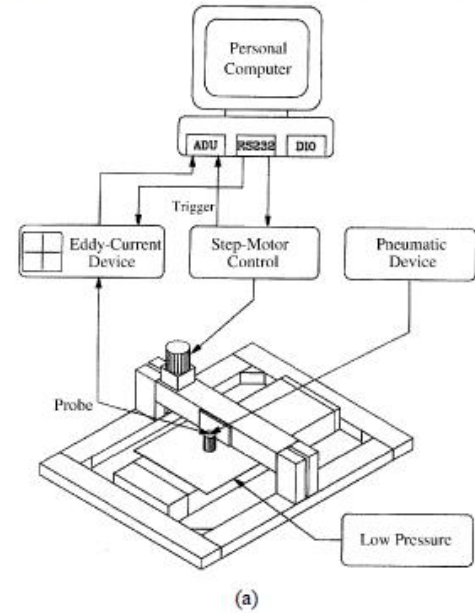


FIG. 19. (a) Schematic view of the xy eddy-current scanning system. (b) Photograph of the new rotating scanning system.

100 kHz corresponding to a penetration depth of 0.5 mm in niobium at room temperature. The maximum scanning speed is 1 m/s. The scanning probe containing the inducing and receiving coils floats on an air pillow to avoid friction. The machined base plate contains holes for evacuating the space between this plate and the Nb sheet. The atmospheric pressure is sufficient to flatten the $265 \times 265 \text{ mm}^2$ niobium sheets to within 0.1 mm, which is important for a high sensitivity scan. The performance

of the apparatus was tested with a Nb test sheet containing implanted tantalum deposits of 0.2 to 1 mm diameter. The scanned picture [Fig. 20(a)] demonstrates that Ta clusters are clearly visible. Using this eddy-current apparatus the tantalum inclusion in cavity C6 was easily detectable.

In the meantime, an improved eddy-current scanning device has been designed and built at BAM which operates similar to a turntable and allows for much higher scanning speeds and better sensitivity since the accelerations of the probe head occurring in *xy* scans are avoided. A two-frequency principle is applied in the new system. Scanning with high frequency (about 1 MHz) allows detection of surface irregularities while the low frequency test (about 150 kHz) is sensitive to bulk inclusions. The high and low frequency signals are picked up simultaneously. Very high sensitivity is achieved by signal subtraction.

3. Neutron activation analysis

The eddy-current scan allows the detection of foreign materials in the niobium but is not suitable for identification. Neutron activation analysis permits a nondestructive determination of the contaminants provided they have radioactive isotopes with a sufficiently long half-life. Experiments were carried out at the research reactor BER II of the Hahn Meitner Institut in Berlin. The niobium sheets are exposed to a thermal neutron flux of $10^9 \text{ cm}^{-2} \text{ s}^{-1}$ for some 5 h. The radioactive isotope ^{94}Nb has a half-life of 6.2 min while ^{182}Ta has a much longer half-life of 115 days. Two weeks after the irradiation the ^{94}Nb activity has dropped to such a low level that tantalum fractions in the ppm range can be identified. Figure 20(b) shows the implanted tantalum clusters in the specially prepared Nb plate with great clarity. Also, the uniformly dissolved Ta is visible and the inferred concentration of 200 ppm is in agreement with the chemical analysis. The activation analysis is far too time consuming for series checks but can be quite useful in identifying special contaminations found with the eddy-current system. Ten Nb sheets from the regular production were investigated without showing any evidence for tantalum clusters.

D. Present status of TTF cavities

1. Improvements in cavity production

For the second series, 25 cavities have been ordered at four firms. The second production differed from the first one in three main aspects:

(1) *Stricter quality control of niobium.* The niobium sheets for the second series were all eddy-current scanned to eliminate material with tantalum or other foreign inclusions before the deep drawing of half-cells. From 715 sheets, 637 were found free of defects, 63 showed grinding marks or imprints from rolling, and 15 exhibited large

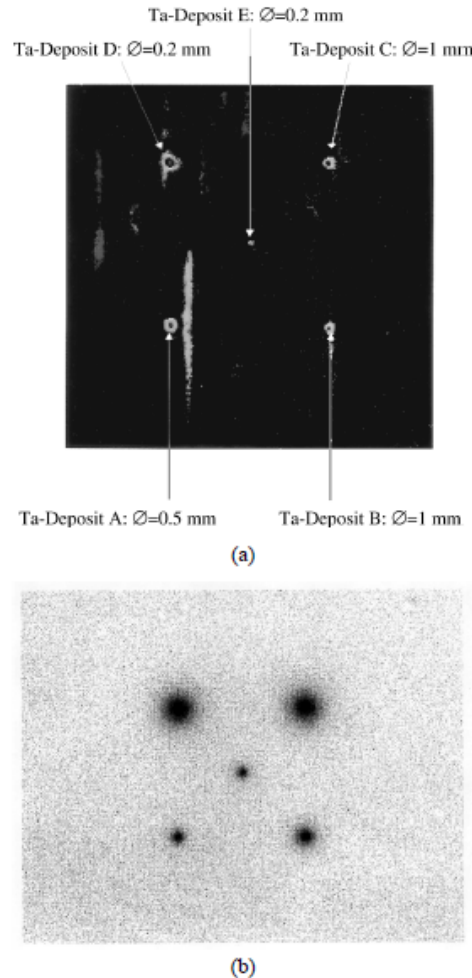


FIG. 20. (a) Eddy-current scan of a specially prepared Nb sheet with Ta implantations at 5 locations. The vertical lines are caused by microphonics. (b) Neutron activation analysis of the same sheet.

signals which, in most cases, were due to small iron chips. No further Nb sheets with tantalum inclusions were found. Most of the rejected sheets will be recoverable by applying some chemical etching. The iron inclusions were caused by mechanical wear of the rolls used for sheet rolling. In the meantime new rolls have been installed. The eddy-current check has turned out to be an important quality control not only for the cavity manufacturer but also for the supplier of the niobium sheets.

(2) *Weld preparation.* Stringent requirements were imposed on the electron-beam welding procedure to prevent the degraded performance at the equator welds encountered in the first series. After mechanical trimming the weld regions were requested to be cleaned by a slight chemical etching, ultrapure water rinsing, and clean room drying not more than 8 h in advance of the EB welding. The success of these two additional quality control measures has been convincing: no foreign material inclusions nor weld contaminations were found in the cavities tested so far.

(3) *Replacement of Nb flanges by NbTi flanges.* In the first cavity series the flanges at the beam pipes and the coupler ports were made by rolling over the 2 mm thick niobium pipes. The sealing against the stainless steel counter flanges was provided by Helicoflex gaskets. This simple design appeared satisfactory in a number of prototype cavities but proved quite unreliable in the series production, mainly due to a softening of the niobium during the 1400°C heat treatment. Most of the 9-cell cavities had to be flanged more than once to become leak tight in superfluid helium. This caused not only time delays but also severe problems with contamination and field emission. Therefore an alternative flange design was needed [29]. The material was selected to be EB weldable to niobium and to possess a surface hardness equivalent to that of standard UHV flange material (stainless steel 316 LN/DIN 4429). Niobium-titanium conforms to these requirements at a reasonable cost. Contrary to pure niobium, the alloy NbTi (ratio 45/55 in wt. %) shows no softening after the 1400°C heat treatment and only a moderate crystal growth. O-ring-type aluminum gaskets provide reliable seals in superfluid helium and are easier to clean than Helicoflex gaskets. During cavity etching the sealing surface must be protected from the acid.

2. Test results in vertical cryostat

All new cavities were subjected to the standard treatment described in Sec. IV B, including the postpurification with titanium getter at 1400°C. Twenty resonators have been tested to date. Only one rf test was performed for each resonator in the first round. If some limitation was found, the cavity was put aside for further treatment. The results of the first test sequence are summarized in Fig. 21. It is seen that eight cavities reach or exceed the TESLA specification of $E_{acc} \geq 25$ MV/m with a quality

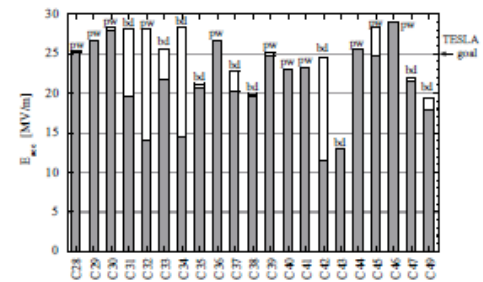


FIG. 21. Test results of the second cavity series (crosshatched bars); plotted is the highest gradient achieved in the first rf test of each cavity at $Q_0 \geq 5 \times 10^9$. Cavities with poor initial performance were subjected to an additional BCP and high pressure water rinsing and tested again (open bars). Field limitation by amplifier power (pw) or thermal breakdown (bd) is indicated for the best gradient.

factor above 5×10^9 . Eight cavities are in the range of 18 to 23 MV/m while four cavities show a much lower performance. In cavity C43 a hole was burned during equator welding which was repaired by welding in a niobium plug; the cavity quenched at 13 MV/m at exactly this position. It is rather unlikely that C43 can be recovered by repeating the repair. Therefore, in future cavity production repaired holes in EB welds will no longer be acceptable. The cavities C32, C34, and C42 showed very strong field emission in the first test. They have been improved in the meantime by additional BCP and high pressure water rinsing; see Fig. 21. Excluding the defective cavity C43, the average gradient is 25.0 ± 3.2 MV/m at $Q_0 = 5 \times 10^9$.

3. Tests with main power coupler in horizontal cryostat

After the successful test in the vertical bath cryostat the cavities are welded into their liquid helium container and equipped with the main power coupler. The external Q is typically 2×10^6 , while in the vertical test an input antenna with an external Q of more than 10^{11} is used. Four cavities of the first production series and 13 of the second series have been tested together with their main power coupler in a horizontal cryostat. The accelerating fields achieved in the vertical and horizontal test are quite similar, as shown in Fig. 22. In a few cases, reduced performance was seen due to field emission while several cavities improved their field capability due to the fact that with the main power coupler pulsed operation is possible instead of the cw operation in the vertical cryostat. These results indicate that the good performance of the cavities can indeed be preserved after assembly of the liquid helium container and the power coupler provided extreme care is taken to avoid foreign particles from entering the cavity during these assembly steps.

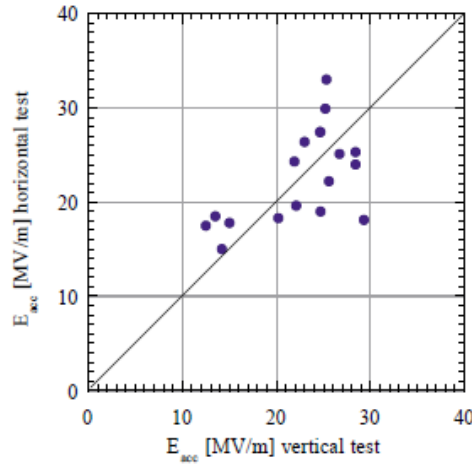


FIG. 22. Comparison of vertical and horizontal test results. The average accelerating field achieved in the vertical test with cw excitation is 22.3 MV/m, in the horizontal test with pulsed excitation 22.5 MV/m. Most of these cavities are from the second production.

4. Cavity improvement by heat treatment

The beneficial effect of the 800 °C and 1400 °C heat treatments has been shown in Fig. 13(c). Ten of the 9-cell cavities have been tested after the intermediate 800 °C step yielding an average gradient of 20.7 MV/m. The 1400 °C treatment with titanium getter raised the average gradient to 24.4 MV/m. It should be noted that part of the 3.7 MV/m improvement may be due to the additional etching of about 80 μm. An interesting correlation is obtained by plotting the maximum gradient as a function of the measured RRR of the cavity; see Fig. 23. This figure clearly indicates that a higher heat conductivity leads to higher accelerating fields, at least if the standard BCP treatment is applied to prepare the cavity surface.

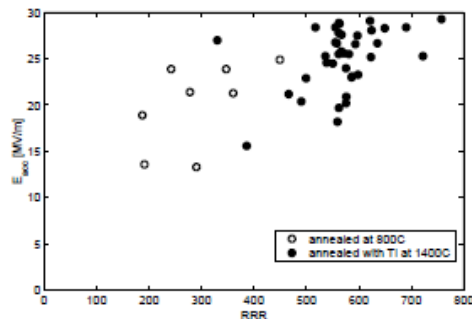


FIG. 23. Maximum gradient as a function of RRR.

VI. RF CONTROL SYSTEM AND PERFORMANCE OF THE CAVITIES WITH ELECTRON BEAM

A. General demands on the rf control system

The requirements on the stability of the accelerating field in a superconducting acceleration structure are comparable to those in a normal-conducting cavity. However, the nature and magnitude of the perturbations to be controlled are rather different. Superconducting cavities possess a very narrow bandwidth and are therefore highly susceptible to mechanical perturbations. Significant phase and amplitude errors are induced by the resulting frequency variations. Perturbations can be excited by mechanical vibrations (microphonics), changes in helium pressure and level, or Lorentz forces. Slow changes in frequency, on the time scale of minutes or longer, are corrected by a frequency tuner, while faster changes are counteracted by an amplitude and phase modulation of the incident rf power.

The demands on amplitude and phase stability of the TESLA Test Facility cavities are driven by the maximum tolerable energy spread in the TTF linac. The design goal is a relative spread of $\sigma_E/E = 2 \times 10^{-3}$ implying a gradient and phase stability of the order of 1×10^{-3} and 1.6° , respectively. For cost reasons, up to 32 cavities will be powered by a single klystron. Hence it is not possible to control individual cavities but only the vector sum of the field vectors in these 32 cavities.

One constraint to be observed is that the rf power needed for control should be minimized. The rf control system must also be robust against variations of system parameters such as beam loading and klystron gain.

The pulsed structure of the rf power and the beam at TTF, shown in Fig 24, puts demanding requirements on the rf control system. Amplitude and phase control is obviously needed during the flattop of 800 μs when the beam is accelerated, but it is equally desirable to control the field during cavity filling to ensure proper beam injection

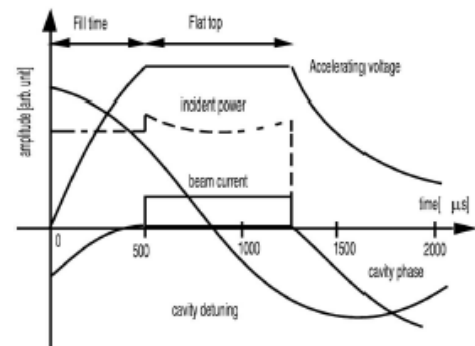


FIG. 24. Pulse structure of TTF cavity operation. Shown are accelerating voltage with 500 μs filling time and 800 μs flattop, incident power, beam current, cavity phase, and cavity detuning.

conditions. Field control is aggravated by the transients induced by the subpicosecond electron bunches which have a repetition rate of 1 to 9 MHz.

For a detailed discussion of the basic principles of rf systems used in superconducting electron linacs and their operational performance, refer to Refs. [30,31].

B. Sources of field perturbations

There are two basic mechanisms which influence the magnitude and phase of the accelerating field in a superconducting cavity: (i) variations in klystron power or beam loading (bunch charge) and (ii) modulation of the cavity resonance frequency.

Perturbations of the accelerating field through time-varying field excitations are dominated by changes in beam loading. One must distinguish between transients caused by the pulsed structure of the beam current and stochastic fluctuations of the bunch charge. The transients caused by the regular bunch train in the TTF linac (800 subpicosecond bunches of 8 nC each, spaced by 1 μ s) are of the order of 1% per 10 μ s; the typical bunch charge fluctuations of 10% induce field fluctuations of about 1%. In both cases the effect of the fast source fluctuations on the cavity field is diminished by the long time constant of the cavity.¹³

Mechanical changes of the shape and eigenfrequency of the cavities caused by microphonics are a source of amplitude and phase jitter which has bothered superconducting accelerator technology throughout its development. In the TTF cavities the sensitivity of the resonance frequency to a longitudinal deformation is about 300 Hz/ μ m. Heavy machinery can transmit vibrations through the ground, the support, and the cryostat to the cavity. Vacuum pumps can interact with the cavity through the beam tubes, and the compressors and pumps of the refrigerator may generate mechanical vibrations which travel along the He transfer line into the cryostat. Also, helium pressure variations lead to changes in resonance frequency, as shown in Fig. 25(a). The rms frequency spread due to microphonics, measured in 16 cavities, is 9.5 ± 5.3 Hz and is thus surprisingly small for a superconducting cavity system [see Fig. 25(b)].

At high accelerating gradients the Lorentz forces become a severe perturbation. The corresponding frequency shift is proportional to the square of the accelerating field according to $\Delta f = -KE_{acc}^2$ with $K \approx 1 \text{ Hz}(\text{MV}^{-1} \text{m}^{-1})^2$. Figure 26(a) shows a cw measurement of the resonance curve with a strong distortion

¹³The cavity with power coupler is adjusted to an external Q of 3×10^6 at 25 MV/m, corresponding to a time constant of about 700 μ s. The consequence is a low-pass filter characteristic.

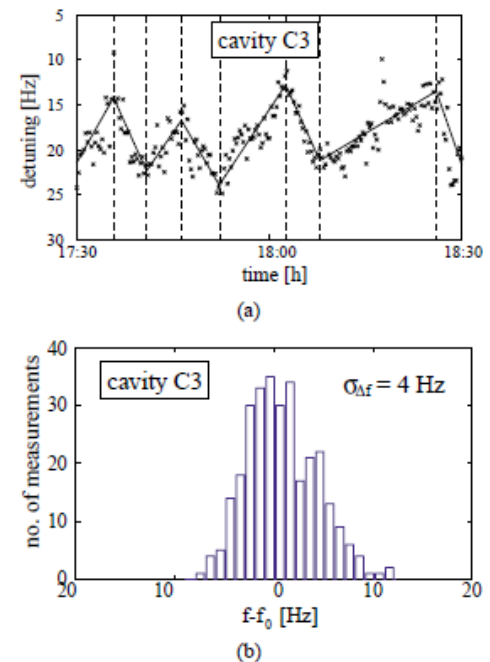


FIG. 25. Fluctuations of the cavity resonance frequency. (a) Slow drifts caused by helium pressure variations. The sensitivity is 10 Hz/mbar. (b) Random variations of resonance frequency after correction for the slow drift.

caused by Lorentz forces. In cw operation the frequency shift can be easily corrected for by mechanical tuning. In the pulsed mode employed at the TTF linac this is not possible since the mechanical tuner is far too slow. Hence a time-dependent detuning is unavoidable. In order to keep the deviation from the nominal resonance frequency within acceptable limits the cavities are predetuned before filling. The measured dynamic detuning of cavity C39 during the 1.3 ms long rf pulse is shown in Fig. 26(b) for accelerating fields of 15 to 30 MV/m. Choosing a predetuning of +300 Hz, the eigenfrequency at 25 MV/m changes dynamically from +100 to -120 Hz during the 800 μ s duration of the beam pulse.

In steady state (cw) operation, at a gradient of 25 MV/m and a beam current of 8 mA, a klystron power of 210 kW is required per 9-cell cavity. In pulsed mode $\approx 15\%$ additional rf power is needed to maintain a constant accelerating gradient in the presence of cavity detuning. The frequency changes from microphonics and helium pressure fluctuations lead to comparable extra power requirements. The klystron should be operated 10% below saturation to guarantee sufficient gain in the feedback loop.

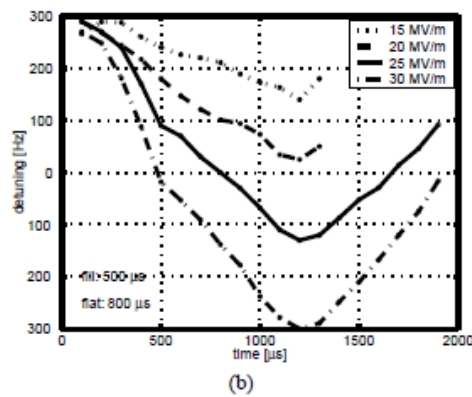
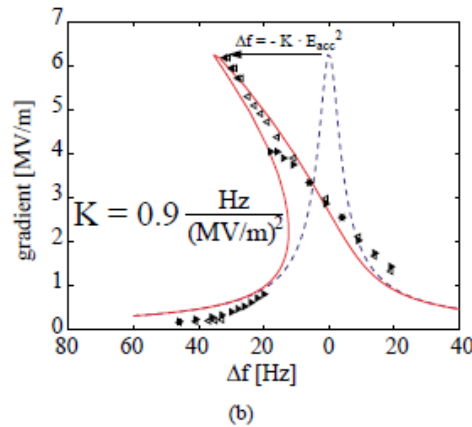


FIG. 26. (Color) (a) Influence of Lorentz forces on the shape of the resonance curve of a sc cavity in cw operation. The left part of the curve was mapped out by approaching the resonance from below, the right part by coming from above. (b) Dynamical detuning of cavity C39 during the TESLA pulse. In pulsed operation the resonance is approached from above.

C. rf control design considerations

The amplitude and phase errors from Lorentz force detuning, beam transients, and microphonics are of the order of 5% and 20°, respectively. These errors must be suppressed by 1–2 orders of magnitude. Fortunately, the dominant errors are repetitive (Lorentz forces and beam transients) and can be largely eliminated by means of a feedforward compensation. It should be noted, however, that bunch-to-bunch fluctuations of the beam current cannot be suppressed by the rf control system since the gain bandwidth product is limited to about 1 MHz due to the low-pass characteristics of the cavity, the bandwidth limitations of electronics and klystrons, and cable delay.

Fast amplitude and phase control can be accomplished by modulation of the incident rf wave which is common

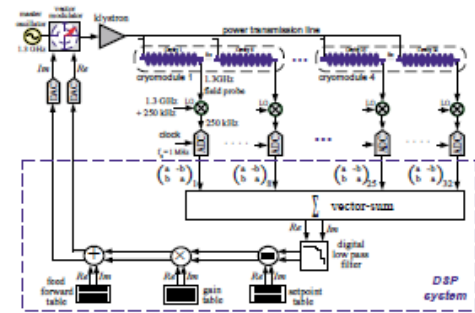


FIG. 27. (Color) Schematic of the digital rf control system.

to 32 cavities. The control of an individual cavity field is not possible. The layout of the TTF digital rf control system is shown in Fig. 27. The vector modulator for the incident wave is designed as a so-called “I/Q modulator” controlling the real and imaginary parts of the complex cavity field vector instead of amplitude and phase. This has the advantage that the coupling between the two feedback loops is minimized and the problem of large phase uncertainties at small amplitude is avoided.

The detectors for cavity field, incident, and reflected wave are implemented as digital detectors for the real and imaginary parts. The rf signals are converted to an intermediate frequency of 250 kHz and sampled at a rate of 1 MHz, which means that two subsequent data points yield the real and the imaginary parts of the cavity field vectors. These vectors are multiplied with 2×2 rotation matrices to correct for phase offsets and to calibrate the gradients of the individual cavity probe signals. The vector sum is calculated and a Kalman filter is applied which provides an optimal state (cavity field) estimate by correcting for delays in the feedback loop and by taking stochastic sensor and process noise into account. Finally, the nominal set point is subtracted and a time-optimal gain matrix is applied to calculate the new actuator setting (the Re and Im control inputs to the vector modulator). Adaptive feedforward is realized by means of a table containing the systematic variations, thereby reducing the task of the feedback loop to control the remaining stochastic fluctuations. The feedforward tables are continuously updated to take care of slow changes in parameters such as average detuning angle, microphonic noise level, and phase shift in the feedforward path.

D. Operational experience

The major purpose of the TESLA Test Facility linac is to demonstrate that all major accelerator subsystems meet the technical and operational requirements of the TESLA collider. Currently the TTF linac is equipped with two cryomodules each containing eight cavities. The cavities

are routinely operated at the design gradient of TTF of 15 MV/m, providing a beam energy of 260 MeV.

An important prerequisite of the proper functioning of the vector-sum control of 16 to 32 cavities is an equal response of the field pickup probes in the individual cavities. A first step is to adjust the phase of the incident rf wave to the same value in all cavities by means of three-stub tuners in the waveguides. Secondly, the transients induced by the bunched beam are used to obtain a relative calibration of the pickup probes, in terms of both amplitude and phase. Typical data taken at the initial start-up of a linac run are shown in Fig. 28. Ideally the lengths of the field vectors should all be identical since the signals are induced by the same electron bunch in all cavities. The observed length differences indicate a variation in the coupling of the pickup antenna to the beam-induced cavity field, which has to be corrected. The different phase angles of the field vectors are mainly due to different signal delays. The complex field vectors are rotated by matrix multiplication in digital signal processors to yield all zero phase. Moreover they are normalized to the same amplitude to correct for the different couplings of the pickup antennas to the cavity fields. Once this calibration has been performed the vector sum of the 16 or 32 cavities is a meaningful measure of the total accelerating voltage supplied to the beam. The calibration is verified with a measurement of the beam energy in a magnetic spectrometer.

The required amplitude stability of 1×10^{-3} and phase stability of $\sigma_\phi \leq 1.6^\circ$ can be achieved during most of the

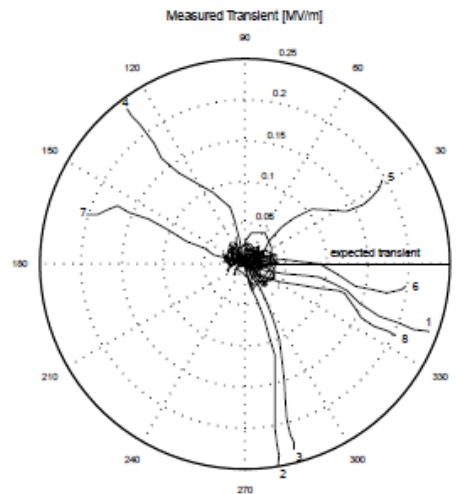


FIG. 28. Beam induced transients (cavity field vectors) obtained by measuring the cavity fields with and without beam pulses. The noise in the signals can be estimated from the erratic motion at the center of the plot. This region represents the first 50 μs of the measurement before the arrival of the beam pulse.

092001-21

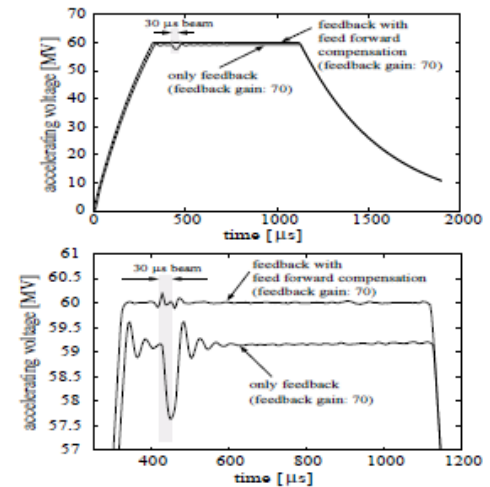


FIG. 29. Field regulation of the vector sum of eight cavities without and with adaptive feedforward. The lower graph shows an enlarged view of the plateau region.

beam pulse duration with the exception of the beam transient induced when turning on the beam. Without feedback the transient of a 30 μs beam pulse at 8 mA would be of the order of 1 MV/m. This transient can be reduced to about 0.2 MV/m by turning on feedback. The effectiveness of the feedback system is limited by the loop delay of 5 μs and the unity-gain bandwidth of about 20 kHz. The 0.2 MV/m transient is repetitive with a high degree of reproducibility. Using feedforward it can be further suppressed by more than 1 order of magnitude, as shown in Fig. 29. Slow drifts are corrected for by making the feedforward system adaptive [32]. The feedforward tables are updated on a time scale of minutes.

VII. CAVITIES OF HIGHER GRADIENTS

Both the TESLA collider and the x-ray FEL would profit from the development of cavities which can reach higher accelerating fields (i.e., higher particle energies) and higher quality factors (i.e., reduced operating costs of the accelerators). The TESLA design energy of 250 GeV per beam requires a gradient of 25 MV/m in the present 9-cell cavities. The results shown in Sec. VD demonstrate that TESLA could indeed be realized with a moderate improvement in the present cavity fabrication and preparation methods. However, for particle physics an energy upgrade of the collider would be of highest interest, and hence there is a strong motivation to push the field capability of the cavities closer to the physical limit of about 50 MV/m, which is determined by the superheating field of niobium. There are three main reasons that the theoretical limit has not yet

092001-21

been attained in multicell resonators: (1) foreign material contamination in the niobium, (2) insufficient quality and cleanliness of the inner rf surface, and (3) insufficient mechanical stability of the resonators. An R&D program has been initiated aiming at improvements in all three directions. Furthermore, the feasibility of seamless cavities is being investigated.

A. Quality improvement of niobium

Niobium for microwave resonators has to be of high purity for several reasons: (i) dissolved gases such as hydrogen, oxygen, and nitrogen reduce the heat conductivity at liquid helium temperature and degrade the cooling of the rf surface; (ii) contamination by foreign metals may lead to magnetic flux pinning and heat dissipation in rf fields; (iii) normal-conducting or weakly superconducting clusters close to the rf surface are particularly dangerous. The Nb ingots contain about 500 ppm of finely dispersed tantalum. It appears unlikely that the Ta clusters found in some early TTF cavities might have been caused by this "natural" Ta content. Rather there is some suspicion that Ta grains might have dropped into the Nb melt during the various remeltings of the Nb ingot in an electron-beam melting furnace because such furnaces are often used for Ta production as well. To avoid contamination by foreign metals, a dedicated electron-beam melting furnace would appear highly desirable but seems to be too cost intensive in the present R&D phase of TESLA. Also, more stringent requirements on the quality of the furnace vacuum (lower pressure, absence of hydrocarbons) would improve the Nb purity. The production steps following the EB melting (machining, forging, and sheet rolling of the ingot) may also introduce dirt. The corresponding facilities need careful inspection and probably some upgrading. The present TTF cavities have been made from niobium with gas contents in the few ppm range and an RRR of 300. Ten 9-cell cavities have been measured after both 800 °C and 1400 °C firings. The average gain in gradient was about 4 MV/m. It would be highly desirable to eliminate the tedious and costly 1400 °C heat treatment of complete cavities. One possibility might be to produce a niobium ingot with an RRR of more than 500. This is presently not our favored approach, mainly for cost reasons.

For the present R&D program, the main emphasis is on the production of ingots with $RRR \geq 300$, but with improved quality by starting from niobium raw material with reduced foreign material content, especially tantalum well below 500 ppm. Stricter quality assurance during machining, forging, and sheet rolling should prevent metal flakes or other foreign material from being pressed into the niobium surface deeper than a few μm . To increase the RRR from 300 to about 600, it is planned to study the technical feasibility¹⁴ of a 1400 °C heat treatment at the

dumbbell stage (2 half-cells joined by a weld at the iris). This procedure would be preferable compared to the heat treatment of whole cavities which must be carefully supported in a Nb frame to prevent plastic deformation, while such a precaution is not needed for dumbbells. However, there is a strong incentive to find cavity treatment methods which would permit elimination of the 1400 °C heat treatment altogether. According to the results obtained at KEK [33], electropolishing seems to offer this chance (see below).

B. Improvement in cavity fabrication and preparation

Once half-cells or dumbbells of high RRR have been produced, it is then mandatory to perform the electron-beam welding of the cavities in a vacuum of a few times 10^{-6} mbar in order to avoid degradation of the RRR in the welds. The EB welding machines available at industrial companies achieve vacua of only 5×10^{-5} mbar and are hence inadequate for this purpose. An EB welding machine at CERN is equipped with a much better vacuum system. This EB apparatus is being used for a single-cell test program. For the future cavity improvement program a new electron-beam welding apparatus will be installed at DESY with a state-of-the-art electron gun, allowing computer-controlled beam manipulations, and an oil-free vacuum chamber fulfilling UHV standards.

The industrially produced cavities undergo an elaborate treatment at TTF before they can be installed in the accelerator. A 150–200 μm thick damage layer is removed from the rf surface because otherwise gradients of 25 MV/m appear inaccessible. As explained in Sec. IV, the present method is BCP which leads to a rather rough surface with strong etching in the grain boundaries. An alternative method is "electropolishing" (EP) in which the material is removed in an acid mixture under current flow. Sharp edges and burrs are smoothed out and a very glossy surface can be obtained. For a number of years remarkable results have been obtained at KEK with electropolishing of 1-cell niobium cavities. Recently, a collaboration between KEK and Saclay has convincingly demonstrated that EP raises the accelerating field by more than 7 MV/m with respect to BCP. Several 1-cell cavities from Saclay, which already showed good performance after the standard BCP, exhibited a clear gain after the application of EP [34]. Conversely, an electropolished cavity which had reached 37 MV/m suffered a degradation after subsequent BCP. These results are a strong indication that electropolishing is the superior treatment method.

¹⁴At Cornell University cavities have been successfully fabricated from $RRR = 1000$ material. Likewise, the TTF cavity C19 was made from postpurified half-cells and showed good performance.

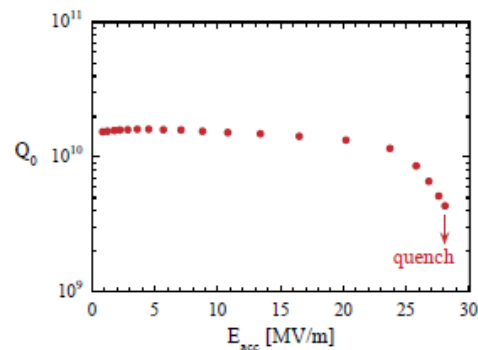


FIG. 30. (Color) Excitation curve of a TESLA 9-cell cavity showing a drop of quality factor without any field emission.

CERN, DESY, KEK, and Saclay started a joint R&D program with electropolishing of half-cells and 1-cell cavities in August, 1998. Recent test results yield gradients around 40 MV/m [35] and hence the same good performance as was achieved at KEK. The transfer of the EP technology to 9-cell resonators requires considerable effort. It is planned to do this in collaboration with industry.

Recently it has been found [36] that an essential prerequisite for achieving gradients in the 40 MV/m regime is a baking at 100 °C to 150 °C for up to 48 h while the cavity is evacuated, after the final high-pressure water rinsing. In electropolished cavities this procedure removes the drop of quality factor towards high gradients which is often observed without any indication of field emission. Such a drop is usually also found in chemically etched cavities; see, for example, Fig. 30. Experiments at Saclay [37] have shown that a baking may improve the $Q(E)$ curve; however, part of the Q reduction at high field may be due to local magnetic field enhancements at the sharp grain boundaries of BCP treated cavities [38].

C. Mechanical stability of the cavities

The stiffening rings joining neighboring cells in the TESLA resonator are adequate to limit Lorentz-force detuning up to accelerating fields of 25 MV/m. Beyond 25 MV/m the cavity reinforcement provided by these rings is insufficient. Hence, an alternative stiffening scheme must be developed for cavities in the 35–40 MV/m regime. A promising approach has been taken at Orsay and Saclay. The basic idea is to reinforce a thin-walled niobium cavity by a 2 mm thick copper layer which is plasma sprayed onto the outer wall. Several successful tests have been made [39]. The copper plating has a potential danger since Nb and Cu have rather different thermal contractions. The deformation of a cavity upon cooldown and the resulting frequency shift need investigation. Another phenomenon has been observed

in cavities made from explosion-bonded niobium-copper sheets: when these cavities were quenched, a reduction in quality factor Q_0 was observed [40]. An explanation may be trapped magnetic flux from thermoelectric currents at the copper-niobium interface. It is unknown whether this undesirable effect happens also in copper-sprayed cavities. An alternative to copper spraying might be the reinforcement of a niobium cavity by depositing some sort of metallic “foam,” using the plasma or high velocity spraying technique. If the layer is porous, the superfluid helium penetrating the voids should provide ample cooling.

The cavity reinforcement by plasma or high-velocity spraying appears to be a promising approach, but considerable R&D work needs to be done to decide whether this is a viable technique for the TESLA cavities.

D. Seamless cavities

The EB welds in the present resonator design are a potential risk. Great care has to be taken to avoid holes, craters, or contamination in the welds which usually have a detrimental effect on the high-field capability. A cavity without weld connections in the regions of high electric or magnetic rf field would certainly be less vulnerable to small mistakes during fabrication. For this reason the TESLA Collaboration decided several years ago to investigate the feasibility of producing seamless cavities. Two routes have been followed: spinning and hydroforming.

At the Legnaro National Laboratory of INFN in Italy, the spinning technique [41] has been successfully applied to form cavities out of niobium sheets. The next step will be to produce a larger quantity of 1-cell, 3-cell, and, finally, 9-cell cavities from seamless Nb tubes with an RRR of 300. In the cavities spun from flat sheets a very high degree of material deformation was needed, leading to a rough inner cavity surface. Gradients between 25 and 32 MV/m were obtained after grinding and heavy etching (removal of more than 500 μm) [42]. Starting from a tube, the amount of deformation will be much less and a smoother inner surface can be expected. This R&D effort is well underway and the first resonators can be expected in early 2000.

The hydroforming of cavities from seamless niobium tubes is being pursued at DESY [43]. Despite initial hydroforming difficulties, related to inhomogeneous mechanical properties of the niobium tubes, four single cell cavities have been successfully built so far. Three of these were tested and reached accelerating fields of 23 to 27 MV/m. In a very recent test¹⁵ 32.5 MV/m was achieved at $Q_0 = 2 \times 10^{10}$. Most remarkable is the fact

¹⁵Preparation and testing of the hydroformed cavities were carried out by P. Kneisel at Jefferson Laboratory, Newport News, Virginia.

that the cavity was produced from low RRR niobium (RRR = 100). It received a 1400 °C heat treatment raising the RRR to 300–400. The surface was prepared by grinding and 250 μm BCP.

E. Niobium sputtered cavities

Recent investigations at CERN [14] and Saclay [44] show that single-cell copper cavities with a niobium sputter layer of about 1 μm thickness are able to reach accelerating fields beyond 20 MV/m. These results appear so promising that CERN and DESY have agreed to initiate an R&D program on 1.3 GHz single-cell sputtered cavities aiming at gradients in the 30 MV/m regime and quality factors above 5×10^9 . High-performance sputtered cavities would certainly be of utmost interest for the TESLA project for cost reasons. Another advantage would be the suppression of Lorentz force detuning by choosing a sufficiently thick copper wall.

F. The superstructure concept

The present TTF cavities are equipped with one main power coupler and two higher order mode couplers per 9-cell resonator. The length of the interconnection between two cavities has been set to $3\lambda/2$ ($\lambda = 0.23$ m is the rf wavelength) in order to suppress cavity-to-cavity coupling of the accelerating mode. A shortening of the interconnection is made possible by the “superstructure” concept, devised by Sekutowicz [45]. Four 7-cell cavities of TESLA geometry are joined by beam pipes of length $\lambda/2$. The pipe diameter is increased to permit an energy flow from one cavity to the next, hence one main power coupler is sufficient to feed the entire superstructure. One HOM coupler per short beam pipe section provides sufficient damping of dangerous higher modes in both neighboring cavities. Each 7-cell cavity will be equipped with its own LHe vessel and frequency tuner. Therefore, in the superstructure the field homogeneity tuning (equal field amplitude in all cells) and the HOM damping can be handled at the subunit level. The main advantages of the superstructure are an increase in the active acceleration length in TESLA—the design energy of 250 GeV per beam can be reached with a gradient of 22 MV/m—and a savings in rf components, especially power couplers.

A copper model of the superstructure is presently used to verify the theoretically predicted performance. This model allows individual cell tuning, field profile adjustment, investigation of transients in selected cells, test of the HOM damping scheme, and measurement of the cavity couplings to the fundamental mode coupler. Also, the influence of mechanical tolerances is studied. First results are promising [46]. A niobium superstructure prototype is under construction and will be tested with beam in the TTF linac in early 2001.

ACKNOWLEDGMENTS

We are deeply indebted to the late distinguished particle and accelerator physicist Bjorn H. Wik who has been the driving force behind the TESLA project and whose determination and enthusiasm were essential for much of the progress that has been achieved. We want to thank the many physicists, engineers, and technicians in the laboratories of the TESLA Collaboration and in the involved industrial companies for their excellent work and support of the superconducting cavity program. We are grateful to P. Kneisel for numerous discussions.

- [1] *Proceedings of the 1st TESLA Workshop, 1990*, edited by H. Padamsee (Cornell University Report No. CLNS-90-1029, 1990).
- [2] TESLA-Report 95-01, 1995.
- [3] C. Reece *et al.*, in *Proceedings of the 1995 Particle Accelerator Conference and International Conference on High Energy Accelerators, Dallas, Texas* (IEEE, Piscataway, NJ, 1995), p. 1512.
- [4] DESY 1997-048, ECFA 1997-182, 1997.
- [5] G. Müller, in *Proceedings of the 3rd Workshop on rf Superconductivity, Argonne, Illinois, 1988*, edited by K. W. Shepard (ANL, Argonne, IL, 1988), p. 331.
- [6] B. Bonin, in *Proceedings of the CERN Accelerator School, Hamburg, 1995*, edited by S. Turner (CERN, Geneva, 1996), p. 191.
- [7] W. Weingarten, in *Proceedings of the CERN Accelerator School, Hamburg, 1995* (Ref. [6]), p. 167.
- [8] T. Schilcher, DESY Report No. TESLA 95-12, 1995.
- [9] B. Bonin, *Supercond. Sci. Technology* 9, 453 (1996).
- [10] K. Schulze, *J. Met.* 33, 33 (1981).
- [11] A. Boucheffa *et al.*, in *Proceedings of the 7th Workshop on rf Superconductivity, Gif-sur-Yvette, France, 1995*, edited by B. Bonin (CEA, Saclay, 1996), p. 659.
- [12] J. Matricon and D. Saint-James, *Phys. Lett.* 24A, 241 (1967).
- [13] T. Hays *et al.*, in *Proceedings of the 7th Workshop on rf Superconductivity, Gif-sur-Yvette, France, 1995* (Ref. [11]), p. 437.
- [14] C. Benvenuti *et al.*, in *Proceedings of the 9th Workshop on rf Superconductivity, Santa Fe, 1999* (to be published).
- [15] R. H. Fowler and L. Nordheim, *Proc. R. Soc. London A* 119, 173 (1928); *Math. Phys. Sci.* 119, 173 (1928).
- [16] H. Padamsee, J. Knobloch, and T. Hays, *RF Superconductivity for Accelerators* (Wiley, New York, 1998).
- [17] H. Padamsee, in *Proceedings of the 5th Workshop on Superconductivity, Hamburg, Germany, 1991*, edited by D. Proch (DESY, Hamburg, 1992), p. 963.
- [18] U. Lauströer *et al.*, DESY Report No. DESY M-87-03, 1987.
- [19] A. W. Chao and M. Tigner, *Handbook of Accelerator Physics and Engineering* (World Scientific, Singapore, 1999).
- [20] W. Albach and G. A. Voss, *Z. Angew. Phys.* 9, 111 (1957).

- [21] W. D. Möller, in *Proceedings of the 9th Workshop on rf Superconductivity*, Santa Fe, New Mexico, 1999 (Ref. [14]).
- [22] J. Tückmantel, in *Proceedings of the 1995 Particle Accelerator Conference and International Conference on High Energy Accelerators*, Dallas, 1995 (Ref. [3]), p. 1642.
- [23] J. Graber, *Nucl. Instrum. Methods Phys. Res., Sect. A* 350, 572 (1994).
- [24] P. Bernard *et al.*, in *Proceedings of the Third European Particle Accelerator Conference, Berlin, 1992*, edited by E. Henke, H. Homeyer, and Ch. Petit-Jean-Genaz (Frontieres, Gif-sur-Yvette, 1992), p. 1269.
- [25] H. Padamsee *et al.*, in *Proceedings of the 4th Workshop on rf Superconductivity, Tsukuba, Japan, 1989*, edited by Y. Kojima (KEK, Ibaraki, 1990), p. 207.
- [26] H. Safa *et al.*, in *Proceedings of the 7th Workshop on rf Superconductivity, Gif-sur-Yvette, France, 1995* (Ref. [11]), p. 649.
- [27] W. Singer, D. Proch, and A. Brinkmann, in *Proceedings of the 8th Workshop on rf Superconductivity, Abano Terme, Italy, 1997*, edited by V. Palmieri and A. Lombardi (LNL-INFN, Padova, 1998), p. 850.
- [28] A. Brinkmann *et al.*, in *Proceedings of the 8th Workshop on rf Superconductivity, Abano Terme, Italy, 1997* (Ref. [27]), p. 452.
- [29] K. Zapfe-Düren *et al.*, in *Proceedings of the 8th Workshop on rf Superconductivity, Abano Terme, Italy, 1997* (Ref. [27]), p. 457.
- [30] H.-D. Gräf, in *Proceedings of the 5th Workshop on rf Superconductivity, Hamburg, Germany, 1991* (Ref. [17]), p. 317.
- [31] S. Simrock, in *Proceedings of the 6th Workshop on rf Superconductivity, Newport News, Virginia, 1993*, edited by R. M. Sundelin (CEBAF, Newport News, 1994), p. 294.
- [32] M. Liepe and S. Simrock, in *Proceedings of the 1998 European Particle Accelerator Conference, Stockholm, Sweden*, edited by S. Myers, L. Liljeby, Ch. Petit-Jean-Genaz, J. Poole, and K.-G. Rensfelt (Institute of Physics, Bristol, UK, 1998), p. 1735.
- [33] K. Saito, in *Proceedings of the 9th Workshop on rf Superconductivity*, Santa Fe, New Mexico, 1999 (Ref. [14]).
- [34] E. Kako *et al.*, in *Proceedings of the 9th Workshop on rf Superconductivity*, Santa Fe, 1999 (Ref. [14]).
- [35] L. Lilje *et al.*, in *Proceedings of the 9th Workshop on rf Superconductivity*, Santa Fe, 1999 (Ref. [14]).
- [36] P. Kneisel, in *Proceedings of the 9th Workshop on rf Superconductivity*, Santa Fe, 1999 (Ref. [14]).
- [37] P. Charrier *et al.*, in *Proceedings of the 1998 European Particle Accelerator Conference, Stockholm, Sweden* (Ref. [32]), p. 1735.
- [38] J. Knobloch *et al.*, in *Proceedings of the 9th Workshop on rf Superconductivity*, Santa Fe, 1999 (Ref. [14]).
- [39] S. Bousson, in *Proceedings of the 9th Workshop on rf Superconductivity*, Santa Fe, 1999 (Ref. [14]).
- [40] T. Fujino *et al.*, in *Proceedings of the 9th Workshop on rf Superconductivity*, Santa Fe, 1999 (Ref. [14]).
- [41] V. Palmieri, in *Proceedings of the 8th Workshop on rf Superconductivity, Abano Terme, Italy, 1997* (Ref. [27]).
- [42] P. Kneisel, V. Palmieri, and K. Saito, in *Proceedings of the 9th Workshop on rf Superconductivity*, Santa Fe, 1999 (Ref. [14]).
- [43] I. Gonin *et al.*, in *Proceedings of the 9th Workshop on rf Superconductivity*, Santa Fe, 1999 (Ref. [14]).
- [44] P. Bosland, A. Aspart, E. Jacques, and M. Ribaudeau, *IEEE Trans. Appl. Supercond* 9, 896 (1999).
- [45] J. Sekutowicz, M. Ferrario, and Ch. Tang, *Phys. Rev. ST Accel. Beams* 2, 062001 (1999).
- [46] H. Chen *et al.*, in *Proceedings of the 9th Workshop on rf Superconductivity*, Santa Fe, 1999 (Ref. [14]).

d. Material Certifications



ATI Allegheny Ludlum
Allegheny Technologies

Ship To
TITANIUM INDUSTRIES
ROCKAWAY SERVICE CENTER
18 GREEN POND RD
ROCKAWAY NJ 07866

UNITI TITANIUM
ONE THORN RUN CTR SU. 325
1187 THORN RUN ROAD EXT
MOON TOWNSHIP PA USA 15108

OUR ORDER NO. UF0383080
YOUR ORDER NO. 5553 / CRP-20244-KS
MEMO NO. 359286-00
DATE 03/17/2010
SALESMAN NO. 341

Tracy McTeel
Tracy McTeel - Director, Corporate Quality Assurance

CERTIFIED MATERIAL TEST REPORT

500 Green Street
Washington, PA 15301

TI
QA
4

Heat	Matl ID	Slip	Sid	Lot No	Size(Inches)	Pcs	Weight(lb)
N57F	6121	07236	AAA	232542	.3750 x 96.0625 x 259.9375	1	1526 PLATE ID N57F-A1
N57F	6121	07237	AAB	232542	.3750 x 96.0625 x 259.8750	1	1526 PLATE ID N57F-A2
N57F	6121	07238	AAC	232542	.3750 x 96.1250 x 259.8750	1	1527 PLATE ID N57F-A3

Lot No	232542	FINAL PRODUCT HYDROGEN: .0020			
Heat	C	TI	N	FE	D
N57F	.011	BAL	.003	.13	.14

Lot No	232542	Gauge	Cond.	Yield	Tensile	Elong %	Area %	Hardness	Bend	Corrosion	Grain
		.3750	LONG	48.6 KSI	70.0 KSI	28.0	50.0				
			TRANS	52.0 KSI	69.0 KSI	27.0	53.0				

MATERIAL WAS NOT WELD REPAIRED
MATERIAL IS OF USA MELT AND MANUFACTURE
DIN EN 10204:2005 3.1 CERTIFICATE
MATERIAL MEETS MICROSTRUCTURAL REQUIREMENTS AND IS FREE OF ALPHA CASE AND SURFACE CONTAMINATION
NOTE: THE RECORDING OF FALSE, FICTITIOUS OR FRAUDULENT STATEMENTS OR ENTRIES ON THIS DOCUMENT MAY BE PUNISHED AS A FELONY UNDER FEDERAL STATUTES INCLUDING FEDERAL LAW, TITLE 18, CHAPTER 47
'URING MANUFACTURING, HANDLING, TESTING, AND INSPECTION THIS MATERIAL DID NOT COME INTO DIRECT CONTACT WITH MERCURY OR ANY DEVICE EMPLOYING A SINGLE BOUNDARY OF CONTAINMENT

STATEMENT OF TEST SHALL NOT BE REPRODUCED IN FULL WITHOUT THE WRITTEN APPROVAL OF THE COMPANY. THE RECORDING OF FALSE, FICTITIOUS, OR FRAUDULENT STATEMENTS OR ENTRIES ON THE CERTIFICATE MAY BE PUNISHED AS A FELONY UNDER FEDERAL LAW. TESTING WAS PERFORMED AT ALC MADCAP AND ISOIEC 17025 APPROVED LABORATORIES LOCATED AT NATRONA HEIGHTS, BRACKENRIDGE, LATROBE, MIDLAND, AND LECHERSBURG, PA FACILITIES OF A MADCAP AND ISOIEC 17025 ACCREDITED LABORATORY. EN 10204 - 3.1 ALLEGHENY LUDLUM IS APPROVED AS MANUFACTURER ACCORDING TO A0-MERKBLATT W01010 100 AND THE PRESSURE EQUIPMENT DIRECTIVE PED 97/23/EC.
IBENY LUDLUM PERFORMS CHEMICAL ANALYSIS BY THE FOLLOWING TECHNIQUES: C, S BY COMBUSTION/INFRARED; N, O, H BY INERT FUSION/THERMAL CONDUCTIVITY; MN, P, SI, CR, NI, MO, CU, CO, V, BY WDXRF; B BY CES; AL AND TI (P-A, 10%) BY OTHERWISE BY CES; PB, BI, AG BY GFAA
VIEW OF TEST STATEMENT & CHEMISTRY STATEMENT EXCEPT AS OTHERWISE NOTED, THIS MATERIAL HAS BEEN MANUFACTURED AND TESTED IN ACCORDANCE WITH THE LISTED SPECIFICATIONS AND RESULTS CONFORM TO THE SPECIFICATION AND OTHER REQUIREMENTS

PLANSEE Metall GmbH
 A - 6900 Raasdorf
 Tel. +43 720 2000
 Fax +43 720 2000
 http://www.plansee.com



INSPECTION CERTIFICATE
 acc. to DIN EN 10204 - 3.1

Report No.: **8646061B000010**
 Date: **13.11.2009**
 Customer: **NIOWAVE, INC. / US**
 PLANSEE-Order No./Pos.No.: **6845267 / 10**
 PLANSEE-Material-No.: **11491247**
 PLANSEE-Segment / PoC. / **/ Schenk / 1232**
 Customer Order No.: **08-0028-001** dated **18.11.2008**
 Specification No.:

Material / Products: **NbM / NbM-RRR 300 sheet 540x800x2,8 mm**
 Condition of material / Quality:

Dimensions: **2,8 + -0,15 x 540 x 800 mm**
 Quantity / Weight: **20,880 KG / KG**
 Batch/lot: **0000548850 20,880 KG**

SHEET No.: 225,230.

CHEMICAL ANALYSIS (INGOT H3212)

Ta = 108 µg/g	Zr = < 2 µg/g	Fe = 3 µg/g
Si = 7 µg/g	W = 5 µg/g	Ni = 3 µg/g
Mo = 4 µg/g	Hf = 4 µg/g	O = 2 µg/g
C = 1 µg/g	N = 3 µg/g	
H = 1 µg/g	Nb remainder	

GAS CONTENT (FINAL PRODUCT)

C = < 10 µg/g	N = < 5 µg/g	O = < 5 µg/g
H = < 1 µg/g		

MECHANICAL PROPERTIES (FINAL PRODUCT): acc. to DIN EN 10002-1

	LONGITUDINAL DIRECTION	TRANSVERSE DIRECTION
0,2 % Yield stress (N/mm ²)	66 - 77	67 - 74
Ultimate tensile strength (N/mm ²)	141 - 168	148 - 170
Percentage elongation (%)	49,9 - 72,5	52,1 - 67,7

Hardness HV10: acc. to EN ISO 6507-1 45,4 - 64,1

Grain size No.: acc. to ASTM E112 6,0 - 7,5 (100% recrystallization)

RRR: 338 - 428

SURFACE FINISH:

Both sides have comparable surface finish, therefore no marking of Rfside was made.

Surface roughness: acc. to DIN EN ISO 4287

Ra: 0,95-1,11 µm Rz: 6,87-7,82 µm Rmax: 12,94-14,16 µm

FINAL QUALITY OF SHEET:

Sheet(s) manufactured by rolling-surface treatment-final heat treatment-grinding by machine (overall)-manual grinding of local defects-etching-final inspection.

REMARKS: -

PLANSEE Werk GmbH
 4-11-01 1749
 Tel: +493723400-0
 Fax: +493723400-500
 info@www.plansee.com



INSPECTION CERTIFICATE
 acc. to DIN EN 10204 - 3.1

Report No.: **86547972000010**
 Date: **17.12.2009**
 Customer: **NIOWAVE, INC. / US**
 PLANSEE-Order No./Pos.No.: **6845267 / 30**
 PLANSEE-Material-No.: **11551120**
 PLANSEE-Segment / PoC / Lot: **/ Schenk / t232**
 Customer Order No.: **06-0020-001 dated 18.11.2009**
 Specification No.:

Material / Product: **NEM / NEM -RRR300 sheet 270 x 270 x 2,8 mm**
 Condition of material / Quality:

Dimensions: **2,8 + 0,10 x 270 + 1,0 x 270 + 1,0 mm**
 Quantity / Weight: **82,015 KG / KG**
 Batch(es): **0890530977 82,015 KG**

SHEET No.: 303-313,315-332,334-351.

CHEMICAL ANALYSIS (INGOT H8212)

Ta = 108 µg/g	Zr = < 2 µg/g	Fe = 3 µg/g
Si = 7 µg/g	W = 5 µg/g	Ni = 3 µg/g
Mo = 4 µg/g	Hf = 4 µg/g	
C = 1 µg/g	N = 3 µg/g	O = 2 µg/g
H = 1 µg/g	Nb remainder	

GAS CONTENT (FINAL PRODUCT)

C = < 10 µg/g	N = < 5 µg/g	O = < 5 µg/g
H = < 1 µg/g		

MECHANICAL PROPERTIES (FINAL PRODUCT): acc. to DIN EN 10002-1

	LONGITUDINAL DIRECTION	TRANSVERSE DIRECTION
0,2 % Yield stress (N/mm ²)	68 - 77	87 - 74
Ultimate tensile strength (N/mm ²)	141 - 160	148 - 170
Percentage elongation (%)	49,3 - 72,6	62,1 - 87,7

Hardness HV10: acc. to EN ISO 6507-1 45,4 - 64,1
 Grain size No.: acc. to ASTM E112 6.0 - 7.5 (100% recrystallization)
 RRR: 338 - 428

SURFACE FINISH:

Both sides have comparable surface finish, therefore no marking of Rfside was made.
 Surface roughness: acc. to DIN EN ISO 4287
 Ra: 0,95-1,11 µm Rz: 6,07-7,82 µm Rmax: 12,94-14,16 µm

FINAL QUALITY OF SHEET:

Sheet(s) manufactured by rolling-surface treatment-final heat treatment-grinding by machine (overall)-manual grinding of local defects-etching-final inspection.

REMARKS: circumference water jet cut (es)

PLANSEE Werk GmbH
 A - 5000 Ried
 Tel: +43 (0) 74 20 04
 Fax: +43 (0) 74 20 10
 E-Mail: office@plansee.com



INSPECTION CERTIFICATE
 acc. to DIN EN 10204 - 3.1

Report No.: **68458790000010**
 Date: **17.11.2009**
 Customer: **NIOWAVE, INC. / US**
 PLANSEE Order No./Pos.No.: **6845267 / 30**
 PLANSEE-Material-No.: **11551120**
 PLANSEE-Signature / Pa.C. / No.: **/ Schenk / 1232**
 Customer Order No.: **06-0028-001** dated **16.11.2008**
 Specification No.:

Material / Product: **NBM / NSM -RRR300 sheet 270 x 270 x 2,8 mm**
 Condition of material / Quality:

Dimensions: **2,8 + -0,10 x 270 + -1,0 x 270 + -1,0 mm**
 Quantity / Weight: **67,910 KG / KG**
 Batch(es): **090980977 67,910 KG**

SHEET No.: 201-214,216-218,220,222,223,226-229,232-235,237-243,245-248.

CHEMICAL ANALYSIS (INGOT H3212)

Ta = 106 µg/g	Zr = < 2 µg/g	Fe = 5 µg/g
Si = 7 µg/g	W = 5 µg/g	Ni = 3 µg/g
Mo = 4 µg/g	Hf = 4 µg/g	
C = 1 µg/g	N = 3 µg/g	O = 2 µg/g
H = 1 µg/g	Nb remainder	

GAS CONTENT (FINAL PRODUCT)

C = < 10 µg/g	N = < 5 µg/g	O = < 5 µg/g
H = < 1 µg/g		

MECHANICAL PROPERTIES (FINAL PRODUCT): acc. to DIN EN 10002-1

	LONGITUDINAL DIRECTION	TRANSVERSE DIRECTION
0,2 % Yield stress (N/mm ²)	88 - 77	87 - 74
Ultimate tensile strength (N/mm ²)	141 - 188	148 - 170
Percentage elongation (%)	49,3 - 72,5	52,1 - 67,7

Hardness HV10: acc. to EN ISO 6507-1 45,4 - 64,1
 Grain size No.: acc. to ASTM E112 6,0 - 7,5 (100% recrystallization)
 RRR: 338 - 428

SURFACE FINISH:

Both sides have comparable surface finish, therefore no marking of RFSide was made.
 Surface roughness: acc. to DIN EN ISO 4287
 Ra: 0,95-1,11 µm Rz: 6,87-7,82 µm Rmax: 12,94-14,16 µm

FINAL QUALITY OF SHEET:

Sheet(s) manufactured by rolling-surface treatment-final heat treatment-grinding by machine (overall)-manual grinding of local defects-etching-final inspection.

REMARKS:

PLANSEE Metall GmbH
 1. 49K 2009
 Tel. +49(0)2090-4
 Fax. +49(0)2090-529
 E-Mail: www.plansee.com



INSPECTION CERTIFICATE

acc. to DIN EN 10204 - 3.1

Report No.: **86413018000010**
 Date: **02.11.2009**
 Customer: **NIOWAVE, INC. / US**
 PLANSEE-Order No./Poc.No.: **6845267 / 30**
 PLANSEE-Material-No.: **11551120**
 PLANSEE-Segment / Poc. / = **/ Schenk / 1232**
 Customer Order No.: **08-0028-001** dated **18.11.2008**
 Specification No.:

Material / Products: **NBM / NBM -RRR300 sheet 270 x 270 x 2,8 mm**
 Condition of material / Quality:

Dimensions: **2,8 + -0,10 x 270 + -1,0 x 270 + -1,0 mm**
 Quantity / Weight: **38,390 KG / KG**
 Batchcode: **009060877 38,390 KG**

SHEET No.: 163-165,167-179,181-186.

CHEMICAL ANALYSIS (INGOT HS205)

Ta = 145 µg/g	Zr = 2 µg/g	Fe = 3 µg/g
Si = 7 µg/g	W = 29 µg/g	Ni = 3 µg/g
Mo = 4 µg/g	Hf = 4 µg/g	
C = 2 µg/g	N = 4 µg/g	O = 5 µg/g
H = 1 µg/g	Nb remainder	

GAS CONTENT (FINAL PRODUCT)

C = < 10 µg/g	N = < 5 µg/g	O = < 5 µg/g
H = < 1 µg/g		

MECHANICAL PROPERTIES (FINAL PRODUCT): acc. to DIN EN 10002-1

	LONGITUDINAL DIRECTION	TRANSVERSE DIRECTION
0,2 % Yield stress (N/mm²)	68 - 73	72 - 81
Ultimate tensile strength (N/mm²)	153 - 181	182 - 182
Percentage elongation (%)	46,4 - 59,5	45,7 - 66,1

Hardness HV10: acc. to EN ISO 6507-1 47,9 - 57,9

Grain size No.: acc. to ASTM E112 5.4 - 6.5 (100% recrystallization)

RRR: 304 - 405

SURFACE FINISH:

Both sides have comparable surface finish, therefore no marking of Rfside was made.

Surface roughness: acc. to DIN EN ISO 4287

Ra: 0,95-1,11 µm Rz: 6,87-7,82 µm Rmax: 12,94 - 14,16 µm

FINAL QUALITY OF SHEET:

Sheet(s) manufactured by rolling-surface treatment-final heat treatment-grinding by machine (overall)-manual grinding of local defects-etching-final inspection.

REMARKS: -

PLANSEE Metall Fein
 A - 600 Road
 Tel: +4356703600
 Fax: +435670160-900
 http://www.plansee.com



INSPECTION CERTIFICATE

acc. to DIN EN 10204 - 3.1

Report No.: **8578353800010**
 Date: **30.01.2009**
 Customer: **NIOWAVE, INC. / US**
 PLANSEE-Order No./Par.No.: **6962614 / 10**
 PLANSEE-Material-No.: **11503996**
 PLANSEE-Segment / PoC. / : **/ Schenk / 1232**
 Customer Order No.: **Jerry Hollister dated 29.01.2009**
 Specification No.:

Material / Product: **NBM / NBM-RRH 250 Sheet 640x800x2,8 mm**

Dimensions: **540 x 800 x 2,8 ±0,15 mm**
 Quantity / Weight: **20,840 KG / KG**
 Batch(es): **0090509278 20,840 KG**
 SHEET No.: 124, 125

CHEMICAL ANALYSIS (INGOT 3201)

Ta = 76 µg/g	W = <5 µg/g	Zr = <2 µg/g
Hf = <4 µg/g	Fe = <3 µg/g	Ni = <3 µg/g
Si = <7 µg/g	Mo = <8 µg/g	
H = 1 µg/g	N = 7 µg/g	C = 2 µg/g
O = 3 µg/g	Nb remainder	

GAS CONTENT (FINAL PRODUCT)

H = <1 µg/g	N = 6 µg/g
O = 7 µg/g	C = 1 µg/g

MECHANICAL PROPERTIES (FINAL PRODUCT): acc. to DIN EN 10002-1
 LONGITUDINAL DIRECTION

0,2 % Yield stress (N/mm ²)	65 - 70
Ultimate tensile strength (N/mm ²)	137 - 147
Percentage elongation (%)	54,2 - 58,9

Hardness HV10: acc. to EN ISO 6507-1	40 - 60
Grain size No.: acc. to ASTM E112	6,2 - 6,8 (100% recrystallization)

ELECTRICAL PROPERTIES:

RRR: 286 (measured at HERAEUS)

Surface Finish:

Both sides have comparable surface finish, therefore no marking of Rfside was made.

Surface roughness: acc. to DIN EN ISO 4287

Ra	1,23 - 1,40 µm
Rz	7,83 - 9,91 µm
Rmax	8,85 - 12,48 µm

PLANSEE Metall GmbH
 A - 9693 Reitz
 Tel: + 43/5072/690 0
 Fax: + 43/5072/690 100
 http://www.plansee.com



INSPECTION CERTIFICATE

acc. to DIN EN 10204 - 3.1

Report No.: **86159167000010**
 Date: **21.07.2009**
 Customer: **NIOWAVE, INC. / US**
 PLANSEE-Order No./Pos.No.: **6845267 / 10**
 PLANSEE-Material-No.: **11491247**
 PLANSEE-Segment / PoC. / **S**: **/ Schenk / 1232**
 Customer Order No.: **08-0028-001** dated **18.11.2008**
 Specification No.:

Material / Product: **NBM / NbM-RRR 300 sheet 540x800x2,8 mm**
 Condition of material / Quality: **/**

Dimensions: **2,8 + -0,15 x 540 x 800 mm**
 Quantity / Weight: **134,550 KG / KG**
 Batch(es): **0090512418 134,550 KG**

SHEET No.: 129-132,135,136,139,142,143,145,146,148,149.

CHEMICAL ANALYSIS (INGOT H3205)

Ta = 145 µg/g	Zr = 2 µg/g	Fe = 3 µg/g
Si = 7 µg/g	W = 29 µg/g	Ni = 3 µg/g
Mo = 4 µg/g	Hf = 4 µg/g	O = 5 µg/g
C = 2 µg/g	N = 4 µg/g	
H = 1 µg/g	Nb remainder	

GAS CONTENT (FINAL PRODUCT)

C = < 10 µg/g	N = < 5 µg/g	O = < 5 µg/g
H = < 1 µg/g		

MECHANICAL PROPERTIES (FINAL PRODUCT): acc. to DIN EN 10002-1

	LONGITUDINAL DIRECTION	TRANSVERSE DIRECTION
0,2 % Yield stress (N/mm ²)	68 - 73	72 - 81
Ultimate tensile strength (N/mm ²)	153 - 161	162 - 182
Percentage elongation (%)	46,4 - 59,5	45,7 - 66,1

Hardness HV10: acc. to EN ISO 6507-1 **44,7 - 48,2**
 Grain size No.: acc. to ASTM E112 **4.7 - 7.5 (100% recrystallization)**
 RRR: **average 317,6**

SURFACE FINISH:

Both sides have compareable surface finish, therefore no marking of Rfside was made.

Surface roughness: acc. to DIN EN ISO 4287

Ra: **0,95-1,11 µm** Rz: **6,87-7,82 µm** Rmax: **12,94-14,16 µm**

FINAL QUALITY OF SHEET:

Sheet(s) manufactured by rolling-surface treatment-final heat treatment-grinding by machine (overall)-manual grinding of local defects-etching-final inspection.

REMARKS: -

INSPECTION CERTIFICATE

acc. DIN EN 10204 - 3.1

Report No.: 86159167000010

Date: 20.01.2010

Certified that the supplies/services detailed hereon have been inspected and tested in accordance with the conditions and requirements of the contract or purchase order and unless otherwise noted below, conform in all respects to the specification(s), drawing(s) relevant thereto.

This certificate has been generated by computer and need not to be signed for validity according to EN 10204.

Authorized inspection representative

(Dr. Thurner)

PLANSEE Metall GmbH
High Performance Materials
Inspection Department QM

(Partner)

N/8



NINGXIA ORIENT TANTALUM INDUSTRY CO., LTD

ADDRESS: P.O.BOX 105, SHIZUISHAN CITY, NINGXIA 753000, P.R.CHINA

TEL: 86-952-2098888

FAX: 86-952-2098889

Quality Control Report

For Nb55Ti Plate

Customer: Niowave, Inc.	Date: Oct 14, 2010
Lot No.: 2010-4-9-368-101014	State: Annealed
Size: 90x485x6.4 (mm)	Standard: Technical Specifications Nb55Ti Alloy
Quantity: 3 Pieces	Net Weight: 52 kg
PO No.: 10-1103-005	

1. Chemical Composition

Content	guaranteed	Analysis Result (%)
Ti	55%±0.1%	53.78
O	≤0.1%	0.072
C	≤0.015%	0.0036
N	≤0.015%	0.008
H	≤0.004%	0.0005
Ta	≤0.25%	0.0099
Fe	≤0.03%	0.018
NE	≤0.01%	0.003
Si	≤0.01%	0.005

2. Conditions and Microstructure

Item	Requirement	Results
Conditions	Forged - Annealed - Machined	OK
Microstructure	Recrystallization degree: Min 95%	>95%

NINGXIA ORIENT TANTALUM INDUSTRY CO.LTD

ADDRESS:P.O.BOX 105;SHIZUISHAN CITY ,NINGXIA 753000,CHINA
 TEL:86-952-209 8538 FAX:86-952- 2012018

CERTIFICATE OF QUALITY

NG

Nb55%Ti alloy bar

Customer: Niowave,Inc	Date: June.2 , 2010
Specification: Nb55%Ti alloy Version A	Number : 2
Lot No: Nb-55TiD-2-10001	Net weight : 83 (kg)
Purchase order number:10-1105-005	Size: Φ 142×500(mm)

Impurities:

Element	Value (%. wt)	Element	Value (%. wt)
C	0.0036	Fe	0.018
O	0.072	Si	0.005
N	0.008	Ni	0.003
H	0.0005	Ti	55.78
W	0.005	Ta	0.0098

Properties:

Recrystallization degree	HV/10N
≥95	167/168/177

QUALITY ASSURANCE REPRESENTATIVE

SIGNATURE





NINGXIA ORIENT TANTALUM INDUSTRY CO., LTD
 ADDRESS: P.O.BOX 105, SHIZUISHAN CITY, NINGXIA 753000, P.R.CHINA
 TEL: 86-952-2098888 FAX: 86-952-2098889

Quality Control Report
For Niobium Plate

Customer: Niowave, Inc. Date: Oct 18, 2010
 Lot No.: 2010-4-9-368-101018 State: Annealed
 Size: 2.8*810*810 (mm) Standard: DFSY
 Quantity: 2 Pcs Net Weight: 32.4kg
 P/O No.: 10-1105-005

N4-24,25

1. Chemical Composition

The ingot meets the chemical analysis for following elements

Content	guaranteed	Analysis Result
Ta	≤0.05%	0.005
W	≤0.007%	0.0012
Ti	≤0.005%	<0.0005
Fe	≤0.003%	0.0005
Si	≤0.003%	0.0010
Mo	≤0.005%	0.0010
Ni	≤0.003%	<0.0005

Content of interstitial elements in the annealed Nb

Content	guaranteed	Analysis Result
H	≤2ppm	1
N	≤10ppm	7
O	≤10ppm	5
C	≤10ppm	7

2. Mechanical Properties (Room Temperature)

Item	Requirement	Results
Tensile strength, Rm (N/mm ²)	Rm>140	184.9~185.4 (Parallel Direction)
		182.3~183.0 (Orthogonal Direction)
0.2% Nonproportional elongation, Rp0.2 (N/mm ²)	50<Rp0.2<100	80.2~87.9 (Parallel Direction)
		80.7~94.6 (Orthogonal Direction)



NINGXIA ORIENT TANTALUM INDUSTRY CO., LTD
 ADDRESS: P.O.BOX 105, SHIZUIZHAN CITY, NINGXIA 753000, P.R.CHINA
 TEL: 86-952-2098888 FAX: 86-952-2098889

Quality Control Report
For Niobium Plate

N4-22,23

Customer: Niowave, Inc. Date: Nov. 11, 2016
 Lot No.: 2016-4-9-368-101111 State: Annealed
 Size: 2.8*810*810 (mm) Standard: DUESY
 Quantity: 2 Pcs Net Weight: 32.42g
 P/O No.: 10-1105-005

1. Chemical Composition

The ingot meets the chemical analysis for following elements

Content	guaranteed	Analysis Result
Ta	≤0.05%	0.007
W	≤0.007%	0.0010
Ti	≤0.005%	<0.0005
Fe	≤0.003%	0.0005
Si	≤0.003%	0.0010
Mo	≤0.005%	0.0010
N	≤0.005%	0.0005

Content of interstitial elements in the annealed Nb

Content	guaranteed	Analysis Result
H	≤2ppm	2
N	≤10ppm	5
O	≤10ppm	5
C	≤10ppm	9

2. Mechanical Properties (Room Temperature)

Item	Requirement	Results
Tensile strength, Rm (N/mm ²)	Rm≥tCG	185.4~185.1 (Parallel Direction)
		183.9~184.9 (Orthogonal Direction)
0.2% Nonproportional elongation, Rp0.2 (N/mm ²)	50≤Rp0.2<100	78.7~79.0 (Parallel Direction)
		78.1~84.2 (Orthogonal Direction)



NINGXIA ORIENT TANTALUM INDUSTRY CO., LTD

ADDRESS: P.O.BOX 105, SHIZUISHAN CITY, NINGXIA 753000, P.R.CHINA

TEL: 86-952-2098888

FAX: 86-952-2098889

N4-18:21

Quality Control Report

For Niobium Plate

Customer: Niowave, Inc.

Date: Sep.29, 2010

Lot No.: 2010-4-9-265-100909

State: Annealed

Size: 2.8x810x810 (mm)

Standard: DE5Y

Quantity: 1 Pcs

Net Weight: 63.3kg

PO No.: 10-1105-005

1. Chemical Composition

The ingot meets the chemical analysis for following elements

Content	guaranteed	Analysis Result
H	≤0.05%	0.005
W	≤0.007%	0.007
T	≤0.005%	<0.0005
Fe	≤0.003%	0.0035
Si	≤0.003%	0.0020
Mn	≤0.005%	0.0010
Ni	≤0.003%	<0.0005

Content of interstitial elements in the annealed Nb

Content	guaranteed	Analysis Result
H	≤2ppm	1
N	≤10ppm	5
O	≤10ppm	5
C	≤10ppm	5

2. Mechanical Properties (Room Temperature)

Item	Requirement	Results
Tensile strength, Rm (N/mm ²)	Rm>140	171.3~175.6 (Parallel Direction)
		172.7~175.6 (Orthogonal Direction)
0.2% Non-proportional elongation, Rp0.2 (N/mm ²)	50<Rp0.2<700	79.0~80.3 (Parallel Direction)
		79.4~80.6 (Orthogonal Direction)



NINGXIA ORIENT TANTALUM INDUSTRY CO., LTD
 ADDRESS: P.O.BOX 105, SHIZUISHAN CITY, NINGXIA 753000, P.R.CHINA
 TEL: 86-952-2098888 FAX: 86-952-2098889

Quality Control Report
For Niobium Plate

*For Invoice
 Ser. N7*

Customer: Niowave, Inc. Date: Sep.9, 2010
 Lot No.: 2010-4-9-368- 00909 State: Annealed
 Size: 2.8x810x810 (mm) *N7-14:17* Standard: DESY
 Quantity: 4 Pcs Net Weight: 63.7kg
 P/O No.: 10-1105-035

1. Chemical Composition

The ingot meets the chemical analysis for following elements

Content	guaranteed	Analysis Result
Ta	≤0.05%	0.005
W	≤0.007%	0.0017
Ti	≤0.005%	<0.0005
Fe	≤0.003%	0.0005
Si	≤0.003%	0.0020
Mo	≤0.005%	0.0010
Ni	≤0.003%	<0.0005

Content of interstitial elements in the annealed Nb

Content	guaranteed	Analysis Result
H	≤2ppm	1
N	≤10ppm	6
O	≤10ppm	5
C	≤10ppm	5

2. Mechanical Properties (Room Temperature)

Item	Requirement	Results
Tensile strength, Rm (N/mm ²)	Rm>140	171.3~175.6 (Parallel Direction)
		173.7~176.6 (Orthogonal Direction)
0.2% Non-proportional elongation, Rp0.2 (N/mm ²)	50·Rp0.2<100	79.0~80.3 (Parallel Direction)
		79.4~80.6 (Orthogonal Direction)



NINGXIA ORIENT TANTALUM INDUSTRY CO., LTD

ADDRESS: P.O. BOX 108, SHUOZHUISHAN CITY, NINGXIA 753000, P.R.CHINA

TEL: 86-952-2098888

FAX: 86-952-2098889

Quality Control Report

For Niobium Plate

Customer: Niowave, Inc	Date: Aug 13, 2012
Lot No.: 2012-09-368-003-71	State: Arizona
Size: 2.888" (76.12 mm)	Standard: JISY
Quantity: 13 Pcs	Net Weight: 209.5g
P.O No.: 10-105-005	

1. Chemical Composition

The following is the chemical analysis for following elements

Content	guaranteed	Analysis Result
Fe	≤0.005%	0.005
W	≤0.007%	0.007
Bi	≤0.005%	≤0.005
Zr	≤0.003%	0.003
Si	≤0.003%	0.003
Mo	≤0.005%	0.005
Ni	≤0.005%	≤0.005

Content of interstitial elements in the amount of Nb

Content	guaranteed	Analysis Result
H	≤10ppm	1
N	≤10ppm	6
O	≤10ppm	5
C	≤10ppm	5

2. Mechanical Properties (Room Temperature)

Item	Requirement	Results
Tensile strength, R _m (N/mm ²)	Rm≥110	171.3~175.6 (Parallel Direction)
		177.7~176.6 (Orthogonal Direction)
0.2% Nonproportional elongation, Rel.2 (N/mm ²)	50~Rm0.01~100	85.0~88.1 (Parallel Direction)
		70.3~85.6 (Orthogonal Direction)



NINGXIA ORIENT TANTALUM INDUSTRY CO., LTD
 ADDRESS: P.O. BOX 108, SHUOZILISHAN CITY, NINGXIA 753000, P.R.CHINA
 TEL: 86-952-2098888 FAX: 86-952-2098889

Quality Control Report
For Niobium Plate

Customer: Niowave, Inc. Date: Aug.10, 2010
 Lot No.: 2010-09-368-003-71 State: Arizona
 Size: 2.888" (76.12 mm) Standard: JISY
 Quantity: 13 Pcs Net Weight: 209.5g
 P.O No.: 10-105-005

1. Chemical Composition

The following is the chemical analysis for following elements

Content	guaranteed	Analysis Result
Fe	≤0.005%	0.005
W	≤0.007%	0.007
Bi	≤0.005%	≤0.005
Zr	≤0.003%	0.003
Si	≤0.003%	0.003
Mo	≤0.005%	0.005
Ni	≤0.005%	≤0.005

Content of interstitial elements in the amount of Nb

Content	guaranteed	Analysis Result
H	≤10ppm	1
N	≤10ppm	6
O	≤1.0ppm	5
C	≤10ppm	5

2. Mechanical Properties (Room Temperature)

Item	Requirement	Results
Tensile strength, R _m (N/mm ²)	Rm≥110	171.3~175.6 (Parallel Direction)
		177.7~176.6 (Orthogonal Direction)
0.2% Nonproportional elongation, Rel.2 (N/mm ²)	50~Rm0.2≤100	85.0~88.1 (Parallel Direction)
		70.3~85.6 (Orthogonal Direction)



~~NINGXIA ORIENT TANTALUM INDUSTRY CO., LTD~~ N15

ADDRESS: P.O.BOX 105, SHIZUISHAN CITY, NINGXIA 753000, P.R.CHINA

TEL: 86-952-2098888

FAX: 86-952-2098889

Quality Control Report

For Niobium Plate

Customer: Niowave, Inc.

Date: Dec.7, 2010

Lot No.: 2010-4-9-368-101207

State: Annealed

Size: 350×230×9.5 (mm)

Standard: DESY

Quantity: 1 PIECE

Net Weight: 6.5kg

P/O No.: 109-1105-005

1. Chemical Composition

The ingot meets the chemical analysis for following elements

Content	guaranteed	Analysis Result
Ta	≤0.05%	0.0061
W	≤0.007%	0.0011
Ti	≤0.005%	<0.0005
Fe	≤0.003%	0.0005
Si	≤0.003%	0.0010
Mo	≤0.005%	0.0010
Ni	≤0.003%	<0.0005

Content of interstitial elements in the annealed Nb

Content	guaranteed	Analysis Result
H	≤2ppm	1
N	≤10ppm	5
O	≤10ppm	5
C	≤10ppm	7

2. Mechanical Properties (Room Temperature)

Item	Requirement	Results
Tensile strength, Rm (N/mm ²)	Rm>140	215.2~223.1 (Parallel Direction)
		211.5.2~231.1 (Orthogonal Direction)
0.2% Nonproportional elongation, Rp0.2 (N/mm ²)	50<Rp0.2<100	90.1~93.1 (Parallel Direction)
		93.1~95.6 (Orthogonal Direction)

Percentage elongation after fracture Using min 30 mm Gauge Length, AL30	$\geq 30\%$	31.2~32.4 (Parallel Direction)
		31.2~36.0 (Orthogonal Direction)
Hardness, HV10	≤ 60	1*

1* (HVS/10N)

No.	1#
Result	57.6 ~ 59.9

3. Inspecture results

Item	Requirement	Results
RRR values	≥ 300	306
Grain Size	-ASTM #6 or finer -Local grain sizes ASTM 4-5	ASTM 7.0-8.0
Surface roughness	$R_t \leq 15 \mu m$	$< 15 \mu m$
Flatness	Surface flatness according to -ASTM B 708: 2% or better	$< 2\%$
Ultrasonic measurements	No defects	ok
Surface inspection (Defects)	(1) Non niobium material, (2) Visible clusters from niobium oxides, segregation, cracks, blisters. (3) Grease and finger prints on the surface. (4) Scratches and marks of more than $R_t \geq 15 \mu m$ for the RF side or of $R_t \geq 60 \mu m$ for the back side, even if free from non niobium material.	ok
Visual inspection	No defect	ok
Size	350x230x9.5	ok

QC Judgment	Pass
-------------	------

Quality Control Representative

Signature: 

NORTHWEST RARE METAL MATERIAL INSTITUTE

ADDRESS: P.O.BOX 105, SHIZUIZHAN CITY, NINGXIA 753000.P.R.CHINA

TEL:86-952-2098206 FAX:86-952-2098205 E-mail:nmiec@public.yc.nx.cn

Quality Control Report**For Niobium Plate**

Customer: NIOWAVE INC.	Date: Mar.23,2009
Lot No.: W2009-02-16-090323	Material No.: E ₃ NT-16
Size: 4X675X775 (mm)	Quantity: 10 Pcs Net Weight: 108.9 kg
2.8X670X330 (mm)	2 Pcs Net Weight: 10.7 kg
State : Annealed	P/O No.: 08-0006-906

1. Chemical Properties**Chemical composition of niobium ingot (wt%):**

Element	Requirement	Analysis Result
Ta	≤0.050	<0.0100 100
W	≤0.007	0.0010 15
Ti	≤0.005	<0.0005 5
Fe	≤0.003	0.0005 5
Si	≤0.003	<0.0010 10
Mo	≤0.005	0.0010 10
Ni	≤0.003	<0.0005 5

Content of Interstitial elements in the annealed niobium plate

Element	Requirement	Analysis Result
H	≤2ppm	2
N	≤10ppm	10
O	≤10ppm	5
C	≤10ppm	8

2. Mechanical Properties(Room Temperature)

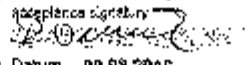
	Results
1) Ultimate Tensile Strength (N/mm ²)	176.2~187.7
2) 0.2% Nonproportional Elongation (N/mm ²)	83.2~91.4
3) Elongation (%)(30mm AL)	53.2~66.8
4) Hardness (HVS/0.05N)	56.5~59.8
5) RRR	315~420
6) Grain Size	ASIM 6.0

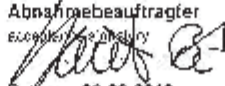
QUALITY CONTROL REPRESENTATIVE

SIGNATURE

WANG LI HUA

HS

Blatt 1/1		Abnahmeprüfzeugnis 3.1		Heraeus
Ausgabe: [D] 28.07.2010 8 K		EN 10204/3.1		
Customer Kunde	Niowave	Product Produkt	Niobium RRR 300 rod 133 x 636 mm	
Part No. Teil-Nr.	81 067 318	Ident No. Ident-Nr.	81 067 318	
Specification No. Satz-Nr.		Quantity Liefermenge	1 pcs	
Order No. Auftrag-Nr.	173 000 66	Material Werkstoff	Nb	
Purchase order No. Bestell-Nr.	PO 10-1105-004 dated 18.03.2010	Lot No. Charge-Nr.	3159 / G 109183	
Pos. Nrn	Prüfparameter Inspection parameter	Nennwert nom. value	Istwert actual	Bemerkung remarks
1	Ingot Nb (µg/g)	remainder	remainder	chemical requirements according to ASTM B352-03-R04210
2	Ta (µg/g)	< 300	330	
3	Zr (µg/g)	< 200	< 2	
4	Fe (µg/g)	< 100	< 3	
5	Si (µg/g)	< 50	< 7	
6	W (µg/g)	< 500	< 6	
7	Ni (µg/g)	< 50	< 3	
8	Mo (µg/g)	< 200	< 4	
9	Hf (µg/g)	< 200	< 4	
10	C (µg/g)	< 100	2	
11	N (ppm)	< 100	7	
12	O (µg/g)	< 250	3	
13	H (µg/g)	< 16	1	
14	RRR	> 300	329	
		Abnahmebeauftragter acceptance signatory  Datum 08.08.2010 date		

Blatt 1/1		Abnahmeprüfzeugnis 3.1		HERMELUS
Ausgabe :		Inspection certificate 3.1		
[C] 28.07.2010 SK		EN 10204/3.1		
customer Kunde	Niowave	product Produkt	Niobium RRR 300 rod 12.0 x 570 mm	
part No. Teil-Nr.	81 067 348	ident No. Ident-Nr.	81 067 345	
specification No. Spezifikations-Nr.		quantity Liefermenge	4 pcs	
order No. Auftrags-Nr.	170 D00 68	material Werkstoff	Nb	
purchase order No. Bestell-Nr.	PO 10-1105-004 dated 19.02.2010	lot No. Chargen-Nr.	3199 / S 103036	
Pos. Item	Prüfparameter inspection parameter	Nennwert nom. value	Istwert actual	Bemerkung remarks
	Ingot			chemical requirements according to ASTM B392-03-R04210
1	Nb (µg/g)	remainder	remainder	
2	Ta (µg/g)	< 300	99	
3	Zr (µg/g)	< 200	< 2	
4	Fe (µg/g)	< 100	< 3	
5	Si (µg/g)	< 50	< 7	
6	W (µg/g)	< 500	13	
7	Ni (µg/g)	< 50	< 3	
8	Mo (µg/g)	< 200	< 4	
9	Hf (µg/g)	< 200	< 4	
10	C (µg/g)	< 100	2	
11	N (µg/g)	< 100	8	
12	O (µg/g)	< 250	4	
13	H (µg/g)	< 15	1	
14	RRR	>300	348	
		Abnahmebeauftragter Accepted by:  Datum 02.08.2010 date:		

Blatt 1/1		Abnahmeprüfzeugnis 3.1		HERAEUS
Ausgabe:		Inspection certificate 3.1		
[0] 23.07.2010 BK		EN 10204/3.1		
customer Kunde	Niowave	product Produkt	Niobium RRR 300 rod 40 x 49 x 466 mm	
part No. Teil-Nr.	81 087 373	ident No. Ident-Nr.	81 087 373	
specification No. Spezifikations-Nr.		quantity Liefermenge	9 pcs	
order No. Auftrag-Nr.	170 030 BR	material Werkstoff	Ni	
purchase order No. Bestell-Nr.	PO 10-1105-004 dated 19.03.2010	lot No. Charge-Nr.	3189 J S 103034	
Poa. Icn:	Prüfparameter Inspection parameter	Nennwert nom. value	Istwert actual	Bemerkung remark
	Ingot			chemical requirements according to ASTM B392-03-R04210
1	Nb (µg/g)	remainder	remainder	
2	Ta (µg/g)	< 300	99	
3	Zr (µg/g)	< 200	< 2	
4	Fe (µg/g)	< 100	< 3	
5	Si (µg/g)	< 50	< 7	
6	W (µg/g)	< 500	13	
7	Rh (µg/g)	< 50	< 3	
8	Mo (µg/g)	< 200	< 4	
9	Hf (µg/g)	< 200	< 4	
10	C (µg/g)	< 100	2	
11	H (µg/g)	< 100	6	
12	O (µg/g)	< 250	4	
13	N (µg/g)	< 15	1	
14	RRR	> 300	364	
		Abnahmebeauftragter [Signature] Datum 02.08.2010 date		

144

Blatt 1/1	Abnahmeprüfzeugnis 3.1 Inspection certificate 3.1	Heraeus
Ausgabe : [0] 20.07.10 DM		EN 10204/3.1
customer Kunde part No. Teile-Nr. specification No. Spezifikations-Nr. order No. Auftrags-Nr. purchase order No. Bestell-Nr.	Niowave Inc. 17000075 PO 10-0013-002 dtd.07/16/2010	product Produkt Ident No. Ident-Nr. quantity Liefermenge material Werkstoff lot No. Chargen-Nr.
		Coupler Housing NB 300 45,00x2,50x66,20 64 003 390 7 pcs Nb RRR 300 3192

Pos. tm	Prüfparameter inspection parameter	Nennwert nom. value	Istwert actual	Bemerkung remarks
	ingot			* chemical requirements according to ASTM B 391-03-R04200
1	Nb (µg/g)	remainder	remainder	
2	Ta (µg/g)	< 1000	65	
3	Fe (µg/g)	< 50	< 3	
4	Si (µg/g)	< 50	< 7	
5	W (µg/g)	< 300	< 6	
6	Ni (µg/g)	< 50	< 3	
7	Mo (µg/g)	< 100	< 4	
8	Ti (µg/g)	< 200	< 2	
9	C (µg/g)	< 100	2	**
10	O (µg/g)	< 160	2	**
11	H (µg/g)	< 15	1	**
12	N (µg/g)	< 100	6	**
13	RRR	> 300	337	

<p>* metallic impurities determined at the ingot</p> <p>** interstitials determined at the final product</p>	<p>Abnahmebeauftragter acceptance signatory Datum 20.07.2010</p> <p style="text-align: right;">H. C. Heraeus SAP - CR</p>
--	--



10-0013-0003-P04

10-0013-0003-P04

10-0013-0003-P04

10-0013-0003-P04

PART NUMBER: 10-0013-0003-P04
 PART NAME: NW 78 END TUBE FLANGE
 NEXT ASSEMBLY: Flange to beam tube EBW
 MATERIAL: NBTI

PROCESS SHEET
 SHEET 1 OF 1

OP	OPERATION DESCRIPTION	OPERATION DRAWING	DATE COMPLETED	OPERATOR INITIALS
1	SAW CUT BAR INTO .800" DISKS	NONE	9/19/2010	JT
2	MILL DISKS TO .790" THICKNESS	SEE SKETCH	9/21/2010	JT
3	WATERJET FLANGE ID TO PRINT	10-0013-R001-P07	9/27/2010	LT
4	QA FLANGE ID	10-0013-R001-P07	9/28/2011	TL
5	MACHINE TO PRINT	10-0013-0003-P04	9/30/2010	TG
6	ENGRAVE SERIAL # ON OD		10/4/2010	TL
7	QA FLANGE	10-0013-0003-P04	10/5/2010	TL
8	MACHINE ID TO FIT BEAM TUBES	10-0013-0003-P04	3/7/2011	DD
9	QA FLANGE	10-0013-0003-P04	3/8/2011	DF
10	PREP FLANGE FOR EBW			TS



NOTE: 1: .020 [.508] HAS BEEN ADDED TO THE FLANGE THICKNESS FOR CLEANUP AFTER THE FIRST WELDING PROCEDURE. SEALING SURFACE TO REMAIN .039 [1] BENEATH THE FACE OF THE FLANGE.

2: COPIED FROM 070034-104 ON 10-22-2008

NIOWAVE		EDDY CURRENT SCAN			PROCESS SHEET	
PART NUMBER: 10-0013-R001-P02		NB SHEET NUMBER:		SHEET 1 OF 1		
PART NAME: HALF-CELL BLANK		MATERIAL: RRR 300 Nb				
OP	OPERATION DESCRIPTION	OPERATION DRAWING	DATE COMPLETED	OPERATOR INITIALS	REFERENCE SKETCH	
1	EDDY CURRENT SCAN	SEE SKETCH	FNAL	FNAL		



MID-CELL FABRICATION TRACKER

COMPONENT TRAVELLER

Parent Material	Stamping		Coming		Check Fixture		Weld Prep Machining		Visual Inspection			DynaBraid			Final Visual Inspection			Notes	
	Date	Operator	Date	Operator	Pass/Fail	Operator	Date	CNC Operator	Rust, scratches, etc.	Date	Inspector	Date	Operator	Pass/Fail	Date	Operator			
N4-24-3	12/21/2010	K2	12/21/2010	K2	PASS	K2	1/6/2011	JNS	SEE MID-CELL CLEAN TRACKER										
N4-24-1	12/21/2010	K2	12/21/2010	K2	PASS	K2	1/6/2011	JNS	SEE MID-CELL CLEAN TRACKER										
N4-24-2	12/21/2010	K2	12/21/2010	K2	PASS	K2	12/29/2010	ECL	SEE MID-CELL CLEAN TRACKER										
N4-24-5	12/21/2010	K2	12/21/2010	K2	PASS	K2	1/5/2011	KC	SEE MID-CELL CLEAN TRACKER										
N4-24-4	12/21/2010	K2	12/21/2010	K2	PASS	K2	1/5/2011	JNS	SEE MID-CELL CLEAN TRACKER										
N4-24-6	12/21/2010	K2	12/21/2010	K2	PASS	K2	1/5/2011	JNS	SEE MID-CELL CLEAN TRACKER										
N4-24-8	12/21/2010	K2	12/21/2010	K2	PASS	K2	1/5/2011	JNS	SEE MID-CELL CLEAN TRACKER										
N4-24-9	12/21/2010	K2	12/21/2010	K2	PASS	K2	12/30/2010	KC	SEE MID-CELL CLEAN TRACKER										
N4-24-7	12/21/2010	K2	12/21/2010	K2	PASS	K2	12/29/2010	ECL	SEE MID-CELL CLEAN TRACKER										
N4-18-2	12/22/2010	K2	12/22/2010	K2	PASS	K2	12/29/2010	ECL	SEE MID-CELL CLEAN TRACKER										
N4-18-3	12/22/2010	K2	12/22/2010	K2	PASS	K2	1/4/2011	ECL	SEE MID-CELL CLEAN TRACKER										
N4-19-7M	12/22/2010	JRW	12/22/2010	JRW	PASS	JRW	12/30/2010	KC	SEE MID-CELL CLEAN TRACKER										
N4-18-5	12/22/2010	K2	12/22/2010	K2	PASS	K2	12/30/2010	JNS	SEE MID-CELL CLEAN TRACKER										
N4-19-8	12/22/2010	JRW	12/22/2010	JRW	PASS	JRW	12/29/2010	ECL	SEE MID-CELL CLEAN TRACKER										
N4-19-4	12/22/2010	K2	12/22/2010	K2	PASS	K2	12/29/2010	ECL	SEE MID-CELL CLEAN TRACKER										
N4-19-5	12/22/2010	JRW	12/22/2010	JRW	PASS	JRW	1/6/2011	JNS	SEE MID-CELL CLEAN TRACKER										
N4-19-6	12/22/2010	JRW	12/22/2010	JRW	PASS	JRW	1/2/2011	ECL	SEE MID-CELL CLEAN TRACKER										
N4-19-1	12/22/2010	K2	12/22/2010	K2	PASS	K2	1/6/2011	ECL	SEE MID-CELL CLEAN TRACKER										
N4-19-2	12/22/2010	K2	12/22/2010	K2	PASS	K2	1/6/2011	JNS	SEE MID-CELL CLEAN TRACKER										
N4-19-3	12/22/2010	K2	12/22/2010	K2	PASS	K2	1/2/2011	K2	SEE MID-CELL CLEAN TRACKER										
N4-25-2	12/22/2010	K2	12/22/2010	K2	PASS	K2	1/4/2011	ECL	SEE MID-CELL CLEAN TRACKER										
N4-25-1	12/22/2010	JRW	12/22/2010	JRW	PASS	JRW	1/5/2011	KC	SEE MID-CELL CLEAN TRACKER										
N4-25-3	12/22/2010	JRW	12/22/2010	JRW	PASS	JRW	1/5/2011	KC	SEE MID-CELL CLEAN TRACKER										
N4-25-5	12/22/2010	K2	12/22/2010	K2	PASS	K2	1/6/2011	JNS	SEE MID-CELL CLEAN TRACKER										
N4-25-8	12/22/2010	K2	12/22/2010	K2	PASS	K2	1/2/2011	K2	SEE MID-CELL CLEAN TRACKER										
N4-25-9	12/22/2010	K2	12/22/2010	K2	PASS	K2	1/6/2011	KC	SEE MID-CELL CLEAN TRACKER										
N4-25-7	12/22/2010	K2	12/22/2010	K2	PASS	K2	1/6/2011	ECL	SEE MID-CELL CLEAN TRACKER										
N4-23-1	12/22/2010	K2	12/22/2010	K2	PASS	K2	1/6/2011	ECL	SEE MID-CELL CLEAN TRACKER										
N4-23-3	12/22/2010	K2	12/22/2010	K2	PASS	K2	1/4/2011	ECL	SEE MID-CELL CLEAN TRACKER										
N4-23-5	12/22/2010	K2	12/22/2010	K2	PASS	K2	1/4/2011	ECL	SEE MID-CELL CLEAN TRACKER										
N4-25-4	12/22/2010	K2	12/22/2010	K2	PASS	K2	1/7/2011	JNS	SEE MID-CELL CLEAN TRACKER										
N4-2-9	1/10/2011	JRW	12/22/2010	JRW	PASS	JRW	1/15/2011	JNS	SEE MID-CELL CLEAN TRACKER										
N4-5-3	1/10/2011	JRW	12/22/2010	JRW	PASS	JRW	1/15/2011	JNS	SEE MID-CELL CLEAN TRACKER										
N4-7-7	1/10/2011	JRW	12/22/2010	JRW	PASS	JRW	1/14/2011	JNS	SEE MID-CELL CLEAN TRACKER										
N4-1-6	1/10/2011	JRW	12/22/2010	JRW	PASS	JRW	1/14/2011	JNS	SEE MID-CELL CLEAN TRACKER										
N4-8-9	1/10/2011	JRW	12/22/2010	JRW	PASS	JRW	1/14/2011	KC	SEE MID-CELL CLEAN TRACKER										
N4-1-9	1/10/2011	JRW	12/22/2010	JRW	PASS	JRW	1/14/2011	JNS	SEE MID-CELL CLEAN TRACKER										
N4-5-2	1/10/2011	JRW	12/22/2010	JRW	PASS	JRW	1/14/2011	JNS	SEE MID-CELL CLEAN TRACKER										
N4-5-9	1/10/2011	JRW	12/22/2010	JRW	PASS	DD	1/4/2011	KC	SEE MID-CELL CLEAN TRACKER										
N4-7-5	1/10/2011	JRW	12/22/2010	JRW	PASS	DD	1/4/2011	DD	SEE MID-CELL CLEAN TRACKER										
N4-9-9	1/10/2011	JRW	12/22/2010	JRW	PASS	JRW	1/13/2011	DDK	SEE MID-CELL CLEAN TRACKER										
N4-7-2	1/10/2011	JRW	12/22/2010	JRW	PASS	JRW	1/13/2011	DDK	SEE MID-CELL CLEAN TRACKER										
N4-5-5	1/10/2011	JRW	12/22/2010	JRW	PASS	JRW	1/13/2011	DDK	SEE MID-CELL CLEAN TRACKER										
N4-8-3	1/10/2011	JRW	12/22/2010	JRW	PASS	JRW	1/14/2011	KC	SEE MID-CELL CLEAN TRACKER										
N4-8-2	1/10/2011	JRW	12/22/2010	JRW	PASS	JRW	1/14/2011	KC	SEE MID-CELL CLEAN TRACKER										
N4-5-4	1/10/2011	JRW	12/22/2010	JRW	PASS	JRW	1/14/2011	KC	SEE MID-CELL CLEAN TRACKER										

PART NUMBER: 10-0013-0005-P01 PART NAME: MID HALF-CELL MATERIAL: RRR 300 Nb NEXT ASSEMBLY: Mid Half Cell to Mid Half Cell EBW SHEET 2 OF 4



MID-CELL FABRICATION TRACKER

COMPONENT TRAVELLER

Parent Material	Stamping		Coming		Check Fixture		Weld Prep Machining		Visual Inspection			DynaBraid			Final Visual Inspection			Notes
	Date	Operator	Date	Operator	Pass/Fail	Operator	Date	CNC Operator	Rust, scratches, etc.	Date	Inspector	Date	Operator	Pass/Fail	Date	Operator		
N4-5-6	1/10/2011	JRW	1/10/2011	JRW	PASS	JRW	1/14/2011	KC	SEE MID-CELL CLEAN TRACKER									
N4-1-7	1/10/2011	JRW	1/10/2011	JRW	PASS	JRW	1/14/2011	KC	SEE MID-CELL CLEAN TRACKER									
N4-5-8	1/10/2011	JRW	1/10/2011	JRW	PASS	JRW	1/14/2011	KC	SEE MID-CELL CLEAN TRACKER									
N4-5-7	1/10/2011	JRW	1/10/2011	JRW	PASS	JRW	1/14/2011	JNS	SEE MID-CELL CLEAN TRACKER									
N4-1-8	1/10/2011	JRW	1/10/2011	JRW	PASS	JRW	1/17/2011	JNS	SEE MID-CELL CLEAN TRACKER									
N4-6-8	1/10/2011	JRW	1/10/2011	JRW	PASS	JRW	1/17/2011	KC	SEE MID-CELL CLEAN TRACKER									
N4-2-4	1/10/2011	JRW	1/10/2011	JRW	PASS	JRW	1/15/2011	JNS	SEE MID-CELL CLEAN TRACKER									
N4-4-7	1/10/2011	JRW	1/10/2011	JRW	PASS	JRW	1/14/2011	KC	SEE MID-CELL CLEAN TRACKER									SMALL DING ON OUTSIDE
N4-2-7	1/10/2011	JRW	1/10/2011	JRW	PASS	JRW	1/14/2011	KC	SEE MID-CELL CLEAN TRACKER									
N4-7-8	1/10/2011	JRW	1/10/2011	JRW	PASS	JRW	1/14/2011	KC	SEE MID-CELL CLEAN TRACKER									
N4-8-5	1/10/2011	JRW	1/10/2011	JRW	PASS	JRW	1/14/2011	JNS	SEE MID-CELL CLEAN TRACKER									
N4-6-4	1/10/2011	JRW	1/10/2011	JRW	PASS	JRW	1/15/2011	JNS	SEE MID-CELL CLEAN TRACKER									
N4-6-6	1/10/2011	JRW	1/10/2011	JRW	PASS	JRW	1/15/2011	JNS	SEE MID-CELL CLEAN TRACKER									
N4-6-2	1/10/2011	JRW	1/10/2011	JRW	PASS	JRW	1/15/2011	JNS	SEE MID-CELL CLEAN TRACKER									
N4-6-6	1/10/2011	JRW	1/10/2011	JRW	PASS	JRW	1/15/2011	JNS	SEE MID-CELL CLEAN TRACKER									
N4-6-8	1/10/2011	JRW	1/10/2011	JRW	PASS	JRW	1/15/2011	JNS	SEE MID-CELL CLEAN TRACKER									
N4-6-9	1/10/2011	JRW	1/10/2011	JRW	PASS	JRW	1/15/2011	JNS	SEE MID-CELL CLEAN TRACKER									
N4-6-3	1/10/2011	JRW	1/10/2011	JRW	PASS	JRW	1/15/2011	JNS	SEE MID-CELL CLEAN TRACKER									
N4-9-2	1/10/2011	JRW	1/10/2011	JRW	PASS	JRW	1/15/2011	JNS	SEE MID-CELL CLEAN TRACKER									
N4-3-6	1/10/2011	SAK	1/10/2011	SAK	PASS	JRW	1/17/2011	KC	SEE MID-CELL CLEAN TRACKER									
N4-7-3	1/10/2011	SAK	1/10/2011	JRW	PASS	JRW	1/15/2011	JNS	SEE MID-CELL CLEAN TRACKER									
N4-4-3	1/10/2011	JRW	1/10/2011	JRW	PASS	JRW	1/15/2011	JNS	SEE MID-CELL CLEAN TRACKER									
N4-3-9	1/11/2011	JRW	1/11/2011	JRW	PASS	JRW	1/18/2011	JNS	SEE MID-CELL CLEAN TRACKER									
N4-7-4	1/11/2011	JRW	1/11/2011	JRW	PASS	JRW	1/18/2011	DNK	SEE MID-CELL CLEAN TRACKER									
N4-2-1	1/11/2011	JRW	1/11/2011	JRW	PASS	JRW	1/17/2011	KC	SEE MID-CELL CLEAN TRACKER									
N4-3-8	1/11/2011	SAK	1/11/2011	SAK	PASS	JRW	1/18/2011	JNS	SEE MID-CELL CLEAN TRACKER									
N4-3-5	1/11/2011	JRW	1/11/2011	JRW	PASS	JRW	1/18/2011	JNS	SEE MID-CELL CLEAN TRACKER									
N4-3-4	1/11/2011	JRW	1/11/2011	JRW	PASS	JRW	1/18/2011	JNS	SEE MID-CELL CLEAN TRACKER									
N4-1-1	1/11/2011	JRW	1/11/2011	JRW	PASS	JRW	1/18/2011	DNK	SEE MID-CELL CLEAN TRACKER									
N4-4-7	1/11/2011	JRW	1/11/2011	JRW	PASS	JRW	1/18/2011	DNK	SEE MID-CELL CLEAN TRACKER									
N4-3-1	1/11/2011	JRW	1/11/2011	JRW	PASS	JRW	1/18/2011	JNS	SEE MID-CELL CLEAN TRACKER									
N4-6-3	1/11/2011	JRW	1/11/2011	JRW	PASS	JRW	1/18/2011	DNK	SEE MID-CELL CLEAN TRACKER									
N4-3-3	1/11/2011	JRW	1/11/2011	JRW	PASS	JRW	1/17/2011	JNS	SEE MID-CELL CLEAN TRACKER									
N4-5-1	1/11/2011	JRW	1/11/2011	JRW	PASS	JRW	1/18/2011	DNK	SEE MID-CELL CLEAN TRACKER									
N4-2-6	1/11/2011	JRW	1/11/2011	JRW	PASS	JRW	1/17/2011	KC	SEE MID-CELL CLEAN TRACKER									
N4-9-1	1/11/2011	JRW	1/11/2011	JRW	PASS	JRW	1/16/2011	ECL	SEE MID-CELL CLEAN TRACKER									
N4-4-1	1/11/2011	JRW	1/11/2011	JRW	PASS	JRW	1/18/2011	JNS	SEE MID-CELL CLEAN TRACKER									
N4-3-2	1/11/2011	JRW	1/11/2011	JRW	PASS	JRW	1/17/2011	KC	SEE MID-CELL CLEAN TRACKER									
N4-8-2	1/11/2011	JRW	1/11/2011	JRW	PASS	JRW	1/16/2011	ECL	SEE MID-CELL CLEAN TRACKER									
N4-3-2	1/11/2011	JRW	1/11/2011	JRW	PASS	JRW	1/16/2011	ECL	SEE MID-CELL CLEAN TRACKER									
N4-6-2	1/11/2011	JRW	1/11/2011	JRW	PASS	JRW	1/16/2011	ECL	SEE MID-CELL CLEAN TRACKER									
N4-7-6	1/11/2011	JRW	1/11/2011	JRW	PASS	JRW	1/16/2011	ECL	SEE MID-CELL CLEAN TRACKER									
N4-4-4	1/11/2011	JRW	1/11/2011	JRW	PASS	JRW	1/16/2011	ECL	SEE MID-CELL CLEAN TRACKER									
N4-3-4	1/11/2011	JRW	1/11/2011	JRW	PASS	JRW	1/16/2011	ECL	SEE MID-CELL CLEAN TRACKER									
N4-8-5	1/11/2011	JRW	1/11/2011	JRW	PASS	JRW	1/16/2011	ECL	SEE MID-CELL CLEAN TRACKER									
N4-4																		
N4-4																		

PART NUMBER: 10-0013-0005-P01 PART NAME: MID HALF-CELL TRACKER MATERIAL: RRR 300 Nb NEXT ASSEMBLY: Mid Half Cell to Mid Half Cell EBW SHEET 3 OF 4



COMPONENT TRAVELER

MID-CELL CLEANING TRACKER

Cell ID	24 Hr Tap-water Soak		Rust Spot Visual Inspection		Dynamabraid		Cleanroom Prep		USC Processing		30 µm Yield Prep Etch		Final Inspect & Clean-room Pkg.		Notes	
	Date	Operator	Pass/Fail	Date	Inspector	Date	Operator	Date	Operator	Date	Operator	Date	Operator	Pass/Fail		Date
N4-01-1	2/1/2011	TS	Pass	2/7/2011	JK			2/7/2011	TS	2/28/2011	JK	3/1/2011	TS	Pass	3/3/2011	TS
N4-01-2	2/1/2011	TS	Fail	2/7/2011	JK	2/9/2011	SAK	2/9/2011	TS	3/14/2011	JK	3/17/2011	CMK	Pass	3/18/2011	JK
N4-01-3	2/1/2011	TS	Fail	2/7/2011	JK	2/9/2011	SAK	2/9/2011	TS	3/14/2011	JK	3/17/2011	CMK	Pass	3/18/2011	JK
N4-01-4	1/20/2011	TS	Pass	1/21/2011	JK			1/26/2011	JH	1/27/2011	JK	2/7/2011	TS	Pass	2/17/2011	JK
N4-01-5	2/2/2011	TS	Pass	2/7/2011	JK			2/28/2011	TS	2/28/2011	JK	3/2/2011	TS	Pass	3/9/2011	TS
N4-01-6	1/18/2011	TS	Fail	1/20/2011	JK	1/20/2011	SAK	1/26/2011	JH	1/27/2011	JK	3/1/2011	CMK	Pass	3/18/2011	JK
N4-01-7	1/17/2011	JK	Pass	1/18/2011	JK			1/26/2011	JH	1/27/2011	JK	3/1/2011	CMK	Pass	3/18/2011	JK
N4-01-8	1/18/2011	TS	Pass	1/19/2011	JK			1/26/2011	JH	1/27/2011	JK	2/9/2011	TS	Pass	2/17/2011	JK
N4-01-9	1/18/2011	TS	Pass	1/20/2011	JK			1/26/2011	JH	1/27/2011	JK	2/9/2011	CMK	Pass	3/18/2011	JK
N4-02-1	1/18/2011	TS	Pass	1/19/2011	JK			1/26/2011	JH	1/27/2011	JK	2/9/2011	CMK	Pass	3/18/2011	JK
N4-02-2	2/1/2011	JW	Fail	2/7/2011	JK	2/9/2011	SAK	2/9/2011	TS	3/14/2011	JK	3/17/2011	CMK	Pass	3/18/2011	JK
N4-02-3	2/2/2011	TS	Pass	2/7/2011	JK			2/27/2011	TS	2/28/2011	JK	3/3/2011	TS	Pass	3/18/2011	JK
N4-02-4	1/17/2011	JK	Pass	1/18/2011	JK			1/26/2011	TS	1/27/2011	JK	2/9/2011	CMK	Pass	2/17/2011	JK
N4-02-5	2/1/2011	TS	Pass	2/7/2011	JK	2/9/2011	SAK	2/9/2011	TS	3/14/2011	JK	3/17/2011	CMK	Pass	3/18/2011	JK
N4-02-6	1/18/2011	TS	Fail	1/20/2011	JK	1/20/2011	SAK	1/26/2011	JH	1/27/2011	JK	2/10/2011	TS	Pass	2/17/2011	JK
N4-02-7	1/17/2011	JK	Pass	1/18/2011	JK			1/26/2011	JH	1/27/2011	JK	2/9/2011	CMK	Pass	3/18/2011	JK
N4-02-8	2/1/2011	TS	Fail	2/7/2011	JK	2/9/2011	SAK	2/9/2011	TS	3/17/2011	JK	3/8/2011	CMK	Pass	3/18/2011	JK
N4-02-9	1/18/2011	TS	Pass	1/20/2011	JK			1/26/2011	JH	1/27/2011	JK	2/9/2011	TS	Pass	2/17/2011	JK
N4-03-1	1/18/2011	TS	Pass	1/20/2011	JK			1/26/2011	JH	1/27/2011	JK	2/9/2011	TS	Pass	2/17/2011	JK
N4-03-2	1/18/2011	TS	Fail	1/20/2011	JK	1/21/2011	SAK	1/26/2011	JH	1/27/2011	JK	3/30/2011	TS	Pass	2/17/2011	JK
N4-03-3	1/18/2011	TS	Pass	1/20/2011	JK			1/26/2011	JH	1/27/2011	JK	2/9/2011	CMK	Pass	2/17/2011	JK
N4-03-4	1/18/2011	TS	Pass	1/20/2011	JK			1/26/2011	JH	1/27/2011	JK	2/9/2011	CMK	Pass	2/17/2011	JK
N4-03-5	1/18/2011	TS	Pass	1/20/2011	JK			1/26/2011	JH	1/27/2011	JK	2/9/2011	TS	Pass	2/17/2011	JK
N4-03-6	1/18/2011	TS	Fail	1/20/2011	JK	1/20/2011	SAK	1/26/2011	JH	1/27/2011	JK	3/30/2011	TS	Pass	2/17/2011	JK
N4-03-7	1/18/2011	TS	Fail	1/20/2011	JK	1/21/2011	SAK	1/26/2011	JH	1/27/2011	JK	3/30/2011	TS	Pass	2/17/2011	JK
N4-03-8	1/18/2011	TS	Pass	1/20/2011	JK			1/26/2011	JH	1/27/2011	JK	2/9/2011	TS	Pass	2/17/2011	JK
N4-03-9	1/18/2011	TS	Fail	1/20/2011	JK	1/20/2011	SAK	1/26/2011	JH	1/27/2011	JK	3/30/2011	TS	Pass	2/17/2011	JK
N4-04-1	1/20/2011	TS	Pass	1/21/2011	JK			1/26/2011	JH	1/27/2011	JK	2/9/2011	CMK	Pass	2/17/2011	JK
N4-04-2	2/1/2011	TS	Fail	2/7/2011	JK	2/9/2011	SAK	2/9/2011	TS	3/17/2011	JK	3/8/2011	CMK	Pass	3/18/2011	JK
N4-04-3	1/17/2011	JK	Pass	1/18/2011	JK			1/26/2011	JH	1/27/2011	JK	2/9/2011	CMK	Pass	2/17/2011	JK
N4-04-4	2/1/2011	TS	Pass	2/7/2011	JK			2/27/2011	TS	2/28/2011	JK	3/3/2011	TS	Pass	3/9/2011	TS
N4-04-5	2/2/2011	TS	Pass	2/7/2011	JK			2/27/2011	TS	2/28/2011	JK	3/3/2011	TS	Pass	3/9/2011	TS
N4-04-6	2/2/2011	TS	Fail	2/7/2011	JK	2/9/2011	SAK	2/9/2011	TS	3/17/2011	JK	3/8/2011	CMK	Pass	3/18/2011	JK
N4-04-7	1/17/2011	JK	Pass	1/18/2011	JK			1/26/2011	JH	1/27/2011	JK	2/9/2011	TS	Pass	2/17/2011	JK
N4-04-8	2/1/2011	TS	Pass	2/7/2011	JK			2/27/2011	TS	2/28/2011	JK	3/3/2011	TS	Pass	3/9/2011	TS
N4-04-9	2/1/2011	TS	Pass	2/7/2011	JK			2/27/2011	TS	2/28/2011	JK	3/3/2011	TS	Pass	3/9/2011	TS
N4-05-1	N/A	N/A	N/A	N/A	N/A	N/A	N/A	N/A	N/A	N/A	N/A	N/A	N/A	N/A	N/A	N/A
N4-05-2	1/17/2011	JK	Pass	1/18/2011	JK			1/26/2011	TS	1/26/2011	JK	1/27/2011	TS	Pass	1/27/2011	JK
N4-05-3	1/18/2011	TS	Fail	1/20/2011	JK	1/21/2011	SAK	1/26/2011	JH	1/27/2011	JK	2/10/2011	TS	Pass	2/17/2011	JK
N4-05-4	1/17/2011	JK	Pass	1/18/2011	JK			1/26/2011	JH	1/27/2011	JK	2/9/2011	CMK	Pass	2/17/2011	JK
N4-05-5	1/17/2011	JK	Pass	1/18/2011	JK			1/26/2011	JH	1/27/2011	JK	2/9/2011	CMK	Pass	2/17/2011	JK
N4-05-6	1/17/2011	JK	Pass	1/18/2011	JK			1/26/2011	JH	1/27/2011	JK	2/9/2011	CMK	Pass	2/17/2011	JK
N4-05-7	1/17/2011	JK	Pass	1/20/2011	JK			1/26/2011	JH	1/27/2011	JK	2/9/2011	TS	Pass	2/17/2011	JK
N4-05-8	1/17/2011	JK	Fail	1/18/2011	JK	1/18/2011	SAK	1/26/2011	JH	1/27/2011	JK	2/9/2011	CMK	Pass	2/17/2011	JK
N4-06-1	2/1/2011	TS	Pass	2/7/2011	JK			2/27/2011	TS	2/28/2011	JK	3/3/2011	TS	Pass	3/9/2011	TS
N4-06-2	1/17/2011	JK	Pass	1/18/2011	JK			1/26/2011	TS	1/27/2011	JK	2/9/2011	CMK	Pass	2/17/2011	JK
N4-06-3	N/A	N/A	N/A	N/A	N/A	N/A	N/A	N/A	N/A	N/A	N/A	N/A	N/A	N/A	N/A	N/A
N4-06-4	1/18/2011	TS	Fail	1/19/2011	JK	1/20/2011	SAK	1/26/2011	JK	1/27/2011	JK	2/9/2011	CMK	Pass	2/17/2011	JK
N4-06-5	2/1/2011	TS	Fail	2/7/2011	JK	2/9/2011	SAK	2/9/2011	TS	3/7/2011	JK	3/8/2011	CMK	Pass	3/18/2011	JK

SHEET 1 OF 4



MID-CELL CLEANING TRACKER

COMPONENT TRAVELER

Cell ID	24 Hr Tap-water Soak		Rust Spot Visual Inspection		Dynamabraid		Cleanroom Prep		USC Processing		30 µm Yield Prep Etch		Final Inspect & Clean-room Pkg.		Notes	
	Date	Operator	Pass/Fail	Date	Inspector	Date	Operator	Date	Operator	Date	Operator	Date	Operator	Pass/Fail		Date
N4-06-6	1/17/2011	JK	Pass	1/18/2011	JK			1/18/2011	TS	1/27/2011	JK	CMK	2/8/2011	JK	2/17/2011	JK
N4-06-7	2/1/2011	TS	Pass	2/7/2011	JK			2/7/2011	TS	2/28/2011	JK	TS	3/1/2011	TS	3/3/2011	TS
N4-06-8	2/2/2011	TS	Pass	2/7/2011	JK			2/7/2011	TS	2/28/2011	JK	TS	3/1/2011	TS	3/3/2011	TS
N4-06-9	1/17/2011	JK	Pass	1/18/2011	JK			1/18/2011	TS	1/27/2011	JK	CMK	3/8/2011	JK	3/18/2011	JK
N4-07-1	1/20/2011	TS	Pass	1/21/2011	JK			1/24/2011	JK	1/26/2011	JK	TS	2/9/2011	TS	2/9/2011	JK
N4-07-2	1/17/2011	JK	Fail	1/18/2011	JK	1/18/2011	SAK	1/26/2011	JH	1/27/2011	JK	TS	3/9/2011	TS	3/9/2011	JK
N4-07-3	1/18/2011	TS	Fail	1/20/2011	JK	1/21/2011	SAK	1/26/2011	JH	1/27/2011	JK	CMK	3/17/2011	JK	3/18/2011	JK
N4-07-4	1/20/2011	TS	Pass	1/21/2011	JK			1/26/2011	JH	1/27/2011	JK	CMK	3/17/2011	JK	3/18/2011	JK
N4-07-5	1/17/2011	JK	Fail	1/18/2011	JK	1/18/2011	SAK	1/26/2011	JH	1/27/2011	JK	TS	2/9/2011	TS	2/9/2011	JK
N4-07-6	2/1/2011	TS	Fail	2/7/2011	JK	2/9/2011	SAK	2/9/2011	TS	3/14/2011	JK	CMK	3/17/2011	JK	3/18/2011	JK
N4-07-7	1/18/2011	TS	Pass	1/20/2011	JK			1/24/2011	JK	1/27/2011	JK	CMK	2/8/2011	JK	2/17/2011	JK
N4-07-8	1/18/2011	TS	Fail	1/20/2011	JK	1/20/2011	SAK	1/26/2011	JH	1/27/2011	JK	TS	2/9/2011	TS	2/17/2011	JK
N4-07-9	1/17/2011	JK	Pass	1/18/2011	JK			1/18/2011	TS	1/27/2011	JK	CMK	2/8/2011	JK	2/17/2011	JK
N4-08-1	2/1/2011	TS	Pass	2/7/2011	JK			2/7/2011	TS	2/28/2011	JK	TS	3/1/2011	TS	3/3/2011	TS
N4-08-2	1/17/2011	JK	Pass	1/18/2011	JK			1/18/2011	TS	1/27/2011	JK	TS	3/1/2011	TS	3/3/2011	TS
N4-08-3	2/1/2011	TS	Fail	1/18/2011	JK	1/18/2011	SAK	1/18/2011	TS	1/27/2011	JK	CMK	3/17/2011	JK	3/18/2011	JK
N4-08-4	2/1/2011	TS	Fail	2/7/2011	JK	2/9/2011	SAK	2/9/2011	TS	3/14/2011	JK	CMK	3/17/2011	JK	3/18/2011	JK
N4-08-5	1/17/2011	JK	Pass	1/18/2011	JK			1/18/2011	TS	1/27/2011	JK	CMK	3/8/2011	JK	3/18/2011	JK
N4-08-6	1/18/2011	TS	Pass	1/20/2011	JK			1/26/2011	JH	1/27/2011	JK	TS	2/7/2011	TS	2/17/2011	JK
N4-08-7	2/1/2011	TS	Fail	2/7/2011	JK	2/9/2011	SAK	2/9/2011	TS	3/7/2011	JK	CMK	3/8/2011	JK	3/18/2011	JK
N4-08-8	2/1/2011	TS	Fail	2/7/2011	JK	2/9/2011	SAK	2/9/2011	TS	3/7/2011	JK	CMK	3/8/2011	JK	3/18/2011	JK
N4-08-9	1/17/2011	JK	Fail	1/18/2011	JK	1/18/2011	SAK	1/18/2011	TS	1/26/2011	JK	TS	2/9/2011	TS	2/17/2011	JK
N4-08-10	2/1/2011	TS	Fail	2/7/2011	JK	2/9/2011	SAK	2/9/2011	TS	3/14/2011	JK	CMK	3/17/2011	JK	3/18/2011	JK
N4-08-11	1/18/2011	TS	Pass	1/18/2011	JK			1/18/2011	TS	1/27/2011	JK	CMK	2/8/2011	JK	2/17/2011	JK
N4-08-12	2/2/2011	TS	Pass	2/7/2011	JK			2/7/2011	TS	2/28/2011	JK	TS	3/1/2011	TS	3/3/2011	TS
N4-08-13	1/17/2011	JK	Pass	1/18/2011	JK			1/18/2011	TS	1/27/2011	JK	CMK	3/8/2011	JK	3/18/2011	JK
N4-08-14	2/2/2011	TS	Pass	2/7/2011	JK			2/7/2011	TS	2/28/2011	JK	TS	3/1/2011	TS	3/3/2011	TS
N4-08-15	1/17/2011	JK	Pass	1/18/2011	JK			1/18/2011	TS	1/27/2011	JK	CMK	3/8/2011	JK	3/18/2011	JK
N4-08-16	1/17/2011	JK	Pass	1/18/2011	JK			1/18/2011	TS	1/27/2011	JK	CMK	3/8/2011	JK	3/18/2011	JK
N4-08-17	2/2/2011	TS	Pass	2/7/2011	JK			2/7/2011	TS	2/28/2011	JK	TS	3/1/2011	TS	3/3/2011	TS
N4-08-18	1/17/2011	JK	Pass	1/18/2011	JK			1/18/2011	TS	1/27/2011	JK	CMK	3/8/2011	JK	3/18/2011	JK
N4-08-19	2/2/2011	TS	Pass	2/7/2011	JK			2/7/2011	TS	2/28/2011	JK	TS	3/1/2011	TS	3/3/2011	TS
N4-08-20	1/17/2011	JK	Pass	1/18/2011	JK			1/18/2011	TS	1/27/2011	JK	CMK	3/8/2011	JK	3/18/2011	JK
N4-08-21	1/17/2011	JK	Pass	1/18/2011	JK			1/18/2011	TS	1/27/2011	JK	CMK	3/8/2011	JK	3/18/2011	JK
N4-08-22	2/2/2011	TS	Pass	2/7/2011	JK			2/7/2011	TS	2/28/2011	JK	TS	3/1/2011	TS	3/3/2011	TS
N4-08-23	1/17/2011	JK	Pass	1/18/2011	JK			1/18/2011	TS	1/27/2011	JK	CMK	3/8/2011	JK	3/18/2011	JK
N4-08-24	2/2/2011	TS	Pass	2/7/2011	JK			2/7/2011	TS	2/28/2011	JK	TS	3/1/2011	TS	3/3/2011	TS
N4-08-25	1/17/2011	JK	Pass	1/18/2011	JK			1/18/2011	TS	1/27/2011	JK	CMK	3/8/2011	JK	3/18/2011	JK
N4-08-26	1/17/2011	JK	Pass	1/18/2011	JK			1/18/2011	TS	1/27/2011	JK	CMK	3/8/2011	JK	3/18/2011	JK
N4-08-27	2/2/2011	TS	Pass	2/7/2011	JK			2/7/2011	TS	2/28/2011	JK	TS	3/1/2011	TS	3/3/2011	TS
N4-08-28	2/2/2011	TS	Pass	2/7/2011	JK			2/7/2011	TS	2/28/2011	JK	TS	3/1/2011	TS	3/3/2011	TS
N4-08-29	1/17/2011	JK	Fail	1/18/2011	JK	1/18/2011	SAK	1/18/2011	TS	1/26/2011	JK	TS	2/9/2011	TS	2/17/2011	JK
N4-08-30	1/17/2011	JK	Fail	1/18/2011	JK	1/18/2011	SAK	1/18/2011	TS	1/26/2011	JK	TS	2/9/2011	TS	2/17/2011	JK
N4-08-31	1/17/2011	JK	Pass	1/18/2011	JK			1/18/2011	TS	1/27/2011	JK	CMK	3/17/2011	JK	3/18/2011	JK
N4-09-1	1/18/2011	TS	Pass	1/20/2011	JK			1/26/2011	JH	1/27/2011	JK	CMK	2/8/2011	JK	2/17/2011	JK
N4-09-2	1/18/2011	TS	Pass	1/20/2011	JK			1/26/2011	JH	1/27/2011	JK	CMK	2/8/2011	JK	2/17/2011	JK
N4-09-3	2/1/2011	TS	Pass	2/7/2011	JK			2/7/2011	TS	2/28/2011	JK	TS	3/1/2011	TS	3/3/2011	TS
N4-09-4	2/1/2011	TS	Pass	2/7/2011	JK			2/7/2011	TS	2/28/2011	JK	TS	3/1/2011	TS	3/3/2011	TS
N4-09-5	2/2/2011	TS	Pass	2/7/2011	JK			2/7/2011	TS	2/28/2011	JK	TS	3/1/2011	TS	3/3/2011	TS
N4-09-6	1/18/2011	TS	Pass	1/20/2011	JK			1/26/2011	JH	1/27/2011	JK	CMK	3/17/2011	JK	3/18/2011	JK
N4-09-7	2/2/2011	TS	Pass	2/7/2011	JK			2/7/2011	TS	2/28/2011	JK	TS	3/1/2011	TS	3/3/2011	TS
N4-09-8	1/17/2011	JK	Pass	1/18/2011	JK			1/18/2011	TS	1/27/2011	JK	CMK	3/8/2011	JK	3/18/2011	JK
N4-09-9	1/17/2011	JK	Pass	1/18/2011	JK			1/18/2011	TS	1/27/2011	JK	CMK	3/8/2011	JK	3/18/2011	JK
N4-09-10	2/2/2011	TS	Pass	2/7/2011	JK			2/7/2011	TS	2/28/2011	JK	TS	3/1/2011	TS	3/3/2011	TS
N4-09-11	1/17/2011	JK	Pass	1/18/2011	JK			1/18/2011	TS	1/27/2011	JK	CMK	3/8/2011	JK	3/18/2011	JK
N4-09-12	2/2/2011	TS	Pass	2/7/2011	JK			2/7/2011	TS	2/28/2011	JK	TS	3/1/2011	TS	3/3/2011	TS
N4-09-13	1/17/2011	JK	Pass	1/18/2011	JK			1/18/2011	TS	1/27/2011	JK	CMK	3/8/2011	JK	3/18/2011	JK
N4-09-14	1/17/2011	JK	Pass	1/18/2011	JK			1/18/2011	TS	1/27/2011	JK	CMK	3/8/2011	JK	3/18/2011	JK
N4-09-15	1/17/2011	JK	Pass	1/18/2011	JK			1/18/2011	TS	1/27/2011	JK	CMK	3/8/2011	JK	3/18/2011	JK
N4-09-16	1/17/2011	JK	Pass	1/18/2011	JK			1/18/2011	TS	1/27/2011	JK	CMK	3/8/2011	JK	3/18/2011	JK
N4-09-17	1/17/2011	JK	Fail	1/18/2011	JK	1/18/2011	SAK	1/18/2011	TS	1/26/2011	JK	CMK	3/17/2011	JK	3/18/2011	JK
N4-09-18	1/17/2011	JK	Fail	1/18/2011	JK	1/18/2011	SAK	1/18/2011	TS	1/26/2011	JK	CMK	3/17/2011	JK	3/18/2011	JK
N4-09-19	1/17/2011	JK	Pass	1/18/2011	JK			1/18/2011	TS	1/27/2011	JK	CMK	3/8/2011	JK	3/18/2011	JK
N4-09-20	1/17/2011	JK	Pass	1/18/2011	JK			1/18/2011	TS	1/27/2011	JK	CMK	3/8/2011	JK	3/18/2011	JK
N4-09-21	1/17/2011	JK	Pass	1/18/2011	JK			1/18/2011	TS	1/27/2011	JK	CMK	3/8/2011	JK	3/18/2011	JK
N4-09-22	1/17/2011	JK	Pass	1/18/2011	JK			1/18/2011	TS	1/27/2011	JK	CMK	3/8/2011	JK	3/18/2011	JK
N4-09-23	1/17/2011	JK	Pass	1/18/2011	JK			1/18/2011	TS	1/27/2011	JK	CMK	3/8/2011	JK	3/18/2011	JK
N4-09-24	1/17/2011															



COMPONENT TRAVELER

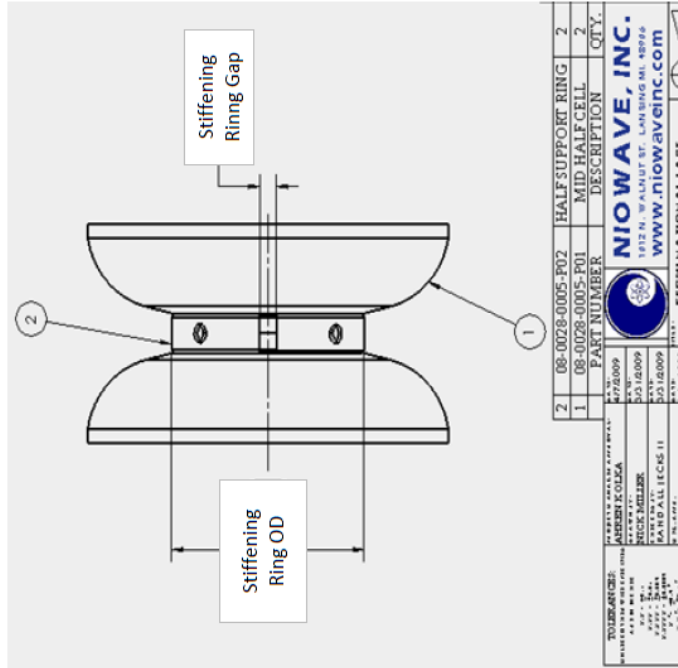
MID-CELL CLEANING TRACKER

Cell ID	24 Hr Tap-water Soak		Rust Spot Visual Inspection		Dynamabraid		Cleanroom Prep		USC Processing		30 µm Yield Prep Etch		Final Inspect & Clean-room Pkg.		Notes		
	Date	Operator	Pass/Fail	Date	Inspector	Date	Operator	Date	Operator	Date	Operator	Date	Operator	Pass/Fail		Date	Operator
N4-16-1	1/6/2011	JK	Pass	1/6/2011	JK			1/7/2011	TS	1/24/2011	JK	1/25/2011	TS	Pass	1/26/2011	JK	
N4-16-2	1/6/2011	JK	Fail	1/6/2011	JK	1/6/2011	SAK	1/7/2011	TS	1/27/2011	JK	2/7/2011	TS	Pass	2/17/2011	JK	
N4-16-3	1/5/2011	TS	Fail	1/5/2011	JK	1/5/2011	SAK	1/5/2011	TS	1/7/2011	JK	1/11/2011	CMK	Pass	1/14/2011	JK	
N4-16-4	1/7/2011	JK	Pass	1/7/2011	JK			1/11/2011	JH	1/24/2011	JK	1/25/2011	CMK	Pass	1/26/2011	JK	
N4-16-5	1/4/2011	JK	Pass	1/4/2011	JK			1/4/2011	JH	1/7/2011	JK	1/12/2011	CMK	Pass	1/14/2011	JK	
N4-16-6	1/4/2011	TS	Pass	1/4/2011	JK			1/4/2011	JH	1/11/2011	JK	1/25/2011	TS	Pass	1/26/2011	JK	
N4-16-7	1/4/2011	TS	Pass	1/4/2011	JK			1/4/2011	TS	1/11/2011	JK	1/26/2011	TS	Pass	1/27/2011	JK	
N4-16-8	1/6/2011	JK	Pass	1/6/2011	JK			1/6/2011	JK	1/7/2011	JK	1/12/2011	CMK	Pass	1/14/2011	JK	
N4-16-9	1/5/2011	TS	Pass	1/5/2011	JK			1/5/2011	JK	1/7/2011	JK	1/12/2011	CMK	Pass	1/14/2011	JK	
N4-17-1	1/4/2011	TS	Pass	1/4/2011	JK			1/4/2011	TS	1/7/2011	JK	1/11/2011	CMK	Pass	1/14/2011	JK	
N4-17-2	1/4/2011	TS	Pass	1/4/2011	JK			1/5/2011	JK	1/7/2011	JK	1/11/2011	CMK	Pass	1/14/2011	JK	
N4-17-3	1/5/2011	TS	Pass	1/5/2011	JK			1/5/2011	JK	1/7/2011	JK	1/11/2011	CMK	Pass	1/14/2011	JK	
N4-17-4	1/4/2011	TS	Pass	1/4/2011	JK			1/4/2011	JK	1/11/2011	JK	1/26/2011	CMK	Pass	1/27/2011	JK	
N4-17-5	1/5/2011	TS	Pass	1/5/2011	JK			1/5/2011	TS	1/7/2011	JK	1/11/2011	CMK	Pass	1/14/2011	JK	
N4-17-6	1/5/2011	TS	Pass	1/5/2011	JK			1/5/2011	JK	1/7/2011	JK	1/11/2011	CMK	Pass	1/14/2011	JK	
N4-17-7	1/6/2011	JK	Pass	1/6/2011	JK			1/7/2011	JK	1/13/2011	JK	1/26/2011	TS	Pass	1/27/2011	JK	
N4-17-8	1/7/2011	JK	Fail	1/7/2011	JK	1/10/2011	SAK	1/7/2011	JH	1/13/2011	JK	1/20/2011	TS	Pass	1/24/2011	JK	
N4-17-9	1/4/2011	TS	Pass	1/4/2011	JK			1/4/2011	JK	1/11/2011	JK	1/25/2011	TS	Pass	1/26/2011	JK	
N4-18-1	1/7/2011	JK	Pass	1/7/2011	JK			1/7/2011	TS	1/27/2011	JK	2/9/2011	CMK	Pass	2/17/2011	JK	
N4-18-2	1/4/2011	TS	Pass	1/4/2011	JK			1/4/2011	TS	1/7/2011	JK	1/11/2011	CMK	Pass	1/14/2011	JK	
N4-18-3	1/5/2011	TS	Pass	1/5/2011	JK			1/5/2011	TS	1/7/2011	JK	1/11/2011	CMK	Pass	1/14/2011	JK	
N4-18-4	1/10/2011	JK	Fail	1/10/2011	JK	1/10/2011	SAK	1/11/2011	JH	1/12/2011	JH	1/26/2011	TS	Pass	1/27/2011	JK	
N4-18-5	1/4/2011	TS	Pass	1/4/2011	JK			1/4/2011	TS	1/7/2011	JK	1/11/2011	CMK	Pass	1/14/2011	JK	
N4-18-6	1/6/2011	JK	Pass	1/6/2011	JK			1/7/2011	TS	1/27/2011	JK	2/7/2011	TS	Pass	2/17/2011	JK	
N4-18-7	1/7/2011	JK	Fail	1/7/2011	JK	1/10/2011	SAK	1/11/2011	JH	1/12/2011	JH	1/26/2011	TS	Pass	1/27/2011	JK	
N4-18-8	1/6/2011	JK	Fail	1/6/2011	JK	1/10/2011	SAK	1/7/2011	JH	1/13/2011	JK	1/20/2011	TS	Pass	1/24/2011	JK	
N4-18-9	1/6/2011	JK	Pass	1/6/2011	JK			1/7/2011	TS	1/13/2011	JK	1/27/2011	TS	Pass	1/24/2011	JK	
N4-19-1	1/7/2011	JK	Pass	1/7/2011	JK			1/7/2011	JK	1/13/2011	JK	1/27/2011	TS	Pass	1/24/2011	JK	
N4-19-2	1/7/2011	JK	Fail	1/7/2011	JK	1/10/2011	SAK	1/11/2011	JH	1/13/2011	JK	1/25/2011	TS	Pass	1/24/2011	JK	
N4-19-3	1/4/2011	TS	Pass	1/4/2011	JK			1/4/2011	JK	1/11/2011	JK	1/25/2011	TS	Pass	1/26/2011	JK	
N4-19-4	1/4/2011	TS	Pass	1/4/2011	JK			1/4/2011	JH	1/11/2011	JK	1/25/2011	TS	Pass	1/26/2011	JK	
N4-19-5	1/7/2011	JK	Fail	1/7/2011	JK	1/10/2011	SAK	1/11/2011	JH	1/11/2011	JK	1/25/2011	TS	Pass	1/26/2011	JK	
N4-19-6	1/4/2011	TS	Pass	1/4/2011	JK			1/4/2011	JK	1/11/2011	JK	1/24/2011	TS	Pass	1/27/2011	JK	
N4-19-7	1/4/2011	TS	Pass	1/4/2011	JK			1/4/2011	JH	1/11/2011	JK	1/24/2011	CMK	Pass	1/14/2011	JK	
N4-19-8	1/4/2011	TS	Pass	1/4/2011	JK			1/4/2011	TS	1/11/2011	JK	1/25/2011	TS	Pass	1/26/2011	JK	
N4-19-9	1/4/2011	TS	Pass	1/4/2011	JK			1/4/2011	JK	1/11/2011	JK	1/24/2011	TS	Pass	1/24/2011	JK	
N4-23-1	1/7/2011	JK	Pass	1/7/2011	JK			1/7/2011	TS	1/24/2011	JK	1/26/2011	TS	Pass	1/26/2011	JK	
N4-23-2	1/5/2011	TS	Fail	1/5/2011	JK	1/5/2011	SAK	1/5/2011	TS	1/7/2011	JK	1/11/2011	CMK	Pass	1/14/2011	JK	
N4-23-3	1/10/2011	JK	Fail	1/10/2011	JK	1/10/2011	SAK	1/11/2011	JH	1/12/2011	JH	1/26/2011	TS	Pass	1/27/2011	JK	
N4-23-4	1/6/2011	JK	Pass	1/6/2011	JK			1/7/2011	TS	1/27/2011	JK	2/10/2011	TS	Pass	2/17/2011	JK	
N4-23-5	1/5/2011	TS	Pass	1/5/2011	JK			1/5/2011	JK	1/11/2011	JK	1/11/2011	CMK	Pass	1/14/2011	JK	
N4-23-6	1/7/2011	JK	Pass	1/7/2011	JK			1/7/2011	TS	1/27/2011	JK	3/3/2011	TS	Pass	3/13/2011	JK	
N4-23-7	1/10/2011	JK	Fail	1/10/2011	JK	1/10/2011	SAK	1/11/2011	JH	1/13/2011	JK	1/21/2011	TS	Pass	1/24/2011	JK	
N4-23-8	1/7/2011	JK	Pass	1/7/2011	JK			1/7/2011	JK	1/25/2011	JK	1/25/2011	TS	Pass	1/26/2011	JK	
N4-23-9	1/10/2011	JK	Pass	1/10/2011	JK			1/11/2011	JH	1/13/2011	JK	1/21/2011	TS	Pass	1/24/2011	JK	
N4-24-1	1/10/2011	JK	Pass	1/10/2011	JK			1/11/2011	JH	1/13/2011	JK	1/21/2011	TS	Pass	1/24/2011	JK	
N4-24-2	1/4/2011	TS	Pass	1/4/2011	JK			1/4/2011	TS	1/11/2011	JK	1/21/2011	TS	Pass	1/26/2011	JK	
N4-24-3	1/6/2011	JK	Pass	1/6/2011	JK			1/7/2011	TS	1/13/2011	JK	1/13/2011	TS	Pass	1/13/2011	JK	
N4-24-4	1/7/2011	JK	Pass	1/7/2011	JK			1/7/2011	JK	1/13/2011	JK	2/10/2011	TS	Pass	2/17/2011	JK	
N4-24-5	1/6/2011	JK	Pass	1/6/2011	JK			1/7/2011	TS	1/27/2011	JK	2/10/2011	TS	Pass	2/17/2011	JK	

SHEET 3 OF 4

QA Data for TB9NR015 Dumbells

DIMENSION	Stiffening Ring OD		Stiffening Ring GAP 1		Stiffening Ring GAP 2	
	TB9NR015	TB9NR015	TB9NR015	TB9NR015	TB9NR015	TB9NR015
N4-6-9/N4-6-2	4.431	0.447	0.447	0.372	0.372	0.372
N4-4-1/N4-8-6	4.510	0.570	0.570	0.476	0.476	0.476
N4-1-6/N4-8-4	4.433	0.484	0.484	0.352	0.352	0.352
N4-15-4/N4-14-5	4.445	0.405	0.405	0.436	0.436	0.436
N4-19-4/N4-16-6	4.456	0.400	0.400	0.438	0.438	0.438
N4-18-4/N4-25-3	4.459	0.397	0.397	0.461	0.461	0.461
N4-17-8/N4-23-7	4.436	0.433	0.433	0.489	0.489	0.489
N4-5-9/N4-7-7	4.458	0.428	0.428	0.424	0.424	0.424
average	4.454	0.446	0.446	0.431	0.431	0.431
max	4.510	0.570	0.570	0.489	0.489	0.489
min	4.431	0.397	0.397	0.352	0.352	0.352



Part Name:	Dumbell
Part Number:	10-0013-0002-A05
Checked By:	KEN KOLP
Date:	10/6/2011
Measuring Devices:	Calipers



COMPONENT TRAVELER

PART NUMBER: 10-0013-0002-A05		PART NAME: DUMBELL		MATERIAL: RRR 300 Nb		NEXT ASSEMBLY: DUMBELL STACK-UP EBW		Dynebraid		SHEET 1 OF 1		
Cell ID	Cell ID	Re-strike		Check Fixture		Flattening Complete		Tuning Complete		Visual Inspection		Notes
		Date	Operator	Pass/Fail	Operator	Date	Machinist	Date	RF Specialist	Rust, scratches, etc.	Date	
N4-16-5	N4-17-1	1/24/2011	JNS	PASS	JNS	4/15/2011	DF	4/20/2011	BK	SEE DUMBELL CLEAN TRACKER	SEE DUMBELL CLEAN TRACKER	SEE DUMBELL CLEAN TRACKER
N4-23-5	N4-17-6	1/24/2011	JNS	PASS	JNS	4/15/2011	DF	4/20/2011	BK	SEE DUMBELL SHEET	BK	SEE DUMBELL CLEAN TRACKER
N4-14-3	N4-14-9	1/24/2011	JNS	PASS	JNS	4/15/2011	DF	4/20/2011	BK	SEE DUMBELL SHEET	BK	SEE DUMBELL CLEAN TRACKER
N4-18-3	N4-18-2	1/24/2011	JNS	PASS	JNS	4/15/2011	DF	4/20/2011	BK	SEE DUMBELL SHEET	BK	SEE DUMBELL CLEAN TRACKER
N4-17-3	N4-16-8	1/24/2011	JNS	PASS	JNS	4/15/2011	DF	4/20/2011	BK	SEE DUMBELL SHEET	BK	SEE DUMBELL CLEAN TRACKER
N4-17-5	N4-14-6	1/24/2011	JNS	PASS	JNS	4/15/2011	DF	4/20/2011	BK	SEE DUMBELL SHEET	BK	SEE DUMBELL CLEAN TRACKER
N4-17-5	N4-25-8	1/24/2011	JNS	PASS	JNS	4/15/2011	DF	4/20/2011	BK	SEE DUMBELL SHEET	BK	SEE DUMBELL CLEAN TRACKER
N4-16-9	N4-25-2	1/24/2011	JNS	PASS	JNS	4/15/2011	DF	4/20/2011	BK	SEE DUMBELL SHEET	BK	SEE DUMBELL CLEAN TRACKER
N4-23-2	N4-19-7	2/2/2011	JNS	PASS	JNS	4/15/2011	DF	4/20/2011	BK	SEE DUMBELL SHEET	BK	SEE DUMBELL CLEAN TRACKER
N4-16-3	N4-18-5	2/2/2011	JNS	PASS	JNS	4/15/2011	DF	4/20/2011	BK	SEE DUMBELL SHEET	BK	SEE DUMBELL CLEAN TRACKER
N4-24-3	N4-14-7	2/2/2011	JNS	PASS	JNS	4/15/2011	DF	4/20/2011	BK	SEE DUMBELL SHEET	BK	SEE DUMBELL CLEAN TRACKER
N4-14-2	N4-15-7	2/2/2011	JNS	PASS	JNS	4/15/2011	DF	4/20/2011	BK	SEE DUMBELL SHEET	BK	SEE DUMBELL CLEAN TRACKER
N4-25-4	N4-24-8	2/2/2011	JNS	PASS	JNS	4/15/2011	DF	4/20/2011	BK	SEE DUMBELL SHEET	BK	SEE DUMBELL CLEAN TRACKER
N4-25-6	N4-18-9	2/2/2011	JNS	PASS	JNS	4/15/2011	DF	4/20/2011	BK	SEE DUMBELL SHEET	BK	SEE DUMBELL CLEAN TRACKER
N4-17-8	N4-23-7	2/14/2011	ECL	PASS	ECL	2/15/2011	ECL	2/15/2011	BK	SEE DUMBELL SHEET	BK	SEE DUMBELL CLEAN TRACKER
N4-14-8	N4-19-6	2/14/2011	ECL	PASS	ECL	2/14/2011	ECL	2/15/2011	BK	SEE DUMBELL SHEET	BK	SEE DUMBELL CLEAN TRACKER
N4-15-8	N4-19-9	2/14/2011	ECL	PASS	ECL	2/15/2011	ECL	2/15/2011	BK	SEE DUMBELL SHEET	BK	SEE DUMBELL CLEAN TRACKER
N4-24-1	N4-18-8	2/14/2011	ECL	PASS	ECL	2/14/2011	ECL	2/15/2011	BK	SEE DUMBELL SHEET	BK	SEE DUMBELL CLEAN TRACKER
N4-5-9	N4-7-7	2/27/2011	ECL	PASS	DKK	2/28/2011	ECL	3/2/2011	BK	SEE DUMBELL SHEET	BK	SEE DUMBELL CLEAN TRACKER
N4-25-5	N4-17-7	2/27/2011	DKK	PASS	DKK	2/28/2011	ECL	3/2/2011	BK	SEE DUMBELL SHEET	BK	SEE DUMBELL CLEAN TRACKER
N4-3-4	N4-7-5	2/27/2011	ECL	PASS	ECL	2/28/2011	ECL	3/2/2011	BK	SEE DUMBELL SHEET	BK	SEE DUMBELL CLEAN TRACKER
N4-17-2	N4-23-3	2/27/2011	DKK	PASS	JNS	2/27/2011	ECL	3/2/2011	BK	SEE DUMBELL SHEET	BK	SEE DUMBELL CLEAN TRACKER
N4-17-3	N4-24-2	2/27/2011	DKK	PASS	DKK	2/28/2011	ECL	3/2/2011	BK	SEE DUMBELL SHEET	BK	SEE DUMBELL CLEAN TRACKER
N4-23-8	N4-19-5	2/27/2011	DKK	PASS	DKK	2/28/2011	ECL	3/2/2011	BK	SEE DUMBELL SHEET	BK	SEE DUMBELL CLEAN TRACKER
N4-2-1	N4-2-1	2/27/2011	DKK	PASS	DKK	2/28/2011	ECL	3/2/2011	BK	SEE DUMBELL SHEET	BK	SEE DUMBELL CLEAN TRACKER
N4-18-6	N4-9-8	2/27/2011	DKK	PASS	DKK	2/28/2011	ECL	3/2/2011	BK	SEE DUMBELL SHEET	BK	SEE DUMBELL CLEAN TRACKER
N4-16-7	N4-24-7	2/28/2011	JNS	PASS	JNS	3/2/2011	ECL	3/2/2011	BK	SEE DUMBELL SHEET	BK	SEE DUMBELL CLEAN TRACKER
N4-18-7	N4-25-9	2/28/2011	JNS	PASS	JNS	3/2/2011	ECL	3/2/2011	BK	SEE DUMBELL SHEET	BK	SEE DUMBELL CLEAN TRACKER
N4-16-4	N4-25-7	2/28/2011	JNS	PASS	JNS	3/2/2011	ECL	3/2/2011	BK	SEE DUMBELL SHEET	BK	SEE DUMBELL CLEAN TRACKER
N4-17-9	N4-23-1	2/28/2011	JNS	PASS	JNS	3/2/2011	ECL	3/2/2011	BK	SEE DUMBELL SHEET	BK	SEE DUMBELL CLEAN TRACKER
N4-16-2	N4-7-9	2/28/2011	JNS	PASS	JNS	3/1/2011	ECL	3/2/2011	BK	SEE DUMBELL SHEET	BK	SEE DUMBELL CLEAN TRACKER
N4-8-3	N4-7-2	2/28/2011	JNS	PASS	JNS	3/1/2011	ECL	3/3/2011	BK	SEE DUMBELL SHEET	BK	SEE DUMBELL CLEAN TRACKER
N4-1-8	N4-15-9	2/28/2011	JNS	PASS	JNS	3/1/2011	ECL	3/3/2011	BK	SEE DUMBELL SHEET	BK	SEE DUMBELL CLEAN TRACKER
N4-7-1	N4-15-6	2/28/2011	JNS	PASS	JNS	3/1/2011	ECL	3/3/2011	BK	SEE DUMBELL SHEET	BK	SEE DUMBELL CLEAN TRACKER
N4-16-1	N4-24-9	2/28/2011	JNS	PASS	JNS	3/2/2011	ECL	3/3/2011	BK	SEE DUMBELL SHEET	BK	SEE DUMBELL CLEAN TRACKER
N4-3-1	N4-25-1	2/28/2011	JNS	PASS	JNS	3/1/2011	ECL	3/3/2011	BK	SEE DUMBELL SHEET	BK	SEE DUMBELL CLEAN TRACKER
N4-24-6	N4-15-3	2/28/2011	JNS	PASS	JNS	3/1/2011	ECL	3/3/2011	BK	SEE DUMBELL SHEET	BK	SEE DUMBELL CLEAN TRACKER
N4-9-3	N4-6-4	3/11/2011	DF	PASS	DF	3/11/2011	DKK	4/1/2011	BK	SEE DUMBELL SHEET	BK	SEE DUMBELL CLEAN TRACKER
N4-8-6	N4-4-1	3/11/2011	DF	PASS	DF	3/16/2011	DKK	4/1/2011	BK	SEE DUMBELL SHEET	BK	SEE DUMBELL CLEAN TRACKER
N4-14-2	N4-17-4	3/11/2011	DF	PASS	DF	3/15/2011	DKK	4/1/2011	BK	SEE DUMBELL SHEET	BK	SEE DUMBELL CLEAN TRACKER
N4-16-6	N4-19-4	3/11/2011	DF	PASS	DF	3/15/2011	DKK	4/1/2011	BK	SEE DUMBELL SHEET	BK	SEE DUMBELL CLEAN TRACKER
N4-2-9	N4-14-4	3/11/2011	DF	PASS	DF	3/16/2011	DKK	4/1/2011	BK	SEE DUMBELL SHEET	BK	SEE DUMBELL CLEAN TRACKER
N4-19-1	N4-5-2	3/11/2011	DF	PASS	DF	3/16/2011	DKK	4/1/2011	BK	SEE DUMBELL SHEET	BK	SEE DUMBELL CLEAN TRACKER
N4-15-2	N4-15-5	3/11/2011	DF	PASS	DF	3/16/2011	DKK	4/1/2011	BK	SEE DUMBELL SHEET	BK	SEE DUMBELL CLEAN TRACKER
N4-14-4	N4-19-8M	3/11/2011	DF	PASS	DF	3/14/2011	DKK	4/1/2011	BK	SEE DUMBELL SHEET	BK	SEE DUMBELL CLEAN TRACKER
N4-15-4	N4-14-5	3/11/2011	DF	PASS	DF	3/15/2011	DKK	4/1/2011	BK	SEE DUMBELL SHEET	BK	SEE DUMBELL CLEAN TRACKER
N4-8-9	N4-4-7	3/11/2011	DF	PASS	DF	3/15/2011	DKK	4/1/2011	BK	SEE DUMBELL SHEET	BK	SEE DUMBELL CLEAN TRACKER



COMPONENT TRAVELLER

PART NUMBER: 10-0013-0002-A05		PART NAME: DUMBELL		MATERIAL: RRR 300 Nd		NEXT ASSEMBLY: DUMBELL STACK-UP ESW		SHEET 1 OF 2							
Cell ID	24 Hr Tap-water Soak Operator	Date	Rust Spot Visual Inspection Pass/Fail	Date	Inspector	Dynabraid Operator	Date	Cleanroom Prep Operator	Date	USC Processing Operator	Date	20 µm Weld Prep Etch Operator	Date	Final Inspect & Clean-room Pkg. Operator	Notes
N4-01-1	N4-06-1	3/24/2011	TS	3/25/2011	TS	DF	3/25/2011	MD	9/15/2011	MD	9/15/2011	TS	9/16/2011	JK	
N4-01-2	N4-07-6	5/5/2011	JK	5/16/2011	JK	SAK	5/16/2011	TS	5/23/2011	JK	5/23/2011	TS	9/16/2011	JK	Week of Sept 12-16, ALL DUMBELLS:
N4-01-3	N4-04-8	5/5/2011	JK	5/16/2011	TS	SAK	5/16/2011	TS	5/23/2011	JK	5/23/2011	TS	9/16/2011	JK	Inspected by Fermi
N4-01-4	N4-05-7	4/4/2011	TS	4/5/2011	TS	SAK	4/5/2011	TS	4/29/2011	JK	4/29/2011	TS	9/16/2011	JK	Dynabraid (if needed)
N4-01-5	N4-08-2	4/4/2011	TS	4/5/2011	TS	SAK	4/5/2011	TS	4/29/2011	JK	4/29/2011	TS	9/16/2011	JK	Re-inspected in House
N4-01-6	N4-08-4	5/5/2011	JK	5/16/2011	TS	SAK	5/16/2011	TS	5/23/2011	JK	5/23/2011	TS	9/16/2011	JK	Acetone/Methanol
N4-01-7	N4-02-8	5/5/2011	JK	5/13/2011	TS	SAK	5/13/2011	TS	5/23/2011	JK	5/23/2011	TS	9/16/2011	JK	20µ etched then dipped
N4-01-8	N4-15-9	3/24/2011	TS	3/25/2011	TS	DF	3/25/2011	TS	4/8/2011	MD	4/8/2011	TS	9/16/2011	JK	Bagged with Nitrogen
N4-01-9	N4-07-4	5/5/2011	JK	5/16/2011	JK	SAK	5/16/2011	JK	5/23/2011	JK	5/23/2011	TS	9/16/2011	JK	Boxed to ship out
N4-02-1	N4-02-7	3/18/2011	JK	3/24/2011	TS	DF	3/24/2011	JK	4/5/2011	JK	4/5/2011	TS	9/16/2011	JK	
N4-02-2	N4-03-7	5/5/2011	JK	5/16/2011	JK	SAK	5/16/2011	TS	5/23/2011	JK	5/23/2011	TS	9/16/2011	JK	
N4-02-3	N4-04-4	4/4/2011	TS	4/5/2011	TS	SAK	4/5/2011	TS	4/29/2011	JK	4/29/2011	TS	9/16/2011	JK	
N4-02-4	N4-16-2	3/24/2011	TS	3/25/2011	JK	SAK	4/11/2011	TS	4/8/2011	MD	4/8/2011	TS	9/16/2011	JK	
N4-02-5	N4-23-6	4/5/2011	TS	4/7/2011	JK	SAK	4/7/2011	JW	4/29/2011	JK	4/29/2011	TS	9/16/2011	JK	
N4-02-6	N4-23-6	4/5/2011	TS	4/7/2011	JK	SAK	4/7/2011	JW	4/29/2011	JK	4/29/2011	TS	9/16/2011	JK	
N4-02-7	N4-14-4	3/23/2011	TS	3/24/2011	TS	DF	3/24/2011	JK	4/5/2011	JK	4/5/2011	TS	9/16/2011	JK	
N4-02-8	N4-03-9	5/5/2011	JK	5/16/2011	JK	SAK	5/16/2011	TS	5/23/2011	JK	5/23/2011	TS	9/16/2011	JK	
N4-02-9	N4-15-6	3/17/2011	JK	3/18/2011	JK	SAK	3/18/2011	JW	4/29/2011	JK	4/29/2011	TS	9/16/2011	JK	
N4-03-1	N4-07-8	4/5/2011	TS	4/7/2011	JK	SAK	4/7/2011	JW	4/29/2011	JK	4/29/2011	TS	9/16/2011	JK	
N4-03-2	N4-07-5	3/17/2011	JK	3/18/2011	JK	SAK	3/18/2011	JW	4/29/2011	JK	4/29/2011	TS	9/16/2011	JK	
N4-03-3	N4-24-4	4/4/2011	TS	4/5/2011	TS	SAK	4/5/2011	TS	4/29/2011	JK	4/29/2011	TS	9/16/2011	JK	
N4-03-4	N4-07-3	5/5/2011	JK	5/16/2011	JK	SAK	5/16/2011	TS	5/23/2011	JK	5/23/2011	TS	9/16/2011	JK	
N4-03-5	N4-09-5	3/24/2011	TS	3/25/2011	TS	SAK	4/11/2011	JW	4/29/2011	JK	4/29/2011	TS	9/16/2011	JK	
N4-03-6	N4-07-3	5/5/2011	JK	5/16/2011	JK	SAK	5/16/2011	TS	5/23/2011	JK	5/23/2011	TS	9/16/2011	JK	
N4-03-7	N4-23-4	4/4/2011	TS	4/5/2011	TS	SAK	4/5/2011	TS	4/29/2011	JK	4/29/2011	TS	9/16/2011	JK	
N4-03-8	N4-12-3	5/5/2011	JK	5/16/2011	TS	SAK	5/16/2011	TS	5/23/2011	JK	5/23/2011	TS	9/16/2011	JK	
N4-04-1	N4-08-6	3/24/2011	TS	3/25/2011	TS	DF	3/25/2011	TS	4/5/2011	JK	4/5/2011	TS	9/16/2011	JK	
N4-04-2	N4-12-3	5/5/2011	JK	5/16/2011	TS	SAK	5/16/2011	TS	5/23/2011	JK	5/23/2011	TS	9/16/2011	JK	
N4-04-3	N4-06-5	4/4/2011	TS	4/5/2011	TS	SAK	4/5/2011	TS	4/29/2011	JK	4/29/2011	TS	9/16/2011	JK	
N4-04-4	N4-09-5	3/24/2011	TS	3/25/2011	TS	DF	3/25/2011	TS	4/5/2011	JK	4/5/2011	TS	9/16/2011	JK	
N4-04-5	N4-09-5	3/24/2011	TS	3/25/2011	TS	DF	3/25/2011	TS	4/5/2011	JK	4/5/2011	TS	9/16/2011	JK	
N4-04-6	N4-08-5	4/4/2011	TS	4/5/2011	TS	SAK	4/5/2011	TS	4/29/2011	JK	4/29/2011	TS	9/16/2011	JK	
N4-04-7	N4-08-9	3/23/2011	TS	3/24/2011	TS	DF	3/24/2011	JK	4/8/2011	MD	4/8/2011	TS	9/16/2011	JK	
N4-04-8	N4-23-9	3/23/2011	TS	3/24/2011	TS	DF	3/24/2011	TS	4/5/2011	JK	4/5/2011	TS	9/16/2011	JK	
N4-04-9	N4-19-1	3/23/2011	TS	3/24/2011	TS	DF	3/24/2011	JK	4/4/2011	JK	4/4/2011	TS	9/16/2011	JK	
N4-05-1	N4-05-6	5/5/2011	JK	5/13/2011	TS	SAK	5/13/2011	TS	5/23/2011	JK	5/23/2011	TS	9/16/2011	JK	
N4-05-2	N4-09-6	4/4/2011	TS	4/5/2011	TS	SAK	4/5/2011	JW	4/29/2011	JK	4/29/2011	TS	9/16/2011	JK	
N4-05-3	N4-08-8	4/4/2011	TS	4/5/2011	TS	SAK	4/5/2011	TS	4/29/2011	JK	4/29/2011	TS	9/16/2011	JK	
N4-05-4	N4-08-8	4/4/2011	TS	4/5/2011	TS	SAK	4/5/2011	TS	4/29/2011	JK	4/29/2011	TS	9/16/2011	JK	
N4-05-5	N4-08-8	4/4/2011	TS	4/5/2011	TS	SAK	4/5/2011	TS	4/29/2011	JK	4/29/2011	TS	9/16/2011	JK	
N4-05-6	N4-07-7	3/24/2011	TS	3/25/2011	TS	DF	3/25/2011	TS	4/5/2011	JK	4/5/2011	TS	9/16/2011	JK	
N4-05-7	N4-06-9	4/4/2011	TS	4/5/2011	TS	DF	4/5/2011	JW	4/29/2011	JK	4/29/2011	TS	9/16/2011	JK	
N4-05-8	N4-06-9	4/4/2011	TS	4/5/2011	TS	DF	4/5/2011	JW	4/29/2011	JK	4/29/2011	TS	9/16/2011	JK	
N4-05-9	N4-07-7	3/24/2011	TS	3/25/2011	TS	DF	3/25/2011	TS	4/5/2011	JK	4/5/2011	TS	9/16/2011	JK	
N4-06-1	N4-06-9	4/4/2011	TS	4/5/2011	TS	DF	4/5/2011	JW	4/29/2011	JK	4/29/2011	TS	9/16/2011	JK	
N4-06-2	N4-06-9	4/4/2011	TS	4/5/2011	TS	DF	4/5/2011	JW	4/29/2011	JK	4/29/2011	TS	9/16/2011	JK	
N4-06-3	N4-07-9	3/23/2011	TS	3/24/2011	TS	DF	3/24/2011	TS	4/5/2011	JK	4/5/2011	TS	9/16/2011	JK	
N4-06-4	N4-07-9	3/23/2011	TS	3/24/2011	TS	DF	3/24/2011	TS	4/5/2011	JK	4/5/2011	TS	9/16/2011	JK	
N4-06-5	N4-07-9	3/23/2011	TS	3/24/2011	TS	DF	3/24/2011	TS	4/5/2011	JK	4/5/2011	TS	9/16/2011	JK	
N4-06-6	N4-09-7	3/23/2011	TS	3/24/2011	TS	DF	3/24/2011	TS	4/5/2011	JK	4/5/2011	TS	9/16/2011	JK	
N4-06-7	N4-09-7	3/23/2011	TS	3/24/2011	TS	DF	3/24/2011	TS	4/5/2011	JK	4/5/2011	TS	9/16/2011	JK	
N4-06-8	N4-09-2	4/5/2011	JK	4/7/2011	JK	SAK	4/7/2011	JW	4/29/2011	JK	4/29/2011	TS	9/16/2011	JK	
N4-06-9	N4-15-6	3/17/2011	JK	3/18/2011	JK	SAK	3/18/2011	JW	4/29/2011	JK	4/29/2011	TS	9/16/2011	JK	
N4-07-1	N4-15-6	3/17/2011	JK	3/18/2011	JK	SAK	3/18/2011	JW	4/29/2011	JK	4/29/2011	TS	9/16/2011	JK	
N4-07-2	N4-08-3	3/17/2011	JK	3/18/2011	JK	SAK	3/18/2011	JW	4/29/2011	JK	4/29/2011	TS	9/16/2011	JK	
N4-08-1	N4-18-1	4/4/2011	TS	4/5/2011	TS	SAK	4/5/2011	TS	4/29/2011	JK	4/29/2011	TS	9/16/2011	JK	
N4-08-2	N4-09-4	5/5/2011	JK	5/16/2011	TS	SAK	5/16/2011	TS	5/23/2011	JK	5/23/2011	TS	9/16/2011	JK	
N4-08-3	N4-18-6	3/17/2011	JK	3/18/2011	JK	SAK	3/18/2011	TS	4/5/2011	JK	4/5/2011	TS	9/16/2011	JK	
N4-08-4	N4-19-8	3/23/2011	TS	3/24/2011	TS	SAK	3/24/2011	TS	4/5/2011	JK	4/5/2011	TS	9/16/2011	JK	
N4-08-5	N4-14-1	3/23/2011	TS	3/24/2011	TS	SAK	3/24/2011	TS	4/5/2011	JK	4/5/2011	TS	9/16/2011	JK	
N4-08-6	N4-14-7	3/23/2011	TS	3/24/2011	TS	SAK	3/24/2011	TS	4/5/2011	JK	4/5/2011	TS	9/16/2011	JK	
N4-08-7	N4-14-9	3/23/2011	TS	3/24/2011	TS	SAK	3/24/2011	TS	4/5/2011	JK	4/5/2011	TS	9/16/2011	JK	
N4-08-8	N4-15-4	3/23/2011	TS	3/24/2011	TS	SAK	3/24/2011	TS	4/5/2011	JK	4/5/2011	TS	9/16/2011	JK	
N4-08-9	N4-15-4	3/23/2011	TS	3/24/2011	TS	SAK	3/24/2011	TS	4/5/2011	JK	4/5/2011	TS	9/16/2011	JK	
N4-09-1	N4-15-4	3/23/2011	TS	3/24/2011	TS	SAK	3/24/2011	TS	4/5/2011	JK	4/5/2011	TS	9/16/2011	JK	
N4-09-2	N4-15-1	3/16/2011	JK	3/18/2011	JK	SAK	3/18/2011	TS	4/4/2011	JK	4/4/2011	TS	9/16/2011	JK	
N4-09-3	N4-14-7	3/16/2011	JK	3/18/2011	JK	SAK	3/18/2011	TS	4/4/2011	JK	4/4/2011	TS	9/16/2011	JK	
N4-09-4	N4-24-3	3/18/2011	JK	3/23/2011	TS	DF	3/23/2011	TS	4/7/2011	JK	4/7/2011	TS	9/16/2011	JK	
N4-09-5	N4-24-3	3/18/2011	JK	3/23/2011	TS	DF	3/23/2011	TS	4/7/2011	JK	4/7/2011	TS	9/16/2011	JK	
N4-09-6	N4-24-3	3/18/2011	JK	3/23/2011	TS	DF	3/23/2011	TS	4/7/2011	JK	4/7/2011	TS	9/16/2011	JK	
N4-09-7	N4-24-3	3/18/2011	JK	3/23/2011	TS	DF	3/23/2011	TS	4/7/2011	JK	4/7/2011	TS	9/16/2011	JK	
N4-09-8	N4-24-3	3/18/2011	JK	3/23/2011	TS	DF	3/23/2011	TS	4/7/2011	JK	4/7/2011	TS	9/16/2011	JK	
N4-09-9	N4-24-3	3/18/2011	JK	3/23/2011	TS	DF	3/23/2011	TS	4/7/2011	JK	4/7/2011	TS	9/16/2011	JK	
N4-10-1	N4-24-3	3/18/2011	JK	3/23/2011	TS	DF	3/23/2011	TS	4/7/2011	JK	4/7/2011	TS	9/16/2011	JK	
N4-10-2	N4-24-3	3/18/2011	JK	3/23/2011	TS	DF	3/23/2011	TS	4/7/2011	JK	4/7/2011	TS	9/16/2011	JK	
N4-10-3	N4-24-3	3/18/2011	JK	3/23/2011	TS	DF	3/23/2011	TS	4/7/2011	JK	4/7/2011	TS	9/16/2011	JK	



COMPONENT TRAVELER

PART NUMBER: 10-0013-0002-A05		PART NAME: DUMBELL		MATERIAL: RRR 300 Nd		NEXT ASSEMBLY: DUMBELL STACK-UP ESW		SHEET 2 OF 2	
Cell ID	24 Hr Tap-water Soak	Rust Spot Visual Inspection	Dynabraid	Cleanroom Prep	USC Processing	20 µm Wet Prep Etch	Final Inspect & Clean-room Pkg.	Operator	Notes
	Date	Date	Date	Date	Date	Date	Date	Date	
N4-14-8	3/18/2011	3/23/2011	3/25/2011	3/25/2011	4/7/2011	9/15/2011	9/16/2011	JK	
N4-15-2	3/18/2011	3/25/2011	3/25/2011	3/25/2011	4/5/2011	9/15/2011	9/16/2011	JK	
N4-15-3	3/18/2011	3/25/2011	3/24/2011	3/24/2011	4/7/2011	9/15/2011	9/16/2011	JK	
N4-15-7	3/18/2011	3/23/2011	3/24/2011	3/24/2011	4/4/2011	9/15/2011	9/16/2011	JK	
N4-15-8	3/18/2011	3/23/2011	3/24/2011	3/24/2011	4/5/2011	9/15/2011	9/16/2011	JK	
N4-15-1	3/18/2011	3/23/2011	3/24/2011	3/24/2011	4/5/2011	9/15/2011	9/16/2011	JK	
N4-16-3	3/17/2011	3/23/2011	3/24/2011	3/24/2011	4/7/2011	9/15/2011	9/16/2011	JK	
N4-16-4	3/17/2011	3/23/2011	3/24/2011	3/24/2011	5/23/2011	9/15/2011	9/16/2011	JK	X
N4-16-5	3/16/2011	3/23/2011	3/24/2011	3/24/2011	4/4/2011	9/15/2011	9/16/2011	JK	
N4-16-6	3/16/2011	3/23/2011	3/24/2011	3/24/2011	4/4/2011	9/15/2011	9/16/2011	JK	
N4-16-7	3/17/2011	3/18/2011	3/18/2011	3/21/2011	4/5/2011	9/15/2011	9/16/2011	JK	
N4-16-8	3/16/2011	3/18/2011	3/18/2011	3/21/2011	4/4/2011	9/15/2011	9/16/2011	JK	
N4-16-9	3/16/2011	3/18/2011	3/18/2011	3/21/2011	4/8/2011	9/15/2011	9/16/2011	JK	
N4-17-2	3/17/2011	3/18/2011	3/18/2011	3/21/2011	4/4/2011	9/15/2011	9/16/2011	JK	
N4-17-5	3/17/2011	3/18/2011	3/18/2011	3/21/2011	4/8/2011	9/15/2011	9/16/2011	JK	
N4-17-6	3/17/2011	3/18/2011	3/18/2011	3/21/2011	4/8/2011	9/15/2011	9/16/2011	JK	
N4-17-7	3/17/2011	3/18/2011	3/18/2011	3/21/2011	4/8/2011	9/15/2011	9/16/2011	JK	
N4-17-8	3/18/2011	3/23/2011	3/24/2011	3/24/2011	4/4/2011	9/15/2011	9/16/2011	JK	
N4-17-9	3/24/2011	3/25/2011	3/25/2011	3/25/2011	4/5/2011	9/15/2011	9/16/2011	JK	
N4-18-2	3/16/2011	3/18/2011	3/18/2011	3/24/2011	4/4/2011	9/15/2011	9/16/2011	JK	
N4-18-4	3/23/2011	3/24/2011	3/24/2011	3/24/2011	4/8/2011	9/15/2011	9/16/2011	JK	
N4-18-7	3/18/2011	3/23/2011	3/24/2011	3/24/2011	4/5/2011	9/15/2011	9/16/2011	JK	
N4-18-8	3/18/2011	3/23/2011	3/24/2011	3/24/2011	4/8/2011	9/15/2011	9/16/2011	JK	
N4-18-9	3/17/2011	3/18/2011	3/18/2011	3/21/2011	4/8/2011	9/15/2011	9/16/2011	JK	
N4-19-3	3/18/2011	3/23/2011	3/24/2011	3/24/2011	4/8/2011	9/15/2011	9/16/2011	JK	
N4-19-5	3/18/2011	3/23/2011	3/24/2011	3/24/2011	4/5/2011	9/15/2011	9/16/2011	JK	
N4-19-7	3/16/2011	3/18/2011	3/18/2011	3/21/2011	4/4/2011	9/15/2011	9/16/2011	JK	
N4-24-8	3/16/2011	3/18/2011	3/18/2011	3/21/2011	4/4/2011	9/15/2011	9/16/2011	JK	
P4-03	COMPLETED IN 08-0028	COMPLETED IN 08-0028	COMPLETED IN 08-0028	COMPLETED IN 08-0028	COMPLETED IN 08-0028	COMPLETED IN 08-0028	9/15/2011	JK	Ahren Added five P4 Dumbells:
P4-06	COMPLETED IN 08-0028	COMPLETED IN 08-0028	COMPLETED IN 08-0028	COMPLETED IN 08-0028	COMPLETED IN 08-0028	COMPLETED IN 08-0028	9/15/2011	JK	Inspected by Ahren
P4-44	COMPLETED IN 08-0028	COMPLETED IN 08-0028	COMPLETED IN 08-0028	COMPLETED IN 08-0028	COMPLETED IN 08-0028	COMPLETED IN 08-0028	9/15/2011	JK	Dynabraid (if needed)
P4-75	COMPLETED IN 08-0028	COMPLETED IN 08-0028	COMPLETED IN 08-0028	COMPLETED IN 08-0028	COMPLETED IN 08-0028	COMPLETED IN 08-0028	9/15/2011	JK	Re-inspected in House
P4-85	COMPLETED IN 08-0028	COMPLETED IN 08-0028	COMPLETED IN 08-0028	COMPLETED IN 08-0028	COMPLETED IN 08-0028	COMPLETED IN 08-0028	9/15/2011	JK	Acetone/Methanol 20u etched then dipped Bagged with Nitrogen Boxed to ship out



LONG END CLEANING TRACKER

COMPONENT TRAVELER

PART NUMBER: 10-0013-0006-P07		PART NAME: LONG HALF-CELL MATERIAL: RRR 300 Nb		NEXT ASSEMBLY: Long End Cell to Transition Ring EBW		SHEET 1 OF 1										
CELL ID	24 Hr Tap-water Soak		Rust Spot Visual Inspection		Dynabraid		Cleanroom Prep		USC Processing		20 µm Weld Prep Etch		Final Inspect & Clean-room Pkg.		Notes	
	Date	Operator	Pass/Fail	Date	Inspector	Date	Operator	Date	Operator	Date	Operator	Date	Operator	Pass/Fail		Date
P7-10-1	11/12/2010	JK	FAIL	11/12/2010	TS	11/15/2010	SK	11/23/2010	TS	12/1/2010	JK	12/2/2010	TS	PASS	12/3/2010	JK
P7-9-1	11/12/2010	JK	PASS	11/12/2010	TS	N/A	N/A	11/23/2010	TS	12/1/2010	JK	12/2/2010	TS	PASS	12/3/2010	JK
P7-9-3	11/12/2010	JK	PASS	11/12/2010	TS	N/A	N/A	11/23/2010	TS	12/1/2010	JK	12/2/2010	TS	PASS	12/3/2010	JK
P7-11-5	11/12/2010	JK	PASS	11/12/2010	TS	N/A	N/A	11/23/2010	TS	12/1/2010	JK	12/2/2010	TS	PASS	12/3/2010	JK
P7-9-2	11/12/2010	JK	PASS	11/12/2010	TS	N/A	N/A	11/23/2010	TS	12/1/2010	JK	12/2/2010	TS	PASS	12/3/2010	JK
P7-11-4	11/12/2010	JK	FAIL	11/12/2010	JK	11/15/2010	SK	11/23/2010	TS	12/1/2010	JK	12/2/2010	TS	PASS	12/3/2010	JK
P7-9-4	11/12/2010	JK	FAIL	11/12/2010	JK	11/15/2010	SK	11/23/2010	TS	12/1/2010	JK	12/2/2010	TS	PASS	12/3/2010	JK
P7-9-5	11/12/2010	JK	PASS	11/12/2010	TS	N/A	N/A	11/23/2010	TS	12/1/2010	JK	12/2/2010	TS	PASS	12/3/2010	JK
P7-11-3	11/12/2010	JK	PASS	11/12/2010	JK	N/A	N/A	11/23/2010	TS	12/1/2010	JK	12/2/2010	TS	PASS	12/3/2010	JK
P7-4-5	11/12/2010	JK	FAIL	11/12/2010	JK	11/15/2010	SK	11/23/2010	TS	12/1/2010	JK	12/2/2010	TS	PASS	12/3/2010	JK
P7-4-4	11/12/2010	JK	FAIL	11/12/2010	TS	11/15/2010	SK	11/23/2010	TS	12/1/2010	JK	12/2/2010	TS	PASS	12/3/2010	JK



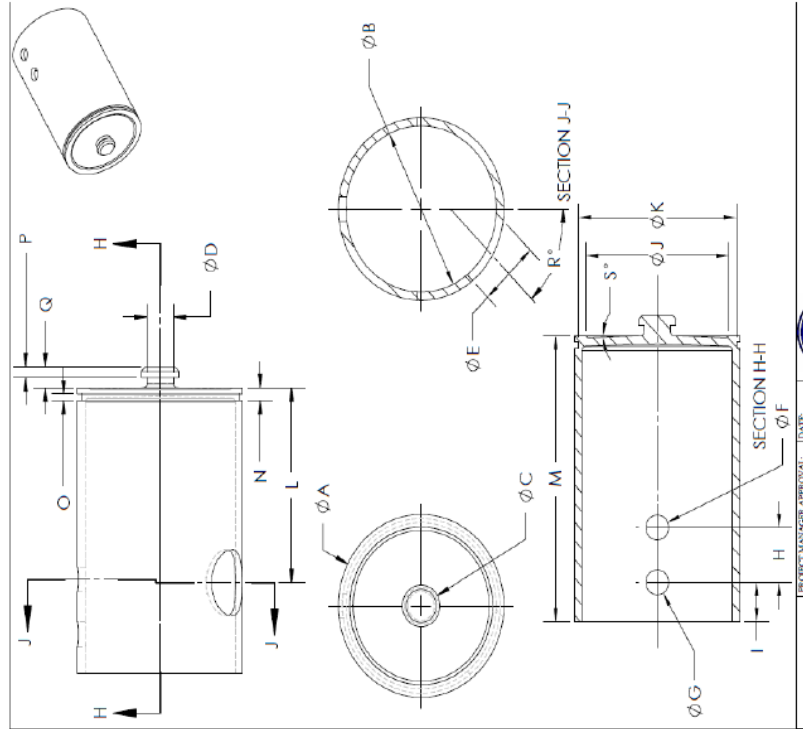
SHORT END CELL FABRICATION TRACKER

COMPONENT TRAVELER

CELL ID	Stamping		Coining		Check Fixture		Weld Prep Machining		Visual Inspection			Dynabraid			Final Inspection			Notes
	Date	Operator	Date	Operator	Pass/Fail	Operator	Date	CNC Operator	Rust, scratches, etc.	Date	Inspector	Date	Operator	Pass/Fail	Date	Operator		
P7-7-3	11/1/2010	DLP	N/A	N/A	PASS	SAK	11/11/2010	ECL	SEE SHORT END CLEANING TRACKER									
P7-4-1	11/1/2010	SAK	N/A	N/A	PASS	DLP	11/11/2010	ECL	SEE SHORT END CLEANING TRACKER									
P7-4-3	11/1/2010	DLP	N/A	N/A	PASS	DLP	11/8/2010	ECL	SEE SHORT END CLEANING TRACKER									
P7-11-2	11/1/2010	DLP	N/A	N/A	PASS	DLP	11/11/2010	ECL	SEE SHORT END CLEANING TRACKER									
P7-4-2	11/1/2010	SAK	N/A	N/A	PASS	SAK	11/11/2010	ECL	SEE SHORT END CLEANING TRACKER									
P7-7-5	11/1/2010	SAK	N/A	N/A	PASS	SAK	11/11/2010	ECL	SEE SHORT END CLEANING TRACKER									
P7-6-5	11/1/2010	DLP	N/A	N/A	PASS	DLP	11/11/2010	ECL	SEE SHORT END CLEANING TRACKER									
P7-2-2	11/1/2010	DLP	N/A	N/A	PASS	DLP	11/11/2010	ECL	SEE SHORT END CLEANING TRACKER									
P7-6-4	11/2/2010	JNS	N/A	N/A	PASS	JNS	11/11/2010	ECL	SEE SHORT END CLEANING TRACKER									
P7-7-1	11/2/2010	JNS	N/A	N/A	PASS	JNS	11/11/2010	ECL	SEE SHORT END CLEANING TRACKER									
P7-7-4	11/20/2010	JNS	N/A	N/A	PASS	JNS	11/11/2010	ECL	SEE SHORT END CLEANING TRACKER									

PART NUMBER: 10-0013-0010-P02 PART NAME: SHORT HALF-CELL MATERIAL: RRR 300 Nb NEXT ASSEMBLY: Short End Cell to Transition Ring EBW SHEET 1 OF 1

QA Data for Long End HOM Housing

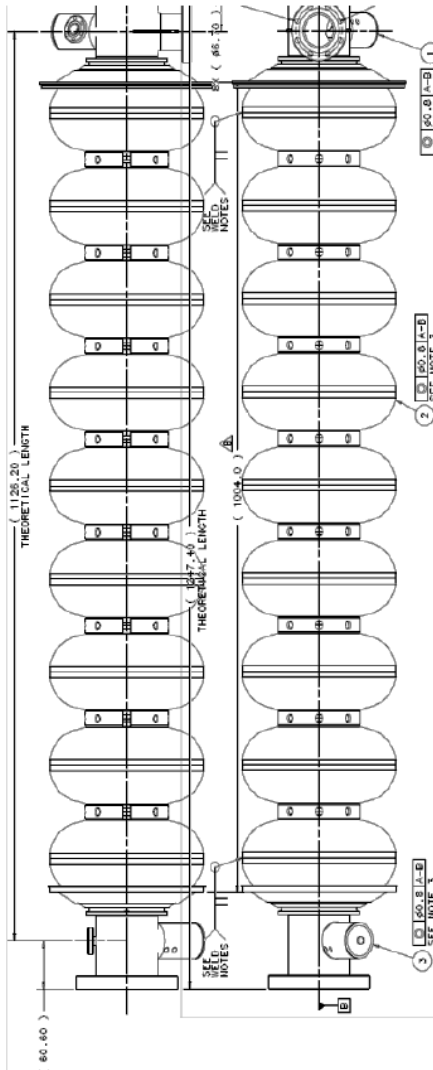


DIMENSION	A	C	D	K	O	P	Q
PART ID							
1 L	1.727	0.389	0.274	1.635	0.065	0.080	0.186
Unused - 2 L							
3 L	1.727	0.388	0.259	1.642	0.066	0.091	0.205
4 L	1.726	0.387	0.260	1.642	0.068	0.097	0.206
Unused - 5 L							
Unused - 6 L							
7 L	1.725	0.391	0.278	1.647	0.062	0.096	0.200
8 L	1.721	0.390	0.271	1.626	0.059	0.099	0.200
9 L	1.727	0.394	0.272	1.654	0.062	0.096	0.193
10 L	1.726	0.394	0.272	1.654	0.064	0.097	0.210
11 L	1.728	0.391	0.274	1.654	0.061	0.095	0.203
12 L	1.727	0.393	0.272	1.645	0.064	0.096	0.202
13 L	1.727	0.390	0.273	1.643	0.067	0.103	0.190
FINAL FIXTURE LIMIT	< 1.742	< 0.424	< 0.280	< 1.670	> 0.055	< 0.103	> 0.180
FINAL FIXTURE NOM.	< 1.752	< 0.434	< 0.285	< 1.675	> 0.050	< 0.108	> 0.170
FINAL FIXTURE TOL.	+/- .010	+/- .010	+/- .005	+/- .005	+/- .005	+/- .005	+/- .010

Part Name: Long End HOM Housing
Part Number: 10-0013-0008-P02
Checked By: KEN KOLP
Date: 10/4/2011
Measuring Devices: height gauge, calipers, depth mics, groove mics

TOLERANCES: PROJECT MANAGER: APPROVAL: DATE:

QA Data for Finished Cavity



DIMENSION	Overall Length	Ti to Ti Ring Length
PART ID		
TB9NR007	1260.00	1012.00
TB9NR008	1250.00	1014.00
TB9NR009	1250.00	1014.00
TB9NR010	1251.00	1014.00
TB9NR011	1250.00	1012.00
TB9NR013	1240.00	1009.00
TB9NR014	1250.00	1013.00
TB9NR015	1251.00	1013.00
TB9NR016	1251.00	1013.00
MIN	1240.00	1009.00
MAX	1260.00	1014.00
AVERAGE	1249.30	1012.60

Part Name:	19 Cell
Part Number:	10-0013-0000-A01
Checked By:	KEN KOLP
Date:	10/5/2011, 01/18/2012
Measuring Devices:	



NIOWAVE, INC

1012 North Walnut Street
Lansing, MI 48906
Phone: (517) 999-3475
Fax: (517) 999-3626
www.niowaveinc.com

**Certification of Processing
1.3 GHz 9-Cell Cavity Leak-check**

Cavity ID: TB9NR007

(Reference P.O. # 593451)

Procedure:

- Remove protective flange covers
- Install flanges with rubber gaskets on all flange surfaces
- Perform helium leak check
- Remove flanges & gaskets from all sealing surfaces
- Re-install protective flange covers

Check One

Cavities conform to FNAL helium leak check specification
(No detectible signal found with a minimum sensitivity of at least $\leq 1 \times 10^{-10}$ mbar L/s)

Cavities failed leak check

Signature: Tim Schade Date: 10-11-11
Tim Schade
Accelerator Engineer



NIOWAVE, INC

1012 North Walnut Street
Lansing, MI 48906
Phone: (517) 999-3475
Fax: (517) 999-3626
www.niowaveinc.com

**Certification of Processing
1.3 GHz 9-Cell Cavity Leak-check**

Cavity ID: TB9NR008

(Reference P.O. # 593451)

Procedure:

- Remove protective flange covers
- Install flanges with rubber gaskets on all flange surfaces
- Perform helium leak check
- Remove flanges & gaskets from all sealing surfaces
- Re-install protective flange covers

Check One

- Cavities conform to FNAL helium leak check specification
(No detectible signal found with a minimum sensitivity of at least $\leq 1 \times 10^{-10}$ mbar L/s)
- Cavities failed leak check

Signature: Tim Schade Date: 10-11-11
Tim Schade
Accelerator Engineer



NIOWAVE, INC

1012 North Walnut Street
Lansing, MI 48906
Phone: (517) 999-3475
Fax: (517) 999-3626
www.niowaveinc.com

**Certification of Processing
1.3 GHz 9-Cell Cavity Leak-check**

Cavity ID: TB9NR016

(Reference P.O. # 593451)

Procedure:

- Remove protective flange covers
- Install flanges with rubber gaskets on all flange surfaces
- Perform helium leak check
- Remove flanges & gaskets from all sealing surfaces
- Re-install protective flange covers

Check One

Cavities conform to FNAL helium leak check specification
(No detectible signal found with a minimum sensitivity of at least $\leq 1 \times 10^{-10}$ mbar L/s)

Cavities failed leak check

Signature: Tim Schade Date: 10-11-11
Tim Schade
Accelerator Engineer



NIOWAVE, INC

1012 North Walnut Street
Lansing, MI 48906
Phone: (517) 999-3475
Fax: (517) 999-3626
www.niowaveinc.com

**Certification of Processing
1.3 GHz 9-Cell Cavity Leak-check**

Cavity ID: TB9NR016

(Reference P.O. # 593451)

Procedure:

- Remove protective flange covers
- Install flanges with rubber gaskets on all flange surfaces
- Perform helium leak check
- Remove flanges & gaskets from all sealing surfaces
- Re-install protective flange covers

Check One

Cavities conform to FNAL helium leak check specification
(No detectible signal found with a minimum sensitivity of at least $\leq 1 \times 10^{-10}$ mbar L/s)

Cavities failed leak check

Signature: Tim Schade Date: 10-11-11
Tim Schade
Accelerator Engineer



NIOWAVE, INC

1012 North Walnut Street
Lansing, MI 48906
Phone: (517) 999-3475
Fax: (517) 999-3626
www.niowaveinc.com

**Certification of Processing
1.3 GHz 9-Cell Cavity Leak-check**

Cavity ID: TB9NR011

(Reference P.O. # 593451)

Procedure:

- Remove protective flange covers
- Install flanges with rubber gaskets on all flange surfaces
- Perform helium leak check
- Remove flanges & gaskets from all sealing surfaces
- Re-install protective flange covers

Check One

- Cavities conform to FNAL helium leak check specification
(No detectible signal found with a minimum sensitivity of at least $\leq 1 \times 10^{-10}$ mbar L/s)
- Cavities failed leak check

Signature: Tim Schade Date: 10-11-11
Tim Schade
Accelerator Engineer



NIOWAVE, INC

1012 North Walnut Street
Lansing, MI 48906
Phone: (517) 999-3475
Fax: (517) 999-3626
www.niowaveinc.com

**Certification of Processing
1.3 GHz 9-Cell Cavity Leak-check**

Cavity ID: TB9NR012

(Reference P.O. # 593451)

Procedure:

- Remove protective flange covers
- Install flanges with rubber gaskets on all flange surfaces
- Perform helium leak check
- Remove flanges & gaskets from all sealing surfaces
- Re-install protective flange covers

Check One

- Cavities conform to FNAL helium leak check specification
(No detectible signal found with a minimum sensitivity of at least $\leq 1 \times 10^{-10}$ mbar L/s)
- Cavities failed leak check

Signature: Tim Schade Date: 10-11-11
Tim Schade
Accelerator Engineer



NIOWAVE, INC

1012 North Walnut Street
Lansing, MI 48906
Phone: (517) 999-3475
Fax: (517) 999-3626
www.niowaveinc.com

**Certification of Processing
1.3 GHz 9-Cell Cavity Leak-check**

Cavity ID: TB9NR013

(Reference P.O. # 593451)

Procedure:

- Remove protective flange covers
- Install flanges with rubber gaskets on all flange surfaces
- Perform helium leak check
- Remove flanges & gaskets from all sealing surfaces
- Re-install protective flange covers

Check One

- Cavities conform to FNAL helium leak check specification
(No detectible signal found with a minimum sensitivity of at least $\leq 1 \times 10^{-10}$ mbar L/s)
- Cavities failed leak check

Signature: Tim Schade Date: 10-11-11
Tim Schade
Accelerator Engineer



NIOWAVE, INC

1012 North Walnut Street
Lansing, MI 48906
Phone: (517) 999-3475
Fax: (517) 999-3626
www.niowaveinc.com

**Certification of Processing
1.3 GHz 9-Cell Cavity Leak-check**

Cavity ID: TB9NR014

(Reference P.O. # 593451)

Procedure:

- Remove protective flange covers
- Install flanges with rubber gaskets on all flange surfaces
- Perform helium leak check
- Remove flanges & gaskets from all sealing surfaces
- Re-install protective flange covers

Check One

Cavities conform to FNAL helium leak check specification
(No detectible signal found with a minimum sensitivity of at least $\leq 1 \times 10^{-10}$ mbar L/s)

Cavities failed leak check

Signature:  Date: 10-11-11
Michael DeRosia
Accelerator Engineer



NIOWAVE, INC

1012 North Walnut Street
Lansing, MI 48906
Phone: (517) 999-3475
Fax: (517) 999-3626
www.niowaveinc.com

**Certification of Processing
1.3 GHz 9-Cell Cavity Leak-check**

Cavity ID: TB9NR015

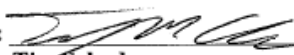
(Reference P.O. # 593451)

Procedure:

- Remove protective flange covers
- Install flanges with rubber gaskets on all flange surfaces
- Perform helium leak check
- Remove flanges & gaskets from all sealing surfaces
- Re-install protective flange covers

Check One

- Cavities conform to FNAL helium leak check specification
(No detectible signal found with a minimum sensitivity of at least $\leq 1 \times 10^{-10}$ mbar L/s)
- Cavities failed leak check

Signature:  Date: 1-19-12
Tim Schade
Accelerator Engineer



NIOWAVE, INC

1012 North Walnut Street
Lansing, MI 48906
Phone: (517) 999-3475
Fax: (517) 999-3626
www.niowaveinc.com

**Certification of Processing
1.3 GHz 9-Cell Cavity Leak-check**

Cavity ID: TB9NR016

(Reference P.O. # 593451)

Procedure:

- Remove protective flange covers
- Install flanges with rubber gaskets on all flange surfaces
- Perform helium leak check
- Remove flanges & gaskets from all sealing surfaces
- Re-install protective flange covers

Check One

- Cavities conform to FNAL helium leak check specification
(No detectible signal found with a minimum sensitivity of at least $\leq 1 \times 10^{-10}$ mbar L/s)
- Cavities failed leak check

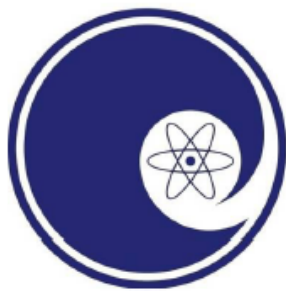
Signature: Tim Schade Date: 1-20-12
Tim Schade
Accelerator Engineer

9-cell Equator Weld Repair Plan
(Cavities TB9NR015, TB9NR016)

**FNAL 1.3GHz 9-cell
10 cavity order**

01/20/12

FNAL PO # 593451



NIOWAVE
www.niowaveinc.com



NIOWAVE, INC
1012 North Walnut Street
Lansing, MI 48906
Phone: (517) 999-3475
Fax: (517) 999-3626
www.niowaveinc.com

EBW Observations

Two cavities out of the ten cavity order had a weld blow-through during the electron beam welding (EBW) of the end assembly equators. All components had been cleaned per DESY specification DESY_Cavity_Spec2005 prior to EBW. The equators that had the EBW blow-throughs looked like the other 18 full penetration welds from this cavity batch, with the exception of the blow-throughs. Niowave did observe intermittent weld spatter during the 20 equator welds and believe that this is due to an unstable vapor column with these weld parameters. The cavity purity is still intact and Niowave proposes to repair these two cavities utilizing the same fabrication techniques for the repairs as the original welds. All Nb will be handled per DESY specification DESY_Cavity_Spec2005 in order to maintain cavity purity and performance for these repairs. The cavities will also be photographed both before and after the repair for future reference.

Cavity Repair Steps

NOTE: UTILIZE NITRILE, LATEX, OR APPROPRIATE CLEAN GLOVES WHEN HANDLING COMPONENTS. DO NOT TOUCH EQUATOR BLOW THROUGH REGIONS OR INTERIOR.

1. Mask off cavity exterior surrounding blowthrough to minimize exterior surface contamination
2. Machine hole of known dimensions to remove blowthrough
 - a. ***UTILIZE VACUUM TO REMOVE ANY CHIPS DURING MACHINING***
3. Machine plug of RRR 300 Nb to match thickness of equator weld prep
4. Engrave beam flange to indicate timing of equator blowthrough for future reference
5. Utilize BCP to perform a 20 μm etch of both the weld region and plug
6. After both cavity and plug are ultra-pure water rinsed & dry in class 100 clean room, install Nb plug in cleanroom
7. Bag cavity in dry nitrogen
8. EBW plug & inspect interior prior to removing from EBW chamber



NIOWAVE, INC

1012 North Walnut Street
Lansing, MI 48906
Phone: (517) 999-3475
Fax: (517) 999-3626
www.niowaveinc.com

Cavity Repair Photographs

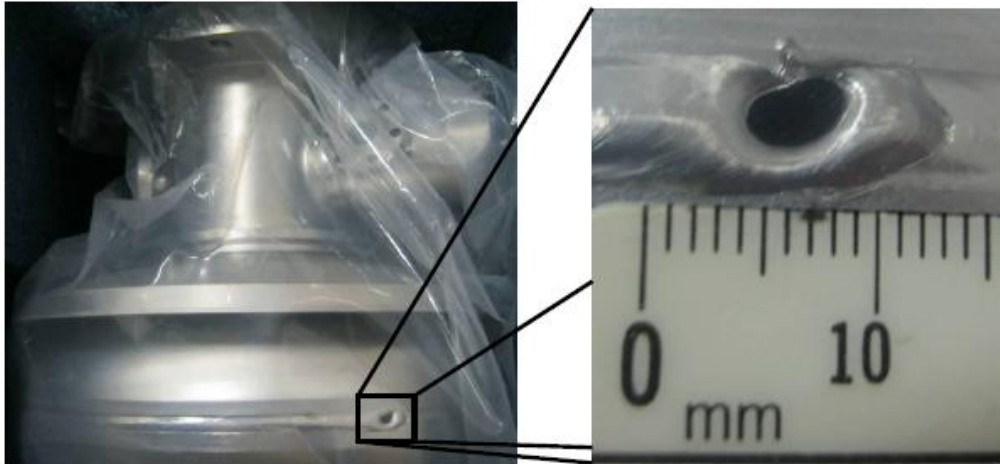


Figure 1 Cavity TB9NR015 long end assembly blow-through (before repair preparation)



Figure 2 Cavity TB9NR015 blow-through (after repair preparation)



NIOWAVE, INC

1012 North Walnut Street
Lansing, MI 48906
Phone: (517) 999-3475
Fax: (517) 999-3626
www.niowaveinc.com



Figure 3 Cavity TB9NR015 blow-through (after repair)



NIOWAVE, INC

1012 North Walnut Street
Lansing, MI 48906
Phone: (517) 999-3475
Fax: (517) 999-3626
www.niowaveinc.com

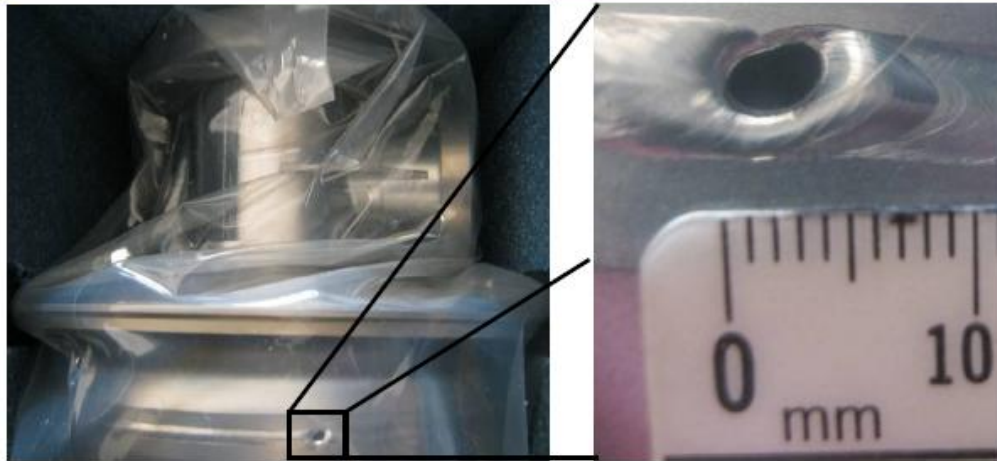


Figure 4 Cavity TB9NR016 short end assembly blow-through (before repair preparation)



Figure 5 Cavity TB9NR016 blow-through (after repair preparation)



NIOWAVE, INC

1012 North Walnut Street
Lansing, MI 48906
Phone: (517) 999-3475
Fax: (517) 999-3626
www.niowaveinc.com



Figure 6 Cavity TB9NR016 blow-through (after repair)